Universidad de Santiago de Compostela

Facultad de Farmacia

Departamento de Farmacia y Tecnología Farmacéutica

Tesis Doctoral

Nanocápsulas multifuncionales para la liberación selectiva de fármacos antitumorales

Carmen Teijeiro Valiño

Santiago de Compostela, 2015

USC
UNIVERSIDADE
DE SANTIAGO
DE COMPOSTELA

Dra. María José Alonso Fernández, Catedrática del Departamento de Tecnología Farmacéutica de la Universidad de Santiago de Compostela

Dra. Noémi Stefania Csaba, Investigadora del Departamento de Tecnología Farmacéutica de la Universidad de Santiago de Compostela

Informan:

Que la presente Memoria Experimental titulada**: "Nanocápsulas multifuncionales para la liberación selectiva de fármacos antitumorales**", elaborada por **Carmen Teijeiro Valiño**, fue realizada bajo su dirección y en el Departamento de Farmacia y Tecnología Farmacéutica y, estando concluida, autorizan su presentación a fin de que pueda ser juzgada por el tribunal correspondiente.

Y para que así conste, expiden y firman el presente certificado en Santiago de Compostela, a 4 de noviembre de 2015.

Fdo. María José Alonso Fernández Fdo. Noémi Stefania Csaba

USC
UNIVERSIDADE
DE SANTIAGO
DE COMPOSTELA

Gracias

Y llegados este momento, quiero acordarme de todos los que de forma directa o aún sin saberlo han contribuido a que pueda concluir esta tesis.

A mis directoras María José Alonso y Noémi Csaba por haberme dado la oportunidad de realizar esta tesis doctoral y por dirigir esta trabajo.

También al proyecto Lymphotarg y a la Diputación de A Coruña por la financiación de este proyecto.

A todos aquellos con los que he compartido colaboraciones; científicos de distintas áreas indispensables para realizar un trabajo multidisciplinar como éste. Gracias a Erea Borrajo, Ramón Novoa, Marta Alonso, María de la Fuente, Anxo Vidal, Elena Santidrián y Laura Sánchez.

A Melissa Guada y María Blanco del departamento de Farmacia y Tecnología Farmacéutica de la Universidad de Navarra; por vuestra amabilidad y disponibilidad, por enseñarme tantas cosas y tan útiles para este proyecto, y también por enseñarme Navarra y sus pintxos. A Fabiana Quaglia, por acogerme en el departamento de Química Farmacéutica y Toxicología de la Universidad de Nápoles.

A todos mis amigos y en especial a Loly, Gema, Alejandra y Raquel, por vuestro interés, vuestra compañía y vuestro apoyo.

A toda mi familia; a mis abuelos, a Tila, a mi hermano Javi; gracias por animarme siempre y muy especialmente a mis padres, por sentar las bases de mi vida y por darme un apoyo y cariño incondicional sin el cual no hubiera podido llegar hasta aquí.

A Zalo, por andar conmigo todo el camino, por tu optimismo y generosidad, por hacerme seguir adelante en los momentos difíciles y por todo. Gracias.

Y gracias a mis nanochachos; Raquel, Ivana, Ana Cadete, Ana Olivera, Belén López, Tania, Howl, Mariajo, Sara, Jorge, Jose Vicente, Ana González, Jose, Irene, Tamara, Imma, Niu, Lungile, Mati, Khair y muy en especial a Adriana, a Elena y a Sonia. Por tantos momentos

compartidos que me acompañarán siempre. Por la ayuda, los ánimos, las risas y por todo el aprendizaje profesional pero sobre todo personal.

Y finalmente al resto de los componentes de Nanobiofar; Desiré, Loly, Marcos, Puri, Rafa por la ayuda y los consejos y en especial a Belén Cuesta por crear buen rollo y ganas.

Índice

USC
UNIVERSIDADE
DE SANTIAGO
DE COMPOSTELA

Resumen/Abstract

USC
UNIVERSIDADE
DE SANTIAGO
DE COMPOSTELA

El trabajo desarrollado en la presente tesis, está enfocado al diseño de nanocápsulas poliméricas con propiedades multifuncionales que les permitan dirigir activamente fármacos quimioterapéuticos a células tumorales.

Para la preparación de estos sistemas nanocapsulares consistentes en un núcleo oleoso y una cubierta polimérica, hemos seleccionado como biomaterial de cubierta el polisacárido natural ácido hialurónico por su aportación de propiedades clave; como su interacción específica con el receptor CD44 sobreexpresado en un gran número de células tumorales, así como su hidrofilia. Este polímero ha sido modificado con el péptido denominado t-Lyp-1, que además de presentar una alta selectividad por el receptor NRP1 presente en muchas células tumorales, promueve la penetración a través del estroma tumoral. Ambos materiales; ácido hialurónico y ácido hialurónico conjugado con t-Lyp-1, fueron empleados para la preparación de nanocápsulas.

La caracterización de estos sistemas mostró unas propiedades físico-químicas favorables para la administración de fármacos quimioterapéuticos; tales como tamaño reducido, estabilidad en medios fisiológicos y capacidad de encapsular el fármaco antitumoral docetaxel en su núcleo oleoso. Además, se ha demostrado la presencia de una cubierta de ácido hialurónico y t-Lyp-1 en la superficie de las nanocápsulas. Posteriormente, estudios *in vitro* confirmaron una interacción específica de estos sistemas a través de sus receptores CD44 y NRP1 en la línea celular de cáncer de pulmón A549.

En la última parte del trabajo, hemos evaluado el comportamiento in vivo de estos sistemas en un modelo de cáncer de pulmón metastásico. El estudio de biodistribución mostró un gran aumento de la acumulación tumoral respecto al tratamiento comercial Taxotere®, especialmente para las nanocápsulas modificadas con t-Lyp-1 (hasta 37 veces más). Ambos prototipos, además, consiguieron incrementar los niveles de fármaco en los ganglios linfáticos, siendo este efecto de gran importancia para frenar la diseminación metastática. El estudio de eficacia antitumoral reveló que las nanocápsulas modificadas con t-Lyp-1 lograron una gran mejora de la eficacia terapéutica, tanto a nivel de reducción del crecimiento tumoral, como en la capacidad para frenar la diseminación metastática.

Estos resultados muestran el éxito logrado con el sistema multifuncional propuesto, capaz de interaccionar con dos receptores tumorales y de promover la penetración a través del tejido tumoral

The main goal of this thesis has been the design of polymeric nanocapsules, with multifunctional properties that allow the targeted delivery of chemotherapeutic drugs to tumour cells.

These nanocapsules formed by an oily core and a polymer shell, are based on hyaluronic acid, selected as shell material for its key properties; such as its specific interaction with CD44 receptor overexpressed in a wide number of tumour cells, as well as its hydrophilicity. This biopolymer has been modified with the tumour homing peptide t-Lyp-1, which, in addition to show high affinity for NRP1 receptor present in many types of tumours, promotes penetration through tumour stroma. Both materials, hyaluronic acid and hyaluronic acid conjugated with t-Lyp-1, were employed for nanocapsules preparation.

The characterization of these systems showed favourable physico-chemical properties, such as small size, satisfactory stability in physiological media and good capacity for encapsulating the antitumoral drug docetaxel inside the oily core. Furthermore, the presence of hyaluronic acid and t-Lyp-1 shell around the nanocapsules has been confirmed. In the next step, *in vitro* studies confirmed a specific interaction of these systems through CD44 and NRP1 receptors overexpressed in the lung cancer cell line A549.

Finally, the in vivo fate of these systems was assessed in a metastatic lung cancer model. Biodistribution data showed a great enhancement of tumour accumulation compared with commercial treatment (Taxotere®), especially for t-Lyp-1 modified nanocapsules (37-fold increase). Additionally, both prototypes achieved increased drug levels in the lymph nodes, this being crucial for the access of the nanosystems to the metastatic cells. Antitumoral efficacy study revealed that t-Lyp-1 modified nanocapsules greatly improve therapeutic efficacy, in terms of reduction of tumour growth, and also hindering the metastatic spreading.

These results highlight the success achieved with the proposed multifunctional nanosystem, exhibiting the capacity for interacting with two cancer cell receptors and promoting penetration through the tumour tissue.

USC
UNIVERSIDADE
DE SANTIAGO
DE COMPOSTELA

Introducción

Nanomedicinas contra el cáncer.

Avances y retos

USC
UNIVERSIDADE
DE SANTIAGO
DE COMPOSTELA

Nanomedicinas contra el cáncer. Avances y retos

1. Nanoterapias actuales: logros y carencias de los sistemas de vectorización pasiva

La quimioterapia constituye hoy en día una de las principales líneas de tratamiento contra el cáncer. Sin embargo y a pesar del descubrimiento de potentes fármacos antitumorales, entre los cuales se encuentran los taxanos [1], la quimioterapia presenta grandes deficiencias; en primer lugar su toxicidad, asociada a la necesidad de utilizar agentes solubilizantes, como el Cremophor® y el Tween® 80, para su administración por vía intravenosa en forma de solución [2]. Sin embargo, el mayor obstáculo a la eficacia de estos fármacos, está en su perfil de biodistribución inespecífico, distribuyéndose en tejidos sanos con la consecuente toxicidad para éstos y sin alcanzar una dosis suficiente en el tejido tumoral que logre el efecto terapéutico deseado [3, 4].

Las terapias antitumorales basadas en la nanotecnología (nanoterapias oncológicas) se presentan como una estrategia prometedora para intentar solventar estos problemas asociados con las terapias convencionales. Por una parte, existen diferentes tipos de sistemas nanométricos incluyendo micelas, liposomas, nanopartículas o nanocápsulas que permiten asociar fármacos hidrofóbicos evitando así el uso de sustancias tóxicas necesarias para su solubilización. Además, la mayor parte de estas nanoestructuras [5] han sido diseñadas específicamente para actuar en determinadas condiciones fisio-patológicas. Así por ejemplo, el incremento de la permeabilidad de los capilares sanguíneos y la disfunción de los capilares linfáticos han sido utilizados en el diseño de sistemas de orientación pasiva basados en el efecto de mayor permeabilidad y retención tumoral (EPR, enhanced permeability and retention effect [6]).

Para lograr este objetivo las propiedades físico-químicas de los nanosistemas, tales como hidrofilicidad, tamaño y carga eléctrica, desempeñan una función primordial. Así, muchos nanosistemas caracterizados por su largo tiempo de circulación presentan en su superficie una cubierta hidrofílica que les confiere protección estérica evitando la opsonización y ofreciéndoles más oportunidades para extravasarse al tumor [7-13]. En cuanto al tamaño, se sabe que sistemas en torno a 100 - 150 nm muestran una mayor resistencia frente a la agregación y, por tanto, una mayor estabilidad [14] y tiempo de

circulación en el torrente sanguíneo [15-19]. Por otra parte, la carga superficial de los nanosistemas genera una repulsión entre partículas que dificulta la agregación mejorando su estabilidad [20] y en concreto, la carga superficial negativa presenta menor grado de interacciones celulares de tipo no específico [21, 22].

Desde el comienzo de la investigación en nanomedicina, se han ido desarrollando y testando un gran número de nanostructuras que han ido aumentando en su complejidad. Las micelas, liposomas y nanopartículas han sido sin duda los sistemas más explorados y los únicos que hasta el momento han conseguido llegar a clínica. La Tabla 1 recoge las principales formulaciones quimioterapéuticas aprobadas o en fase de investigación clínica. Además de éstas, existen otros tipos de nanostructuras poliméricas como son los dendrímeros consistentes en polímeros ramificados de especial interés para la asociación de material genético, o las nanocápsulas, una tecnología reciente constituida por un núcleo oleoso y una cubierta polimérica, muy adecuada para la asociación de fármacos hidrofóbicos.

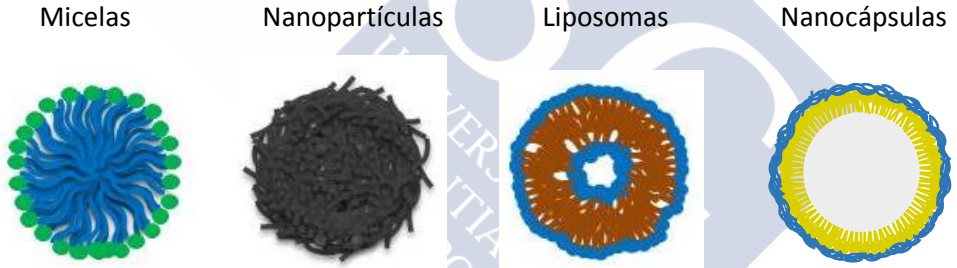

Figura 1. Representación esquemática de los tipos de nanoestructuras con mayor representación

Las micelas, probablemente por su sencillez tecnológica, han sido sin duda el sistema más estudiado. Estas nanoestructuras se forman a partir de moléculas anfifílicas que cuando se encuentran por encima de la concentración micelar crítica en un medio acuoso se autoensamblan espontáneamente, disponiéndose con los grupos polares hacia la superficie externa y la parte hidrofóbica inmersa hacia el interior, donde se pueden asociar fármacos hidrofóbicos (Figura 1). Hay un amplio abanico de polímeros anfifílicos empleados para la formación de formulaciones micelares, algunas de las cuáles han llegado a ensayos clínicos. Tal es el caso del producto denominado NK105 [23] a base de PEG-poliaspartato asociado a paclitaxel, indicado en el tratamiento del

cáncer de estómago, el sistema NK012 compuesto de PEG-poliglutamato [24], asociado a un análogo de la camptotecina, indicado en el tratamiento del cáncer de mama, o el llamado NC-6004™ [25] similar al anterior, pero en este caso con cisplatino, indicado en el tratamiento de cáncer de páncreas. Actualmente, existen dos formulaciones micelares comercializadas, ambas constituidos por micelas de ácido poliláctico pegilado. Una de ellas es la conocida como Genexol®-PM [24], una formulación que contiene paclitaxel y ha sido aprobada para el tratamiento de cáncer de mama, pulmón y ovario. La segunda, Nanoxel®, es una fomulación que contiene docetaxel y que ha sido aprobada para el tratamiento de cáncer de pulmón, mama y de ovario [26]. A pesar del éxito que supuso la comercialización de estos prototipos, una de las grandes limitaciones de las micelas es la falta de estabilidad debido a su disgregación cuando se diluyen por debajo de su concentración micelar crítica, como puede ocurrir tras una administración intravenosa, aspecto que podría limitar el grado de aplicación clínica de estos sistemas [27, 28].

Los liposomas son vesículas nanométricas consistentes en un núcleo acuoso rodeado de una bicapa de fosfolípidos, los fármacos hidrofóbicos en este caso puede asociarse a los componentes lipídicos del sistema (Figura 1). Los liposomas son sin duda, los sistemas que más éxito han tenido hasta ahora en el desarrollo de nanoterapéuticos contra el cáncer. El primero fue comercializado en los 90, con el nombre de Doxil® o Caelyx® [29], y es un liposoma pegilado conteniendo doxorubicina para el tratamiento del cáncer de ovario y el sarcoma de Kaposi. A partir de entonces, muchas otras formulaciones liposomales se han sumado a esta lista: como el Myocet® [30], sistema similar al anterior pero sin pegilar, que se usa en la práctica clínica para el cáncer de mama y ovario, o el DaunoXome® [31] para el tratamiento del sarcoma de Kaposi, ambos para la administración de doxorubicina. Además de los diferentes formatos de doxorubicina liposomal, existen formulaciones para la administración de otros fármacos antitumorales; como por ejemplo el Marquibo® [32], un liposoma conteniendo vincristina para el tratamiento de linfoma no-Hodgkin, el conocido como Lipusu® con paclitaxel para el tratamiento de cáncer de ovario y pulmón [33] y el Depocyt®, un liposoma multivesicular con citarabina para el tratamiento de neoplasmas meníngeas [34]. A parte de estos sistemas comercializados, otros se encuentran en ensayos clínicos

como los liposomas no pegilados CPX-1 [35] y MM-398 [36], ambos con irinotecano para el tratamiento de carcinoma colorectal, cáncer de páncreas metastático y tumores sólidos pediátricos, o los conocidos como LEP-ETU [37] y ATI-1123 [38] ambos con docetaxel para tratar tumores sólidos avanzados.

Los últimos sistemas en sumarse a esta lista de nanomedicamentos en la práctica clínica han sido las nanopartículas. Estas estructuras son sistemas matriciales que presentan una gran versatilidad en cuanto a materiales empleados para su formación, siendo las nanopartículas poliméricas las que han logrado una mayor presencia en la aplicación clínica (Figura 1). Hasta el momento el único tratamiento comercializado es el Abraxane® [39], consistente en nanopartículas de albúmina cargadas de paclitaxel, indicadas en el tratamiento del cáncer de mama. Sin embargo, existen otros candidatos a nanomedicamentos que están siendo evaluados en ensayos clínicos, como es el caso de ABI-009, un derivado del Abraxane® con rapamicina para el tratamiento del cáncer de mama metastático, cáncer de próstata, linfoma y tumores sólidos en general [40], o el conocido como Doxorubicin Transdrug®, constituido por nanopartículas de poliacrilatos conteniendo doxorubicina, indicado en el tratamiento de carcinoma hepatocelular [41]. Otros ejemplos de nanopartículas conteniendo docetaxel son el CRLX301 [42], formulación constituida por ciclodextrinas poliméricas y el docetaxel-PNP [43], formulación formada por ácido poliláctico, ambas para el tratamiento de tumores sólidos.

Nanosistema	Fármaco	Nombre comercial	Indicación	Estado
Micelas	Paclitaxel	Genexol®-PM	Cáncer de mama y pulmón	Comercializado
	Paclitaxel	NK-105	Cáncer de mama	Fase III
	Docetaxel	Nanoxel®	Cáncer de mama y pulmón	Comercializado
	Cisplatino	NC-6004™	Cáncer de páncreas	Fase III
	Camptotecina	NK012	Cáncer de mama	Fase II
Liposomas	Paclitaxel	Lipusu®	Cáncer de ovario y pulmón	Comercializado
	Docetaxel	ATI-1123	Tumores sólidos avanzados	Fase I
	Docetaxel	LEP-ETU	Tumores sólidos avanzados	Fase II
	Doxorubicina	Doxil®	Cáncer de ovario	Comercializado
	Doxorubicina	Myocet®	Cáncer de mama metastásico	Comercializado
	Doxorubicina	DaunoXome®	Sarcoma de Kaposi	Comercializado
	Vincristina	Onco-TCS (Marqibo)®	Linfoma No-Hodgkin	Comercializado
	Citarabina	Depocyt®	Neoplasia meníngea	Comercializado
	Irinotecano	CPX-1	Carcinoma colorectal	Fase II
	Irinotecano	MM-398	Cáncer de páncreas	Fase I

Nanopartículas	Paclitaxel	Abraxane®	Cáncer de mama y pulmón	Comercializado
	Rapamicina	ABI-009	Cáncer de mama y próstata	Fase II
	Docetaxel	Docetaxel-PNP	Tumores sólidos avanzados	Fase II
	Docetaxel	CRLX301	Tumores sólidos avanzados	Fase II
	Doxorubicina	Doxorubicin-Transdrug®	Carcinoma hepatocelular	Fase III

Tabla 1. Principales nanomedicamentos quimioterapéuticos comercializados o en fase clínica.

En mayor o menor medida, estas formulaciones han demostrado un aumento del tiempo de circulación en sangre y una mejora de la biodistribución del fármaco hacia el tumor, mediante el mecanismo de vehiculización pasivo anteriormente comentado [44, 45]. A su vez, estos nanosistemas han conseguido una reducción significativa de efectos tóxicos como cardiotoxicidad, neurotoxicidad y nefrotoxicidad [44-47], permitiendo un aumento de la máxima dosis tolerada, debido tanto a esta biodistribución más selectiva como a la eliminación de los excipientes tóxicos incluidos en las formas de administración convencionales.

A pesar de estas mejoras asociadas a la utilización de estas nanoestructuras, el incremento en la eficacia antitumoral en la práctica clínica ha sido bastante modesto. Esta limitación se debe a distintas causas. En primer lugar, la orientación pasiva no logra el incremento necesario de dosis de fármaco en el tumor. Por otra parte, la limitada penetración de las nanosistemas a través del tejido tumoral [48-51] dificulta el acceso a las células menos accesibles disminuyendo la eficacia terapéutica. Finalmente, otro gran impedimento, es la ineficacia de los actuales tratamientos para detener el avance tumoral una vez que haya comenzado el proceso de la metastásis y las células tumorales comienzan a diseminarse [52-54].

2. Sistemas de orientación o "targeting" activo: Avances recientes y nuevas expectativas

La evolución en el conocimiento sobre la fisiología tumoral y el desarrollo de nuevos materiales, está permitiendo diseñar nanosistemas más adaptados a las necesidades terapéuticas. De hecho, existe una segunda generación de nanosistemas, basados en el uso de biomoléculas que interaccionan específicamente con células tumorales, para mejorar considerablemente la acumulación e interacción con las células diana, estrategia conocida como orientación o "targeting" activo. Entre estas biomoléculas se encuentran los anticuerpos monoclonales, los aptameros y los péptidos, los cuales, al estar localizados en la superficie externa de los nanosistemas, facilitan su unión a receptores sobreexpresados en las células diana. La Tabla 2 muestra las biomoléculas más representativas que han sido utilizadas en el desarrollo de nanomedicamentos dirigidos activamente a células tumorales.

Biomolécula	Nombre	Receptor diana
Anticuerpos	Cetuximab	Factor crecimiento EGFR
	Rituximab	CD20
	Trastuzumab	HER2
Ácidos nucleicos	ACUPA	PSMA
	AS1411	Nucleolina
Péptidos	RGD	Integrinas $\alpha_v B_3$
	iRGD (péptido CendR)	Integrinas $\alpha_n B_3$
	Lyp-1 (péptido CendR)	p32
	t-Lyp-1 (péptido CendR)	NRP1

Proteínas	Transferrina	Receptores transferrina
Vitaminas	Ácido fólico	Receptor folato

Tabla 2. Biomoléculas más usadas para el desarrollo de nanomedicamentos activamente dirigidos a células tumorales

Dada la conocida especificidad de la unión antígeno-anticuerpo, los anticuerpos han sido los primeros ligandos usados para transportar fármacos a tejidos tumorales. Algunos de los más conocidos son los anticuerpos Trastuzumab y Cetuximab, ambos utilizados en la funcionalización de liposomas que están actualmente en ensayos clínicos. Este es el caso del nanomedicamento Doxil® modificado con el anticuerpo Cetuximab, un antagonista del factor de crecimiento EGFR, que ha completado la fase I para el tratamiento de tumores sólidos en estados avanzados [55], o el MM-302, un liposoma con doxorubicina funcionalizado con el anticuerpo Trastuzumab para tumores HER2 positivos de cáncer de mama que también superó la fase I [56]. Pero hay muchos otros ejemplos del uso de estas biomoléculas para la funcionalización de nanopartículas y liposomas. Por ejemplo, las nanopartículas de ácido poliláctico pegilado modificadas con Cetuximab y Rituximab han mostrado un marcado incremento de su internalización en células HER2 positivas y CD20 positivas respectivamente [57]. Igualmente, se ha observado que los liposomas pegilados modificados con Trastuzumab han logrado aumentar su internalización a través de un receptor, presente en una línea celular HER2 positiva [58]. Además, cada vez es más común el uso de los fragmentos del anticuerpo con el epítopo responsable del reconocimiento selectivo, evitando así el uso de moléculas demasiado grandes que complican tanto la química como el desarrollo del nanosistema. Un ejemplo de esta estrategia lo encontramos en nanopartículas de ácido poliláctico pegilado modificadas con el fragmento de un anticuerpo dirigido a células HER2 positivas, que resultaron en un incremento notable en la internalización de las nanopartículas en este tipo celular [59]. A pesar de su alta selectividad, los anticuerpos no están exentos de inconvenientes, entre los que se encuentran sus propiedades inmunogénicas y su inestabilidad en disolventes, a menudo necesarios en la preparación de los nanosistemas.

Los aptámeros, oligonucleótidos como ADN o ARN de cadena sencilla, constituyen otro grupo de biomoléculas de gran interés en la funcionalización de nanosistemas. Al igual

que los anticuerpos, los aptámeros son altamente específicos y además presentan la ventaja de ser más estables. Por ejemplo, la funcionalización de las nanopartículas de ácido poliláctico-glicólico pegilado con el aptámero conocido como AS1411 [60] ha resultado en un aumento de la acumulación de dichas nanopartículas en las células tumorales en un modelo xenograft de glioma [61]. Cabe destacar el sistema de nanopartículas conocido como BIND-014, basadas en ácido poliláctico pegilado con docetaxel modificadas con un ácido nucleico denominado ACUPA, que ha logrado llegar a fase II para el tratamiento del cáncer de próstata [62].

Por último, los péptidos están ganando mucho interés para la formulación de nanosistemas dirigidos, debido a su estabilidad, baja inmunogenicidad y pequeño tamaño. Además, el desarrollo de librerías de péptidos haciendo uso de la técnica conocida como "phage display" ha posibilitado el descubrimiento de nuevos ligandos peptídicos con afinidad por diferentes tipos celulares [63].

Dentro de este grupo, destacan los péptidos denominados RGD. Este grupo de péptidos contiene una secuencia de aminoácidos arginina-glicina-aspartato, que presenta una afinidad por determinadas células tumorales y además es responsable de promover la penetración celular, facilitando así la difusión a través de la matriz tumoral [64, 65]. Hasta el momento, estos péptidos han sido utilizados para la funcionalización de nanopartículas de ácido poliláctico-pegilado y también de liposomas. En concreto, las nanopartículas de ácido poliláctico-pegilado cargadas con paclitaxel y modificadas con el péptido (c(RGDyK), mostraron un incremento de su biodistribución hacia el tumor, seguido de una mayor eficacia antitumoral y de un aumento en su supervivencia en un modelo xenograft de glioma [66]. De forma similar, los liposomas modificados con este tipo de péptidos, resultaron en un aumento del tiempo de supervivencia en dos modelos xenograft de melanoma [67, 68]. No obstante, a pesar de estas mejoras en la eficacia antitumoral, la aplicación de estas moléculas se ve limitada por la existencia de sus receptores ($\alpha_v B_3$) en otros tejidos y por su penetración inespecífica, aumentando la acumulación también en tejidos sanos [66].

Recientemente se ha descubierto un grupo de péptidos de especial interés en este campo, caracterizados por tener una secuencia de aminoácidos (R/K)XX(R/K) (donde R y K son arginina y lisina respectivamente y X es cualquier aminoácido), que además de

dotarles de una afinidad hacia receptores tumorales, es capaz de promover la penetración de una forma específica, que sólo se activa tras la unión al receptor. Es la denominada tecnología CendR, descubierta por *Sugahara y Tessalu* [69-71], empleada con éxito para modificar nanopartículas de Abraxane® con el péptido iRGD, demostrando una mayor penetración a través del estroma tumoral y una reducción significativa del volumen tumoral comparado con el producto comercial Abraxane® en un modelo tumoral ortotópico de próstata [69]. Dentro de este grupo, también son de especial interés los péptidos Lyp-1 y su forma lineal o truncada t-Lyp-1 por su alta selectividad hacia sus receptores sobreexpresados en tejidos tumorales y a nivel muy bajo en tejidos sanos [72-74]. El primero, Lyp-1, es un péptido cíclico que se ha usado para modificar nanopartículas de Abraxane® mejorando la penetración y reduciendo la carga tumoral en un modelo xenograft de cáncer de mama [75]. Posteriormente, *Roth et al* realizó un estudio comparativo con nanopartículas de óxido de hierro modificadas con Lyp-1 y t-Lyp-1, mostrando que la forma lineal t-Lyp-1 produce un marcado aumento de la difusión tumoral comparado con la forma cíclica del péptido Lyp-1 en un modelo ortotópico de cáncer de mama [76].

Además de los tres grandes grupos moleculares comentados anteriormente para la funcionalización de nanosistemas, también existen otro tipo de moléculas de distinta naturaleza, con una gran presencia en la preparación de sistemas de "targeting" activo. Entre ellos se encuentra la proteína transportadora de hierro denominada transferrina, [77, 78], la cual forma parte de una formulación de liposomas cargados de oxaliplatino que se encuentra en ensayos clínicos en fase I (MBP-426) para la indicación del tratamiento de cáncer gástrico [79]. También es destacable, el ácido fólico, una vitamina de pequeño tamaño que se ha usado para modificar liposomas y micelas demostrando una capacidad específica de unión a células tumorales [80, 81].

En general, el éxito de esta estrategia de orientación activa está condicionada por propiedades intrínsecas de estos ligandos, tales como su selectividad y afinidad hacia el receptor, pero también de otras características del nanosistema, como es la densidad de moléculas de ligando en la superficie. Sin embargo, además de la afinidad química de los sistemas funcionalizados, estos sistemas también están sujetos a fenómenos físicos como el EPR, que contribuye al acercamiento al área tumoral y por tanto todas las

características físico-químicas citadas en el apartado anterior, son también clave para el comportamiento *in vivo* de estos nanosistemas.

Finalmente queremos destacar la importante presencia del ácido hialurónico (HA) en el diseño de nanoterapéuticos antitumorales de vectorización activa, que se describe con detalle en el siguiente apartado.

3. El ácido hialurónico en el desarrollo de nano-quimioterapéuticos.

El ácido hialurónico es un polisacárido formado por la unión de ácido glucurónico y acetil glucosamina, que presenta cualidades físicas y biológicas que lo convierten en un biomaterial muy empleado en el desarrollo de nanomedicamentos. En primer lugar, el HA cumple con los requisitos de biodegradabilidad, no toxicidad y no inmunogenicidad necesarios para su uso farmacéutico [82]. Por otra parte, participa en numerosas funciones biológicas reguladas por su interacción con proteínas específicas. Entre sus receptores, el CD44 resulta muy interesante por estar sobreexpresado en una gran número de tumores [83-85], haciendo del HA una molécula muy atractiva para orientar moléculas terapéuticas a células cancerosas en una estrategia de vectorización activa.

Además de este perfil biológico, el HA posee características muy adecuadas para el desarrollo de nanosistemas. Su naturaleza endógena evita el problema del reconocimiento y captación por el sistema inmune propio de algunos anticuerpos y proteínas [86-88]. Su carácter altamente hidrofílico proporciona una repulsión estérica que puede evadir la opsonización, aumentando el tiempo de circulación en sangre de una manera similar al efecto logrado con la pegilación pero evitando la baja internalización celular que a menudo lleva asociado el PEG, tal y como lo muestran diferentes estudios [89-91]. A su vez, la carga negativa proporcionada por los grupos carboxilato del HA disminuye las interacciones celulares de tipo no específico, mejorando su selectividad hacia el tejido diana [21]. Por otra parte, la reactividad química de este polisacárido a través de estos grupos carboxilato [92-96] aporta un sustrato para la unión de otras moléculas posibilitando, por ejemplo, la preparación de derivados anfifílicos del HA para la preparación de micelas o facilitando la unión química del HA a liposomas con el fin de mejorar su afinidad a tejidos tumorales. Prueba de ello

es el gran número de trabajos que hacen uso del HA para el desarrollo de nanosistemas que se muestran en la Tabla 3. Sin embargo, a pesar de sus interesantes propiedades, el HA carece de la selectividad que sería deseable para conseguir una orientación activa efectiva. De hecho, parte de los trabajos que se encuentran en la literatura han descrito su acumulación preferente a nivel hepático [7, 90, 97, 98], atribuida en parte, a la interacción del HA con otro de sus receptores, HARE (hyaluronic acid receptor for endocitosis), localizado en el endotelio de hígado y bazo [83, 99].

Composición	Fármaco	Modelo tumoral estudiado	Referencias
Micelas HA - ácido colánico	Irinotecano Doxorubicina Camptotecina Paclitaxel	Xenograft cancer de mama, colon y carcinoma	[98, 100-108]
Micelas HA – ceramida	Docetaxel Doxorubicina	Xenograft cáncer de mama y carcinoma	[109-111]
Micelas HA - polibencil glutamato	Docetaxel	Xenograft tumor ascítico de Ehrlich	[112]
Micelas HA - polihistidina	Doxorubicina	Xenograft cáncer de mama	[113]
Micelas HA - ácido retinoico	Paclitaxel	Xenograft melanoma	[114]
Liposomas HA - derivado fosfolipídico	Doxorubicin Mitomicina C	Ortotópico y singénico cáncer de pulmón	[89, 90]
Liposomas HA adsorbido electrostáticamente	Paclitaxel	Xenograft carcinoma hepatocelular	[115]

Nanocápsulas HA y aceite de soja	Paclitaxel	Xenograft melanoma	[7]
Nanopartículas HA y quitosano	Doxorubicina	Xenograft cáncer de mama	[116]

Tabla 3. Nanosistemas de HA para dirigir agentes quimioterapéuticos a células tumorales.

Como podemos ver en esta tabla, los sistemas micelares son sin duda los más numerosos, debido seguramente, a la facilidad del HA para reaccionar con otras moléculas formando conjugados anfifílicos que se autoensamblan para formar estos sistemas. Dentro de este grupo, destaca el amplio trabajo con micelas de HA con la sal biliar ácido colánico [98, 100-108]. Estas micelas han sido probadas con diferentes fármacos demostrando una mayor acumulación tumoral mediada por interacciones con CD44, seguida de una reducción del volumen tumoral en diferentes modelos xenograft de cáncer de mama, de colón y carcinoma. También el sistema micelar formado por el conjugado HA-ceramida, un esfingolípido constituyente de la membrana celular, demostró en dos modelos xenograft de cáncer de mama y carcinoma mejorar la acumulación tumoral a través de uniones específicas con el receptor CD44 y un consiguiente aumento de la eficacia antitumoral [109-111].

Entre los liposomas, destaca el trabajo desarrollado con un sistema liposomal donde el HA se encuentra unido covalentemente a la bicapa fosfolipídica. Los cuáles han mostrado un elevado aumento de la acumulación de los fármacos doxorubicina y mitomicina C en el tejido tumoral y una mejora de la eficacia terapéutica en modelos clínicamente más relevantes (modelo ortotópico y modelo singénico) de cáncer de pulmón [89, 90].

Las nanopartículas constituyen un sistema menos explorado para el transporte de antitumorales. Dentro de este grupo encontramos dos sistemas de HA en combinación con quitosano como contraión para la preparación de nanopartículas. Estos sistemas mostraron un aumento de la internalización celular [116, 117] y una mejora de la eficacia en un modelo xenograft de cáncer de mama [116].

Finalmente, las nanocápsulas de HA representan una tecnología más reciente. Este sistema está formado por un núcleo oleoso que resulta muy conveniente para la asociación de fármacos antitumorales hidrofóbicos. De hecho, diferentes prototipos nanocapsulares desarrollados en este grupo con una cubierta polimérica de ácido hialurónico, ácido poliglutámico, quitosano o poliasparagina han conseguido asociar eficazmente este tipo de moléculas [118-121]. Hasta la fecha no se han reportado muchos resultados *in vivo* con este tipo de nanosistemas, como ejemplo encontramos un sistema nanocapsular de HA para el transporte de paclitaxel que logró incrementar la dosis de fármaco en tumor y reducir el volumen tumoral en un modelo xenograft de melanoma [7].

A continuación (Capítulo 1) se realiza una descripción más detallada del perfil biológico del HA y sus aplicaciones biomédicas más importantes, haciendo énfasis en la aportación del HA al desarrollo de nanoterapias antitumorales.

4. Conclusiones

Globalmente, los sistemas de "targeting" activo han demostrado mejoras en relación con otros tratamientos nano-oncológicos ya comercializados, como es el caso del Abraxane® o del Doxil®. Estos nuevos prototipos, desarrollados con biomateriales activos, permiten interaccionar específicamente con las células tumorales, consiguiendo un aumento considerable de la acumulación del fármaco en el tejido diana, así como de la internalización celular a través de este reconocimiento específico con receptores tumorales, con su consiguiente beneficio terapéutico. Entre las diferentes opciones de materiales activos, es particularmente interesante el ácido hialurónico, un polisacárido natural que constituye en sí mismo un polímero con características físico-químicas adecuadas para la preparación de nanosistemas. Por otra parte, el avance en el conocimiento de la fisiología tumoral permite el desarrollo de nuevas moléculas multifuncionales, cada vez más adaptadas a las necesidades terapéuticas. Es el caso de los péptidos CendR, que además de mejorar la selectividad hacia las células diana promueven la penetración a través del estroma tumoral, superando así uno de los grandes obstáculos a la eficacia terapéutica.

Referencias

1. Crown, J., M. O'Leary, and W.-S. Ooi, *Docetaxel and Paclitaxel in the Treatment of Breast Cancer: A Review of Clinical Experience.* The Oncologist, 2004. **9**(suppl 2): p. 24-32.
2. van Zuylen, L., J. Verweij, and A. Sparreboom, *Role of Formulation Vehicles in Taxane Pharmacology.* Investigational New Drugs, 2001. **19**(2): p. 125-141.
3. de Weger, V.A., J.H. Beijnen, and J.H.M. Schellens, *Cellular and clinical pharmacology of the taxanes docetaxel and paclitaxel – a review.* Anti-Cancer Drugs, 2014. **25**(5): p. 488-494.
4. Chu, Q., et al., *Taxanes as first-line therapy for advanced non-small cell lung cancer: A systematic review and practice guideline.* Lung Cancer, 2005. **50**(3): p. 355-374.
5. Maeda, H., G.Y. Bharate, and J. Daruwalla, *Polymeric drugs for efficient tumor-targeted drug delivery based on EPR-effect.* European Journal of Pharmaceutics and Biopharmaceutics, 2009. **71**(3): p. 409-419.
6. Maeda, H., *Toward a full understanding of the EPR effect in primary and metastatic tumors as well as issues related to its heterogeneity.* Advanced Drug Delivery Reviews, (0).
7. Yang, X.-y., et al., *Hyaluronic acid-coated nanostructured lipid carriers for targeting paclitaxel to cancer.* Cancer Letters, 2013. **334**(2): p. 338-345.
8. Chen, D.-B., et al., *In Vitro and in Vivo Study of Two Types of Long-Circulating Solid Lipid Nanoparticles Containing Paclitaxel.* Chemical and Pharmaceutical Bulletin, 2001. **49**(11): p. 1444-1447.
9. Yang, T., et al., *Enhanced solubility and stability of PEGylated liposomal paclitaxel: In vitro and in vivo evaluation.* International Journal of Pharmaceutics, 2007. **338**(1–2): p. 317-326.
10. Ernsting, M.J., et al., *Preclinical pharmacokinetic, biodistribution, and anti-cancer efficacy studies of a docetaxel-carboxymethylcellulose nanoparticle in mouse models.* Biomaterials, 2012. **33**(5): p. 1445-1454.
11. Jiang, X., et al., *PEGylated poly(trimethylene carbonate) nanoparticles loaded with paclitaxel for the treatment of advanced glioma: In vitro and in vivo evaluation.* International Journal of Pharmaceutics, 2011. **420**(2): p. 385-394.
12. Lollo, G., et al., *Enhanced in vivo therapeutic efficacy of plitidepsin-loaded nanocapsules decorated with a new poly-aminoacid-PEG derivative.* International Journal of Pharmaceutics, 2015. **483**(1–2): p. 212-219.
13. Rivera-Rodriguez, G.R., et al., *In vivo evaluation of poly-l-asparagine nanocapsules as carriers for anti-cancer drug delivery.* International Journal of Pharmaceutics, 2013. **458**(1): p. 83-89.
14. Tadros, T., et al., *Formation and stability of nano-emulsions.* Advances in Colloid and Interface Science, 2004. **108–109**(0): p. 303-318.
15. Vonarbourg, A., et al., *Parameters influencing the stealthiness of colloidal drug delivery systems.* Biomaterials, 2006. **27**(24): p. 4356-4373.
16. Dufort, S., L. Sancey, and J.-L. Coll, *Physico-chemical parameters that govern nanoparticles fate also dictate rules for their molecular evolution.* Advanced Drug Delivery Reviews, 2012. **64**(2): p. 179-189.
17. Lux, F., et al., *Ultrasmall Rigid Particles as Multimodal Probes for Medical Applications.* Angewandte Chemie International Edition, 2011. **50**(51): p. 12299-12303.
18. Park, J.-H., et al., *Magnetic Iron Oxide Nanoworms for Tumor Targeting and Imaging.* Advanced Materials, 2008. **20**(9): p. 1630-1635.
19. Faraji, A.H. and P. Wipf, *Nanoparticles in cellular drug delivery.* Bioorganic & Medicinal Chemistry, 2009. **17**(8): p. 2950-2962.

20. Santander-Ortega, M.J., et al., *Hydration forces as a tool for the optimization of core-shell nanoparticle vectors for cancer gene therapy.* Soft Matter, 2012. **8**(48): p. 12080-12092.
21. Alexis, F., et al., *Factors Affecting the Clearance and Biodistribution of Polymeric Nanoparticles.* Molecular pharmaceutics, 2008. **5**(4): p. 505-515.
22. Verma A, S.F., *Effect of surface properties on nanoparticle-cell interactions.* Small, 2010. **6**(1): p. 12-21.
23. Hamaguchi, T., et al., *A phase I and pharmacokinetic study of NK105, a paclitaxel-incorporating micellar nanoparticle formulation.* British Journal of Cancer, 2007. **97**(2): p. 170-176.
24. Matsumura, Y., *Preclinical and clinical studies of NK012, an SN-38-incorporating polymeric micelles, which is designed based on EPR effect.* Advanced Drug Delivery Reviews, 2011. **63**(3): p. 184-192.
25. Wilson, R.H., et al., *Phase I and pharmacokinetic study of NC-6004, a new platinum entity of cisplatin-conjugated polymer forming micelles.* J Clin Oncol (Meeting Abstracts), 2008. **26**(15_suppl): p. 2573-.
26. Lee, S.-W., et al., *Development of docetaxel-loaded intravenous formulation, Nanoxel-PM™ using polymer-based delivery system.* Journal of Controlled Release, 2011. **155**(2): p. 262-271.
27. Gaucher, G., et al., *Block copolymer micelles: preparation, characterization and application in drug delivery.* Journal of Controlled Release, 2005. **109**(1–3): p. 169-188.
28. Lu, Y. and K. Park, *Polymeric micelles and alternative nanonized delivery vehicles for poorly soluble drugs.* International Journal of Pharmaceutics, 2013. **453**(1): p. 198-214.
29. Barenholz, Y., *Doxil® — The first FDA-approved nano-drug: Lessons learned.* Journal of Controlled Release, 2012. **160**(2): p. 117-134.
30. Batist, G., et al., *Reduced Cardiotoxicity and Preserved Antitumor Efficacy of Liposome-Encapsulated Doxorubicin and Cyclophosphamide Compared With Conventional Doxorubicin and Cyclophosphamide in a Randomized, Multicenter Trial of Metastatic Breast Cancer.* Journal of Clinical Oncology, 2001. **19**(5): p. 1444-1454.
31. Rivera, E., *Liposomal Anthracyclines in Metastatic Breast Cancer: Clinical Update.* The Oncologist, 2003. **8**(suppl 2): p. 3-9.
32. Silverman, J.A. and S.R. Deitcher, *Marqibo(®) (vincristine sulfate liposome injection) improves the pharmacokinetics and pharmacodynamics of vincristine.* Cancer Chemotherapy and Pharmacology, 2013. **71**(3): p. 555-564.
33. Hu, L., et al., *Assessing the effectiveness and safety of liposomal paclitaxel in combination with cisplatin as first-line chemotherapy for patients with advanced NSCLC with regional lymph-node metastasis: study protocol for a randomized controlled trial (PLC-GC trial).* Trials, 2013. **14**: p. 45-45.
34. Angst, M. and D. Drover, *Pharmacology of Drugs Formulated with DepoFoam™.* Clinical Pharmacokinetics, 2006. **45**(12): p. 1153-1176.
35. Du, H., et al., *Novel Tetrapeptide, RGDF, Mediated Tumor Specific Liposomal Doxorubicin (DOX) Preparations.* Molecular Pharmaceutics, 2011. **8**(4): p. 1224-1232.
36. Nasongkla, N., et al., *cRGD-Functionalized Polymer Micelles for Targeted Doxorubicin Delivery.* Angewandte Chemie International Edition, 2004. **43**(46): p. 6323-6327.
37. Deeken, J., et al., *A phase I study of liposomal-encapsulated docetaxel (LE-DT) in patients with advanced solid tumor malignancies.* Cancer Chemotherapy and Pharmacology, 2013. **71**(3): p. 627-633.
38. Mahalingam, D., et al., *Phase I study of intravenously administered ATI-1123, a liposomal docetaxel formulation in patients with advanced solid tumors.* Cancer Chemotherapy and Pharmacology, 2014. **74**(6): p. 1241-1250.
39. Desai, N., et al., *Increased antitumor activity, intratumor paclitaxel concentrations, and endothelial cell transport of cremophor-free, albumin-bound paclitaxel, ABI-007,*

compared with cremophor-based paclitaxel. Clinical Cancer Research, 2006. **12**(4): p. 1317-1324.

40. Gonzalez-Angulo, A.M., et al., *Weekly nab-Rapamycin in Patients with Advanced Nonhematologic Malignancies: Final Results of a Phase I Trial.* Clinical Cancer Research, 2013. **19**(19): p. 5474-5484.
41. *Efficacy and Safety Doxorubicin Transdrug Study in Patients Suffering From Advanced Hepatocellular Carcinoma (ReLive).* Clinicaltrials.gov. **https://clinicaltrials.gov/ct2/show/NCT01655693?term=doxorubicin+Transdrug&rank=1**.
42. *Phase 1/2a Dose-Escalation Study of CRLX301 in Patients With Advanced Solid Tumors.* clinicaltrials.gov. **https://clinicaltrials.gov/ct2/show/NCT02380677**.
43. Svenson, S., *Clinical translation of nanomedicines.* Current Opinion in Solid State and Materials Science, 2012. **16**(6): p. 287-294.
44. Fan, Y. and Q. Zhang, *Development of liposomal formulations: From concept to clinical investigations.* Asian Journal of Pharmaceutical Sciences, 2013. **8**(2): p. 81-87.
45. Sriraman, S.K. and V.P. Torchilin, *Recent Advances with Liposomes as Drug Carriers*, in *Advanced Biomaterials and Biodevices*2014, John Wiley & Sons, Inc. p. 79-119.
46. Hofheinz, R.-D., et al., *Liposomal encapsulated anti-cancer drugs.* Anti-Cancer Drugs, 2005. **16**(7): p. 691-707.
47. Swain, S.M., F.S. Whaley, and M.S. Ewer, *Congestive heart failure in patients treated with doxorubicin.* Cancer, 2003. **97**(11): p. 2869-2879.
48. Grantab, R., S. Sivananthan, and I.F. Tannock, *The Penetration of Anticancer Drugs through Tumor Tissue as a Function of Cellular Adhesion and Packing Density of Tumor Cells.* Cancer Research, 2006. **66**(2): p. 1033-1039.
49. Netti, P.A., et al., *Role of Extracellular Matrix Assembly in Interstitial Transport in Solid Tumors.* Cancer Research, 2000. **60**(9): p. 2497-2503.
50. Heldin, C.-H., et al., *High interstitial fluid pressure [mdash] an obstacle in cancer therapy.* Nat Rev Cancer, 2004. **4**(10): p. 806-813.
51. Jain, R.K., *Delivery of molecular and cellular medicine to solid tumors1.* Advanced Drug Delivery Reviews, 2001. **46**(1–3): p. 149-168.
52. Thiele, W. and J.P. Sleeman, *Tumor-induced lymphangiogenesis: A target for cancer therapy?* Journal of Biotechnology, 2006. **124**(1): p. 224-241.
53. Joyce, J.A. and J.W. Pollard, *Microenvironmental regulation of metastasis.* Nat Rev Cancer, 2009. **9**(4): p. 239-252.
54. Weaver, D.L., et al., *Pathologic analysis of sentinel and nonsentinel lymph nodes in breast carcinoma.* Cancer, 2000. **88**(5): p. 1099-1107.
55. Mamot, C., et al., *Tolerability, safety, pharmacokinetics, and efficacy of doxorubicin-loaded anti-EGFR immunoliposomes in advanced solid tumours: a phase 1 dose-escalation study.* The Lancet Oncology, 2012. **13**(12): p. 1234-1241.
56. McDonagh, C.F., et al., *Antitumor Activity of a Novel Bispecific Antibody That Targets the ErbB2/ErbB3 Oncogenic Unit and Inhibits Heregulin-Induced Activation of ErbB3.* Molecular Cancer Therapeutics, 2012. **11**(3): p. 582-593.
57. Nobs, L., et al., *Biodegradable Nanoparticles for Direct or Two-Step Tumor Immunotargeting.* Bioconjugate Chemistry, 2006. **17**(1): p. 139-145.
58. Yang, T., et al., *Preparation and evaluation of paclitaxel-loaded PEGylated immunoliposome.* Journal of Controlled Release, 2007. **120**(3): p. 169-177.
59. Alexis, F., et al., *HER-2-Targeted Nanoparticle–Affibody Bioconjugates for Cancer Therapy.* ChemMedChem, 2008. **3**(12): p. 1839-1843.
60. Soundararajan, S., et al., *The Nucleolin Targeting Aptamer AS1411 Destabilizes Bcl-2 Messenger RNA in Human Breast Cancer Cells.* Cancer Research, 2008. **68**(7): p. 2358-2365.

61. Guo, J., et al., *Aptamer-functionalized PEG–PLGA nanoparticles for enhanced anti-glioma drug delivery.* Biomaterials, 2011. **32**(31): p. 8010-8020.
62. www.bindbio.com.
63. Ladner, R.C., et al., *Phage display-derived peptides as therapeutic alternatives to antibodies.* Drug Discovery Today, 2004. **9**(12): p. 525-529.
64. Desgrosellier, J.S. and D.A. Cheresh, *Integrins in cancer: biological implications and therapeutic opportunities.* Nature reviews. Cancer, 2010. **10**(1): p. 9-22.
65. Ruoslahti, E., *RGD AND OTHER RECOGNITION SEQUENCES FOR INTEGRINS.* Annual Review of Cell and Developmental Biology, 1996. **12**(1): p. 697-715.
66. Zhan, C., et al., *Cyclic RGD conjugated poly(ethylene glycol)-co-poly(lactic acid) micelle enhances paclitaxel anti-glioblastoma effect.* Journal of Controlled Release, 2010. **143**(1): p. 136-142.
67. Xiong, X.-B., et al., *Enhanced intracellular delivery and improved antitumor efficacy of doxorubicin by sterically stabilized liposomes modified with a synthetic RGD mimetic.* Journal of Controlled Release, 2005. **107**(2): p. 262-275.
68. Dubey, P.K., et al., *Liposomes Modified with Cyclic RGD Peptide for Tumor Targeting.* Journal of Drug Targeting, 2004. **12**(5): p. 257-264.
69. Sugahara, K.N., et al., *Tissue-Penetrating Delivery of Compounds and Nanoparticles into Tumors.* Cancer Cell, 2009. **16**(6): p. 510-520.
70. Sugahara, K.N., et al., *Coadministration of a Tumor-Penetrating Peptide Enhances the Efficacy of Cancer Drugs.* Science, 2010. **328**(5981): p. 1031-1035.
71. Teesalu, T., et al., *C-end rule peptides mediate neuropilin-1-dependent cell, vascular, and tissue penetration.* Proceedings of the National Academy of Sciences, 2009. **106**(38): p. 16157-16162.
72. Ellis, L.M., *The role of neuropilins in cancer.* Molecular Cancer Therapeutics, 2006. **5**(5): p. 1099-1107.
73. Guttmann-Raviv, N., et al., *The neuropilins and their role in tumorigenesis and tumor progression.* Cancer Letters, 2006. **231**(1): p. 1-11.
74. Bagri, A., M. Tessier-Lavigne, and R.J. Watts, *Neuropilins in Tumor Biology.* Clinical Cancer Research, 2009. **15**(6): p. 1860-1864.
75. Karmali, P.P., et al., *Targeting of albumin-embedded paclitaxel nanoparticles to tumors.* Nanomedicine: Nanotechnology, Biology and Medicine. **5**(1): p. 73-82.
76. Roth, L., et al., *Transtumoral targeting enabled by a novel neuropilin-binding peptide.* Oncogene, 2012. **31**(33): p. 3754-3763.
77. Kim, K., et al., *Tumor-homing multifunctional nanoparticles for cancer theragnosis: Simultaneous diagnosis, drug delivery, and therapeutic monitoring.* Journal of Controlled Release, 2010. **146**(2): p. 219-227.
78. Sahoo, S.K., W. Ma, and V. Labhasetwar, *Efficacy of transferrin-conjugated paclitaxel-loaded nanoparticles in a murine model of prostate cancer.* International Journal of Cancer, 2004. **112**(2): p. 335-340.
79. Suzuki, R., et al., *Effective anti-tumor activity of oxaliplatin encapsulated in transferrin–PEG-liposome.* International Journal of Pharmaceutics, 2008. **346**(1–2): p. 143-150.
80. Yoo, H.S. and T.G. Park, *Folate receptor targeted biodegradable polymeric doxorubicin micelles.* Journal of Controlled Release, 2004. **96**(2): p. 273-283.
81. Lee, R.J. and P.S. Low, *Folate-mediated tumor cell targeting of liposome-entrapped doxorubicin in vitro.* Biochimica et Biophysica Acta (BBA) - Biomembranes, 1995. **1233**(2): p. 134-144.
82. Teijeiro, C., et al., *Polysaccharide-Based Nanocarriers for Drug Delivery*, in *Handbook of Nanobiomedical Research*. p. 235-277.
83. Harada, H. and M. Takahashi, *CD44-dependent Intracellular and Extracellular Catabolism of Hyaluronic Acid by Hyaluronidase-1 and -2.* Journal of Biological Chemistry, 2007. **282**(8): p. 5597-5607.

84. Lesley, J., R. Hyman, and P.W. Kincade, *CD44 and Its Interaction with Extracellular Matrix*, in *Advances in Immunology*, J.D. Frank, Editor 1993, Academic Press. p. 271-335.
85. Knudson, C.B., *Hyaluronan and CD44: Strategic players for cell–matrix interactions during chondrogenesis and matrix assembly.* Birth Defects Research Part C: Embryo Today: Reviews, 2003. **69**(2): p. 174-196.
86. Park, J.W., et al., *Tumor targeting using anti-her2 immunoliposomes.* Journal of Controlled Release, 2001. **74**(1–3): p. 95-113.
87. Harding, J.A., et al., *Immunogenicity and pharmacokinetic attributes of poly(ethylene glycol)-grafted immunoliposomes.* Biochimica et Biophysica Acta (BBA) - Biomembranes, 1997. **1327**(2): p. 181-192.
88. Benhar, I., et al., *Rapid humanization of the Fv of monoclonal antibody B3 by using framework exchange of the recombinant immunotoxin B3(Fv)-PE38.* Proceedings of the National Academy of Sciences of the United States of America, 1994. **91**(25): p. 12051-12055.
89. Peer, D. and R. Margalit, *Loading mitomycin C inside long circulating hyaluronan targeted nano-liposomes increases its antitumor activity in three mice tumor models.* International Journal of Cancer, 2004. **108**(5): p. 780-789.
90. Peer, D., Margalit, R., *Tumor-Targeted Hyaluronan Nanoliposomes Increase the Antitumor Activity of Liposomal Doxorubicin in Syngeneic and Human Xenograft Mouse Tumor Models.* Neoplasia, 2004. **6**(4): p. 343-353.
91. Dan, P., et al., *Nanocarriers as an emerging platform for cancer therapy.* Nature Nanotechnology, 2007. **2**(12): p. 751-760.
92. Luo, Y., M.R. Ziebell, and G.D. Prestwich, *A Hyaluronic Acid−Taxol Antitumor Bioconjugate Targeted to Cancer Cells.* Biomacromolecules, 2000. **1**(2): p. 208-218.
93. Luo, Y. and G.D. Prestwich, *Synthesis and Selective Cytotoxicity of a Hyaluronic Acid−Antitumor Bioconjugate.* Bioconjugate Chemistry, 1999. **10**(5): p. 755-763.
94. Auzenne, E., et al., *Hyaluronic Acid-Paclitaxel: Antitumor Efficacy against CD44(+) Human Ovarian Carcinoma Xenografts.* Neoplasia (New York, N.Y.), 2007. **9**(6): p. 479-486.
95. Rosato, A., et al., *HYTAD1-p20: A new paclitaxel-hyaluronic acid hydrosoluble bioconjugate for treatment of superficial bladder cancer.* Urologic Oncology: Seminars and Original Investigations, 2006. **24**(3): p. 207-215.
96. Platt, V.M. and F.C. Szoka, *Anticancer Therapeutics: Targeting Macromolecules and Nanocarriers to Hyaluronan or CD44, a Hyaluronan Receptor.* Molecular Pharmaceutics, 2008. **5**(4): p. 474-486.
97. Rivkin, I., et al., *Paclitaxel-clusters coated with hyaluronan as selective tumor-targeted nanovectors.* Biomaterials, 2010. **31**(27): p. 7106-7114.
98. Choi, K.Y., et al., *Self-assembled hyaluronic acid nanoparticles as a potential drug carrier for cancer therapy: synthesis, characterization, and in vivo biodistribution.* Journal of Materials Chemistry, 2009. **19**(24): p. 4102-4107.
99. Zhou, B., et al., *Identification of the Hyaluronan Receptor for Endocytosis (HARE).* Journal of Biological Chemistry, 2000. **275**(48): p. 37733-37741.
100. Lee, D.-E., et al., *Amphiphilic hyaluronic acid-based nanoparticles for tumor-specific optical/MR dual imaging.* Journal of Materials Chemistry, 2012. **22**(21): p. 10444-10447.
101. Choi, K.Y., et al., *Self-assembled hyaluronic acid nanoparticles for active tumor targeting.* Biomaterials, 2010. **31**(1): p. 106-114.
102. Choi, K.Y., et al., *Theranostic nanoparticles based on PEGylated hyaluronic acid for the diagnosis, therapy and monitoring of colon cancer.* Biomaterials, 2012. **33**(26): p. 6186-6193.
103. Yoon, H.Y., et al., *Tumor-targeting hyaluronic acid nanoparticles for photodynamic imaging and therapy.* Biomaterials, 2012. **33**(15): p. 3980-3989.

104. Choi, K.Y., et al., *PEGylation of hyaluronic acid nanoparticles improves tumor targetability in vivo.* Biomaterials, 2011. **32**(7): p. 1880-1889.
105. Choi, K.Y., et al., *Smart Nanocarrier Based on PEGylated Hyaluronic Acid for Cancer Therapy.* ACS Nano, 2011. **5**(11): p. 8591-8599.
106. Yoon, H.Y., et al., *Photo-crosslinked hyaluronic acid nanoparticles with improved stability for in vivo tumor-targeted drug delivery.* Biomaterials, 2013. **34**(21): p. 5273-5280.
107. Han, H.S., et al., *Robust PEGylated hyaluronic acid nanoparticles as the carrier of doxorubicin: Mineralization and its effect on tumor targetability in vivo.* Journal of Controlled Release, 2013. **168**(2): p. 105-114.
108. Han, S.-Y., et al., *Mineralized hyaluronic acid nanoparticles as a robust drug carrier.* Journal of Materials Chemistry, 2011. **21**(22): p. 7996-8001.
109. Cho, H.-J., et al., *Self-assembled nanoparticles based on hyaluronic acid-ceramide (HA-CE) and Pluronic® for tumor-targeted delivery of docetaxel.* Biomaterials, 2011. **32**(29): p. 7181-7190.
110. Cho, H.-J., et al., *Polyethylene glycol-conjugated hyaluronic acid-ceramide self-assembled nanoparticles for targeted delivery of doxorubicin.* Biomaterials, 2012. **33**(4): p. 1190-1200.
111. Park, J.-H., et al., *Development of poly(lactic-co-glycolic) acid nanoparticles-embedded hyaluronic acid–ceramide-based nanostructure for tumor-targeted drug delivery.* International Journal of Pharmaceutics, 2014. **473**(1–2): p. 426-433.
112. Upadhyay, K.K., et al., *In vitro and In vivo Evaluation of Docetaxel Loaded Biodegradable Polymersomes.* Macromolecular Bioscience, 2010. **10**(5): p. 503-512.
113. Qiu, L., et al., *Enhanced effect of pH-sensitive mixed copolymer micelles for overcoming multidrug resistance of doxorubicin.* Biomaterials, 2014. **35**(37): p. 9877-9887.
114. Yao, J., et al., *Efficient Simultaneous Tumor Targeting Delivery of All-Trans Retinoid Acid and Paclitaxel Based on Hyaluronic Acid-Based Multifunctional Nanocarrier.* Molecular Pharmaceutics, 2013. **10**(3): p. 1080-1091.
115. Jiang, T., et al., *Dual-functional liposomes based on pH-responsive cell-penetrating peptide and hyaluronic acid for tumor-targeted anticancer drug delivery.* Biomaterials, 2012. **33**(36): p. 9246-9258.
116. Deng, X., et al., *Hyaluronic acid-chitosan nanoparticles for co-delivery of MiR-34a and doxorubicin in therapy against triple negative breast cancer.* Biomaterials, 2014. **35**(14): p. 4333-4344.
117. Li, J., et al., *Tumor targeting and pH-responsive polyelectrolyte complex nanoparticles based on hyaluronic acid-paclitaxel conjugates and Chitosan for oral delivery of paclitaxel.* Macromolecular Research, 2013. **21**(12): p. 1331-1337.
118. Lozano, M.V., et al., *Intracellular delivery of docetaxel using freeze-dried polysaccharide nanocapsules.* Journal of Microencapsulation, 2012. **30**(2): p. 181-188.
119. Rivera-Rodríguez, G.R., M.J. Alonso, and D. Torres, *Poly-l-asparagine nanocapsules as anticancer drug delivery vehicles.* European Journal of Pharmaceutics and Biopharmaceutics, 2013. **85**(3, Part A): p. 481-487.
120. Lollo, G., et al., *Polyglutamic acid–PEG nanocapsules as long circulating carriers for the delivery of docetaxel.* European Journal of Pharmaceutics and Biopharmaceutics, 2014. **87**(1): p. 47-54.
121. Oyarzun-Ampuero, F.A., et al., *Hyaluronan nanocapsules as a new vehicle for intracellular drug delivery.* European Journal of Pharmaceutical Sciences, 2013. **49**(4): p. 483-490.

Capítulo 1

Polysaccharide-based nanocarriers for drug delivery

USC
UNIVERSIDADE
DE SANTIAGO
DE COMPOSTELA

Polysaccharide-based nanocarriers for drug delivery

Adaptado de "*Polysaccharide-Based Nanocarriers for Drug Delivery*". Carmen Teijeiro, Adam McGlone, Noemi Csaba, Marcos Garcia-Fuentes and María J Alonso. Handbook of Nanobiomedical Research. p. 235-277.

CIMUS Research Center. Faculty of Pharmacy. University of Santiago de Compostela (USC). Santiago de Compostela. Spain

USC
UNIVERSIDADE
DE SANTIAGO
DE COMPOSTELA

1. Introduction

Polysaccharides are complex carbohydrate molecules typically composed of mono- or disaccharide units linked by glycosidic bonds, which allows their structural organization into either linear or highly branched homo- or heteropolysaccharides. These naturally occurring biopolymers represent a large family of structurally and functionally different molecules many of them playing critical roles in plant, animal and human physiology.

Due to their high diversity and abundance in nature, polysaccharides have been applied for several hundred years as traditional pharmaceutical excipients (e.g. stabilizers, lubricants, coagulants etc). In addition, over the past decades polysaccharides have also been implemented in biomedical research as biomaterials for advanced drug delivery applications and tissue engineering.

Within this context, polysaccharides of interest are typically biodegradable, biocompatible, and preferentially water soluble. In addition, they also display additional characteristics such as specific mechanical-rheological properties and/or ease of chemical transformations, which can further expand the possibility of their application as biomaterials in diverse drug delivery strategies. Most relevant examples of natural polysaccharides exhibiting these features are:

Table 1. Relevant examples of polysaccharides as biomaterials and their main characteristics

Name	Origin	Composition	Structure	Charge
Alginate	Algae	Mannuronate Guluronate	Linear	Negative
Dextran	Plant	Glucose	Branched	Neutral
Hyaluronic acid	Animal	Glucuronic acid N-acetyl-	Linear	Negative
Chitosan	Animal - semisynthetic	Glucosamine N-acetyl glucosamine	Linear	Positive

As reflected by the steadily increasing number of scientific reports (Figure 1), over the past ten years these biomaterials have been extensively studied for biomedical applications in many different forms. These include the formulation of films, hydrogels, beads, or micro- and nanostructured carriers, alone or in combination with other polymeric or lipidic materials (1-3). Within the specific field of nanomedicine and nanocarrier mediated drug delivery, chitosan (CS) and hyaluronic acid (HA) are two polysaccharides that have emerged as the most prominent candidates. At first glance, CS and HA may seem very different: CS is produced by deacetylation of chitin, a polysaccharide obtained from crustacean shells, and is polycationic in nature. On the other hand, HA is a polyanionic biomacromolecule widely distributed in the human body as part of the extracellular matrix.

They both, however, share a few common features that explain their extraordinary success in biomedical research. Both materials are hydrophilic, structurally flexible affording possible interaction with other molecules through various types of non-covalent interactions. Another important characteristic is their high gelling capacity, which further expands the possibilities of their formulation as biomaterials for drug delivery. In addition, CS and HA are highly functional biomacromolecules due to their capacity to interact with the biological environment. These properties, together with their biocompatibility and biodegradability, have rendered these two polysaccharides very attractive for a number of different drug delivery strategies such as transmucosal drug delivery, gene therapy and anticancer therapy, among others. Within this chapter we present an updated review of their biological and toxicological profile, followed by the current biomedical applications and future potential of CS and HA as functional materials in nanomedicine.

Figure 1. Evolution of the number of scientific reports on the application of polysaccharides for drug delivery and tissue engineering; legend: (∗) chitosan, (+) hyaluronic acid, (♦) alginate, (▲) dextran

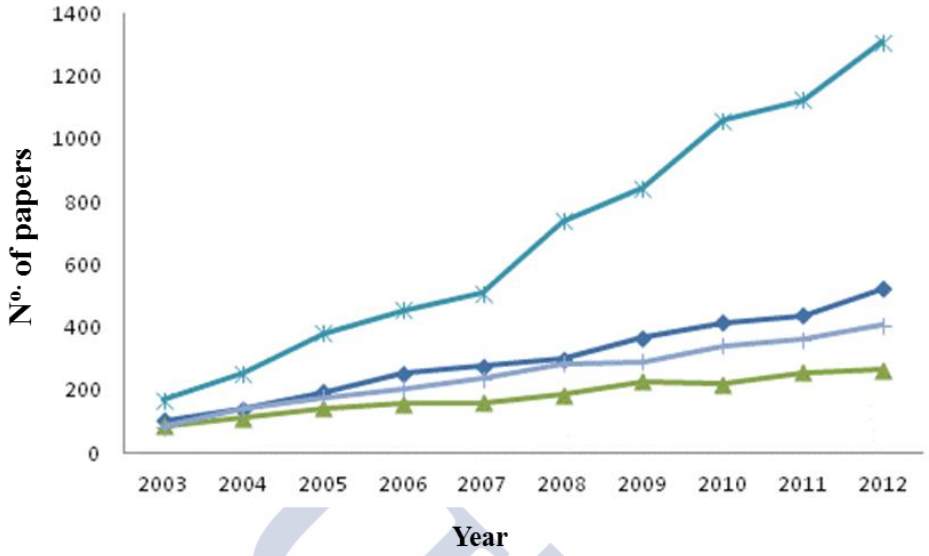

2. Biopharmaceutical and toxicological profile

2.1 Chitosan

Chitosan (CS), derived from deacytalation of chitin, is a copolymer of β-(1-4)-linked D-glucosamine and N-acetyl-D-glucosamine linked through glycosidic bonds. It has basic amine groups with a pK_a around 6.5, which results in various pH-dependent behaviours regarding solubility and polymer conformation. In addition to the protonation of its amines, the amount of acetylated monomers in CS and their distribution throughout the polymer backbone can also affect its solubility and properties in aqueous media. CS can partake in both electrostatic and hydrogen bonding interactions with other entities and molecules, and this is taken advantage for the formation of CS nanocarriers (4, 5).

Not only are these molecular features of interest in the formation of CS-based supramolecular assemblies, they are also critical features by which CS interacts with biological membranes. For example, CS is able to open epithelial tight junctions, an important action for their drug absorption promoting properties. Recent studies in the in vitro Caco-2 cell model have shown that this opening of cell junctions is related to CS electrostatic interaction with integrin-αV-β3, which in turn induces surface clustering of

integrin and reorganization of F(actin) (6, 7). However, this could be just one of the transport enhancing mechanisms for CS. In fact, TEER based studies suggest that there may also exist a degree of transcellular transport for molecules in the presence of CS (8).

In addition to its permeation properties, CS is considered a mucoadhesive polymer. This is due to its ability to interact with the negatively charged mucin strands via electrostatic and hydrogen bonding interactions. Most delivery routes, including ocular, nasal and oral are protected by mucus, and thus the interest in building drug delivery systems around CS becomes obvious (3).

This interest in CS as a pharmaceutical excipient and dietary supplement has led to a number of toxicological studies. CS toxicity in various cell models has been characterized by IC_{50} values between 0.2 to 2 $mg.mL^{-1}$, depending on the specific cell type, but also on CS deacetylation and molecular weight (3, 9, 10). In vivo toxicity values have been determined for several administration routes: toxic levels upon sub-cutaneous administration into rabbits and dogs were in the 5 – 50 $mg.kg^{-1}.day^{-1}$ range; oral toxicity in rats was estimated at 1 – 15 $g.kg^{-1}.day^{-1}$ (11-13). This *in vivo* data seems to translate to humans where oral doses of 6.75 $g.day^{-1}$ have been administered without adverse effects.

Various enzymes present in human mucosas and other physiological fluids participate in CS biodegradation: lysozyme, di-N-acetylchitobiase, chitiotriosidase and N-acetyl-β-D-glucosaminidase (9, 10, 14, 15). While CS is not currently listed as an excipient in any FDA approved formulations, it is included in the FDA GRAS list. CS is also used as a dietary supplement to reduce fat adsorption and has been used in wound dressings (16), indicating that a good understanding of its topical and oral tolerance exists.

The above toxicological data were obtained from CS in solution or in bulk form, which although indicative, cannot be reliably extrapolated to colloidal forms of CS. However, some studies have shown similar cytotoxicity in cell cultures with CS nanocarriers as with CS solutions (17, 18). These results suggest that the safety profile of CS in colloidal form may not be radically different from that of CS solutions.

The described properties have led to intensive study of CS as a biomaterial in a wide range of applications. In this chapter, however, we focus on CS drug nanocarriers, their preparation, and their promise in a range of applications: the transmucosal delivery of biological macromolecules such as DNA, antigens and peptides.

Figure 2: Chemical structure of chitosan and hyaluronic acid.

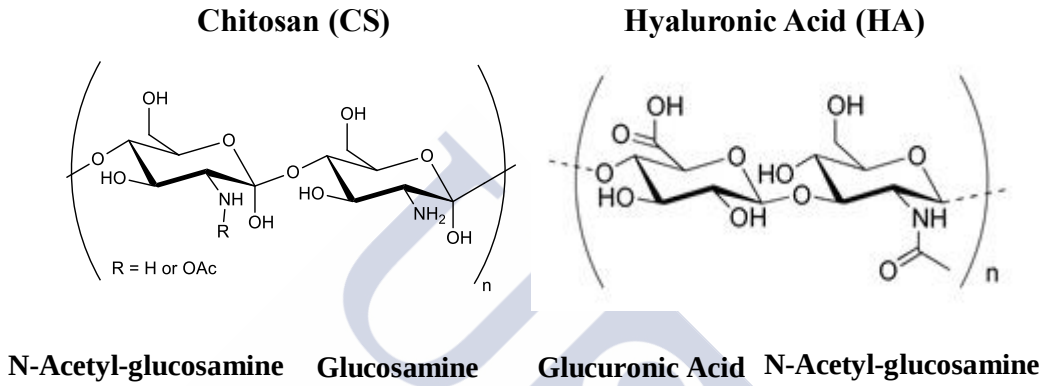

2.2 Hyaluronic acid

Hyaluronic acid (HA), an endogenous biomolecule found in all tissues and body fluids of vertebrates. It is a structural component of the extracellular matrix, sinovial fluids, and soft tissue, which connects and support structures and organs of the body. As in the case of CS, HA is composed by D-glucuronic acid and N-acetylglucosamine linked through alternating β (1 → 4) and β (1→3) glycosidic bonds (figure 2). Native HA has a molecular weight (Mw) of 10000-100000 kDa, however, it can be obtained from commercial sources in a large range of Mws. Within this broad range, HA of Mw up to 10 kDa is normally named as oligomeric HA (19) and HA of Mw up to 45 kDa (20, 21) is generally considered as LMw-HA.

As shown figure 2, the bulky hydroxyl, carboxylate and amide groups are fixed in an equatorial position due to steric repulsion in HA. When placed in physiological solutions HA folds into a random coil structure, the resulting conformation of HA in solution produces hydrophobic patches consisting of the axial hydrogens in the polysaccharide

backbone (22). These regions are also considered to play a part in the mucoadhesivity of HA (23).

In addition to the described interactions, HA is involved in several biological functions mediated by its interaction with specific proteins. For example, its role as a structural tissue component, HA binds to proteoglycans, thus forming complexes with lubricant and viscoelastic properties (20, 24). On the other hand, HA interacts with a number of protein cell receptors, this interaction being critical for HA degradation and elimination from the body.

The best known HA receptor, CD44, is a transmembrane glycoprotein found in lymphocytes, epithelial and endothelial cells, ocular tissue (conjunctival cells), among others. This protein is also overexpressed in many cancer cells participating in angiogenesis, tumor invasion and metastasis (25, 26). Specific HA-CD44 binding is involved in several cellular functions such as cell differentiation, proliferation and migration and contributes as well to HA degradation (26-28).

The binding affinity of HA to CD44 increases with the HA Mw where 6 to 10 oligosaccharide units are considered as the minimum amount for effective receptor binding. Paradoxically, the higher affinity of HMw-HA towards the CD44 receptor does not necessarily lead to its enhanced cellular internalization. Due to the cluster nature of HA-CD44 binding, the increased number of linkages between receptor and ligand may lead to the saturation of the receptor incapacitating it for further binding and internalization of more HA (29). CD44 mediated HA degradation is controlled by two types of hyaluronidases; Hyal-1 and Hyal-2. The degradation process starts extracellularly with Hyal-2 that is only active in presence of CD44. Once HA is bound to CD44, the degradation is predominantly mediated by Hyal-1 (26).

One mechanism for the elimination of HA from blood is via the Hyaluronic Acid Receptor for Endocytosis (HARE) (26, 30). This receptor is located mostly in sinusoidal endothelial cells of liver and spleen and its affinity for HA is Mw dependent. For example, Jadin et al (31) have shown that upon intravenous administration, high Mw HA (1200 KDa) was accumulated in liver and kidney up to a much greater extent than low Mw HA (<160 kDa). Taking this into account, some authors have indicated the possibility to saturate

the HARE receptor with a specific compound (e.g. chondroitin sulfate with high HARE affinity and no CD44 affinity) in order to reduce the elimination rate of HA. This strategy might be of interest for the use of HA as a targeting polymer carrier (32, 33).

Another receptor of interest that participates in the tissue elimination of HA is the Lymphatic Vessel Endothelial Receptor 1 (LYVE-1), mainly located in lymph vessel endothelium. The interaction with this receptor is responsible for the continuous transit of HA from tissues into the lymphatic system, which is the main route of degradation of tissue-derived HA. In fact, the capacity of the lymphatic system to extract HA is known to be up to 90% (34-37). The binding mechanism of HA-LYVE-1 is similar to that of HA-CD44 (both share similar domains) (36). Although this HA receptor has not yet been exploited for the targeting of HA-based nanocarriers, targeting the lymphatic system with this marker represents therapeutic opportunities in several pathologies such as inflammation, autoimmunity and also for metastatic cancer dissemination via lymph nodes since LYVE-1 has recently been related to tumor lymphangiogenesis.

TSG-6 is another HA receptor, found in synovial fluids and also detected in the serum of patients with inflammatory or autoimmune diseases. It´s up-regulation is related with inflammation processes like arthritis and tissue remodeling (38, 39), in which TSG-6 and hyaluronan binding suppresses cartilage degeneration and normalize synovial fluids (20). A schematic overview of the receptors involved HA-binding and their main physiological role is presented in Figure 3.

Figure 3. Schematic overview of the receptors involved in HA-binding and their main physiological role

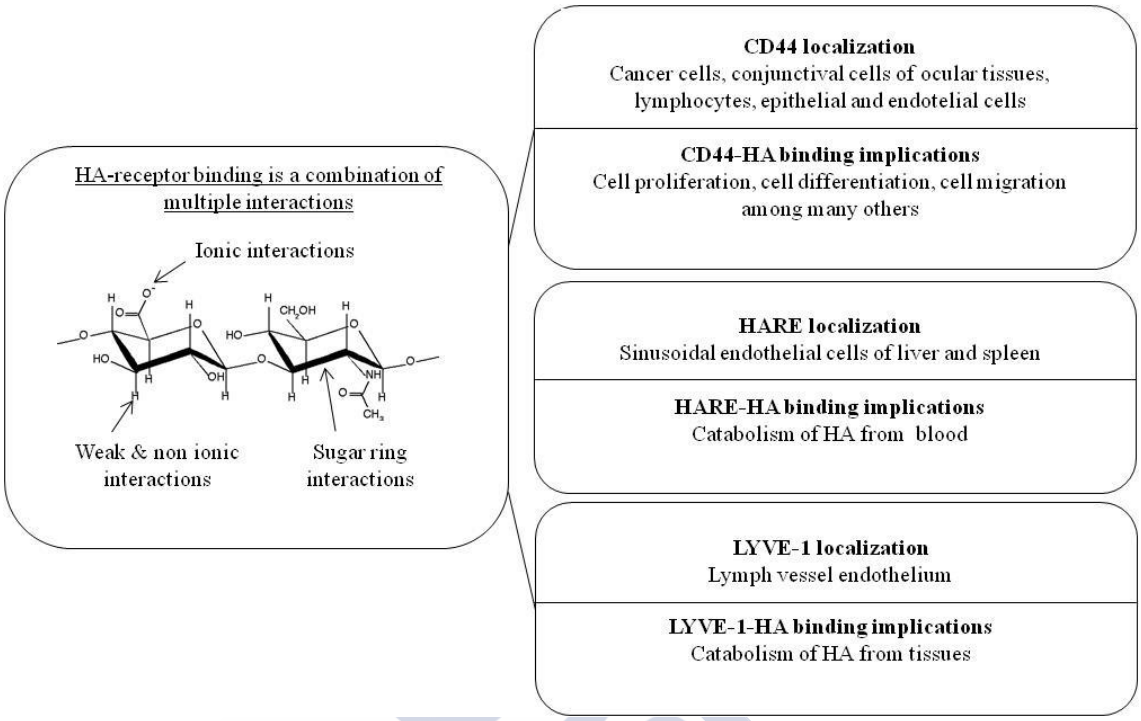

Hyaluronic acid, being both non-toxic and biodegradable, is considered to be a biocompatible material with a wide number of clinical applications and commercial products for topical, ophthalmic, nasal, pulmonary and also parenteral administration. Toxicological studies were performed in order to evaluate the toxicity, immunogenic response, genotoxicity, neurotoxicity, carcinogenicity or effects on reproductive and organogenesis in a wide range of animal species and with different exposure routes (oral, peritoneal, inhalation, topical, intramuscular…). In all cases high doses of HA did not induce any immunogenic or adverse toxicological effects either in the short or long term (40). Although it is important to mention that recent studies have suggested the potential immunogenic properties of LMw-HA (41, 42).

Because of its interesting physicochemical and biological properties, both, HA and CS are regarded as very interesting materials for a wide variety of biomedical applications. Both are currently being used in wound healing and skin care in different forms. Additionally, HA is being employed in intra-articular injections for osteoarthritis treatment, and as eye-drops for dry-eye treatment, whereas CS is being evaluated for this use in clinical trials. In this chapter, however, we focus on CS and HA-based drug

nanocarriers and their potential for transmucosal drug delivery, anticancer-drug targeting and gene therapy.

3. Types of CS and HA-based Nanocarriers

Over the last five years, the reactivity of HA and CS has inspired the synthesis of polymer-drug conjugates (33, 43-47), amphiphilic copolymers (21, 48-64) that have been used to form micelles, and phospholipid linked HA to form hyaluronized liposomes (65-71). For the purpose of simplicity within this chapter we will concentrate in the description of polymer-based nanostructures, namely micelles, liposomes, nanoparticles and nanocapsules. Some specific references of these nanostructures are presented in table 1 and 2. Also an illustration of the different nanostructures is presented in Figure 4.

Figure 4. Schematic illustration of different HA and CS based nanocarriers described in the literature.

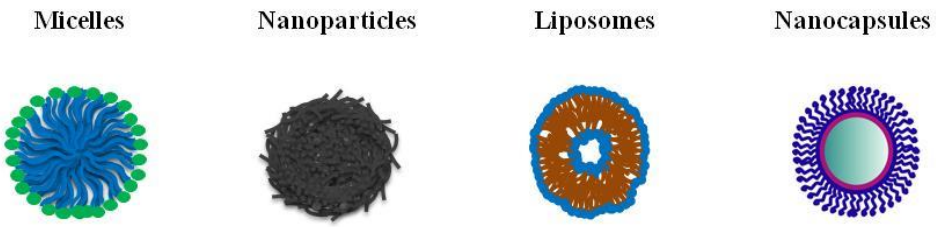

3.1 Hyaluronic acid and chitosan-based micelles

Hydrophobic moieties, e.g. cholanic acid or ceramide, can be conjugated to HA´s carboxylic acid groups through simple reactions to yield amphiphillic copolymers. The resulting polymers can then self-assemble into micelles in physiological conditions (21, 48-62). Similarly, CS has been chemically modified forming, for example, quaternary ammonium palmitoyl glycochitosan (GCPQ), which induces the formation of micelles upon dispersing in water (72, 73). The hydrophobic part of copolymer is oriented inwards, forming a core suited for the encapsulation of hydrophobic drugs (48-53, 55-60, 62, 72). In the case of CS, the positive charge has also led to the efficient entrapment of negatively charged macromolecules, i.e. peptides and nucleic acid-based molecules (74, 75). An illustration of this type of structures is presented in Figure 4.

3.2 Hyaluronic acid and chitosan-based nanoparticles

Electrostatically formed hybrid HA-CS nanoparticles can be achieved avoiding the use of organic solvents by simply ionic gelation using a crosslinking agent like tripolyphosphate or adipic acid dihydrazide. This method takes advantage of the gelling properties of polysaccharides and permits the association of delicate macromolecules without the use of organic solvents or high energy sources (76-79). In the case of CS, other polymers besides hyaluronate, i.e. alginate and poly-γ-glutamate have been used for in the formation of these nanoparticles (61, 80-89). Such techniques also permit the incorporation of additional excipients to modify the properties of CS nanoparticles, for example, cyclodextrins (90-94).

Given that solid matrix nanoparticles are formed and stabilized mainly through ion pair interactions it is important that the pH is controlled during preparation, as alterations in pH will change the degree and state of ionization of the polymers and macromolecules.

Overall, these different nanoparticle types have been designed with the aim of taking advantage of their bioadhesive properties to improve the interactions and contact time with mucosal barriers. A schematic illustration of this type of nanocarrier is shown in Figure 4.

3.3 Hyaluronic acid and chitosan-coated liposomes

The reactivity of HA also allows its conjugation with chemically activated phospholipids with molecules like ethanolamine or stearylamine to form HA liposomes (41, 65-67, 69, 71). This so-called hyaluronization can be achieved previous or post liposome formation. In addition to this strategy, liposomes can be readily coated either with chitosan, or hyaluronic acid or their derivatives based upon the ion-pair formation between the lipid´s groups and the polysaccharide's groups (95-98). Therefore, the formation of the HA or CS-coated liposomes can be easily achieved upon incubation of liposomes in an aqueous solution of the polysaccharide. The resulting system enables the association of hydrophilic molecules (in the aqueous core) or hydrophobic drugs (within the lipid bilayer). An illustration of this type of structures is presented in Figure 4.

3.4 Hyaluronic acid and chitosan nanocapsules

These are vesicular systems with an oily core stabilized by surfactants and a surrounding polymer shell. The formation of the HA or CS polymer shell is mediated by hydrophobic and ionic interactions of the polysaccharides with the surfactants and can be easily achieved using simple emulsification methods, such as the solvent displacement technique (99, 100). Thus, the electrostatic interaction of CS with the oily core has been mediated by negatively charged phospholipids (101-103), whereas that of HA has been is achieved by the incorporation of a cationic surfactant such as cetyl trimethylammoium bromide or bezalkonium chloride (100, 104). The oily core provides high capacity for the encapsulation of hydrophobic cancer drugs while the polymer coating barrier confers capacity to control drug release and optionally allows the association of hydrophilic substances (e.g. nucleic acids). Potential also exists for the formation of nanocapsules via solvent-free methods as it is the case of a described self-double-emulsifying system with an alginate-CS coating (105). An illustration of this type of structures is presented in Figure 4. An overview of HA and CS nanocarriers compositions and their main applications are presented in Tables 2 and 3 respectively.

Table 2: Overview of HA-nanocarriers compositions and their main applications.

Hyaluronic acid micelles		
Description	**Application**	**Ref.**
HA-cholanic acid copolymer	Antitumoral drugs/imaging to CD44 tumor cells	(51, 60, 62)
HA-cholanic acid-PEG copolymer	Antitumoral drugs/imaging to CD44 tumor cells	(50, 52, 56, 57)
HA–cholanic acid–PEG-aminopropylmethacrylamide copolymer	Antitumoral drugs/imaging to CD44 tumor cells	(48)
HA-cholanic acid-PEG and without PEG copolymer mineralized with Ca^{2+} y PO_4^{3-}	Antitumoral drugs/imaging to CD44 tumor cells	(49, 55)

HA-ceramide copolymer and Pluronic® P85	Antitumoral drugs/imaging to CD44 tumor cells	(53, 58)
HA - polybenzyl glutamate copolymer	Antitumoral drugs/imaging to CD44 tumor cells	(59)
HA-spermine-amines copolymer	Gene therapy to CD44 tumor cells	(21, 54)
Hyaluronic acid nanoparticles		
Description	**Application**	**Ref.**
HA, CS or CS-PEG & TPP	Gene therapy through ocular mucosal barriers to CD44 cells	(76-78, 106)
HA & CS	Gene therapy to CD44 tumor cells	(61)
HA, trimethyl CS & TPP with and without PEG	Antigen through nasal mucosal barrier	(107)
HA, adipic acid dihydrazide and TweenR 80	Peptide through oral mucosal barrier	(108)
HA and adipic acid dihydrazide	Viscosupplementation of synovial fluid for osteoarthritis treatment	(109)
HA & CS-ammonium and CS-thiol derivatives	Drug delivery through oral mucosal barrier	(110)
HA:CS or CS derivative	Gene therapy through oral mucosal barriers	(111)
Hyaluronic acid liposomes		
Description	**Application**	**Ref.**
HA covalently linked to ethanolamine derived phospholipid	Antitumoral drugs to CD44 tumor cells	(71)
HA covalently linked to ethanolamine derived phospholipid	Antitumoral drugs to CD44 tumor cells	(69)

HA covalently linked to ethanolamine derived phospholipid	Gene therapy to CD44 tumor cells	(65)
HA covalently linked to stearylamine	Drug delivery to HARE endothelial liver cells	(66)
HA covalently linked to ethanolamine derived phospholipid	Antitumoral drugs to CD44 tumor cells	(67)
HA covalently linked to ethanolamine derived phospholipid	Gene therapy to CD44 tumor cells	(68)
HA electrostatically coated onto cationic liposomes	Imaging agents to CD44 tumor cells	(112)
HA electrostatically coated onto cationic liposomes	Antitumoral drugs to CD44 tumor cells	(113)
Hyaluronic acid nanocapsules		
Description	**Application**	**Ref.**
HA, soybean core and surfactants	Antitumoral drugs to CD44 tumor cells	(104)
HA, Miglyol core and surfactants	Antitumoral drugs to CD44 tumor cells	(100)
HA & hydroxiethyl starch, aqueous core and surfactants	Wound care	(114)
HA, polycaprolactone core with surfactants	Drug delivery through ocular mucosal barriers	(115)

Table 3: Overview of CS-nanocarriers compositions and their main applications.

Chitosan Micelles		
Description	**Application**	**Ref.**
Doxorubicin conjugated and hydrophobised glycol chitosan	Antitumoral	(47)
Cholanic acid modified glycol CS	Antitumoral	(64)
Targeted (transferrine) self-assembled GCPQ chitosan micelles	Antitumoral	(116)
Self-assembled GCPQ chitosan micelles	Gene delivery	(75)
Self-assembled GCPQ chitosan micelles	Oral peptide	(73)
Chitosan nanoparticles		
Description	**Application**	**Ref.**
TMC based nanoparticles	Nasal antigen	(117-123)
CS based nanoparticles	Nasal antigen	(124-127)
PEGylated CS/TPP	Nasal gene delivery	(128)
bfFP-CS/pDNA, dendritic cell targeting	Nasal gene delivery	(129)
Mannosylated CS/pDNA	Nasal gene delivery	(130)
CS/TPP	Nasal peptide	(131)

CS/TPP/cyclodextrin	Nasal peptide	(92)
CS/TPP/alginate	Nasal peptide	(83)
Thiolated CS, binary polyelectrolyte complex	Nasal peptide	(132)
CS-PVA-PLA interpolymer complex	Nasal peptide	(133)
TMC-CS, binary polyelectrolyte complex	Nasal peptide	(134)
CS/TPP nanogel particles	Nasal peptide	(131)
CS-pDNA	Ocular gene delivery	(135, 136)
TMC/pDNA	Oral gene delivery	(137)
Oleoyl-TMC/pDNA/TPP	Oral gene delivery	(138)
Thiolated-TMC/pDNA	Oral gene delivery s	(139)
CS-insulin binary polyelectrolyte complex	Oral peptide	(140)
CS-insulin dispersed in oil or surfactant.	Oral peptide	(141, 142)
CS-alginate Ca^{2+} crosslinked nanoparticles	Oral peptide	(80, 143)
CS-albumin coated alginate-dextran nanoparticles	Oral peptide	(144-147)

Binary polyelectrolyte complex with CS targeting peptide conjugate	Oral peptide	(148)
CS-poly-γ-glutamate nanoparticles	Oral peptide	(85, 86, 89, 149)
Chitosan Nanocapsules		
Description	**Application**	**Ref.**
CS coated emulsion	Nasal antigen	(127)
Miglyol-lecithin-CS coated nanocarriers	Nasal peptide	(150)
CS/poly-L-lysine coated caprolactone nanocapsules	Ocular	(99)
Alginate-CS coated W/O/W nanoemulsion	Oral peptide	(105)
Miglyol-lecithin-CS coated nanocarriers.	Oral peptide	(151-153)

4. Biomedical applications of Hyaluronic acid and chitosan-based nanocarriers

CS and HA-based nanocarriers have been proposed for a wide range of biopharmaceutical applications. Because they share some interesting biological properties, notably their bio-adhesiveness, they have been widely studied regarding their ability to overcome cellular and epithelial barriers. However, while CS-based nanocarriers have been mainly used for overcoming mucosal barriers, those based on HA have mainly been conceived for targeting to specific cell populations, i.e. cancer cells. On the other hand, due to its positive charge, CS has also attracted a great deal of attention in the gene delivery field. In this section we will summarize the advances made towards those specific aims.

4.1 Transmucosal drug/antigen delivery

The bioadhesive properties of HA have been studied in several cases in combination with chitosan. The aim has been to form nanocarriers with enhanced residence time and contact (77, 154-157) with different mucosal surfaces, achieving higher doses of the associated bioactive compound crossing the mucosal barrier.

4.1.1 Ocular drug delivery

CS-based nanocarriers have also been explored as a way to increase the residence time and the penetration of drug either into the corneal or the conjunctival epithelium. The first evidence of this potential was shown with CS-nanocapsules, which exhibited the ability to enter the corneal epithelium and favor the retention of drugs, i.e. indomethacin and cyclosporin A (99, 158). A comparative study of fluorescently marked CS and PEG-CS coated nanocapsules demonstrated that while unmodified CS enhanced the retention in the mucosal layer, the PEGylated derivative accelerated the transport of the nanocarrier through the epithelium (159).

Similarly, CS nanoparticles and CS-lipid hybrid nanostructures were also found to interact with ocular mucosa (160) showing good ocular tolerance and cellular uptake (161-163). Other specific examples are indicated in section 4.3.

Despite the extensive use of HA solutions in the form of artificial tears and the known presence of CD44 receptors in the conjunctival epithelial cells, there has been only minor activity of the use of HA-based nanocarriers for ocular drug delivery. One of the few examples of HA nanocarriers in ocular drug delivery are HA coated polycaprolactone nanocapsules reported by Barbault-Foucher (115, 164). Ocular administration of cyclosporine A loaded nanocapsules yielded a significant increase in the conjunctival and corneal concentration of cyclosporine A when compared to a castor oil solution. Furthermore, cyclosporine A was present for up to 24 hours post-administration in the case of the nanocapsules. This corresponded to a lower cyclosporine A concentration in tear fluid for the nanocapsules than the castor oil control. Both observations show that the ability of the nanocarrier to adhere to the ocular tissues is imperative in the resulting efficacy of the formulations.

Of particular interest is the combination of both polysaccharides, HA and CS, in the form of nanoparticles. In vivo studies performed with fluorescently labeled HA/CS nanoparticles in rabbit ocular mucosa showed the ability of these nanocarriers to efficiently interact with and penetrate the corneal and conjunctival cells (76-78). These nanoparticles have been widely tested as non-viral gene delivery systems in ocular tissues improving transfection efficiency by facilitating interaction with conjunctival CD44 receptors for the treatment of several diseases such as dry eye, immune-mediated diseases and ocular allergy.

4.1.2 Nasal drug/antigen delivery

The nasal route is of particular interest in the development of needle-free vaccinations. Also, the increasing prevalence of peptide drugs in research pipelines and marketed products is behind an ever increasing interest in obtaining efficacious transmucosal delivery systems.

While HA-based nanocarriers have barely been studied for nasal drug delivery, the previously described properties of CS have led to its extensive study in the nasal delivery of drugs and antigens. Early work with insulin-loaded CS nanoparticles demonstrated the potential of CS nanocarriers in nasal insulin delivery (131). This base system led to the development of hybrid nanoparticles consisting of CS and caboxymethyl or sulfobutyl β-CDs (165), CS and alginate (83), or CS and polylactic acid (133), which significantly enhanced insulin response upon nasal administration. Other examples of successful nasal administration of insulin, in terms of pharmacological response, include gold nanoparticles coated with CS (166).

On the other hand, nanoparticles formed with chemically modified CS have proven successful with both TMC and thiolated CS derivatives (132, 134). For example, in a study it was found that thiolated CS nanoparticles produced an improvement in hypoglyceamia compared to the non-thiolated analogue in healthy rats (132). Similarly, the degree of quaternization of TMC was observed to positively affect the absorption of insulin associated to TMC based nanoparticles in rats (134).

Further to the solid matrix nanoparticle systems, salmon calcitonin (sCT) loaded CS nanocapsules produced a hypocalcaemic effect after nasal administration, where the CS coating resulted in an enhanced effect when compared to the control nanoemulsion (150).

Beyond the enhanced absorption of therapeutic peptides, the potential of CS-based nanocarriers as antigen delivery systems is well established. Following the initial studies demonstrating significant transport of tetanus toxoid across the nasal mucosa when associated to CS nanoparticles (126, 167), a range of CS-based nanocarriers has emerged. For example, CS nanocapsules containing the antigen associated to the CS shell have been reported as useful carriers for the nasal delivery of the model antigen, ovalbumin (127) and also the recombinant hepatitis B surface antigen (rHBsAg) (168, 169).

Trimethyl CS based nanocarriers have also yielded promising results regarding nasal antigen delivery. Ovalbumin conjugated to TMC nanocarriers induced a marked increase in the IgG response when compared to a TMC ovalbumin solution (170-172). This positive in vivo performance of TMC nanocarrries has been corroborated with other antigens, namely, influenza and tetanus toxoid (117, 122, 123, 173). Nevertheless, a comparative study of CS and TMC nanoparticles loaded with rHBsAg showed that both were similarly efficacious after either intranasal or intramuscular administration (118). Therefore, the potential advantage of TMC nanoparticles vs. CS nanoparticles for antigen delivery remains to be elucidated.

Other immunostimulating molecules have also been co-associated to CS nanocarriers, where further improvements in immune response have been observed. This was the case when CpG ODN was co-encapsulated with ovalbumin in CS nanoparticles. Interestingly, this combination led to an improved cellular immune response as confirmed by the increased ovalbumin specific T-cell response in the spleen (121). More recently, the same group evaluated a battery of immunostimulants, among which LPS and MDP were found to be the most efficacious in combination with TMC nanocarriers (120).

Finally, HA-CS nanoparticles have been studied for nasal vaccination, however this preliminary study in mice did not demonstrate and enhanced immune response when compared to the plain antigen (107).

4.1.3 Oral administration

The results on the potential of nanocarriers for nasal administration of peptides can serve as a stepping stone toward developing successful nanocarriers for oral peptide delivery. However, this delivery route does pose some additional complications such as the high dilution of the nanocarriers in the harsh gastro-intestinal environment. Therefore, it is imperative that oral delivery platforms offer protection against proteolysis in addition to facilitating mucosal transport.

The main focus of attention regarding oral peptide delivery using nanocarriers has been diabetes treatments, chiefly with insulin, although GLP-1 analogues are also of interest. This has been driven by the current and projected socioeconomic impact of diabetes. Further to showing promising PK/PD results in animal studies CS nanocarriers have also yielded a bank of information regarding the behaviour of colloidal nanocarriers administered orally.

Insulin-loaded CS-alginate nanoparticles showed a clear hypoglycemic effect upon oral administration to rats. A feature of interest of these nanocarriers was that insulin release was found to be pH dependent: i.e. inhibited at gastric pH and sustained at intestinal pH (80, 81, 143). The same authors have more recently presented a second generation of nanoparticles with a dextran-alginate core coated with CS, and with an additional albumin coating to protect the nanoparticle from enzymatic degradation (144-147). In vitro and ex vivo models were used to elucidate the mechanism of absorption of the nanocarriers (147). Overall, the results indicated that the epithelial permeation of Caco-2, Caco-2/HT29MTX cell models and excised rat intestinal tissue increased in the presence of nanoparticles. Fluorescent labeling of alginate and insulin in ex vivo experiments indicated that both alginate and insulin were co-localised in enterocytes.

Another approach that has been explored relies on the formation of CS-insulin or CS-sodium lauryl sulphate insulin nanocomplexes (140-142, 174). A clear hypoglycemic effect was observed upon administration of these formulations, this effect being more pronounced in the case of CS-Insulin nanocomplexes dispersed in an oil (141, 142). In both architectures, either the oily dispersion or the presence of sodium lauryl sulphate would afford protection to insulin from pepsin degradation.

Poly-γ-glutamate has been used to form interpolymer crosslinked CS nanoparticles for oral peptide delivery. When administered to rats in enteric coated capsules these prototypes showed *in vivo* data among the best reported in terms of oral insulin bioavailabilities (15 to 20%) (85, 86, 175). Similar results were obtained for the GLP-1 analogue Exendin-4 with a bioavailability value of 14% (176). In this study it was found that the presence of Fe^{3+} increased greatly the encapsulation efficiency of the peptide due to the coordination between Fe^{3+}, CS and Exendin-4. Further to the high bioavailability, additional SPECT studies provided important information regarding the mechanism of action of CS nanocarriers. Namely, the results indicated that while insulin was absorbed into the villi, CS remained in the mucosa.

Chemical derivatisation of CS offers an interesting pathway to controlling the behaviour of nanocarriers in vivo. The effect of incorporating targeting ligands onto trimethylated CS (TMC)-insulin nanoparticles was recently tested (148). Confocal microscopy of Caco-2/HT29MTX monolayers after incubation with the fluorescently labeled nanoparticles showed an increased cellular uptake of the nanoparticles targeted to the goblet cells when compared to the ligand free TMC-insulin nanoparticles. Indeed, this translated to a moderate improvement in relative bioavailability from 3.69 to 5.66% due to the conjugated ligand.

Besides offering the potential for improvements in bioavailibity chemical modification of CS can also significantly alter the uptake pathway of the polymer. One of the strongest examples is the GCPQ CS polymer that merits special mention here (73) GCPQ is an amidoylalkyl glycochitosan derivative whose amphiphatic character induces self-assembly into micelles. Oral administration of Leu-enkephalin-loaded GCPQ micelles

resulted not only in an increased absorption of the peptide but also in its transport across the blood brain barrier.

In addition to the various solid matrix nanocarriers described previously, CS coated lipid core nanocarriers have also been studied for oral peptide delivery. CS and PEG-CS nanocapsules have been studied for oral salmon calcitonin (sCT) delivery. Interestingly, these nanocapsules gave rise to an enhanced and extended hypocalcaemic effect of at least 24 hours (duration of experiment) (17, 151-153). In a subsequent study, CS was PEGylated via amidation of the primary amine (1% and 0.5% degrees of PEGylation) and its effect on the pharmacological response to sCT-loaded CS nanocapsules was evaluated (152). The results showed that a high PEGylation degree affected negatively the efficacy of the nanocarriers. In all the examples reported in this series of studies, CS was found to be fundamental to the eventual pharmacological activity of the formulations. A more recent approach has been to produce nanocapsules with a mixed CS-alginate polymer shell. This composition has been used to form W/O/W nanocapsules for oral insulin delivery, and resulted in a hypoglycaemic nadir of ~30% at 7 hours post administration (105).

Regarding oral administration with HA-based nanocarriers; the work of Zambito (110) use the combination of CS derivatives and HA to form mucoadhesive nanoparticles for oral drug delivery. CS derivatives consist on quaternary and primary ammonium pendant moieties available for covalent attachment of thiol-bearing compounds. Quaternary ammonium has the ability to open epitelial tight junctions whilst thiols can form disulphide bonds with epithelial mucus increasing the mucoadhesion capacity of the system. Nanoparticles were found to be non toxic in endothelial progenitor cells. Mucoadhesion studies with fluorescently labeled nanoparticles using rat intestinal mucosa, showed a high absorption of nanoparticles and furthermore that this absorption was concentration independent. Moreover, the thiolated nanoparticles proved to be more mucoadhesive than their non-thiolated analogues demonstrating the potential advantages of thiol containing nanoparticles for transmucosal delivery.

Again hybrid HA/CS nanoparticles have also been tested to deliver siRNA by the oral route (111). Trimethyl chitosan or thiolated TMC derivatives were used in order to

improve stability of CS against disolution at acidic pH. Stability studies in gastrointestinal fluids showed that the non-HA containing nanoparticle´s size increased to a much larger extent than the HA/CS nanoparticles. Whilst naked siRNA was rapidly degraded in endogenous nucleases supplemented medium, HA/CS nanoparticles were able to partially protect siRNA from nuclease degradation. The degradation of a fraction of the siRNA loaded into the nanoparticles can be attributed to polysaccharide degradation; more specifically to the presence of chitosanase in colonic mucosa. Permeation studies with fluorescent labeled nanoparticles using rat ileum showed significant enhancement of siRNA transport, this was confirmed by biodistribution studies: in which nanoparticle concentration in the intestine decreased with time while increasing in plasma, liver and spleen, demonstrating that the nanocarrier is capable of promoting adsoption and subsequent entry into systemic circulation and the reticuloendothelial system.

Finally, Han *et al.* proposed HA nanoparticles for insulin delivery. These nanoparticles protected insulin from enzymatic degradation by gastrointenstinal enzymes (97% free insulin degradation versus 31% degradation inside nanoparticles). Transepithelial transport capacity studied by the Caco-2 monolayer cell model and in rat small intestine showed higher efficiently transport compared with insulin solution. A reduction in blood glucose was observed after oral administration of these nanoparticles to diabetic rats helped by the nanocarrier´s aforementioned ability to enhance epithelial permeation and protect insulin from degradation (108).

The systems discussed above show that a wide variety of CS based nanocarriers are effective in facilitating the transmucosal delivery of proteins and peptides, where CS plays a fundamental role in their action. Besides showing good PK/PD data in animal models, which in some cases is on the top end of the reported performances for oral protein delivery, a better understanding of the behaviour of CS in the absorption of the nanocarriers is beginning to emerge. In the case of nanoparticulate CS, the current evidence suggests that the polymer may not translocate into the serosal side of the villi. Instead, it tends to accumulate in the mucosa adjacent to the epithelia. This behaviour, from a toxicological standpoint, is preferred given that internalisation of the nanocarrier or its components may imply a more complicated safety evaluation.

4.2 Anticancer drug delivery

Opposite to what was described for transmucosal drug delivery, CS-based nanocarriers have received little attention for anti-cancer drug delivery; these two works from Alonso´s group being some of the limited examples available (177, 178). The main goal in the delivery of anticancer drugs is to target them to the cancer cells, this enhancing their efficacy and reducing their toxicity. For this specific purpose, in general, the delivery carrier needs to be administered intravenously and the positive charge of CS represents a hurdle from the point of view of the biological stability of the nanocarrier. To overcome this limitation some authors have proposed the use of chemically modified CS such as hydrophobic derivatives (63, 64), or PEGylation (178). Doxorubicin has also been conjugated to glycol CS in nanoparticles (47).

Both specificity and cellular uptake can be improved by incorporating targeting ligands such as folate or transferrine. The previously described GCPQ glycol CS derivative has been further modified to include targeting ligands (116). Here the authors studied the efficacy of both transferrine and glucosamine, where the uptake and cytotoxicity of docetaxel loaded vesicles were improved by conjugating the transferrine ligand. Folate-CS has also been employed to take advantage of folate receptor mediated endocytosis in cancer cells (63, 179). Conjugation of OX26 to CS-PEG based nanoparticles facilitated brain delivery of an antitumoral (180), and dendritic cell targeting for cancer immunotherapy (181).

In contrast, the specific ability of HA to target CD44 overexpressed in many tumors and its shielding effect make HA-based nanocarriers particularly attractive for developing more effective cancer therapies (31, 62, 182, 183). As a consequence of this capacity, a number of different HA based nanocarriers have been developed to deliver antitumoral drugs, gene therapy or imaging contrast agents to many types of cancer like breast, lung, colon, carcinoma, melanoma, liver, among others.

A critical factor to consider for the design of nanocarriers with optimal CD44 affinity is the selection of HA molecular weight. As detailed in Section 1, the affinity of HA for CD44 increases with molecular weight of HA. In accordance with this, studies undertaken with HA-conjugated liposomes of varying HA molecular weight showed that conjugation with

higher molecular weight HA resulted in stronger CD44 binding (41). This observation is also supported by studies with similar liposomes also linked to HA, where increased uptake was achieved with higher Mw in a CD44 cancer cell line (67). However, recent studies suggest that the cluster nature of HA CD44 binding results in a limit to the number of linkages that can be formed before the CD44 receptor is saturated and incapacitated preventing further internalization (29). This is in agreement with Wojcicki et al. (65) where the transfection efficiency of DNA loaded HA-liposomes with two different HA concentrations (10 and 15%) were studied. Here, the authors found that the lower concentration of HA gave higher levels of transfection.

Besides CD44´s targeting potential, the hydrophilicity of HA can diminish carrier opsonization by steric repulsion increasing nanocarrier circulation time after intravenous (69, 70, 184), in turn promoting nanocarrier accumulation in tumors through passive mechanisms (182, 183).

Micelles composed of amphiphilic copolymers of HA and hydrophobic molecules are the most studied systems for tumor targeting. Choi et al carried out extensive studies with micelles of HA conjugated with the bile salt, 5β-cholanic acid. HA-cholanic acid micelles were loaded with antitumoral drugs, e.g. irinotecan, chlorine e6, doxorubicin, paclitaxel, camptothecin, and imag contrasts agents and were used for the targeting of carcinoma, breast, colon or liver cancer (51, 60, 62). Tumor cells overexpressing CD44 could internalize these nanocarriers more readily than normal fibroblasts. Moreover, drug loaded HA-micelles exhibited higher cytotoxicity than the free drug, thus suggesting the role of the nanocarrier at increasing the drug internalization. Finally, following intravenous administration of fluorescently labeled HA-cholanic acid micelles in tumor bearing mice it was observed that micellar HA remained in the blood circulation for a much longer time than HA in solution. This prolonged circulation time produced a preferential accumulation of the micelles in tumoral tissue and consequently a significant increase in antitumoral efficacy, measured in terms or reduction of tumoral volume. Although a significant amount of nanocarriers were also detected in the liver. Similar results have also been obtained with other HA nanocarriers such as polybenzyl glutamate conjugated HA micelles (59).

The hepatic accumulation of HA micelles was attributed to their uptake the Mononuclear Phagocytic System (MPS) but also to their specific interaction with the HARE receptors. Based on these results HA micelles were proposed for hepatic cancer imaging (185). Nevertheless, hepatic accumulation may represent a major drawback for cancer therapies directed to organs. In order to reduce the hepatic uptake of HA-cholanic acid micelles, PEGylation of the HA backbone (50, 52, 56, 57) has been studied. In vitro experiments showed a reduced internalization of PEGylated micelles, both in tumor cells and normal fibroblasts, most likely due to a shielding effect of PEG.
However, in vivo studies with breast and colon tumor bearing mice demonstrated a reduced hepatic accumulation and increased circulation time of the PEGylated micelles in comparison with the non PEGylated analogue. This difference in nanocarrier biodistribution and pharmacokinetics was associated to an improvement in the accumulation of the PEGylated nanocarrier in tumoral tissue. Although PEGylation may be of interest for inhibiting hepatic acumulation it may also reduce binding to CD44, thus reducing in part the benefits of HA based nanocarriers.

Additional strategies aimed at improving the behavior of HA micelles have been oriented to improve their stability and controlled release properties. One strategy relied on coating micelles with calcium and phosphate salts, termed by the authors as mineralization (49, 55). These minerals acted as a stabilizing barrier which inhibited drug release at pH 7.4. However, at the more acidic pH environment of tumor tissues, the dissolution of this mineral barrier facilitated the release of the encapsulated drug. Biodistribution studies with fluorescent labeled micelles showed significant enhancement of the tumor/liver accumulation ratio compared with non-mineralized micelles. Overall, the combination of these factors allow drug-loaded mineralized HA micelles to reduce tumor volume more efficiently than non-mineralized micelles or the free drug.

A further strategy to improve the stability and release properties of HA micelles has been the crosslinking of carboxylates of HA with aminopropylmethacrylamide (48). The result was a slower drug release rate, without altering the affinity for the CD44 receptors. The in vitro studies in Hyal-1 supplemented medium showed that drug release can be achieved intracellularly (80% of drug released in these conditions). Fluorescent labeled

crosslinked HA micelles also showed increased accumulation in tumor tissues and improved antitumoral efficacy.

Other authors have developed oligomeric HA micelles, PEGylated or not, conjugated to ceramide (53, 58), a cell membrane sphingolipid involved in apoptosis of cancer cells (186). These micelles also contain Pluronic® 85, a surfactant with abilities to overcome multidrug resistance, a major cause in the lack of efficacy in many chemotherapeutic treatments. The resulting micelles were found to be stable to dilution and exhibited controlled release properties, partially attributed to Pluronic® 85. In vitro studies in tumoral cell lines confirmed that oligomeric HA-ceramide micelles presented a high CD44 affinity. Again, the control drug release and enhanced structural stability of these HA micelles resulted in a markedly preferential accumulation in tumor and increased efficacy compared with free drug for both PEGylated and non-PEGylated system.

HA-coated liposomes have also been investigated for targeting the CD44 receptor in cancer cells. In some instances, hyaluronized liposomes loaded with anticancer drugs, e.g. doxorubicin and mytomicin C, presented an increased cytotoxicity in cancer cell lines when compared with non hyaluronized liposomes or free drug (69, 71). In vivo these drug-loaded liposomes exhibited a significant reduction in toxicity - assessed by loss of body weight - a prolongation of their circulation time and an increase in their tumor uptake as compared to the free drug. This favorable biodistribution pattern of HA liposomes resulted in a 2-fold decrease in the tumor volume as compared to the free drug.

HA nanocapsules represent a new type of nanocarrier consisting of an oily core conveniently stabilized and surrounded by a HA shell, which are particularly attractive for the encapsulation of hydrophobic antitumoral drugs. The first report presented by Orzayun-Ampuero et al. showed the efficient internalization and increase of cytotoxicity of docetaxel-loaded HA nanocapsules as compared to the free drug (100). A similar type of nanocarrier consisting of a solid lipid core and soybean oil (104) was used for the delivery of paclitaxel. Upon systemic administration to tumor bearing mice, paclitaxel-loaded HA nanocapsules exhibited longer circulation time, and reduced toxicity, in terms

of body weight loss, and enhanced efficacy as compared to the commercial paclitaxel formulation (Taxol®).

4.3 Gene delivery

Both CS and HA have been used as carriers in gene therapy. However, while CS is positively charged and, thus, able to condense oligonucleotide-based molecules, HA has to be associated to other positively charged molecules in order to be useful for gene therapy approaches. In some instances both, CS and HA have been included together in order to entrap oligonucleotides, such as DNA and siRNA (76-78) (106). These combinations are particularly interesting where CD44 targeting or mucosal delivery are involved; such as ocular delivery or cancer cell targeting. Entrapment of oligonucleotides inside solid matrix nanoparticles can protect them from nuclease degradation, further, the specific interaction with CD44 increase cellular uptake resulting in higher transfection efficiency.

HA has also been combined with other positively charged molecules for the targeting of gene therapy approaches to cancer cells. For example, Shen et al. developed siRNA-loaded HA micelles in which low Mw HA was conjugated with hydrophobic alkylamines and spermines (21, 54). Here the hydrophobic and cationic spermine formed a hydrophobic core within which the oligonucleotide was condensed, due to the polycationic nature of spermine, thus protecting the genetic material from enzymatic degradation. This resulted in improved transfection and gene silencing in cancer cells when compared to other established transfection agents like lipofectamine and polyethyleneimine.

In another study, Wojcicki et al. (65) developed HA liposomes with HA covalently linked to ethanolamine derived phospholipid in which plasmid DNA is electrostatically complexed to the lipid chains of the liposome. In this case the HA shell was found to protect DNA from nuclease degradation and the transfection studies in a cancer cell line showed a significant expression of the encoded protein (green fluorescent protein, GFP). Similarly, HA liposomes loaded with anti-telomerasa siRNA targeted to CD44 lung cancer cells resulted in an improve protection of siRNA from degradation and a higher transfection efficiency in vitro (68).

In the case of CS, its great ability to complex genetic material (e.g. pDNA or siRNA) has led not only to a great amount of literature but also to the commercial development of a CS-based transfection agent. Early work carried out by Leong´s research group (187-189) pioneered the concept of CS-mediated gene delivery and the attention to this concept has increased over the years (3, 190). Several studies have shown that the good *in vitro* observations can be translated into excellent *in vivo* transfection efficiencies (136, 191-193). The high performance of these systems has been linked to CS´s capacity to enter cells and deliver the associated genetic material in a proper form intracellularly. CS is able to promote endosomal escape, aided by its buffering capacity, i.e. CS acting as a proton sponge (189, 194). A recent study suggests that CS´s buffering capacity may be closer to that of polyethlyeneimine (a well established proton sponge) than originally thought (195).

As with protein delivery, a wide variety of CS based vectors have been studied. The majority are based on direct complexation between CS and the nucleic acid (187), although ore sophisticated systems incorporating lipids or polymers, e.g. HA, have also been reported (78, 128, 196-199).

CS nanocarriers have shown high transfection levels not only in HEK293 cell lines (137, 200, 201), but also in HeLa, CaLu-3 and MDCK cell lines, known to be more challenging for transfection (78, 92, 137, 191, 202-207). Supporting this high efficacy, siRNA-loaded CS nanocarriers have also been reported to reduce gene expression to similar levels to those obtained with lipofectaminee (~50%) (196, 208).

Further to determining the transfection capacity of CS nanocarriers the current body of work gives some indications regarding the design features required for effective transfection. Firstly, a reduced particle size and cationic surface charge are essential for transfection (209). Various studies have highlighted the role played by CS molecular weight, where shorter polymer chains have proven to be more effective due to the easier decomplexation and release of pDNA after internalization (61, 203, 210-213). Although CS chain length, particle size and surface charge appear to have clear correlations with transfection, the role of deacetylation degree cannot be correlated with the same clarity. Whereas, in vitro studies showed better results with highly

deacetylated CS (214, 215), better in vivo results (intramuscular administration) were found with a low degree of deacetylation (215).

The colloidal stability of CS nanocarriers is of importance in obtaining effective transfection vectors. One of the more salient properties is the pH dependence of surface charge where the pH of physiological fluids reduces the degree of protonation, thus neutralizing surface charge and affecting stability. Although, this destabilisation can be offset by the coating of CS nanocarriers with serum proteins (216), some other strategies have been investigated. These include chemical modifications of CS such as quarternization of the amine groups, ensuring that the surface charge remains unaffected by pH (201, 202, 213, 217), PEG-CS conjugated polymers have also been reported (128).

A further alternative has been the preparation branched CS derivatives with higher water solubility (206, 218, 219). Both transfection efficiency and cell uptake were found to be improved by these modifications. Grafting of polymers, such as cell penetrating peptides (CPP) or PEG, onto a CS polymer backbone yielded some interesting observations regarding cellular uptake. For example, CPPs such as TAT (220-222) and poly-arginines (223-229) have been employed to improve cellular uptake. It was also observed that poly arginine grafted CS was internalized via a caveolae mechanism, while CS nanoparticles were taken up via a clathrin-mediated pathway (227, 228). Similarly, Reitan *et al*. studied the mechanisms behind the different transfection efficiencies observed for glycosylated oligomeric CS and oligomeric CS (230). Here glycosylated CS internalized DNA to a higher degree and over a longer period than oligomeric CS.

Various systems have been reported with the aim of further improving endosomal escape and cytosol-specific release characteristic of CS based systems. Thiolation of CS is one such strategy where S-S bridges are reduced in the intracellular environment thus inducing site-specific release in the cytosol (231, 232). CS has also been modified with polyethyleneimine, imidazole and histidines to further improve its endosomolytic activity (206, 233, 234). Both temperature dependence and biodegradation have also been exploited as mechanisms for improving intracellular release of gene medicines (198, 207).

An alternative to the aforementioned chemical modifications is the formation of gene-loaded CS nanoparticles prepared via ionotropic gelation (e.g. with TPP). As indicated above, these nanoparticles can be further optimized using additional polymers, e.g. HA. Various studies have demonstrated that this approach results in an improved transfection when compared to classical CS-oligonucleotides complexes (191, 196, 235, 236). Folate has also been postulated as a receptor mediated approach to improve cellular uptake, although this has not been studied to the same extent as hyaluronic acid (192, 237, 238).

As indictaed in Section 4.1, the potential of CS as a gene delivery vector is well established and studied with various covalent and non-covalent modifications being employed to improve stability, uptake and targeting (128-130, 135-36, 138-39, 213). This has led to the emergence of various *in vivo* studies supporting the potential of CS based gene delivery vectors in this field (181, 192, 193, 238-241).

Table 4: Outline of CS & HA properties and their main biomedical applications

Property	CS	HA	Applications
Positive charge	√	--	• Ionic interactions with biological surfaces • Condensation of oligonucleotides
Viscoelasticity	√	√	• Dermal applications • Ocular applications • Intra-articular applications
Penetration enhancement	√	--	• Mucosal drug delivery
Mucoadhesion	√	√	• Mucosal drug delivery
Targeting capacity	--	√	• Anticancer drug delivery to CD44 cancer cells • Drug delivery to HARE epithelial liver cells

5. Comparative prospect analysis of the potential of CS and HA-based nanocarriers

Based on the reviewed works, it becomes clear that the potential of chitosan (CS) and hyaluronic acid (HA) for nanotechnology-based drug delivery is there. The field of application of these technologies has been, however, driven by differences in the regulatory and safety profile of both materials. CS is approved as dietary fibre and as hemostatic bandages, but, from our knowledge, no regulatory study regarding human parenteral administration or implantation has been performed. On the other hand, HA is FDA-approved since 2003 for injection as tissue filler either during cataract removal and there are currently other clinical applications, such as intra-articular injection and topical ocular application, as well as a myriad of clinical studies involving its administration by different modalities of administration.

CS is well known for its high capacity to strongly interact with mucus, and recent studies have also shown specific cell binding through integrins. This specific cell interaction seems to be critical for CS permeation enhancing properties (6, 7), and we expect further research to clarify whether it may also drive CS nanoparticle endocytosis. On this basis, it is not surprising that CS nanocarries have become some of the most successful transmucosal drug delivery systems, with proven efficacy for nasal and oral delivery. Nasal delivery has been applied mostly to vaccination since this route is more suitable to biopharmaceuticals active at low doses, and not requiring chronic administration. Antigens administered intranasaly in CS nanocarriers elicit a strong mucosal immune response, but also systemic immunity levels well above the protective level (118, 126). Viral challenge studies have proven the capacity of CS nanocarrier-based vaccines to prevent several viral infections (122).

Another area of extensive research for CS nanocarriers has been oral protein delivery. Beginning in the late 90's, a few groups including ours reported effective oral delivery of therapeutic peptides and proteins upon integration in a CS-based nanocarrier (131, 242). Further developments in this line have optimized these basic prototypes, reporting some of the best bioavailabity results for oral insulin formulations (86). As indicated, these positive results are eexplained by the capacity of CS nanoparticles to penetrate the mucus and to bioadhere to the apical membrane of enterocytes (243). However,

how CS nanocarriers behave in the body is not yet fully understood. For example, there is still limited information regarding the fate of CS nanoparticles upon oral administration (73).

On the other hand, beyond the current application to the ocular mucosa, HA degradation in the presence of the gut's microflora questions the potential of HA for oral delivery (244). However, as a major component of the extracellular matrix, HA has shown capacity to bind to a few cell receptors with a broad spectrum of activities indicating potential for other medical uses (26-28, 30, 34-37). This specific binding of HA has stimulated research regarding its potential for cell or tissue targeting, and to improve cellular uptake by receptor-mediated endocytosis. It has also opened the possibility to use nanocarriers in combined therapies where HA receptor activation would act as co-signaling supporting specific cellular pathways. For instance, CD44 activation can result in regenerative effects and also stimulate cell migration (245). HA activation of TSG-6 could have an effect on immunomodulation (38, 39). Based on this profile, and considering its excellent biocompatibility, HA-based nanomedicines have found the greatest interest for the design of new oncological therapies, however, we could anticipate increased interest in HA nanomedicines for immune diseases and regenerative medicine.

Future breakthroughs in HA-based nanomedicines will require a better understanding of HA interactions and processing in the body. Also an improvement of HA targeting abilities could arise from chemically controlling the binding of HA to several potential receptor targets. This would ovoid competition between receptors of interest and possible off-targets. For instance, suppressing HARE binding while preserving CD44 affinity could improve current HA nanocarrier delivery to most cancer tumors, since the active targeted carrier will not have extensive affinity for the liver. Apart from the areas currently under research, we speculate that targeting to cancer stem cells and lymphatic targeting could be two emerging areas of application of HA in cancer therapy.

Despite the different profile of CS and HA, there are two common areas where both nanocarriers could have a bright future, these are gene therapy and ocular drug delivery. The use of CS nanocarriers for gene therapy is largely documented and there is now a

considerable body of knowledge and a marketed transfection agent supporting this application. The success of CS is based in the reported ability of CS to enhance its penetration through cellular and epithelial barriers, its cationic nature capable of compacting gene medicines, and its buffering properties important for endosomal escape (189, 195). A potential weakness of CS for gene therapy is its general cationic character that would drive opsonization upon parenteral administration. Due to this limitation, some of the most successful applications of CS in gene delivery are related to mucosal administration (128, 135, 138, 139). Alternatively, several groups have reported the PEGylation of CS as a method to improve the behavior upon parenteral administration of these nanocarriers (128, 206).

Although much less explored than CS, HA can also be used to generate nanocarriers that are taken up by specific cell receptor endocytosis. HA offers no major limitations for parenteral administration, but has not shown the same performance upon transmucosal administration as CS. The main limitation of HA for gene therapy relies on its polyanionic nature, making it incapable of condensing oligonucleotides. To address this, researchers are trying to synthesize HA derivatives bearing cationic groups (21, 54, 65, 68), or to engineer nanocarriers combining HA with other cationic condensing agents (21, 54, 65, 68).

Ocular drug delivery is often seen as a niche application, but its industrial interest has grown steadily in the last decade; many drugs would benefit from improved retention on the ocular surface, and enhanced corneal and conjunctival penetration. This is an application where both CS and HA have already shown promising data. CS nanocapsules, with their intrinsic capacity to overcome mucosal barriers have shown enhanced levels of indomethatin and cyclosporin A upon ocular instillation (99, 158). HA-acid nanoparticles have also shown high penetration, in this case of gene medicines, a result that can be related to the widespread expression of CD44 in corneal tissue (76-78).

In conclusion, HA and CS-based nanocarriers have shown outstanding results for several applications, justifying the intense interest and study in the development of CS nanocarriers. In the future, a general challenge for both nanocarrier platforms would be

translating the promising results, mostly obtained in rodents, to large mammals and ultimately to humans. Interestingly, despite the difficulties for analyzing the clinical development of CS and HA in a “nano” format, we have identified a number of nanocarrier prototypes undergoing early clinical trials. It is therefore expected that, if successful, the clinical development of these technologies will open interesting avenues for the exploitation of polysaccharide-based nanomedicines.

References

1. Wang Y, Wang PG. Polysaccharide-based systems in drug and gene delivery. Advanced Drug Delivery Reviews. 2013;65(9):1121-2.
2. Khan F, Ahmad SR. Polysaccharides and Their Derivatives for Versatile Tissue Engineering Application. Macromolecular Bioscience. 2013;13(4):395-421.
3. Garcia-Fuentes M, Alonso MJ. Chitosan-based drug nanocarriers: Where do we stand? Journal of Controlled Release. 2012;161(2):496-504.
4. Payne GF, Raghavan SR. Chitosan: a soft interconnect for hierarchical assembly of nano-scale components. Soft Matter. 2007;3(5):521-7.
5. Schneider H-J, Strongin RM. Supramolecular Interactions in Chemomechanical Polymers. Accounts of Chemical Research. 2009;42(10):1489-500.
6. Hsu L-W, Lee P-L, Chen C-T, Mi F-L, Juang J-H, Hwang S-M, et al. Elucidating the signaling mechanism of an epithelial tight-junction opening induced by chitosan. Biomaterials. 2012;33(26):6254-63.
7. Hsu L-W, Ho Y-C, Chuang E-Y, Chen C-T, Juang J-H, Su F-Y, et al. Effects of pH on molecular mechanisms of chitosan-integrin interactions and resulting tight-junction disruptions. Biomaterials. 2013;34(3):784-93.
8. Rosenthal R, Guenzel D, Finger C, Krug SM, Richter JF, Schulzke J-D, et al. The effect of chitosan on transcellular and paracellular mechanisms in the intestinal epithelial barrier. Biomaterials. 2012;33(9):2791-800.
9. Gorzelanny C, Poeppelmann B, Pappelbaum K, Moerschbacher BM, Schneider SW. Human macrophage activation triggered by chitotriosidase-mediated chitin and chitosan degradation. Biomaterials. 2010;31(33):8556-63.
10. Kean T, Thanou M. Biodegradation, biodistribution and toxicity of chitosan. Advanced Drug Delivery Reviews. 2010;62(1):3-11.
11. Minami S, OhOka M, Okamoto Y, Miyatake K, Matsuhashi A, Shigemasa Y, et al. Chitosan-inducing hemorrhagic pneumonia in dogs. Carbohydrate Polymers. 1996;29(3):241-6.
12. CarrenoGomez B, Duncan R. Evaluation of the biological properties of soluble chitosan and chitosan microspheres. International Journal of Pharmaceutics. 1997;148(2):231-40.
13. Baldrick P. The safety of chitosan as a pharmaceutical excipient. Regulatory Toxicology and Pharmacology. 2010;56(3):290-9.
14. Muzzarelli RAA. Human enzymatic activities related to the therapeutic administration of chitin derivatives. Cellular and Molecular Life Sciences. 1997;53(2):131-40.
15. Varum KM, Myhr MM, Hjerde RJN, Smidsrod O. In vitro degradation rates of partially N-acetylated chitosans in human serum. Carbohydrate Research. 1997;299(1-2):99-101.
16. Boateng JS, Matthews KH, Stevens HNE, Eccleston GM. Wound healing dressings and drug delivery systems: A review. Journal of Pharmaceutical Sciences. 2008;97(8):2892-923.
17. Prego C, Garcia M, Torres D, Alonso MJ. Transmucosal macromolecular drug delivery. Journal of Controlled Release. 2005;101(1-3):151-62.
18. Garcia-Fuentes M, Prego C, Torres D, Alonso MJ. A comparative study of the potential of solid triglyceride nanostructures coated with chitosan or poly(ethylene glycol) as carriers for oral calcitonin delivery. European Journal of Pharmaceutical Sciences. 2005;25(1):133-43.
19. Yang C, Cao M, Liu H, He Y, Xu J, Du Y, et al. The High and Low Molecular Weight Forms of Hyaluronan Have Distinct Effects on CD44 Clustering. Journal of Biological Chemistry. 2012;287(51):43094-107.
20. Girish KS, Kemparaju K. The magic glue hyaluronan and its eraser hyaluronidase: A biological overview. Life Sciences. 2007;80(21):1921-43.
21. Shen Y, Li Q, Tu J, Zhu J. Synthesis and characterization of low molecular weight hyaluronic acid-based cationic micelles for efficient siRNA delivery. Carbohydrate Polymers. 2009;77(1):95-104.

22. Scott JE. Supramolecular organization of extracellular matrix glycosaminoglycans, in vitro and in the tissues. The FASEB Journal. 1992;6(9):2639-45.
23. Pritchard K, Lansley AB, Martin GP, Helliwell M, Marriott C, Benedetti LM. Evaluation of the bioadhesive properties of hyaluronan derivatives: detachment weight and mucociliary transport rate studies. International Journal of Pharmaceutics. 1996;129(1):137-45.
24. Laurent TC, Laurent UBG, Fraser JRE. Functions of hyaluronan. Annals of the Rheumatic Diseases. 1995;54(5):429-32.
25. Lesley J, Hyman R, Kincade PW. CD44 and Its Interaction with Extracellular Matrix. In: Frank JD, editor. Advances in Immunology: Academic Press; 1993. p. 271-335.
26. Harada H, Takahashi M. CD44-dependent Intracellular and Extracellular Catabolism of Hyaluronic Acid by Hyaluronidase-1 and -2. Journal of Biological Chemistry. 2007;282(8):5597-607.
27. Knudson CB. Hyaluronan and CD44: Strategic players for cell–matrix interactions during chondrogenesis and matrix assembly. Birth Defects Research Part C: Embryo Today: Reviews. 2003;69(2):174-96.
28. Li H, Guo, L., Li, J., Liu, N., Qi, R., & Liu, J. Expression of
hyaluronan receptors CD44 and RHAMM in stomach cancers: relevance
with tumor progression. International Journal of Oncology. 2000;17(5):927-59.
29. Almalik A, Karimi S, Ouasti S, Donno R, Wandrey C, Day PJ, et al. Hyaluronic acid (HA) presentation as a tool to modulate and control the receptor-mediated uptake of HA-coated nanoparticles. Biomaterials. 2013;34(21):5369-80.
30. Zhou B, Weigel JA, Fauss L, Weigel PH. Identification of the Hyaluronan Receptor for Endocytosis (HARE). Journal of Biological Chemistry. 2000;275(48):37733-41.
31. Jadin L, Bookbinder LH, Frost GI. A comprehensive model of hyaluronan turnover in the mouse. Matrix Biology. 2012;31(2):81-9.
32. Harris EN, Kyosseva SV, Weigel JA, Weigel PH. Expression, Processing, and Glycosaminoglycan Binding Activity of the Recombinant Human 315-kDa Hyaluronic Acid Receptor for Endocytosis (HARE). Journal of Biological Chemistry. 2007;282(5):2785-97.
33. Luo Y, Ziebell MR, Prestwich GD. A Hyaluronic Acid−Taxol Antitumor Bioconjugate Targeted to Cancer Cells. Biomacromolecules. 2000;1(2):208-18.
34. J R Fraser WGK, T C Laurent, R N Cahill and N Vakakis. Uptake and degradation of hyaluronan in lymphatic tissue. Biochemical Journal. 1988;256:153-8.
35. Fraser JRE, Laurent TC, Laurent UBG. Hyaluronan: its nature, distribution, functions and turnover. Journal of Internal Medicine. 1997;242(1):27-33.
36. Jackson DG, Prevo R, Clasper S, Banerji S. LYVE-1, the lymphatic system and tumor lymphangiogenesis. Trends in Immunology. 2001;22(6):317-21.
37. Jackson DG. The Lymphatics Revisited: New Perspectives from the Hyaluronan Receptor LYVE-1. Trends in Cardiovascular Medicine. 2003;13(1):1-7.
38. Kohda D, Morton CJ, Parkar AA, Hatanaka H, Inagaki FM, Campbell ID, et al. Solution Structure of the Link Module: A Hyaluronan-Binding Domain Involved in Extracellular Matrix Stability and Cell Migration. Cell. 1996;86(5):767-75.
39. Milner CM, Day AJ. TSG-6: a multifunctional protein associated with inflammation. Journal of Cell Science. 2003;116(10):1863-73.
40. Becker LC, Bergfeld WF, Belsito DV, Klaassen CD, Marks JG, Shank RC, et al. Final Report of the Safety Assessment of Hyaluronic Acid, Potassium Hyaluronate, and Sodium Hyaluronate. International Journal of Toxicology. 2009;28(4 suppl):5-67.
41. Mizrahy S, Raz SR, Hasgaard M, Liu H, Soffer-Tsur N, Cohen K, et al. Hyaluronan-coated nanoparticles: The influence of the molecular weight on CD44-hyaluronan interactions and on the immune response. Journal of Controlled Release. 2011;156(2):231-8.
42. Ke C, Wang D, Sun Y, Qiao D, Ye H, Zeng X. Immunostimulatory and antiangiogenic activities of low molecular weight hyaluronic acid. Food and Chemical Toxicology. 2013;58(0):401-7.

43. Luo Y, Prestwich GD. Synthesis and Selective Cytotoxicity of a Hyaluronic Acid−Antitumor Bioconjugate. Bioconjugate Chemistry. 1999;10(5):755-63.
44. Edmond Auzenne SCG, Mojgan Khodadadian, Belinda Rivera, David Farquhar, Roger E Price, Murali Ravoori, Vikas Kundra, Ralph S Freedman, and Jim Klostergaard. Hyaluronic Acid-Paclitaxel: Antitumor Efficacy against CD44(+) Human Ovarian Carcinoma Xenografts. Neoplasia. 2007;9(6):479–86.
45. Rosato A, Banzato A, De Luca G, Renier D, Bettella F, Pagano C, et al. HYTAD1-p20: A new paclitaxel-hyaluronic acid hydrosoluble bioconjugate for treatment of superficial bladder cancer. Urologic Oncology: Seminars and Original Investigations. 2006;24(3):207-15.
46. Lee H, Mok H, Lee S, Oh Y-K, Park TG. Target-specific intracellular delivery of siRNA using degradable hyaluronic acid nanogels. Journal of Controlled Release. 2007;119(2):245-52.
47. Hyung Park J, Kwon S, Lee M, Chung H, Kim J-H, Kim Y-S, et al. Self-assembled nanoparticles based on glycol chitosan bearing hydrophobic moieties as carriers for doxorubicin: in vivo biodistribution and anti-tumor activity. Biomaterials. 2006;27(1):119-26.
48. Yoon HY, Koo H, Choi KY, Chan Kwon I, Choi K, Park JH, et al. Photo-crosslinked hyaluronic acid nanoparticles with improved stability for in vivo tumor-targeted drug delivery. Biomaterials. 2013;34(21):5273-80.
49. Han HS, Lee J, Kim HR, Chae SY, Kim M, Saravanakumar G, et al. Robust PEGylated hyaluronic acid nanoparticles as the carrier of doxorubicin: Mineralization and its effect on tumor targetability in vivo. Journal of Controlled Release. 2013;168(2):105-14.
50. Yoon HY, Koo H, Choi KY, Lee SJ, Kim K, Kwon IC, et al. Tumor-targeting hyaluronic acid nanoparticles for photodynamic imaging and therapy. Biomaterials. 2012;33(15):3980-9.
51. Lee D-E, Kim AY, Yoon HY, Choi KY, Kwon IC, Jeong SY, et al. Amphiphilic hyaluronic acid-based nanoparticles for tumor-specific optical/MR dual imaging. Journal of Materials Chemistry. 2012;22(21):10444-7.
52. Choi KY, Jeon EJ, Yoon HY, Lee BS, Na JH, Min KH, et al. Theranostic nanoparticles based on PEGylated hyaluronic acid for the diagnosis, therapy and monitoring of colon cancer. Biomaterials. 2012;33(26):6186-93.
53. Cho H-J, Yoon I-S, Yoon HY, Koo H, Jin Y-J, Ko S-H, et al. Polyethylene glycol-conjugated hyaluronic acid-ceramide self-assembled nanoparticles for targeted delivery of doxorubicin. Biomaterials. 2012;33(4):1190-200.
54. Shen Y, Wang B, Lu Y, Ouahab A, Li Q, Tu J. A novel tumor-targeted delivery system with hydrophobized hyaluronic acid–spermine conjugates (HHSCs) for efficient receptor-mediated siRNA delivery. International Journal of Pharmaceutics. 2011;414(1–2):233-43.
55. Han S-Y, Han HS, Lee SC, Kang YM, Kim I-S, Park JH. Mineralized hyaluronic acid nanoparticles as a robust drug carrier. Journal of Materials Chemistry. 2011;21(22):7996-8001.
56. Choi KY, Yoon HY, Kim J-H, Bae SM, Park R-W, Kang YM, et al. Smart Nanocarrier Based on PEGylated Hyaluronic Acid for Cancer Therapy. ACS Nano. 2011;5(11):8591-9.
57. Choi KY, Min KH, Yoon HY, Kim K, Park JH, Kwon IC, et al. PEGylation of hyaluronic acid nanoparticles improves tumor targetability in vivo. Biomaterials. 2011;32(7):1880-9.
58. Cho H-J, Yoon HY, Koo H, Ko S-H, Shim J-S, Lee J-H, et al. Self-assembled nanoparticles based on hyaluronic acid-ceramide (HA-CE) and Pluronic® for tumor-targeted delivery of docetaxel. Biomaterials. 2011;32(29):7181-90.
59. Upadhyay KK, Bhatt AN, Castro E, Mishra AK, Chuttani K, Dwarakanath BS, et al. In vitro and In vivo Evaluation of Docetaxel Loaded Biodegradable Polymersomes. Macromolecular Bioscience. 2010;10(5):503-12.
60. Choi KY, Chung H, Min KH, Yoon HY, Kim K, Park JH, et al. Self-assembled hyaluronic acid nanoparticles for active tumor targeting. Biomaterials. 2010;31(1):106-14.
61. Duceppe N, Tabrizian M. Factors influencing the transfection efficiency of ultra low molecular weight chitosan/hyaluronic acid nanoparticles. Biomaterials. 2009;30(13):2625-31.

62. Choi KY, Min KH, Na JH, Choi K, Kim K, Park JH, et al. Self-assembled hyaluronic acid nanoparticles as a potential drug carrier for cancer therapy: synthesis, characterization, and in vivo biodistribution. Journal of Materials Chemistry. 2009;19(24):4102-7.
63. Wang H, Zhao P, Liang X, Gong X, Song T, Niu R, et al. Folate-PEG coated cationic modified chitosan - Cholesterol liposomes for tumor-targeted drug delivery. Biomaterials. 2010;31(14):4129-38.
64. Min KH, Park K, Kim Y-S, Bae SM, Lee S, Jo HG, et al. Hydrophobically modified glycol chitosan nanoparticles-encapsulated camptothecin enhance the drug stability and tumor targeting in cancer therapy. Journal of Controlled Release. 2008;127(3):208-18.
65. Dufaÿ Wojcicki A, Hillaireau H, Nascimento TL, Arpicco S, Taverna M, Ribes S, et al. Hyaluronic acid-bearing lipoplexes: Physico-chemical characterization and in vitro targeting of the CD44 receptor. Journal of Controlled Release. 2012;162(3):545-52.
66. Toriyabe N, Hayashi Y, Hyodo M, Harashima H. Synthesis and Evaluation of Stearylated Hyaluronic Acid for the Active Delivery of Liposomes to Liver Endothelial Cells. Biological and Pharmaceutical Bulletin. 2011;34(7):1084-9.
67. Qhattal HSS, Liu X. Characterization of CD44-Mediated Cancer Cell Uptake and Intracellular Distribution of Hyaluronan-Grafted Liposomes. Molecular Pharmaceutics. 2011;8(4):1233-46.
68. Taetz S, Bochot A, Surace C, Arpicco S, Renoir JM, Schaefer UF, et al. Hyaluronic acid-modified DOTAP/DOPE liposomes for the targeted delivery of anti-telomerase siRNA to CD44-expressing lung cancer cells. Oligonucleotides. 2009;19(2):103-16.
69. Peer D, Margalit R. Loading mitomycin C inside long circulating hyaluronan targeted nano-liposomes increases its antitumor activity in three mice tumor models. International Journal of Cancer. 2004;108(5):780-9.
70. Peer D, Margalit, R. Tumor-Targeted Hyaluronan Nanoliposomes Increase the Antitumor Activity of Liposomal Doxorubicin in Syngeneic and Human Xenograft Mouse Tumor Models. Neoplasia. 2004;6(4):343-53.
71. Eliaz RE, Szoka FC. Liposome-encapsulated Doxorubicin Targeted to CD44: A Strategy to Kill CD44-overexpressing Tumor Cells. Cancer Research. 2001;61(6):2592-601.
72. Siew A, Le H, Thiovolet M, Gellert P, Schatzlein A, Uchegbu I. Enhanced Oral Absorption of Hydrophobic and Hydrophilic Drugs Using Quaternary Ammonium Palmitoyl Glycol Chitosan Nanoparticles. Molecular Pharmaceutics. 2012;9(1):14-28.
73. Lalatsa A, Garrett NL, Ferrarelli T, Moger J, Schaetzlein AG, Uchegbu IF. Delivery of Peptides to the Blood and Brain after Oral Uptake of Quaternary Ammonium Palmitoyl Glycol Chitosan Nanoparticles. Molecular Pharmaceutics. 2012;9(6):1764-74.
74. Thompson CJ, Tetley L, Uchegbu IF, Cheng WP. The complexation between novel comb shaped amphiphilic polyallylamine and insulin-Towards oral insulin delivery. International Journal of Pharmaceutics. 2009;376(1-2):46-55.
75. Uchegbu IF, Sadiq L, Pardakhty A, El-Hammadi M, Gray AI, Tetley L, et al. Gene transfer with three amphiphilic glycol chitosans - the degree of polymerisation is the main controller of transfection efficiency. Journal of Drug Targeting. 2004;12(8):527-39.
76. María de la Fuente BS, María J. Alonso. Design of novel polysaccharidic nanostructures for gene delivery. Nanotechnology. 2008;19:075105.
77. Fuente Mdl, Seijo B, Alonso MJ. Bioadhesive hyaluronan–chitosan nanoparticles can transport genes across the ocular mucosa and transfect ocular tissue. Gene Therapy. 2008;15(9):668-76.
78. de la Fuente M, Seijo B, Alonso MJ. Novel Hyaluronic Acid-Chitosan Nanoparticles for Ocular Gene Therapy. Investigative Ophthalmology & Visual Science. 2008;49(5):2016-24.
79. Calvo P, Remuñan-López C, Vila-Jato J, Alonso M. Chitosan and Chitosan/Ethylene Oxide-Propylene Oxide Block Copolymer Nanoparticles as Novel Carriers for Proteins and Vaccines. Pharmaceutical Research. 1997;14(10):1431-6.

80. Sarmento B, Ribeiro A, Veiga F, Sampaio P, Neufeld R, Ferreira D. Alginate/Chitosan nanoparticles are effective for oral insulin delivery. Pharmaceutical Research. 2007;24(12):2198-206.
81. Sarmento B, Ribeiro A, Veiga F, Ferreira D, Neufeld R. Oral bioavailability of insulin contained in polysaccharide nanoparticles. Biomacromolecules. 2007;8(10):3054-60.
82. Mi F-L, Wu Y-Y, Lin Y-H, Sonaje K, Ho Y-C, Chen C-T, et al. Oral delivery of peptide drugs using nanoparticles self-assembled by poly(gamma-glutamic acid) and a chitosan derivative functionalized by trimethylation. Bioconjugate Chemistry. 2008;19(6):1248-55.
83. Goycoolea FM, Lollo G, Remunan-Lopez C, Quaglia F, Alonso MJ. Chitosan-Alginate Blended Nanoparticles as Carriers for the Transmucosal Delivery of Macromolecules. Biomacromolecules. 2009;10(7):1736-43.
84. Ravina M, Cubillo E, Olmeda D, Novoa-Carballal R, Fernandez-Megia E, Riguera R, et al. Hyaluronic Acid/Chitosan-g-Poly(ethylene glycol) Nanoparticles for Gene Therapy: An Application for pDNA and siRNA Delivery. Pharmaceutical Research. 2010;27(12):2544-55.
85. Sonaje K, Lin K-J, Wey S-P, Lin C-K, Yeh T-H, Nguyen H-N, et al. Biodistribution, pharmacodynamics and pharmacokinetics of insulin analogues in a rat model: Oral delivery using pH-Responsive nanoparticles vs. subcutaneous injection. Biomaterials. 2010;31(26):6849-58.
86. Sonaje K, Chen Y-J, Chen H-L, Wey S-P, Juang J-H, Nguyen H-N, et al. Enteric-coated capsules filled with freeze-dried chitosan/poly(gamma-glutamic acid) nanoparticles for oral insulin delivery. Biomaterials. 2010;31(12):3384-94.
87. Sonaje K, Lin K-J, Wang J-J, Mi F-L, Chen C-T, Juang J-H, et al. Self-Assembled pH-Sensitive Nanoparticles: A Platform for Oral Delivery of Protein Drugs. Advanced Functional Materials. 2010;20(21):3695-700.
88. Moon H-J, Lee J-S, Talactac MR, Chowdhury MYE, Kim J-H, Park M-E, et al. Mucosal immunization with recombinant influenza hemagglutinin protein and poly gamma-glutamate/chitosan nanoparticles induces protection against highly pathogenic influenza A virus. Veterinary Microbiology. 2012;160(3-4):277-89.
89. Chuang E-Y, Nguyen GTH, Su F-Y, Lin K-J, Chen C-T, Mi F-L, et al. Combination therapy via oral co-administration of insulin- and exendin-4-loaded nanoparticles to treat type 2 diabetic rats undergoing OGTT. Biomaterials. 2013;34(32):7994-8001.
90. Maestrelli F, Garcia-Fuentes M, Mura P, Alonso MJ. A new drug nanocarrier consisting of chitosan and hydoxypropyleyclodextrin. European Journal of Pharmaceutics and Biopharmaceutics. 2006;63(2):79-86.
91. Trapani A, Garcia-Fuentes M, Alonso MJ. Novel drug nanocarriers combining hydrophilic cyclodextrins and chitosan. Nanotechnology. 2008;19(18).
92. Teijeiro-Osorio D, Remunan-Lopez C, Jose Alonso M. Chitosan/cyclodextrin nanoparticles can efficiently transfect the airway epithelium in vitro. European Journal of Pharmaceutics and Biopharmaceutics. 2009;71(2):257-63.
93. Trapani A, Lopedota A, Franco M, Cioffi N, Ieva E, Garcia-Fuentes M, et al. A comparative study of chitosan and chitosan/cyclodextrin nanoparticles as potential carriers for the oral delivery of small peptides. European Journal of Pharmaceutics and Biopharmaceutics. 2010;75(1):26-32.
94. Nahaei M, Valizadeh H, Baradaran B, Nahaei MR, Asgari D, Hallaj-Nezhadi S, et al. Preparation and characterization of chitosan/beta-cyclodextrin nanoparticles containing plasmid DNA encoding interleukin-12. Drug research. 2013;63(1):7-12.
95. Werle M, Takeuchi H. Chitosan-aprotinin coated liposomes for oral peptide delivery: Development, characterisation and in vivo evaluation. International Journal of Pharmaceutics. 2009;370(1-2):26-32.
96. Takeuchi H, Matsui Y, Yamamoto H, Kawashima Y. Mucoadhesive properties of carbopol or chitosan-coated liposomes and their effectiveness in the oral administration of calcitonin to rats. Journal of Controlled Release. 2003;86(2-3):235-42.

97. Liu W, Liu J, Liu W, Li T, Liu C. Improved Physical and in Vitro Digestion Stability of a Polyelectrolyte Delivery System Based on Layer-by-Layer Self-Assembly Alginate-Chitosan-Coated Nanoliposomes. Journal of Agricultural and Food Chemistry. 2013;61(17):4133-44.
98. Kowapradit J, Apirakaramwong A, Ngawhirunpat T, Rojanarata T, Sajomsang W, Opanasopit P. Methylated N-(4-N,N-dimethylaminobenzyl) chitosan coated liposomes for oral protein drug delivery. European Journal of Pharmaceutical Sciences. 2012;47(2):359-66.
99. Calvo P, VilaJato JL, Alonso MJ. Evaluation of cationic polymer-coated nanocapsules as ocular drug carriers. International Journal of Pharmaceutics. 1997;153(1):41-50.
100. Oyarzun-Ampuero FA, Rivera-Rodríguez GR, Alonso MJ, Torres D. Hyaluronan nanocapsules as a new vehicle for intracellular drug delivery. European Journal of Pharmaceutical Sciences. 2013;49(4):483-90.
101. Calvo P, RemunanLopez C, VilaJato JL, Alonso MJ. Development of positively charged colloidal drug carriers: Chitosan coated polyester nanocapsules and submicron-emulsions. Colloid and Polymer Science. 1997;275(1):46-53.
102. Santander-Ortega MJ, Peula-Garcia JM, Goycoolea FM, Ortega-Vinuesa JL. Chitosan nanocapsules: Effect of chitosan molecular weight and acetylation degree on electrokinetic behaviour and colloidal stability. Colloids and Surfaces B-Biointerfaces. 2011;82(2):571-80.
103. Goycoolea FM, Valle-Gallego A, Stefani R, Menchicchi B, David L, Rochas C, et al. Chitosan-based nanocapsules: physical characterization, stability in biological media and capsaicin encapsulation. Colloid and Polymer Science. 2012;290(14):1423-34.
104. Yang X-y, Li Y-x, Li M, Zhang L, Feng L-x, Zhang N. Hyaluronic acid-coated nanostructured lipid carriers for targeting paclitaxel to cancer. Cancer Letters. 2013;334(2):338-45.
105. Li X, Qi J, Xie Y, Zhang X, Hu S, Xu Y, et al. Nanoemulsions coated with alginate/chitosan as oral insulin delivery systems: preparation, characterization, and hypoglycemic effect in rats. International Journal of Nanomedicine. 2013;8:23-32.
106. Raviña M, Cubillo E, Olmeda D, Novoa-Carballal R, Fernandez-Megia E, Riguera R, et al. Hyaluronic Acid/Chitosan-g-Poly(ethylene glycol) Nanoparticles for Gene Therapy: An Application for pDNA and siRNA Delivery. Pharmaceutical Research. 2010;27(12):2544-55.
107. Verheul RJ, Slütter B, Bal SM, Bouwstra JA, Jiskoot W, Hennink WE. Covalently stabilized trimethyl chitosan-hyaluronic acid nanoparticles for nasal and intradermal vaccination. Journal of Controlled Release. 2011;156(1):46-52.
108. Han L, Zhao Y, Yin L, Li R, Liang Y, Huang H, et al. Insulin-Loaded pH-Sensitive Hyaluronic Acid Nanoparticles Enhance Transcellular Delivery. AAPS PharmSciTech. 2012;13(3):836-45.
109. Fakhari A, Phan Q, Thakkar SV, Middaugh CR, Berkland C. Hyaluronic Acid Nanoparticles Titrate the Viscoelastic Properties of Viscosupplements. Langmuir. 2013;29(17):5123-31.
110. Zambito Y, Felice F, Fabiano A, Di Stefano R, Di Colo G. Mucoadhesive nanoparticles made of thiolated quaternary chitosan crosslinked with hyaluronan. Carbohydrate Polymers. 2013;92(1):33-9.
111. Zhang J, He C, Tang C, Yin C. Ternary Polymeric Nanoparticles for Oral siRNA Delivery. Pharmaceutical Research. 2013;30(5):1228-39.
112. Esposito G, Geninatti Crich S, Aime S. Efficient Cellular Labeling by CD44 Receptor-Mediated Uptake of Cationic Liposomes Functionalized with Hyaluronic Acid and Loaded with MRI Contrast Agents. ChemMedChem. 2008;3(12):1858-62.
113. Jiang T, Zhang Z, Zhang Y, Lv H, Zhou J, Li C, et al. Dual-functional liposomes based on pH-responsive cell-penetrating peptide and hyaluronic acid for tumor-targeted anticancer drug delivery. Biomaterials. 2012;33(36):9246-58.
114. Baier G, Cavallaro A, Vasilev K, Mailänder V, Musyanovych A, Landfester K. Enzyme Responsive Hyaluronic Acid Nanocapsules Containing Polyhexanide and Their Exposure to Bacteria To Prevent Infection. Biomacromolecules. 2013;14(4):1103-12.
115. Barbault-Foucher S, Gref R, Russo P, Guechot J, Bochot A. Design of poly-ε-caprolactone nanospheres coated with bioadhesive hyaluronic acid for ocular delivery. Journal of Controlled Release. 2002;83(3):365-75.

116. Dufes C, Muller JM, Couet W, Olivier JC, Uchegbu IF, Schatzlein AG. Anticancer drug delivery with transferrin targeted polymeric chitosan vesicles. Pharmaceutical Research. 2004;21(1):101-7.
117. Verheul RJ, Hagenaars N, van Es T, van Gaal EVB, de Jong PHJLF, Bruijns S, et al. A step-by-step approach to study the influence of N-acetylation on the adjuvanticity of N,N,N-trimethyl chitosan (TMC) in an intranasal nanoparticulate influenza virus vaccine. European Journal of Pharmaceutical Sciences. 2012;45(4):467-74.
118. Tafaghodi M, Saluja V, Kersten GFA, Kraan H, Sluetter B, Amorij J-P, et al. Hepatitis B surface antigen nanoparticles coated with chitosan and trimethyl chitosan: Impact of formulation on physicochemical and immunological characteristics. Vaccine. 2012;30(36):5341-8.
119. Subbiah R, Ramalingam P, Ramasundaram S, Kim DY, Park K, Ramasamy MK, et al. N,N,N-Trimethyl chitosan nanoparticles for controlled intranasal delivery of HBV surface antigen. Carbohydrate Polymers. 2012;89(4):1289-97.
120. Bal SM, Slutter B, Verheul R, Bouwstra JA, Jiskoot W. Adjuvanted, antigen loaded N-trimethyl chitosan nanoparticles for nasal and intradermal vaccination: Adjuvant- and site-dependent immunogenicity in mice. European Journal of Pharmaceutical Sciences. 2012;45(4):475-81.
121. Slutter B, Jiskoot W. Dual role of CpG as immune modulator and physical crosslinker in ovalbumin loaded N-trimethyl chitosan (TMC) nanoparticles for nasal vaccination. Journal of Controlled Release. 2010;148(1):117-21.
122. Hagenaars N, Verheul RJ, Mooren I, de Jong PHJLF, Mastrobattista E, Glansbeek HL, et al. Relationship between structure and adjuvanticity of N,N,N-trimethyl chitosan (TMC) structural variants in a nasal influenza vaccine. Journal of Controlled Release. 2009;140(2):126-33.
123. Amidi M, Romeijn SG, Verhoef JC, Junginger HE, Bungener L, Huckriede A, et al. N-Trimethyl chitosan (TMC) nanoparticles loaded with influenza subunit antigen for intranasal vaccination: Biological properties and immunogenicity in a mouse model. Vaccine. 2007;25(1):144-53.
124. Sharma S, Benson HAE, Mukkur TKS, Rigby P, Chen Y. Preliminary studies on the development of IgA-loaded chitosan-dextran sulphate nanoparticles as a potential nasal delivery system for protein antigens. Journal of Microencapsulation. 2013;30(3):283-94.
125. Wu Y, Wu S, Hou L, Wei W, Zhou M, Su Z, et al. Novel thermal-sensitive hydrogel enhances both humoral and cell-mediated immune responses by intranasal vaccine delivery. European Journal of Pharmaceutics and Biopharmaceutics. 2012;81(3):486-97.
126. Vila A, Sanchez A, Janes K, Behrens I, Kissel T, Jato JLV, et al. Low molecular weight chitosan nanoparticles as new carriers for nasal vaccine delivery in mice. European Journal of Pharmaceutics and Biopharmaceutics. 2004;57(1):123-31.
127. Nagamoto T, Hattori Y, Takayama K, Maitani Y. Novel chitosan particles and chitosan-coated emulsions inducing immune response via intranasal vaccine delivery. Pharmaceutical Research. 2004;21(4):671-4.
128. Csaba N, Koping-Hoggard M, Fernandez-Megia E, Novoa-Carballal R, Riguera R, Jose Alonso M. Ionically Crosslinked Chitosan Nanoparticles as Gene Delivery Systems: Effect of PEGylation Degree on In Vitro and In Vivo Gene Transfer. Journal of Biomedical Nanotechnology. 2009;5(2):162-71.
129. Raghuwanshi D, Mishra V, Das D, Kaur K, Suresh MR. Dendritic Cell Targeted Chitosan Nanoparticles for Nasal DNA Immunization against SARS CoV Nucleocapsid Protein. Molecular Pharmaceutics. 2012;9(4):946-56.
130. Yao W, Peng Y, Du M, Luo J, Zong L. Preventative vaccine-loaded mannosylated chitosan nanoparticles intended for nasal mucosal delivery enhance immune responses and potent tumor immunity. Molecular Pharmaceutics. 2013;10(8):2904-14.

131. Fernandez-Urrusuno R, Calvo P, Remunan-Lopez C, Vila-Jato JL, Alonso MJ. Enhancement of nasal absorption of insulin using chitosan nanoparticles. Pharmaceutical Research. 1999;16(10):1576-81.
132. Wang X, Zheng C, Wu Z, Teng D, Zhang X, Wang Z, et al. Chitosan-NAC Nanoparticles as a Vehicle for Nasal Absorption Enhancement of Insulin. Journal of Biomedical Materials Research Part B-Applied Biomaterials. 2009;88B(1):150-61.
133. Simon M, Wittmar M, Kissel T, Linn T. Insulin containing nanocomplexes formed by self-assembly from biodegradable amine-modified poly(vinyl alcohol)-graft-poly(L-lactide): Bioavailability and nasal tolerability in rats. Pharmaceutical Research. 2005;22(11):1879-86.
134. du Plessis LH, Kotze AF, Junginger HE. Nasal and rectal delivery of insulin with chitosan and N-trimethyl chitosan chloride. Drug Delivery. 2010;17(6):399-407.
135. Jiang M, Gan L, Zhu C, Dong Y, Liu J, Gan Y. Cationic core-shell liponanoparticles for ocular gene delivery. Biomaterials. 2012;33(30):7621-30.
136. Klausner EA, Zhang Z, Chapman RL, Multack RF, Volin MV. Ultrapure chitosan oligomers as carriers for corneal gene transfer. Biomaterials. 2010;31(7):1814-20.
137. Lee D, Zhang W, Shirley SA, Kong X, Hellermann GR, Lockey RF, et al. Thiolated chitosan/DNA nanocomplexes exhibit enhanced and sustained gene delivery. Pharmaceutical Research. 2007;24(1):157-67.
138. Yin L, Song Z, Qu Q, Kim KH, Zheng N, Yao C, et al. Supramolecular Self-Assembled Nanoparticles Mediate Oral Delivery of Therapeutic TNF-alpha siRNA against Systemic Inflammation. Angewandte Chemie-International Edition. 2013;52(22):5757-61.
139. He C, Yin L, Tang C, Yin C. Multifunctional polymeric nanoparticles for oral delivery of TNF-alpha siRNA to macrophages. Biomaterials. 2013;34(11):2843-54.
140. Mukhopadhyay P, Sarkar K, Chakraborty M, Bhattacharya S, Mishra R, Kundu PP. Oral insulin delivery by self-assembled chitosan nanoparticles: In vitro and in vivo studies in diabetic animal model. Materials Science & Engineering C-Materials for Biological Applications. 2013;33(1):376-82.
141. Elsayed A, Al-Remawi M, Qinna N, Farouk A, Al-Sou'od KA, Badwan AA. Chitosan-Sodium Lauryl Sulfate Nanoparticles as a Carrier System for the In Vivo Delivery of Oral Insulin. Aaps Pharmscitech. 2011;12(3):958-64.
142. Elsayed A, Al Remawi M, Qinna N, Farouk A, Badwan A. Formulation and characterization of an oily-based system for oral delivery of insulin. European Journal of Pharmaceutics and Biopharmaceutics. 2009;73(2):269-79.
143. Sarmento B, Ferreira DC, Jorgensen L, van de Weert M. Probing insulin's secondary structure after entrapment into alginate/chitosan nanoparticles. European Journal of Pharmaceutics and Biopharmaceutics. 2007;65(1):10-7.
144. Woitiski CB, Neufeld RJ, Ribeiro AJ, Veiga F. Colloidal carrier integrating biomaterials for oral insulin delivery: Influence of component formulation on physicochemical and biological parameters. Acta Biomaterialia. 2009;5(7):2475-84.
145. Woitiski CB, Veiga F, Ribeiro A, Neufeld R. Design for optimization of nanoparticles integrating biomaterials for orally dosed insulin. European Journal of Pharmaceutics and Biopharmaceutics. 2009;73(1):25-33.
146. Woitiski CB, Neufeld RJ, Soares AF, Figueiredo IV, Veiga FJ, Carvalho RA. Evaluation of hepatic glucose metabolism via gluconeogenesis and glycogenolysis after oral administration of insulin nanoparticles. Drug Development and Industrial Pharmacy. 2012;38(12):1441-50.
147. Woitiski CB, Sarmento B, Carvalho RA, Neufeld RJ, Veiga F. Facilitated nanoscale delivery of insulin across intestinal membrane models. International Journal of Pharmaceutics. 2011;412(1-2):123-31.
148. Jin Y, Song Y, Zhu X, Zhou D, Chen C, Zhang Z, et al. Goblet cell-targeting nanoparticles for oral insulin delivery and the influence of mucus on insulin transport. Biomaterials. 2012;33(5):1573-82.

149. Sonaje K, Lin Y-H, Juang J-H, Wey S-P, Chen C-T, Sung H-W. In vivo evaluation of safety and efficacy of self-assembled nanoparticles for oral insulin delivery. Biomaterials. 2009;30(12):2329-39.
150. Prego C, Torres D, Alonso MJ. Chitosan nanocapsules: a new carrier for nasal peptide delivery. Journal of Drug Delivery Science and Technology. 2006;16(5):331-7.
151. Prego C, Torres D, Alonso MJ. Chitosan nanocapsules as carriers for oral peptide delivery: Effect of chitosan molecular weight and type of salt on the in vitro behaviour and in vivo effectiveness. Journal of Nanoscience and Nanotechnology. 2006;6(9-10):2921-8.
152. Prego C, Torres D, Fernandez-Megia E, Novoa-Carballal R, Quinoa E, Alonso MJ. Chitosan-PEG nanocapsules as new carriers for oral peptide delivery - Effect of chitosan pegylation degree. Journal of Controlled Release. 2006;111(3):299-308.
153. Prego C, Fabre M, Torres D, Alonso MJ. Efficacy and mechanism of action of chitosan nanocapsules for oral peptide delivery. Pharmaceutical Research. 2006;23(3):549-56.
154. Grabovac V, Guggi D, Bernkop-Schnürch A. Comparison of the mucoadhesive properties of various polymers. Advanced Drug Delivery Reviews. 2005;57(11):1713-23.
155. Snyman D., Hamman J. and Kotze A. Evaluation of the Mucoadhesive Properties of N-Trimethyl Chitosan Chloride. Drug Development and Industrial Pharmacy. 2003;29(1):61-9.
156. Greaves JL, Wilson CG. Treatment of diseases of the eye with mucoadhesive delivery systems. Advanced Drug Delivery Reviews. 1993;11(3):349-83.
157. Snyman D, Hamman JH, Kotze AF. Evaluation of the mucoadhesive properties of N-trimethyl chitosan chloride. Drug Development and Industrial Pharmacy. 2003;29(1):61-9.
158. De Campos AM, Sanchez A, Alonso MJ. Chitosan nanoparticles: a new vehicle for the improvement of the delivery of drugs to the ocular surface. Application to cyclosporin A. International Journal of Pharmaceutics. 2001;224(1-2):159-68.
159. De Campos AM, Sanchez A, Gref R, Calvo P, Alonso MJ. The effect of a PEG versus a chitosan coating on the interaction of drug colloidal carriers with the ocular mucosa. European Journal of Pharmaceutical Sciences. 2003;20(1):73-81.
160. de Campos AM, Diebold Y, Carvalho ELS, Sanchez A, Alonso MJ. Chitosan nanoparticles as new ocular drug delivery systems: in vitro stability, in vivo fate, and cellular toxicity. Pharmaceutical Research. 2004;21(5):803-10.
161. Diebold Y, Jarrin M, Saez V, Carvalho ELS, Orea M, Calonge M, et al. Ocular drug delivery by liposome-chitosan nanoparticle complexes (LCS-NP). Biomaterials. 2007;28(8):1553-64.
162. Carvalho ELS, Grenha A, Remunan-Lopez C, Jose Alonso M, Seijo B. MUCOSAL DELIVERY OF LIPOSOME-CHITOSAN NANOPARTICLE COMPLEXES. In: Duzgunes N, editor. Methods in Enzymology Liposomes, Pt G2009. p. 289-312.
163. Battaglia L, D'Addino I, Peira E, Trotta M, Gallarate M. Solid lipid nanoparticles prepared by coacervation method as vehicles for ocular cyclosporine. Journal of Drug Delivery Science and Technology. 2012;22(2):125-30.
164. Yenice İ, Mocan MC, Palaska E, Bochot A, Bilensoy E, Vural İ, et al. Hyaluronic acid coated poly-ε-caprolactone nanospheres deliver high concentrations of cyclosporine A into the cornea. Experimental Eye Research. 2008;87(3):162-7.
165. Teijeiro-Osorio D, Remunan-Lopez C, Jose Alonso M. New Generation of Hybrid Poly/Oligosaccharide Nanoparticles as Carriers for the Nasal Delivery of Macromolecules. Biomacromolecules. 2009;10(2):243-9.
166. Bhumkar DR, Joshi HM, Sastry M, Pokharkar VB. Chitosan reduced gold nanoparticles as novel carriers for transmucosal delivery of insulin. Pharmaceutical Research. 2007;24(8):1415-26.
167. Vila A, Sanchez A, Tobio M, Calvo P, Alonso MJ. Design of biodegradable particles for protein delivery. Journal of Controlled Release. 2002;78(1-3):15-24.

168. Prego C, Paolicelli P, Diaz B, Vicente S, Sanchez A, Gonzalez-Fernandez A, et al. Chitosan-based nanoparticles for improving immunization against hepatitis B infection. Vaccine. 2010;28(14):2607-14.
169. Vicente SPMD-F, Belén; González-Fernández África; Sanchez, Alejandro; Alonso, MJ. Co-delivery of viral proteins and TLR7 agonist from polysaccharide nanocapsules: a needle-free vaccination strategy. Journal of Controlled Release. 2013:In press.
170. Slutter B, Plapied L, Fievez V, Alonso Sande M, des Rieux A, Schneider Y-J, et al. Mechanistic study of the adjuvant effect of biodegradable nanoparticles in mucosal vaccination. Journal of Controlled Release. 2009;138(2):113-21.
171. Slutter B, Soema PC, Ding Z, Verheul R, Hennink W, Jiskoot W. Conjugation of ovalbumin to trimethyl chitosan improves immunogenicity of the antigen. Journal of Controlled Release. 2010;143(2):207-14.
172. Slutter B, Bal S, Keijzer C, Mallants R, Hagenaars N, Que I, et al. Nasal vaccination with N-trimethyl chitosan and PLGA based nanoparticles: Nanoparticle characteristics determine quality and strength of the antibody response in mice against the encapsulated antigen. Vaccine. 2010;28(38):6282-91.
173. Sayin B, Somavarapu S, Li XW, Sesardic D, Senel S, Alpar OH. TMC-MCC (N-trimethyl chitosan-mono-N-carboxymethyl chitosan) nanocomplexes for mucosal delivery of vaccines. European Journal of Pharmaceutical Sciences. 2009;38(4):362-9.
174. Assaf SM, Al-Jbour ND, Eftaiha AaF, Elsayed AM, Al-Remawi MM, Qinna NA, et al. Factors Involved in Formulation of Oily Delivery System for Proteins Based on PEG-8 Caprylic/Capric Glycerides and Polyglyceryl-6 Dioleate in a Mixture of Oleic Acid with Chitosan. Journal of Dispersion Science and Technology. 2011;32(5):623-33.
175. Sonaje K, Lin K-J, Tseng MT, Wey S-P, Su F-Y, Chuang E-Y, et al. Effects of chitosan-nanoparticle-mediated tight junction opening on the oral absorption of endotoxins. Biomaterials. 2011;32(33):8712-21.
176. Nguyen H-N, Wey S-P, Juang J-H, Sonaje K, Ho Y-C, Chuang E-Y, et al. The glucose-lowering potential of exendin-4 orally delivered via a pH-sensitive nanoparticle vehicle and effects on subsequent insulin secretion in vivo. Biomaterials. 2011;32(10):2673-82.
177. Janes KA, Fresneau MP, Marazuela A, Fabra A, Alonso MJ. Chitosan nanoparticles as delivery systems for doxorubicin. Journal of Controlled Release. 2001;73(2-3):255-67.
178. Lozano MV, Torrecilla D, Torres D, Vidal A, Dominguez F, Alonso MJ. Highly efficient system to deliver taxanes into tumor cells: Docetaxel-loaded chitosan oligomer colloidal carriers. Biomacromolecules. 2008;9(8):2186-93.
179. Rata-Aguilar A, Sanchez-Moreno P, Jodar-Reyes AB, Martin-Rodriguez A, Boulaiz H, Marchal-Corrales JA, et al. Colloidal stability and "in vitro" antitumor targeting ability of lipid nanocapsules coated by folate-chitosan conjugates. Journal of Bioactive and Compatible Polymers. 2012;27(4):388-404.
180. Aktas Y, Yemisci M, Andrieux K, Gursoy RN, Alonso MJ, Fernandez-Megia E, et al. Development and brain delivery of chitosan-PEG nanoparticles functionalized with the monoclonal antibody OX26. Bioconjugate Chemistry. 2005;16(6):1503-11.
181. Zhao Q-Q, Hu Y-L, Zhou Y, Li N, Han M, Tang G-P, et al. Gene-carried hepatoma targeting complex induced high gene transfection efficiency with low toxicity and significant antitumor activity. International Journal of Nanomedicine. 2012;7:3191-202.
182. Iyer AK, Khaled G, Fang J, Maeda H. Exploiting the enhanced permeability and retention effect for tumor targeting. Drug Discovery Today. 2006;11(17–18):812-8.
183. Torchilin V. Tumor delivery of macromolecular drugs based on the EPR effect. Advanced Drug Delivery Reviews. 2011;63(3):131-5.
184. Dan P, Jeffrey MK, Seungpyo H, Omid CF, Rimona M, Robert L. Nanocarriers as an emerging platform for cancer therapy. Nature Nanotechnology. 2007;2(12):751-60.

185. Min HS, Son S, Lee TW, Koo H, Yoon HY, Na JH, et al. Liver-Specific and Echogenic Hyaluronic Acid Nanoparticles Facilitating Liver Cancer Discrimination. Advanced Functional Materials. 2013:n/a-n/a.
186. Saddoughi S, Song P, Ogretmen B. Roles of Bioactive Sphingolipids in Cancer Biology and Therapeutics. In: Quinn P, Wang X, editors. Lipids in Health and Disease: Springer Netherlands; 2008. p. 413-40.
187. Leong KW, Mao HQ, Truong-Le VL, Roy K, Walsh SM, August JT. DNA-polycation nanospheres as non-viral gene delivery vehicles. Journal of Controlled Release. 1998;53(1-3):183-93.
188. Roy K, Mao HQ, Huang SK, Leong KW. Oral gene delivery with chitosan-DNA nanoparticles generates immunologic protection in a murine model of peanut allergy. Nature Medicine. 1999;5(4):387-91.
189. Mao HQ, Roy K, Troung-Le VL, Janes KA, Lin KY, Wang Y, et al. Chitosan-DNA nanoparticles as gene carriers: synthesis, characterization and transfection efficiency. Journal of Controlled Release. 2001;70(3):399-421.
190. Shukla SK, Mishra AK, Arotiba OA, Mamba BB. Chitosan-based nanomaterials: A state-of-the-art review. International Journal of Biological Macromolecules. 2013;59:46-58.
191. Csaba N, Koeping-Hoeggard M, Jose Alonso M. Ionically crosslinked chitosan/tripolyphosphate nanoparticles for oligonucleotide and plasmid DNA delivery. International Journal of Pharmaceutics. 2009;382(1-2):205-14.
192. Jiang H-L, Xu C-X, Kim Y-K, Arote R, Jere D, Lim H-T, et al. The suppression of lung tumorigenesis by aerosol-delivered folate-chitosan-graft-polyethylenimine/Akt1 shRNA complexes through the Akt signaling pathway. Biomaterials. 2009;30(29):5844-52.
193. Steg AD, Katre AA, Goodman B, Han H-D, Nick AM, Stone RL, et al. Targeting the Notch Ligand Jagged1 in Both Tumor Cells and Stroma in Ovarian Cancer. Clinical Cancer Research. 2011;17(17):5674-85.
194. Ishii T, Okahata Y, Sato T. Mechanism of cell transfection with plasmid/chitosan complexes. Biochimica Et Biophysica Acta-Biomembranes. 2001;1514(1):51-64.
195. Richard I, Thibault M, De Crescenzo G, Buschmann MD, Lavertu M. Ionization Behavior of Chitosan and Chitosan-DNA Polyplexes Indicate That Chitosan Has a Similar Capability to Induce a Proton-Sponge Effect as PEI. Biomacromolecules. 2013;14(6):1732-40.
196. Katas H, Alpar HO. Development and characterisation of chitosan nanoparticles for siRNA delivery. Journal of Controlled Release. 2006;115(2):216-25.
197. Haas J, Kumar M, Borchard G, Bakowsky U, Lehr CM. Preparation and characterization of chitosan and trimethyl-chitosanmodified poly-(epsilon-caprolactone) nanoparticles as DNA carriers. Aaps Pharmscitech. 2005;6(1).
198. Yuan X, Shah BA, Kotadia NK, Li J, Gu H, Wu Z. The Development and Mechanism Studies of Cationic Chitosan-Modified Biodegradable PLGA Nanoparticles for Efficient siRNA Drug Delivery. Pharmaceutical Research. 2010;27(7):1285-95.
199. de la Fuente M, Seijo B, Alonso MJ. Bioadhesive hyaluronan-chitosan nanoparticles can transport genes across the ocular mucosa and transfect ocular tissue. Gene Therapy. 2008;15(9):668-76.
200. Strand SP, Issa MM, Christensen BE, Varum KM, Artursson P. Tailoring of Chitosans for Gene Delivery: Novel Self-Branched Glycosylated Chitosan Oligomers with Improved Functional Properties. Biomacromolecules. 2008;9(11):3268-76.
201. Gao Y, Zhang Z, Chen L, Gu W, Li Y. Synthesis of 6-N,N,N-Trimethyltriazole Chitosan via "Click Chemistry" and Evaluation for Gene Delivery. Biomacromolecules. 2009;10(8):2175-82.
202. Germershaus O, Mao S, Sitterberg J, Bakowsky U, Kissel T. Gene delivery using chitosan, trimethyl chitosan or polyethylenglycol-graft-trimethyl chitosan block copolymers: Establishment of structure-activity relationships in vitro. Journal of Controlled Release. 2008;125(2):145-54.

203. Turan K, Nagata K. Chitosan-DNA nanoparticles: The effect of cell type and hydrolysis of chitosan on in vitro DNA transfection. Pharmaceutical Development and Technology. 2006;11(4):503-12.
204. Fattahi A, Sadrjavadi K, Golozar MA, Varshosaz J, Fathi M-H, Mirmohammad-Sadeghi H. Preparation and characterization of oligochitosan-tragacanth nanoparticles as a novel gene carrier. Carbohydrate Polymers. 2013;97(2):277-83.
205. Wang B, Zhang S, Cui S, Yang B, Zhao Y, Chen H, et al. Chitosan enhanced gene delivery of cationic liposome via non-covalent conjugation. Biotechnology Letters. 2012;34(1):19-28.
206. Tripathi SK, Goyal R, Kumar P, Gupta KC. Linear polyethylenimine-graft-chitosan copolymers as efficient DNA/siRNA delivery vectors in vitro and in vivo. Nanomedicine-Nanotechnology Biology and Medicine. 2012;8(3):337-45.
207. Bao H, Ping Y, Pan Y, Li L, Li J, Gan LH. Thermo-responsive transfection of DNA complexes with well-defined chitosan terpolymers. Soft Matter. 2012;8(8):2518-26.
208. Rojanarata T, Opanasopit P, Techaarpornkul S, Ngawhirunpat T, Ruktanonchai U. Chitosan-Thiamine Pyrophosphate as a Novel Carrier for siRNA Delivery. Pharmaceutical Research. 2008;25(12):2807-14.
209. Gaspar VM, Sousa F, Queiroz JA, Correia IJ. Formulation of chitosan-TPP-pDNA nanocapsules for gene therapy applications. Nanotechnology. 2011;22(1).
210. Strand SP, Lelu S, Reitan NK, Davies CdL, Artursson P, Varum KM. Molecular design of chitosan gene delivery systems with an optimized balance between polyplex stability and polyplex unpacking. Biomaterials. 2010;31(5):975-87.
211. Thibault M, Nimesh S, Lavertu M, Buschmann MD. Intracellular Trafficking and Decondensation Kinetics of Chitosan-pDNA Polyplexes. Molecular Therapy. 2010;18(10):1787-95.
212. Yang X, Yuan X, Cai D, Wang S, Zong L. Low molecular weight chitosan in DNA vaccine delivery via mucosa. International Journal of Pharmaceutics. 2009;375(1-2):123-32.
213. Zheng F, Shi X-W, Yang G-F, Gong L-L, Yuan H-Y, Cui Y-J, et al. Chitosan nanoparticle as gene therapy vector via gastrointestinal mucosa administration: Results of an in vitro and in vivo study. Life Sciences. 2007;80(4):388-96.
214. Huang M, Fong CW, Khor E, Lim LY. Transfection efficiency of chitosan vectors: Effect of polymer molecular weight and degree of deacetylation. Journal of Controlled Release. 2005;106(3):391-406.
215. Kiang T, Wen H, Lim HW, Leong KW. The effect of the degree of chitosan deacetylation on the efficiency of gene transfection. Biomaterials. 2004;25(22):5293-301.
216. Nimesh S, Thibault MM, Lavertu M, Buschmann MD. Enhanced Gene Delivery Mediated by Low Molecular Weight Chitosan/DNA Complexes: Effect of pH and Serum. Molecular Biotechnology. 2010;46(2):182-96.
217. Varkouhi AK, Schiffelers RM, van Steenbergen MJ, Lammers T, Hennink WE, Storm G. Photochemical internalization (PCI)-mediated enhancement of gene silencing efficiency of polymethacrylates and N,N,N-trimethylated chitosan (TMC) based siRNA polyplexes. Journal of Controlled Release. 2010;148(1):E98-E9.
218. Malmo J, Varum KM, Strand SP. Effect of Chitosan Chain Architecture on Gene Delivery: Comparison of Self-Branched and Linear Chitosans. Biomacromolecules. 2011;12(3):721-9.
219. Deng J, Zhou Y, Xu B, Mai K, Deng Y, Zhang L-M. Dendronized Chitosan Derivative as a Biocompatible Gene Delivery Carrier. Biomacromolecules. 2011;12(3):642-9.
220. Katas H, Dzulkefli NNSN, Sahudin S. Synthesis of a New Potential Conjugated TAT-Peptide-Chitosan Nanoparticles Carrier via Disulphide Linkage. Journal of Nanomaterials. 2012.
221. Malhotra M, Tomaro-Duchesneau C, Saha S, Kahouli I, Prakash S. Development and characterization of chitosan-PEG-TAT nanoparticles for the intracellular delivery of siRNA. International Journal of Nanomedicine. 2013;8.

222. Malhotra M, Tomaro-Duchesneau C, Prakash S. Synthesis of TAT peptide-tagged PEGylated chitosan nanoparticles for siRNA delivery targeting neurodegenerative diseases. Biomaterials. 2013;34(4):1270-80.
223. Gaspar VM, Marques JG, Sousa F, Louro RO, Queiroz JA, Correia IJ. Biofunctionalized nanoparticles with pH-responsive and cell penetrating blocks for gene delivery. Nanotechnology. 2013;24(27).
224. Chang J, Xu X, Li H, Jian Y, Wang G, He B, et al. Components Simulation of Viral Envelope via Amino Acid Modified Chitosans for Efficient Nucleic Acid Delivery: In Vitro and In Vivo Study. Advanced Functional Materials. 2013;23(21):2691-9.
225. Park S, Jeong EJ, Lee J, Rhim T, Lee SK, Lee KY. Preparation and characterization of nonaarginine-modified chitosan nanoparticles for siRNA delivery. Carbohydrate Polymers. 2013;92(1):57-62.
226. Plianwong S, Opanasopit P, Ngawhirunpat T, Rojanarata T. Chitosan Combined with Poly-L-arginine as Efficient, Safe, and Serum-Insensitive Vehicle with RNase Protection Ability for siRNA Delivery. Biomed Research International. 2013.
227. Zhang H, Zhu D, Song L, Liu L, Dong X, Liu Z, et al. Arginine conjugation affects the endocytic pathways of chitosan/DNA nanoparticles. Journal of Biomedical Materials Research Part A. 2011;98A(2):296-302.
228. Noh SM, Park MO, Shim G, Han SE, Lee HY, Huh JH, et al. Pegylated poly-L-arginine derivatives of chitosan for effective delivery of siRNA. Journal of Controlled Release. 2010;145(2):159-64.
229. Zheng H, Tang C, Yin C. The effect of crosslinking agents on the transfection efficiency, cellular and intracellular processing of DNA/polymer nanocomplexes. Biomaterials. 2013;34(13):3479-88.
230. Reitan NK, Sporsheim B, Bjorkoy A, Strand S, Davies Cdl. Quantitative 3-D colocalization analysis as a tool to study the intracellular trafficking and dissociation of pDNA-chitosan polyplexes. Journal of Biomedical Optics. 2012;17(2).
231. Varkouhi AK, Verheul RJ, Schiffelers RM, Lammers T, Storm G, Hennink WE. Gene Silencing Activity of siRNA Polyplexes Based on Thiolated N,N,N-Trimethylated Chitosan. Bioconjugate Chemistry. 2010;21(12):2339-46.
232. Zhao X, Li Z, Pan H, Liu W, Lv M, Leung F, et al. Enhanced gene delivery by chitosan-disulfide-conjugated LMW-PEI for facilitating osteogenic differentiation. Acta Biomaterialia. 2013;9(5):6694-703.
233. Moreira C, Oliveira H, Pires LR, Simoes S, Barbosa MA, Pego AP. Improving chitosan-mediated gene transfer by the introduction of intracellular buffering moieties into the chitosan backbone. Acta Biomaterialia. 2009;5(8):2995-3006.
234. Chang K-L, Higuchi Y, Kawakami S, Yamashita F, Hashida M. Efficient Gene Transfection by Histidine-Modified Chitosan through Enhancement of Endosomal Escape. Bioconjugate Chemistry. 2010;21(6):1087-95.
235. Liao Z-X, Ho Y-C, Chen H-L, Peng S-F, Hsiao C-W, Sung H-W. Enhancement of efficiencies of the cellular uptake and gene silencing of chitosan/siRNA complexes via the inclusion of a negatively charged poly(gamma-glutamic acid). Biomaterials. 2010;31(33):8780-8.
236. Peng S-F, Yang M-J, Su C-J, Chen H-L, Lee P-W, Wei M-C, et al. Effects of incorporation of poly(gamma-glutamic acid) in chitosan/DNA complex nanoparticles on cellular uptake and transfection efficiency. Biomaterials. 2009;30(9):1797-808.
237. Fernandes JC, Qiu X, Winnik FM, Benderdour M, Zhang X, Dai K, et al. Low molecular weight chitosan conjugated with folate for siRNA delivery in vitro: optimization studies. International Journal of Nanomedicine. 2012;7:5833-45.
238. Kim Y-K, Minai-Tehrani A, Lee J-H, Cho C-S, Cho M-H, Jiang H-L. Therapeutic efficiency of folated poly(ethylene glycol)-chitosan-graft-polyethylenimine-Pdcd4 complexes in H-ras12V mice with liver cancer. International Journal of Nanomedicine. 2013;8:1489-98.

239. Liu Z, Lv D, Liu S, Gong J, Wang D, Xiong M, et al. Alginic Acid-Coated Chitosan Nanoparticles Loaded with Legumain DNA Vaccine: Effect against Breast Cancer in Mice. Plos One. 2013;8(4).
240. Liang X, Li X, Chang J, Duan Y, Li Z. Properties and Evaluation of Quaternized Chitosan/Lipid Cation Polymeric Liposomes for Cancer-Targeted Gene Delivery. Langmuir. 2013;29(27):8683-93.
241. Han HD, Mangala LS, Lee JW, Shahzad MMK, Kim HS, Shen D, et al. Targeted Gene Silencing Using RGD-Labeled Chitosan Nanoparticles. Clinical Cancer Research. 2010;16(15):3910-22.
242. Calvo P, RemunanLopez C, VilaJato JL, Alonso MJ. Chitosan and chitosan ethylene oxide propylene oxide block copolymer nanoparticles as novel carriers for proteins and vaccines. Pharmaceutical Research. 1997;14(10):1431-6.
243. Sonaje K, Chuang E-Y, Lin K-J, Yen T-C, Su F-Y, Tseng MT, et al. Opening of Epithelial Tight Junctions and Enhancement of Paracellular Permeation by Chitosan: Microscopic, Ultrastructural, and Computed-Tomographic Observations. Molecular Pharmaceutics. 2012;9(5):1271-9.
244. Hooper LV, Midtvedt T, Gordon JI. How host-microbial interactions shape the nutrient environment of the mammalian intestine. Annual Review of Nutrition. 2002;22:283-307.
245. Meinel AJ, Kubow KE, Klotzsch E, Garcia-Fuentes M, Smith ML, Vogel V, et al. Optimization strategies for electrospun silk fibroin tissue engineering scaffolds. Biomaterials. 2009;30(17):3058-67.

USC
UNIVERSIDADE
DE SANTIAGO
DE COMPOSTELA

Antecedentes, hipótesis y objetivos

USC
UNIVERSIDADE
DE SANTIAGO
DE COMPOSTELA

1. La nanotecnología se ha posicionado como una estrategia de formulación, capaz de mejorar el balance eficacia-seguridad de las terapias antitumorales convencionales. El uso de transportadores nanométricos permite, no sólo evitar el uso de disolventes tóxicos [1], sino también modificar el perfil de biodistribución del fármaco, facilitando su acumulación en el tumor y reduciendo su concentración en órganos vitales. Esta capacidad de orientación pasiva del fármaco antitumoral está relacionada con el tamaño de las nanostructuras, preferentemente en torno a los 100 - 150 nm, así como con su superficie hidrofílica [2].
2. Los estudios llevados a cabo recientemente en relación con el potencial de la nanotecnología para promover el acceso de los fármacos al sistema linfático han permitido apreciar la importancia del tamaño e hidrofilia superficial de los nanosistemas. El estado de conocimiento actual sugiere que las características físico-químicas que favorecen la acumulación en el tumor, contribuyen también al acceso a las células que se diseminan a través del sistema linfático [3, 4].
3. Las nanocápsulas poliméricas desarrolladas por nuestro grupo de investigación son sistemas versátiles, cuyo núcleo oleoso permite la asociación de fármacos hidrofóbicos antitumorales, mientras que el polímero formador de su cubierta puede ser de naturaleza variada, permitiendo dotar al sistema de distintas propiedades en función de las necesidades de la aplicación terapéutica [5-7]. En este sentido, el desarrollo de biopolímeros y biomoléculas con capacidad de interaccionar de forma selectiva con poblaciones celulares tumorales han inspirado el diseño de nuevos nanosistemas multifuncionales con un nivel superior de vectorización y penetración tumoral.
4. El ácido hialurónico es un polisacárido natural ampliamente utilizado para el desarrollo de nanosistemas destinados a esta aplicación, principalmente por su afinidad hacia células tumorales mediada por su receptor CD44, pero también por aportar una cubierta hidrofílica a los sistemas formados. Además de esto, la reactividad química de esta material facilita su unión a otras moléculas con el fin de aportar una multifuncionalidad al sistema desarrollado [8].
5. El péptido t-Lyp-1, es una molécula de gran interés en el diseño de nanosistemas de orientación selectiva debido a su alta selectividad hacia el receptor NRP1

sobreexpresado en muchos tumores, así como por su capacidad de penetración específica a través del estroma tumoral [9]

Referencias

1. van Zuylen, L., J. Verweij, and A. Sparreboom, Role of Formulation Vehicles in Taxane Pharmacology. Investigational New Drugs, 2001. 19(2): p. 125-141.

2. Maeda, H., Toward a full understanding of the EPR effect in primary and metastatic tumors as well as issues related to its heterogeneity. Advanced Drug Delivery Reviews, (0).

3. Ryan, G.M., L.M. Kaminskas, and C.J.H. Porter, Nano-chemotherapeutics: Maximising lymphatic drug exposure to improve the treatment of lymph-metastatic cancers. Journal of Controlled Release, 2014. 193(0): p. 241-256.

4. Svenson, S., What nanomedicine in the clinic right now really forms nanoparticles? Wiley Interdisciplinary Reviews: Nanomedicine and Nanobiotechnology, 2014. 6(2): p. 125-135.

5. Lollo, G., et al., Polyglutamic acid–PEG nanocapsules as long circulating carriers for the delivery of docetaxel. European Journal of Pharmaceutics and Biopharmaceutics, 2014. 87(1): p. 47-54.

6. Rivera-Rodríguez, G.R., M.J. Alonso, and D. Torres, Poly-l-asparagine nanocapsules as anticancer drug delivery vehicles. European Journal of Pharmaceutics and Biopharmaceutics, 2013. 85(3, Part A): p. 481-487.

7. Oyarzun-Ampuero, F.A., et al., Hyaluronan nanocapsules as a new vehicle for intracellular drug delivery. European Journal of Pharmaceutical Sciences, 2013. 49(4): p. 483-490.

8. Teijeiro, C., et al., Polysaccharide-Based Nanocarriers for Drug Delivery, in Handbook of Nanobiomedical Research. p. 235-277.

9. Roth, L., et al., Transtumoral targeting enabled by a novel neuropilin-binding peptide. Oncogene, 2012. 31(33): p. 3754-3763.

USC
UNIVERSIDADE
DE SANTIAGO
DE COMPOSTELA

El desarrollo de un sistema nanocapsular compuesto por un núcleo oleoso y una cubierta polimérica de ácido hialurónico o de ácido hialurónico conjugado con el péptido t-Lyp-1, podría representar una interesante estrategia de formulación para la administración de fármacos antitumorales como el docetaxel, motivada por los aspectos y características que se detallan a continuación:

1. El tamaño nanométrico de las citadas nanocápsulas, así como su superficie hidrofílica proporcionada por esta cubierta polimérica podría facilitar la acumulación tumoral y también su extravasación al sistema linfático desde el sistema circulatorio de forma pasiva.

2. El uso de materiales funcionales en la cubierta de estos sistemas, como son el ácido hialurónico y el péptido t-Lyp-1, permite contribuir de forma activa a aumentar los niveles de fármaco en el tejido tumoral. Además, la capacidad de penetración específica de t-Lyp-1, puede favorecer la difusión de los nanosistemas a través del estroma tumoral alcanzando las células tumorales más inaccesibles.

USC
UNIVERSIDADE
DE SANTIAGO
DE COMPOSTELA

Considerando los antecedentes e hipótesis planteados, el objetivo general de este trabajo se ha centrado en el diseño de sistemas capaces de transportar activamente fármacos quimioterapéuticos a tejidos tumorales y a los nodos linfáticos. Dichos sistemas consisten en nanocápsulas cargadas con el fármaco docetaxel, cuya cubierta de ácido hialurónico o de ácido hialurónico modificado con el péptido t-Lyp-1, aporta una afinidad específica hacia receptores de células tumorales. Además, de una capacidad promotora de la penetración a través del tejido tumoral proporcionada por este péptido. Para conseguir este objetivo se han planteado las siguientes etapas:

Diseño y desarrollo de nanocápsulas de ácido hialurónico y ácido hialurónico modificado con el péptido t-Lyp-1

1. Síntesis y caracterización del nuevo conjugado químico ácido hialurónico-t-Lyp-1.
2. Preparación de nanocápsulas de ácido hialurónico y de ácido hialurónico-t-Lyp-1 cargadas con docetaxel. Caracterización físico-química de los sistemas desarrollados. Estudio de estabilidad en medios biológicos. Evaluación de capacidad de carga y de liberación del fármaco en un medio fisiológico simulado.

Estos resultados se describen en el **capítulo 2 y en el anexo 1** de la memoria.

Estudio de especificidad in vitro de las nanocápsulas desarrolladas

3. Estudios celulares en modelos bi y tri-dimensionales para valorar la capacidad de interacción específica de las nanocápsulas a través de sus receptores celulares CD44 y NRP1 en la línea celular de cáncer de pulmón A519.

Estos resultados se describen en el **anexo 2 de la memoria**.

Evaluación del comportamiento in vivo de los potenciales nanomedicamentos desarrollados

4. Estudio de la biodistribución y la farmacocinética de los sistemas cargados con docetaxel, tras su administración intravenosa en un modelo ortotópico de cáncer de pulmón metastásico. Estudio de la eficacia antitumoral de las nanocápsules

cargadas con docetaxel tras su administración intravenosa en el mismo modelo tumoral.

Estos resultados se describen en el **capítulo 3** de la memoria.

Asimismo, al margen de los objetivos citados, las características distintivas de las nanocápsulas desarrolladas nos llevaron a estudiar su comportamiento biológico en el modelo animal "pez cebra". Los resultados de estos estudios se recogen en el **anexo 3** de la presente memoria.

Capítulo 2

Design, preparation and characterization of multifunctional anticancer drug delivery nanocapsules

USC
UNIVERSIDADE
DE SANTIAGO
DE COMPOSTELA

Design, preparation and characterization of multifunctional anticancer drug delivery nanocapsules

Este trabajo ha sido elaborado en colaboración con Ramón Novoa Carballal. 3B´s Research group - Biomaterials, Biodegradable and Biomimetics. University of Minho, Headquarters of the European Institute of Excellence of Tissue Engineering and Regenerative Medicine. AvePark, 4806-909 Taipas, Guimaraes, Portugal

USC
UNIVERSIDADE
DE SANTIAGO
DE COMPOSTELA

Abstract

The design of nanocarriers for the targeted delivery of anticancer drugs is expected to contribute to a drastic improvement of oncological therapies. The combination of favorable physico-chemical properties, such as small size and a hydrophilic surface, combined with the use of smart materials that present affinity for specific cells represent a promising strategy to improve the therapeutic response of oncological drugs. The objective of this work was the rational design of multifunctional Hyaluronic acid (HA) nanocapsules for the selective delivery of the anticancer drug docetaxel. The natural polysaccharide, HA was selected because of its safety profile and its affinity for the CD44 receptor, generally overexpressed in cancer cells. Furthermore, this polymer was functionalized with t-Lyp-1, a tumour homing peptide, which has shown selective affinity for cancer cells through NRP1 receptor cancer cells, in addition to an exceptional capacity to facilitate the penetration of the nanocarrier across the tumour stroma. The resulting multifunctional nanocapsules were characterized with regard to the composition of the shell (HA or t-Lyp-1 functionalized HA) and their physicochemical and biopharmaceutical properties. The results indicated that the nanocapsules have a small size and polydispersity (112- 149 nm), a negatively surface charge (from -49 to -27 mV), an adequate stability in simulated physiological fluids and a capacity for carrying the antitumoural drug docetaxel (1.5 % w/w). In brief, this is the first report on the development of multifunctional t-Lyp-1 targeted HA nanocapsules.

1. Introduction

The design of selective and effective treatments remains a huge challenge in cancer therapy. Within this broad frame, the potential of nano-delivery systems intended to help drugs overcoming the biological barriers and reach their target is still under-explored. The combination of the physico-chemical properties of the nanocarriers together with the use of smart biomaterials with affinity for cancer cells and the surrounding environment may represent a promising strategy towards improving the targeting, and thus the therapeutic effect of oncological drugs. For the design of these targeted nano-oncologicals a number of key properties have to be fulfilled.

First of all, the nanocarrier must be able to load a significant amount of antitumoural drug and release it in the target tissue. Regarding physico-chemical properties, the surface hydrophilicity and electrostatic charge of nanocarriers are known to highly influence the stability of the nanocarriers in the biological fluids [1]. Namely, hydrophilic surface contribute significantly to reduce the uptake by the mononuclear phagocyte system [2], while, surface charge prevents from aggregation contributing nanosystems with improved stability [3] and, specifically negatively surface charge decrease nonspecific cellular uptake [4], thereby increasing their opportunity to reach their target. The size of the nanocarrier is a critical issue that influences the in vivo fate. It is known that the small size helps nanocarriers to avoid opsonization [2, 5-8]. Moreover, the size determines the capacity to extravasate into the tumour. In this regard, it has been shown that small size nanocarriers (below 150 nm) may facilitate tumour penetration [9, 10] and lymphatic drainage [11-13], this being important for the access of the nanocarriers to the metastatic cells [14-16]. Overall, these properties, small size and hydrophilic surface are crucial for either passive or active targeting. Finally, chemical composition of the outer shell can endow nanocarriers with specific capacity to interact with tumour cell receptors, increasing drug dose in cancer tissue [17, 18] and can also provide penetration enhancer properties [19, 20] for improving limited drug penetration throughout the dense collagen matrix [21, 22] and high interstitial fluid pressure of tumour tissue [23, 24].

Hyaluronic acid (HA), a polysaccharide formed by D-glucuronic acid and D-N-acetylglucosamine linked through alternating beta-1,4 and beta-1,3 glycosidic bonds, is a well-known naturally occurring biopolymer. As disclosed in a review article [25], HA has a crucial function as a structural component of the extracellular matrix and it is also involved in several biological functions mediated by its interaction with specific cellular receptors. The best known HA receptor, CD44, is located in lymphocytes, epithelial and endothelial cells and it is overexpressed in many cancer cells [26-28]. Other HA receptors are the Hyaluronic acid receptor for endocytosis (HARE), mostly located in the endothelial cells of liver and spleen [26, 29], Lymphatic Vessel Endothelial Receptor 1 (LYVE-1), mainly located in lymph vessel endothelium [29, 30] or TSG-6 found in synovial fluids [31, 32]. In particular, the capacity of HA to interact with the cancer cells and the lymph vessel epithelium, makes it an attractive biomaterial for the design of nanocarriers for the delivery of oncological drugs. In addition, because of its hydrophilic character HA has been shown to prevent the opsonisation of nanocarriers, thus, providing them with long circulating properties [33-35]. A great number of HA based nanocarriers including liposomes [33, 34], micelles [9, 36] and nanocapsules [37, 38] have been already explored for their ability to increase the efficacy of cytotoxic drugs. A limitation to the HA targeting behaviour has been, however, associated to the presence of CD44 and other receptors in a variety of non-cancerous cells, for instance, liver and spleen endothelial cells [39, 40].

Recently, a new family of tumour homing peptides, denominated CendR peptides [19, 20] characterized by containing the aminoacid sequence (R/K)XX(R/K) has been reported [19, 20, 41]. These peptides are endowed with selectivity for several tumour receptors and with a specific penetration capacity that is only active after peptide-receptor binding. Within this group, Lyp-1 is a peptide with a cryptic (R/K)XX(R/K) motif, that presents high affinity for p32 receptor located in tumoural lymphatic vessels, tumour cells and tumour associated macrophages [42]. After binding to p32, Lyp-1 is proteolytically cleaved exposing the CendR motif, and therefore, activating the penetration capacity. The targeting capacity of this peptide has already been assessed for liposomes [43] and micelles [44]. In addition, the tumour penetration capacity has also been validated for paclitaxel-loaded albumin nanoparticles (Abraxane®) [45].

Interestingly, this cleaved form of Lyp-1, called truncated Lyp-1 (t-Lyp-1), is known to interact with neuropilin-1 (NRP1, over-expressed in the majority of tumours) and to enhance penetration capacity due to the presence of the unmasked (R/K)XX(R/K) motif in this peptide, actually, t-Lyp-1 bound to iron oxide nanoparticles have probed augmented diffusion within tumour [46].

In this context, polymer nanocapsules developed in our group [47-50] represent a smart platform for carrying hydrophobic antitumoural drugs like taxanes, that are easily solubilized in the inner oily core of the nanovehicle surrounded and protected by a tunable polymer shell that provides steric hindrance and targeting properties.

Taking this background information into account, the main objective of this work has been to develop multifunctional hyaluronic acid (HA) nanocapsules, which are functionalized with the tumour homing peptide t-Lyp-1 (HA-t-Lyp-1). For this, first we synthesized HA-t-Lyp-1 using carbodiimide and maleimide chemistry [51-54] and used this biomaterial to form the nanocapsules shell. The nanocapsules consisting of an oily core and a HA or HA-t-Lyp-1 corona have been characterized with regard to their physicochemical properties, chemical composition of the shell, capacity to load and deliver docetaxel and their stability in plasma.

2. Materials and methods

2.1. Materials

Sodium hyaluronate (HA, Mw 57 KDa) was purchased from Lifecore Biomedical (Chaska, MN, USA). N-(2-Aminoethyl) maleimide trifluoroacetate salt (AEM), N-Hydroxysuccinimide (NHS), N-(3-Dimethylaminopropyl)-N´-ethylcarbodiimide hydrochloride (EDC), MES hydrate buffer, deuterium oxide, sodium chloride hexadeciltrymethylammonium bromide (CTAB), sodium phosphate monobasic, carbazole and sulphuric acid were obtained from Sigma-Aldrich (Spain). The truncated Lyp-1 peptide with the aminoacid sequence CGNKRTR was purchased from BCN peptides (Barcelona, Spain). Miglyol® 812, a neutral oil formed by esters of caprylic and capric fatty acids and glycerol, was donated by Cremer Oleo GmbH & Co (Germany). Docetaxel was donated by Teva Pharmaceutical Industries (Israel). The surfactant Epikuron 145V,

a phosphatidylcholine-enriched fraction of soybean lecithin, was donated by Cargill (Spain). Dulbecco´s modified Eagle´s Medium (DMEM) and Fetal Bovine Serum were purchased from Gibco®, Lifetechnologies. Milli-Q water was used throughout the experiments and organic solvents were of HPLC or MS grade.

2.2. Synthesis of HA-t-Lyp-1

First, Hyaluronic acid (HA) was modified with the maleimide (AEM). Different molar ratios between carboxylic acid groups of HA and the EDC, NHS, AEM were tested. For this purpose, HA were dissolved in 0.1 M MES buffer at pH 6 at a final concentration of 2 mg/mL and the corresponding amount of EDC, NHS and AEM were also dissolved in 0.1 M MES buffer, added to HA solution and maintained under magnetic stirring for 4h at room temperature. The maleimide functionalized HA (HA-Mal) was purified by dyalisis (regenerated cellulose, SnakeSkin 3.5K MWCO, Thermo Scientific), first against NaCl 50mM and then against MilliQ water.

To link the t-Lyp-1 to the maleimide groups incorporated in the first reaction, HA-Mal was diluted in 0.1 M MES buffer at a final HA concentration of 1 mg/mL. This solution was mixed with a 5-fold molar excess of the peptide in respect to maleimide groups linked to ensure the complete modification of its vinyl groups with t-Lyp-1. The reaction mixture was maintained 4 h under magnetic stirring at room temperature and the final HA-t-Lyp-1 product was purified by dialysis as described previously, freeze-dried (Labconzo Frezze Dry System) and stored at 4 ºC.

2.3. NMR spectroscopy

NMR experiments were acquired on a Bruker DRX-500 and Varian Inova 750 spectrometers. The chemical shifts are reported in ppm. The spectra were recorded in deuterium oxide at a HA concentration between 0.4-0.8 mg/mL. ^{1}H-NMR analysis was performed at 500 MHz with 256 scans and 10 s of delay between each scan. ^{1}H Pulsed Field Gradient (PFG) NMR experiments were acquired on a 750 MHz spectrometer (Varian INOVA) equipped with a triple gradient shielded probe. The gradient was varied linearly from 2 to 65 G.cm^{-1} to obtain the diffusion dimension. The pulse sequence used includes the bipolar-gradient pulse pairs and stimulated echo experiment with an

additional delay time of 0.2 ms for longitudinal eddy current compensation (LED-BPPSTE). The diffusion time □ was varied from 2 to 20 s. The duration of the gradients in the sequence was set to 1ms and the recovery delay was 10 s. MestreNova Software (Mestrelab Research) was used for spectral processing. The extent of HA conjugation was quantified as a percent of substitution calculated as the number of maleimide or t-Lyp-1 molecules per 100 carboxylic acid groups of HA (degree of substitution, DS).

2.4. Preparation of HA and HA-t-Lyp-1 nanocapsules

All nanocapsule prototypes were prepared by the solvent displacement technique described previously [38] and conveniently optimized. The organic phase was composed of 4.75 mL of acetone and 0.25 mL of ethanol containing 0.75 mg/mL of Epikuron 145V, 0.15 mg/mL of CTAB, 2.96 mg/mL of Miglyol® 812 and 150 µg/mL of docetaxel and an aqueous phase consisted of 10 mL of HA or HA-t-Lyp-1 solution at 0.25 mg/mL. The organic phase was added drop-wise into the aqueous phase under magnetic stirring, leading to the immediate formation of the nanodroplets and the deposition of the polymer around them. After nanocapsule formation organic solvents were removed by rotaevaporation.

The nanocapsules were isolated by ultracentrifugation (Optima™ L-90K Ultracentrifuge, Beckman Coulter; Fullerton, CA) at 84035 g for 1 h at 15 °C. Then infranatant was removed from the media, nanocarriers were collected and diluted up to a known concentration.

2.5. Physico-chemical characterization

Mean particle size and polydispersity index (PI) were determined by photon correlation spectroscopy (PCS). Samples were diluted in MilliQ Water and the analysis was carried out at 25 ºC with an angle detection of 173º. Zeta potential measurements were performed by laser Doppler anemometry (LDA) and the samples were diluted in KCl 1mM aqueous solution. PCS and LDA analysis were performed in triplicate using a NanoZS® (Malvern Instruments, Malvern, UK).

2.6. Morphological characterization

The morphology of the nanocapsules was studied by transmission electron microscopy (TEM, CM12 Philips, Netherlands). Samples were stained with 2 % w/v phosphotungstic acid solution, and placed on copper grids with Formvar® films for analysis.

2.7. Density of hyaluronic acid shell and t-Lyp-1 shell

HA was quantified by colorimetric derivatization method using carbazole with slight modifications to the procedure described previously [55]. The estimation of HA association to the nanocapsules was calculated by difference between the total amount of HA added for nanocapsule preparation and the free HA found in the nanocapsules suspending medium. For this, nanocapsules were isolated by ultracentrifugation and 0.5 mL of the infranatant containing the free HA was added to 3 mL of H_2SO_4 and the mixture was heated at 100 ºC for 20 minutes in order to digest HA to uronic acid. Then, 100 µL of 0.2 % of a carbazole solution in ethanol was added to the previous mixture for obtaining a coloured product. After 2.5 h the resulting pink product was quantified by spectrophotometry at 528 nm (DU® 730, Beckman Coulter). Calibration standards were prepared in the same way by spiking with HA stock solution a blank infranatant obtained from a nanoemulsion without HA coating, in order to simulate the sample matrix.

The density of HA shell was calculated as the disaccharide number of HA or t-Lyp-1 molecules per unit surface of nanocapsules. For this calculation, we determined the total surface obtained in 1 batch of nanocapsules from the yield production assuming that the nanocapsules have the same density as the main compound (Miglyol® 812) and the average size from PCS measure. The amount of t-Lyp-1 molecules per surface unit (density) was calculated from the total amount of HA molecules and taking into account the substitution degree as indicated in section “NMR spectroscopy”.

2.8. Stability of HA and HA-t-Lyp-1 nanocapsules

The physical stability of nanocapsules was studied simulating in vitro and in vivo conditions. For the first, isolated nanocapsules were diluted ten times in phosphate buffer at pH 7.5 or in cell culture medium consisting of Dulbecco´s Modified Eagle´s Medium (DMEM), supplemented with 10 % (v/v) of fetal bovine serum (FBS) and were maintained under horizontal shaking at 37ºC. Particle size and polydispersity index were

analysed at different time points as described in the section “Physico-chemical characterization”.

For the simulated in vivo conditions, isolated nanocapsules were diluted ten times with human plasma (obtained from patients of the University Hospital of Santiago de Compostela, CHUS) and were maintained under horizontal shaking at 37 ºC. Then, size measurements with DLS were performed by diluting this mixture 20 times with MilliQ water and analysing size of highest intensity peak instead of the average size. A control sample of plasma without nanocapsules was analyzed in the same conditions.

2.9. Loading capacity and release profile of the antitumoural drug docetaxel

The quantification of the drug loading capacity and drug release profile of the nanocapsules was performed using an UPLC-MS technique originally developed by us. The UPLC system consisted of an Acquity UPLC® H-class system (Waters Corp, Milford, USA) with thermostatized autosampler and a column compartment ((BEH C18 column (2.1 x 100mm, 1.7µm; Waters, USA). The experimental analytical conditions were as follows: the mobile phase system consisted of 0.1 % formic acid aqueous solution (A) and acetonitrile (B). A linear gradient program was used, with 80 % to 20 % of mobile phase A from 0 to 5 min, then from 5 to 5.5 min returns to 80 % of A and it was kept up to 6 min for initial conditioning. The flow rate was 0.6 mL/min, the total run time was 6 min. The temperature of the column was maintained at 40 ºC and the autosampler was thermostatized at 4 ºC. The injected volume was 10 µL. Under these conditions, DCX was eluted at 4.11 ± 0.02 min. The UPLC system was coupled to a Xevo® Triple Quadrupole Detector (TQD) (Waters Corp, Milford, USA) with an electrospray ionization (ESI) interface. Mass spectrometric detection was operated in positive mode and set up for multiple reaction monitoring (MRM) to monitor the transitions of m/z 830.4 → 304.1 and 830.4 → 549.2 with auto dwell time conditions. 525 ºC was selected as source temperature and 150 ºC as desolvation temperature, capillary voltage was 3.1 kV and the cone voltage was 40 V. Nitrogen was used for the desolvation and as cone gas at a flow rate of 600 L/h and 80 L/h respectively. Argon was used as the collision gas. The optimized collision energy was 30 eV. Data acquisition and analysis were performed using TargetLynx v4.1 software (Waters Corp., Milford, USA).

The loading capacity of the antitumoural drug docetaxel was expressed as the percentage (w/w) of drug encapsulated with respect to the total amount of nanocapsules. Accordingly, the encapsulated drug was determined in an aliquot of isolated nanocapsules and the total amount of drug was estimated in an aliquot of non-isolated nanocapsules. A volume of 50 µL of both aliquots was first mixed in 950 µL of acetonitrile for the extraction of the drug from the nanocapsules and, then, 50 µL of this solution was diluted with 950 µL of water prior to the chromatographic analysis.

For the determination of the docetaxel release profile from the nanocapsules, a volume of the nanocapsule suspension was diluted in phosphate buffer pH 7.5 up to "sink conditions". The system was maintained under horizontal shaking at 37 ºC for 24 h. At different time points, 1 mL of diluted nanocapsules were taken, the free docetaxel was separated from the nanocapsules by ultracentrifugation and processed accordingly for quantification in the UPLC-MS. Namely, 200 µL of nanocapsules suspending medium was mixed with 800 µL of acetonitrile and then 200 µL of this solution was diluted with 800 µL of water.

3. Results and discussion

3.1. Synthesis and NMR spectroscopy characterization of HA-t-Lyp-1

Besides the biological considerations underlined in the introduction, HA is an attractive biomaterial from the chemical reactivity viewpoint. Indeed, HA contains 1 carboxylic acid per disaccharide of HA, which allows the conjugation of ligands via amide bond formation, using mild reaction conditions. An example of this is the high number of HA conjugates reported so far for different biomedical applications, most of them using simple carbodiimide chemistry [56-60]. Despite this abundant literature in HA conjugation, here we describe for the first time the modification of HA with the tumour homing peptide t-Lyp-1.

Different percentages of t-Lyp-1 were successfully bound to the HA backbone using a two-step reaction, as shows Figure 1. First, using carbodiimide chemistry, maleimide motifs were added to the carboxylic acids of HA via amide bonding between the amine groups of aminoethylmaleimide (AEM) and the carboxylic acid groups. Afterwards, t-

Lyp-1 was linked to the vinyl groups of maleimide through the thiol group of cysteine residues of the peptide via Michael type addition reaction. This method of synthesis enabled the chemical modification of the thiol groups located at the terminal end of the peptide without compromising the distant epitopes responsible for the biological activity (Figure 1).

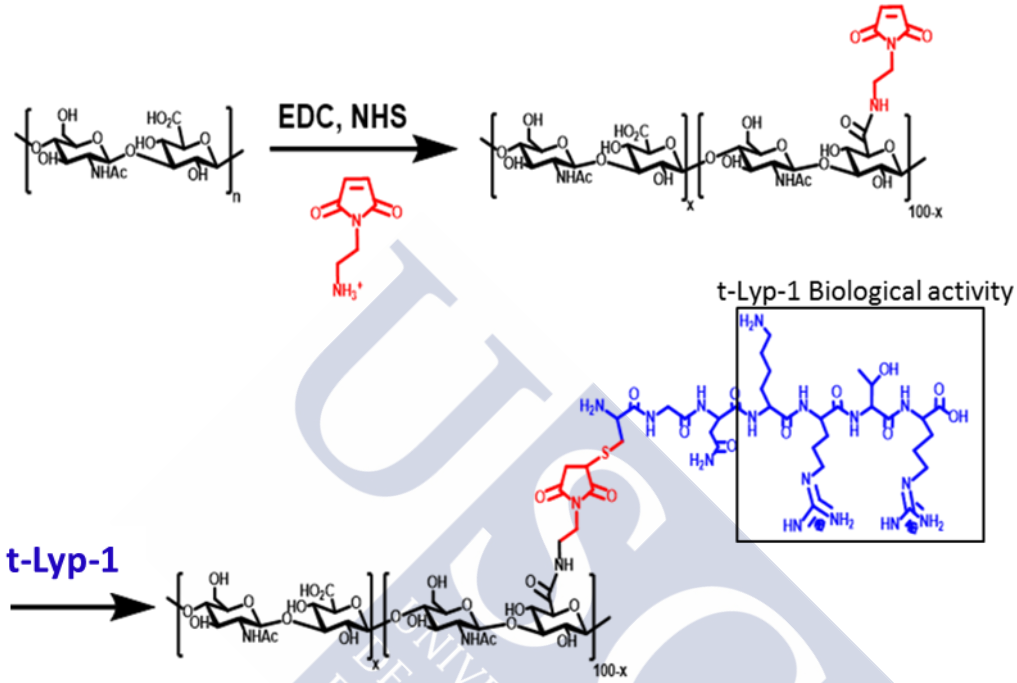

Figure 1. Two-step chemical reaction for obtaining HA-t-Lyp-1.

The ^{1}H-NMR spectrum of HA-Mal presented the characteristic signal of vinyl protons of maleimide at δ 7.0 (See blue arrow in Figure 2). The degree of substitution was determined by comparing this peak with the signal corresponding to the acetamide methyl protons of HA at δ 2.0 in the HA-Mal ^{1}H-NMR spectrum. The ^{1}H-NMR spectrum of HA-t-Lyp-1 showed characteristic ^{1}H-NMR signals of HA and t–Lyp-1 (See Figure 2). The disappearance of a signal of the peptide at 2.9 ppm in the spectrum of the HA-t-Lyp-1, associated to a methylene close to the thiol in the peptide (see red arrow in Figure 2), suggests that the peptide has been chemically bound to HA. The DS of HA with t-Lyp-1 was calculated by comparing the signals of the peptide between 1.4 and 1.6 (assigned as the two CH_2 of Arginine and one CH_2 of Lysine) with the acetamide methyl protons of HA in the ^{1}H-NMR spectrum of HA-t-Lyp-1.

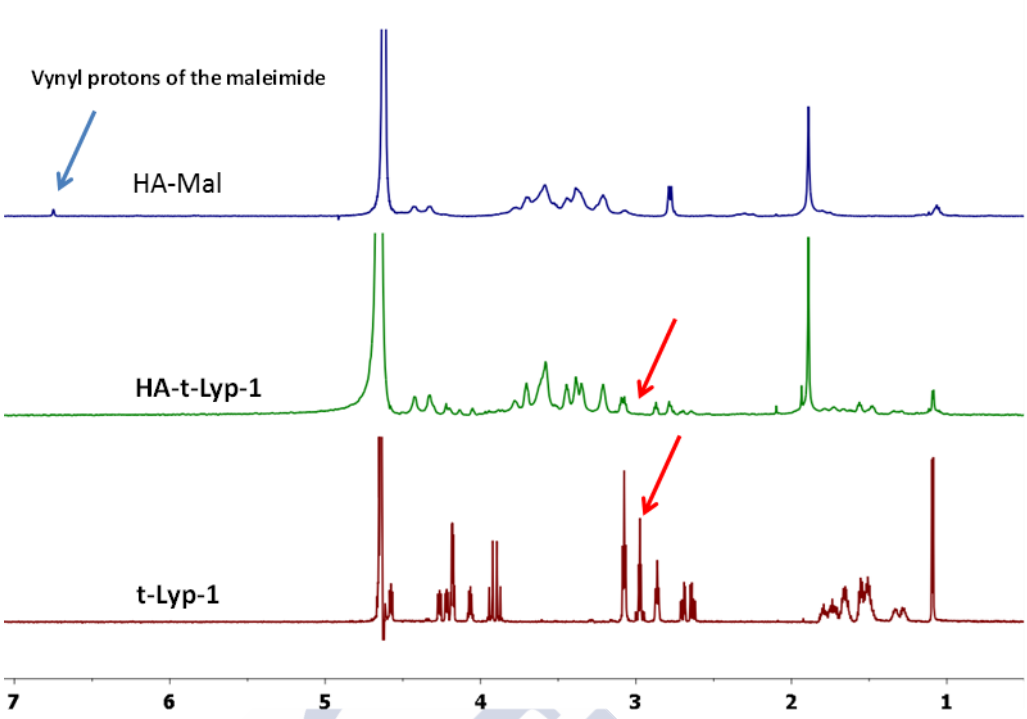

Figure 2. ^{1}H-NMR spectrum of HA-Mal (blue), HA-t-Lyp-1 (green) and t-Lyp-1 (red) in D_2O at 25 ºC.

The covalent binding of t-Lyp-1 and HA was confirmed using Pulsed field gradient NMR. In these NMR experiments, also known as diffusion ordered spectroscopy, the signal intensity of the molecules that move faster in solution decay faster with the increase of the pulsed field gradient. As shown in Figure 3, water signals (D_2O) decay very fast with the increase of the gradient while HA and t-Lyp-1 signals decay exactly with the same rate. This experiment supports that HA and t-Lyp-1 are covalently linked and therefore diffuse together. These results, together with the disappearance of the triplet signal of t-Lyp-1 at 2.9 ppm assure the accomplishment of the designed synthetic approach.

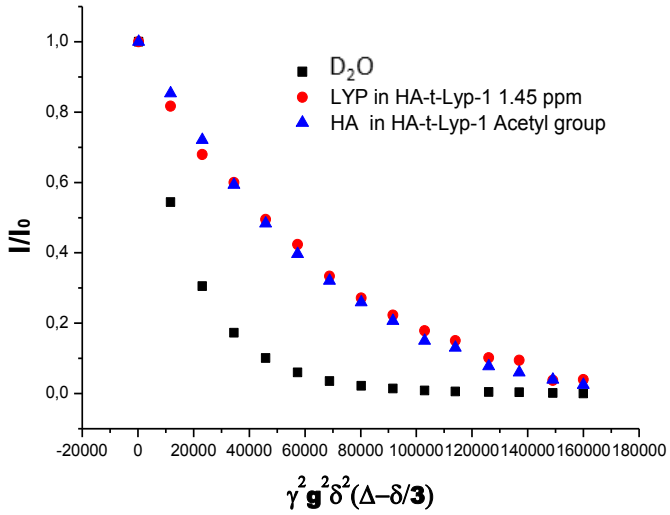

Figure 3. Stejskal-Tanner plots of HA-t-Lyp-1 in D_2O (δ = 1 ms, Δ =20ms).

Following the confirmation of the functionalization reaction we studied different molar ratios of carboxylic acid groups of HA and EDC, NHS and AEM (Table 1). For each of these ratios, in a first attempt, we added a 5-fold molar excess of the peptide with respect to the maleimide groups attached to HA backbone. According to the disappearance of the vinyl protons signal of maleimide in the NMR spectra of HA-t-Lyp-1, a complete modification of maleimide groups with t-Lyp-1 molecules was achieved.

	COOH (HA)	EDC	NHS	AEM
Ratio 1	1	1.5	0.25	0.05
Ratio 2	1	2.16	0.36	0.072
Ratio 3	1	3	0.5	0.1
Ratio 4	1	6	1	0.2
Ratio 5	1	9	1.5	0.3

Table 1. Feed molar ratio of carboxylic acid (COOH) of HA: EDC:NHS:AEM

As described below (Preparation and physico-chemical characterization of HA and HA-t-Lyp-1 nanocapsules), among the different HA-t-Lyp-1 polymer conjugates obtained, those with the two lowest molar ratios (ratio 1 and ratio 2) were adequate for the formation of the nanocapsules and, hence, they were studied in further detail by NMR.

The accurate determination of the degree of substitution (DS) is very complex due to the slow dynamics (reduced flexibility) associated to the tertiary structure and intramolecular binding of the polysaccharide molecules in solution. In this sense, it is important to underline that only a few articles on functionalized HA have described the quantification of DS [54, 61, 62]. Based on the information disclosed by Novoa-Carballal et al., [63], we performed the NMR analysis at different temperature (25, 60, 70 and 80 ºC) in order to increase the dynamics of the HA chain. The results shown in Table 2 indicate that at 60 ºC, we reach a consistent DS and, thus, this was selected as the optimal temperature for performing NMR analysis.

DS HA-t-Lyp-1 at 25 ºC (%)	DS HA-t-Lyp-1 at 60 ºC (%)	DS HA-t-Lyp-1 at 70 ºC (%)	DS HA-t-Lyp-1 at 80 ºC (%)
3.4 ± 0.1	2.8 ± 0.2	2.8 ± 0.1	2.7 ± 0.1

Table 2. Degree of substitution (%) of HA with t-Lyp-1 determined at different temperatures. Results are presented as mean ± SD of 3 replicates.

Accordingly, DS for HA-Mal intermediate conjugate and HA-t-Lyp-1 of the two lowest ratios (ratio 1 and ratio 2) were determined by NMR at 60 ºC as it can be observed in Table 3. In the case of ratio 1, the DS of HA-Mal is lower than the DS of HA-t-Lyp-1, however this difference may be attributed to the fact that NMR is not a highly sensitive technique to discriminate between the small signals corresponding to low DS.

DS HA-Mal ratio 1 (%)	DS HA-Mal ratio 2 (%)	DS HA-t-Lyp-1 ratio 1 (%)	DS HA-t-Lyp-1 ratio 2 (%)
0.6 ± 0.2	2.7 ± 0.4	1.5± 0.1	2.9 ± 0.2

Table 3. Degree of substitution (%) of HA with AEM and t-Lyp-1 for ratio 1 and 2. Results are presented as mean ± SD of 3 replicates

3.2. Preparation and physico-chemical characterization of HA and HA-t-Lyp-1 nanocapsules

Small size HA nanocapsules were prepared using the solvent displacement technique, as previously disclosed by our group [38]. In order to achieve a significant reduction in the particle size (from more than 200 nm to less than 150 nm), we first conducted a study aimed at identifying the critical formulation parameters that influenced particle size. For this, an extensive evaluation of these parameters was carried out in collaboration with Raquel Abellán and these results are described in detail in Annex 1 of this thesis. Briefly, the most marked effect on size was achieved by combining two critical formulation parameters: i) the concentration of the lipid components required for the formation of the lipid droplets, and ii) the incorporation rate of the organic phase into the aqueous phase. Using these modifications we could obtain HA and HA-t-Lyp-1 nanocapsules below 150 nm, a size that was considered suitable for the nanocapsules to exhibit long circulating properties [2, 5, 6], enhanced tumour tissue penetration [9, 10] and improved lymphatic drainage from blood vasculature towards metastatic lymph nodes [11, 12].

The components selected for the formation of the nanocapsule's oily core were Miglyol® 812, used to dissolve docetaxel, and lecithin Epikuron 145V and CTAB, used as surfactants, for the stabilization of the oily droplets. CTAB was also selected because of its critical role as a bridge between the oily droplets and the HA polymer coating. Indeed, CTAB is able to form strong complexes [64-66] with HA by electrostatic interaction and this provided the basis for the formation of the HA shell over the nanocapsules. In previous studies, we have found that all these materials, when combined in the form of nanocapsules, have an acceptable toxicity profile [38, 50] .

	Size (nm)	PI	Zeta potential (mV)
HA NCs	112 ± 7	0.1	-49 ± 3
HA-t-Lyp-1 (DS 1.5%) NCs	130 ± 12	0.1	-31 ± 4
HA-t-Lyp-1 (DS 2.9%) NCs	149 ± 13	0.1	-27 ± 3

Table 4. Size, PI and Zeta potential of HA and HA-t-Lyp-1 NCs (t-Lyp-1 substitution degree of 1.5% and 2.9%). Results are presented as mean ± SD of 3 replicates

As shown in Table 4, nanocapsules obtained with this methodology form a mono-dispersed (PI 0.1) population with a mean size smaller than 150 nm. t-Lyp-1 functionalized nanocapsules could be produced with a substitution degree of the HA backbone of 1.5 and 2.9 %. Higher percentages of the peptide led to the aggregation of the nanocapsules during the preparation process. This might be due to the reduction in the number of anionic carboxylate groups, which were substituted by positive ammonium groups of the peptide.

The linking of the peptide to the HA shell led to a small increase in the particle size, an effect previously observed for other functionalized nanostructures [41, 67], and also to a reduction of the zeta potential that could be logically explained by the substitution of anionic carboxylate groups for positive ammonium groups from the peptide. This possible outward orientation of t-Lyp-1 molecules on the nanocapsule's surface is considered to be essential for the active targeting purposes.

3.3. Morphological characterization

The use of TEM microscopy allowed us to confirm that, irrespective of their functionalization, the nanocapsules exhibit a spherical shape (Figure 4) and a size between 100 and 150 nm (similar to that observed by photon-correlation spectroscopy, Table 4). Moreover, the difference in the core-shell density of the nanocapsules could also be clearly noted, illustrating the robustness of the polymer shell around the oily nanodroplets.

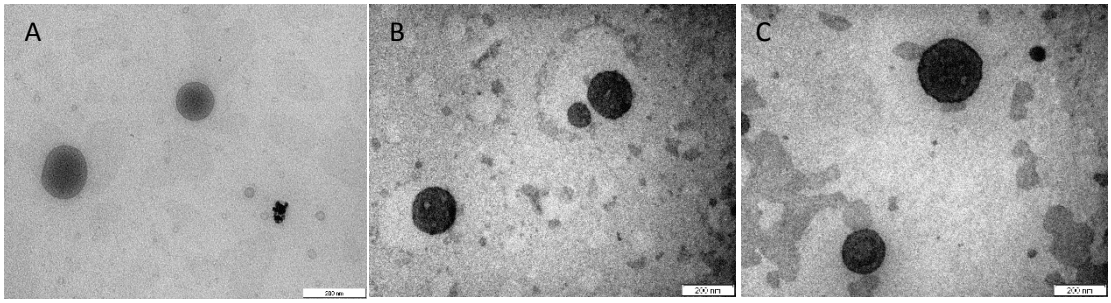

Figure 4. TEM images of HA NCs (A), HA-t-Lyp-1 NCs with a substitution degree of 1.5% (B) and HA-t-Lyp-1 NCs with a substitution degree of 2.9% (C)

3.4. Density of hyaluronic acid shell and t-Lyp-1 shell

One of the key parameters of the design of functionalized nanocarriers relies on their density of targeting ligands, given its importance on the targeting ability of nanocarriers [68-70]. Despite this, generally, most works do not report this information. Our approach has included a characterization of both HA and t-Lyp-1 shell density. These parameters could influence the target affinity of nanocapsules through CD44 and NRP1 interactions as well as the stability of the nanocapsules in biological environment.

As shown in Table 5, the HA shell density is expressed as the quantity of HA disaccharides per nanocapsule's surface area (nm2). It can be observed that HA density increases slightly with the t-Lyp-1 degree of substitution. This could be a consequence of the higher size of HA-t-Lyp-1 nanocapsules, leading to less specific surface available for attaching the same number of HA molecules.

	HA shell density (disaccharide	**t-Lyp-1 density (t-Lyp-1 molecules /nm2)**
HA NCs	2.05 ± 0.19	--
HA-t-Lyp-1 (DS 1.5%) NCs	2.33 ± 0.32	0.035 ± 0.005
HA-t-Lyp-1 (DS 2.9%) NCs	2.68 ± 0.15	0.079 ± 0.004

Table 5. Density number of disaccharides of HA and t-Lyp-1 molecules on the nanocapsules surface of HA and HA-t-Lyp-1 NCs (t-Lyp-1 substitution degree of 1.5% and 2.9%). Results are presented as mean ± SD of 3 replicates.

In the case of t-Lyp-1 density, Table 5 shows that, as expected, the two substitution degrees of HA-t-Lyp-1, resulted in a marked difference in the t-Lyp-1 density of the nanocapsules. To our knowledge, there is no previous work describing HA or t-Lyp-1 shell density on any nanocarriers surface, hence, it is not possible to make a comparative analysis. Nevertheless, in this work the dual targeting efficiency for CD44 and NRP1 has been evaluated with a cancer cell line, and therefore the effect of the different t-Lyp-1 density in HA-t-Lyp-1 nanocapsules has been assessed and described in Annex 2.

3.5. Stability of HA and HA-t-Lyp-1 nanocapsules

The assessment of an adequate stability in physiological conditions is a critical issue in the design of a nanocarrier. Often, the lack of efficacy of nanocarriers is a result of their aggregation in complex media, and this may result from the high ionic strength [3, 71] and/or the presence of proteins in biological media [72, 73]. The HA nanocapsules reported here have a HA coating firmly adhered to the oily core that helps to preserve the nanocapsule's structure in accelerated (high-speed centrifugation (84035 g, 1 hour) or long term stability studies (at least one month at 4ºC) and also upon exposure to phosphate buffer at pH 7.5 for at least three days.

In addition to the above indicated conditions, the stability of the nanocapsules in biologically relevant media was explored. Concretely, stability studies were performed in Dulbecco´s modified Eagle´s Medium (DMEM) supplemented with 10 % of fetal bovine serum (FBS), a medium frequently used in cell culture studies. The results in Figure 5 indicate that nanocapsules were stable in these media. Therefore, it could be inferred that proteins do not interact with the nanocapsules or, if they interact, they do not compromise their integrity.

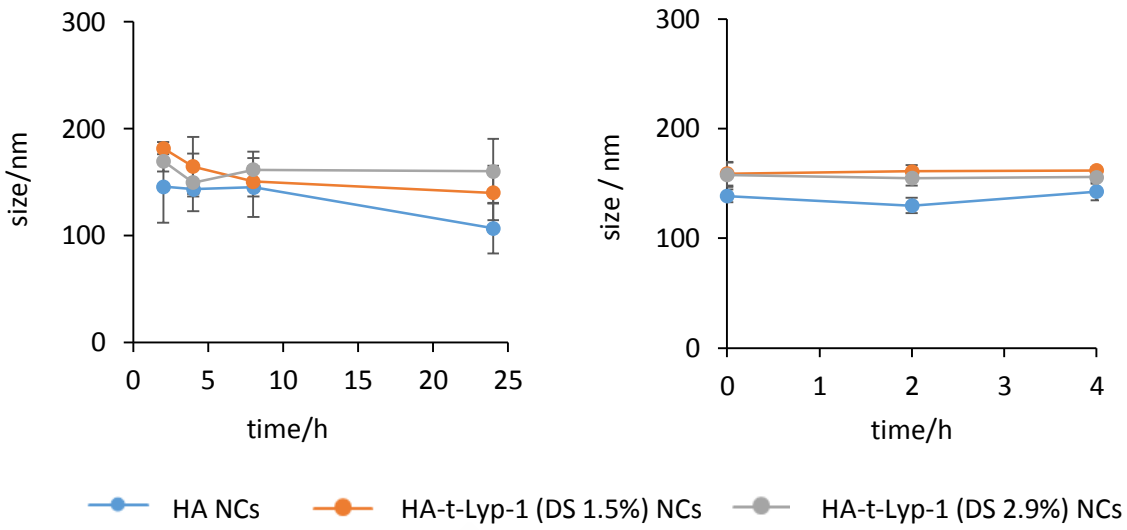

Figure 5. Stability of HA and HA-t-Lyp-1 NCs (t-Lyp-1 substitution degree of 1.5% and 2.9%) in DMEM + FBS (10 %) (left) and in human plasma (right). Results are presented as the mean ± SD of 3 replicates.

Stability studies simulating in vivo conditions were also performed by incubating the nanocapsules in human plasma, then at different time points of the study, this mixture was diluted in water in order to have a suitable viscosity media without affecting the Brownian movement and therefore size measurement, as reported by *Jiang et al* [74]. The analysis of size evolution was based on the size of the highest intensity peak in order to discriminate interferences from the colloidal proteins of plasma. Furthermore, the analysis of a control plasma sample without nanocapsules allowed us to distinguish the highest intensity peak of the plasma proteins at each time from the highest intensity peak of nanocapsules in the plasma medium. The results in Figure 5 indicate that nanocapsules remained stable upon incubation in human plasma for up to 24 h.

Overall, these results indicate that the proposed HA nanocapsules are robust nanocarriers that maintain their nanometric range even in complex media such as human plasma. This could be a consequence of the steric hindrance protection provided by the HA shell, as previously reported [1, 74]. Furthermore, this shell endows the nanocapsules with a high surface charge, which prevents them from aggregation [3]. This firm hydrophilic and negative shell is also a consequence of the appropriate choice of the surfactants and their interaction with HA.

3.6. Loading capacity and release profile of the antitumoural drug docetaxel.

Table 6 shows that, irrespective of the nature of the polymer shell, the final drug loading was above 1.5 %. The oily core of the nanocapsules can dissolve hydrophobic molecules providing high capacity for loading taxanes, similar to that reported for other lipophilic nanocarriers with drug contents between 1-4 % [37, 75-77]

	HA NCs	HA-t-Lyp-1 (DS 1.5%) NCs	HA-t-Lyp-1 (DS 2.9%) NCs
Docetaxel loading (% w/w)	1.54 ± 0.08	1.54 ± 0.11	1.53 ± 0.08

Table 6. Loading of DCX in HA and HA-t-Lyp-1 NCs (t-Lyp-1 substitution degree of 1.5% and 2.9%) expressed as weight of DCX per weight of nanocapsules (%). Results are presented as mean ± SD of 3 replicates.

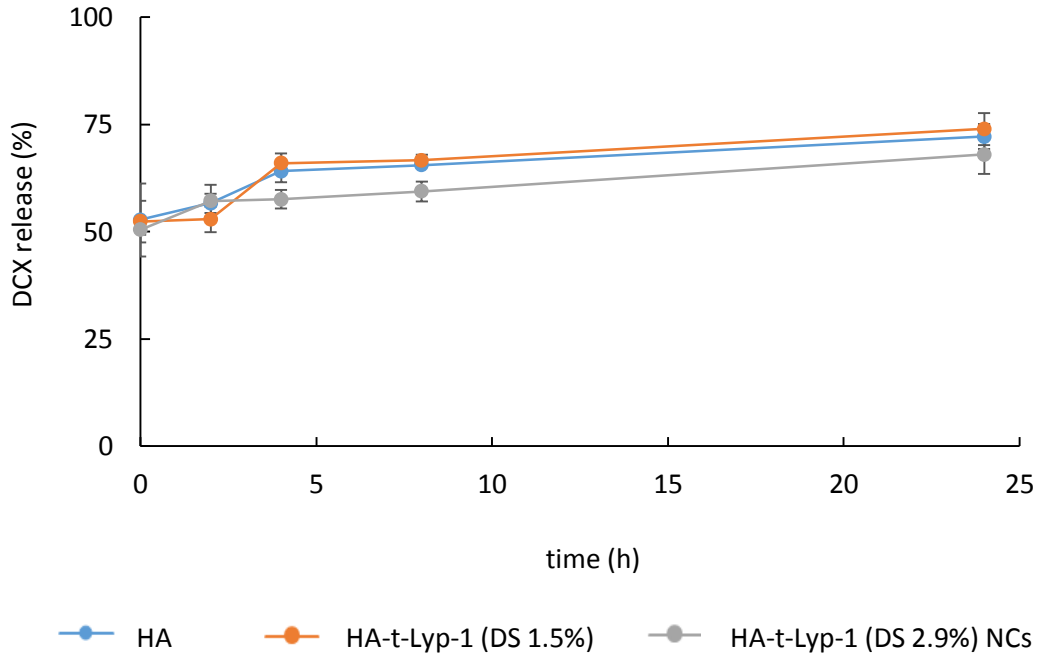

Figure 5. In vitro DCX release from HA and HA-t-Lyp-1 NCs (t-Lyp-1 substitution degree of 1.5% and 2.9%). Results are presented as mean ± SD of 3 replicates.

The ultimate success of nano-chemoterapeutics depends on their capacity for carrying enough drug to the target tissue, therefore, it is crucial to ensure that nanocarriers do not release all the cargo upon dilution. DCX was released under physiological conditions in vitro over 24 h. An initial burst release of 50 % could be observed upon dilution, which was followed by a slow and sustained release profile reaching around 74 % of drug release at the end of the study with little differences regardless of the three nanocapsule prototypes (Figure 5). This initial burst of release is a consequence of the drug partition between the oily phase of the nanocapsules and the water phase. The second slow release phase suggests that the surfactants and polymer coating works as a barrier to the transport of docetaxel that diffuses gradually to the external media. Similar kinetics have also been observed with other HA based nanocarriers, indicating that HA coating can help to control drug release [39, 78, 79].

4. Conclusions

In this work, we report for the first time the functionalization of the biopolymer HA with the tumour homing peptide t-Lyp-1. Simple carbodiimide and maleimide chemistry was employed avoiding the use of organic solvents or catalysts that can compromise the safety for a future *in vivo* application. Further, peptide binding was achieved through the terminal thiol groups, ensuring the preservation of the epitopes responsible for the biological activity. Functionalized HA nanocapsules exhibited a size in the range of 100-150 nm, a negative surface charge and a shell density in the range of 2.05 – 2.68 HA disaccharide molecules/nm2 and 0.035 – 0.079 t-Lyp-1 molecules/nm2. Associated to this firm polymer coating was the optimal stability profile of these nanocapsules upon their incubation in complex media, including plasma. Moreover, the nanocapsules were able to load docetaxel and control its release. In future work we will study the targeting capacity *in vitro* and *in vivo* for evaluating whether the present nanocarriers may contribute to the current research in cancer nanotherapeutics.

References

1. Santander-Ortega, M.J., et al., *Hydration forces as a tool for the optimization of core-shell nanoparticle vectors for cancer gene therapy.* Soft Matter, 2012. **8**(48): p. 12080-12092.
2. Vonarbourg, A., et al., *Parameters influencing the stealthiness of colloidal drug delivery systems.* Biomaterials, 2006. **27**(24): p. 4356-4373.
3. Heurtault, B., et al., *Physico-chemical stability of colloidal lipid particles.* Biomaterials, 2003. **24**(23): p. 4283-4300.
4. Alexis, F., et al., *Factors Affecting the Clearance and Biodistribution of Polymeric Nanoparticles.* Molecular pharmaceutics, 2008. **5**(4): p. 505-515.
5. Dufort, S., L. Sancey, and J.-L. Coll, *Physico-chemical parameters that govern nanoparticles fate also dictate rules for their molecular evolution.* Advanced Drug Delivery Reviews, 2012. **64**(2): p. 179-189.
6. Lux, F., et al., *Ultrasmall Rigid Particles as Multimodal Probes for Medical Applications.* Angewandte Chemie International Edition, 2011. **50**(51): p. 12299-12303.
7. Park, J.-H., et al., *Magnetic Iron Oxide Nanoworms for Tumor Targeting and Imaging.* Advanced Materials, 2008. **20**(9): p. 1630-1635.
8. Faraji, A.H. and P. Wipf, *Nanoparticles in cellular drug delivery.* Bioorganic & Medicinal Chemistry, 2009. **17**(8): p. 2950-2962.
9. Choi, K.Y., et al., *Self-assembled hyaluronic acid nanoparticles for active tumor targeting.* Biomaterials, 2010. **31**(1): p. 106-114.
10. Shen, Y., et al., *Synthesis and characterization of low molecular weight hyaluronic acid-based cationic micelles for efficient siRNA delivery.* Carbohydrate Polymers, 2009. **77**(1): p. 95-104.
11. Ryan, G.M., L.M. Kaminskas, and C.J.H. Porter, *Nano-chemotherapeutics: Maximising lymphatic drug exposure to improve the treatment of lymph-metastatic cancers.* Journal of Controlled Release, 2014. **193**(0): p. 241-256.
12. Svenson, S., *What nanomedicine in the clinic right now really forms nanoparticles?* Wiley Interdisciplinary Reviews: Nanomedicine and Nanobiotechnology, 2014. **6**(2): p. 125-135.
13. Abellan-Pose R, C.N., Alonso MJ, *Lymphatic Targeting of Nanosystems for Anticancer Drug Therapy.* Curr. Pharm. Des. In press.
14. Thiele, W. and J.P. Sleeman, *Tumor-induced lymphangiogenesis: A target for cancer therapy?* Journal of Biotechnology, 2006. **124**(1): p. 224-241.
15. Joyce, J.A. and J.W. Pollard, *Microenvironmental regulation of metastasis.* Nat Rev Cancer, 2009. **9**(4): p. 239-252.
16. Weaver, D.L., et al., *Pathologic analysis of sentinel and nonsentinel lymph nodes in breast carcinoma.* Cancer, 2000. **88**(5): p. 1099-1107.
17. Brannon-Peppas, L. and J.O. Blanchette, *Nanoparticle and targeted systems for cancer therapy.* Advanced Drug Delivery Reviews, 2004. **56**(11): p. 1649-1659.
18. Jin, S.-E., H.-E. Jin, and S.-S. Hong, *Targeted Delivery System of Nanobiomaterials in Anticancer Therapy: From Cells to Clinics.* BioMed Research International, 2014. **2014**: p. 23.
19. Sugahara, K.N., et al., *Coadministration of a Tumor-Penetrating Peptide Enhances the Efficacy of Cancer Drugs.* Science, 2010. **328**(5981): p. 1031-1035.
20. Teesalu, T., et al., *C-end rule peptides mediate neuropilin-1-dependent cell, vascular, and tissue penetration.* Proceedings of the National Academy of Sciences, 2009. **106**(38): p. 16157-16162.

21. Grantab, R., S. Sivananthan, and I.F. Tannock, *The Penetration of Anticancer Drugs through Tumor Tissue as a Function of Cellular Adhesion and Packing Density of Tumor Cells.* Cancer Research, 2006. **66**(2): p. 1033-1039.
22. Netti, P.A., et al., *Role of Extracellular Matrix Assembly in Interstitial Transport in Solid Tumors.* Cancer Research, 2000. **60**(9): p. 2497-2503.
23. Heldin, C.-H., et al., *High interstitial fluid pressure [mdash] an obstacle in cancer therapy.* Nat Rev Cancer, 2004. **4**(10): p. 806-813.
24. Jain, R.K., *Delivery of molecular and cellular medicine to solid tumors1.* Advanced Drug Delivery Reviews, 2001. **46**(1–3): p. 149-168.
25. Teijeiro, C., et al., *Polysaccharide-Based Nanocarriers for Drug Delivery*, in *Handbook of Nanobiomedical Research*. p. 235-277.
26. Harada, H. and M. Takahashi, *CD44-dependent Intracellular and Extracellular Catabolism of Hyaluronic Acid by Hyaluronidase-1 and -2.* Journal of Biological Chemistry, 2007. **282**(8): p. 5597-5607.
27. Lesley, J., R. Hyman, and P.W. Kincade, *CD44 and Its Interaction with Extracellular Matrix*, in *Advances in Immunology*, J.D. Frank, Editor 1993, Academic Press. p. 271-335.
28. Knudson, C.B., *Hyaluronan and CD44: Strategic players for cell–matrix interactions during chondrogenesis and matrix assembly.* Birth Defects Research Part C: Embryo Today: Reviews, 2003. **69**(2): p. 174-196.
29. Zhou, B., et al., *Identification of the Hyaluronan Receptor for Endocytosis (HARE).* Journal of Biological Chemistry, 2000. **275**(48): p. 37733-37741.
30. J R Fraser, W.G.K., T C Laurent, R N Cahill and N Vakakis, *Uptake and degradation of hyaluronan in lymphatic tissue.* Biochemical Journal, 1988. **256**: p. 153-158.
31. Kohda, D., et al., *Solution Structure of the Link Module: A Hyaluronan-Binding Domain Involved in Extracellular Matrix Stability and Cell Migration.* Cell, 1996. **86**(5): p. 767-775.
32. Milner, C.M. and A.J. Day, *TSG-6: a multifunctional protein associated with inflammation.* Journal of Cell Science, 2003. **116**(10): p. 1863-1873.
33. Peer, D. and R. Margalit, *Loading mitomycin C inside long circulating hyaluronan targeted nano-liposomes increases its antitumor activity in three mice tumor models.* International Journal of Cancer, 2004. **108**(5): p. 780-789.
34. Peer, D., Margalit, R., *Tumor-Targeted Hyaluronan Nanoliposomes Increase the Antitumor Activity of Liposomal Doxorubicin in Syngeneic and Human Xenograft Mouse Tumor Models.* Neoplasia, 2004. **6**(4): p. 343-353.
35. Dan, P., et al., *Nanocarriers as an emerging platform for cancer therapy.* Nature Nanotechnology, 2007. **2**(12): p. 751-760.
36. Choi, K.Y., et al., *Self-assembled hyaluronic acid nanoparticles as a potential drug carrier for cancer therapy: synthesis, characterization, and in vivo biodistribution.* Journal of Materials Chemistry, 2009. **19**(24): p. 4102-4107.
37. Yang, X.-y., et al., *Hyaluronic acid-coated nanostructured lipid carriers for targeting paclitaxel to cancer.* Cancer Letters, 2013. **334**(2): p. 338-345.
38. Oyarzun-Ampuero, F.A., et al., *Hyaluronan nanocapsules as a new vehicle for intracellular drug delivery.* European Journal of Pharmaceutical Sciences, 2013. **49**(4): p. 483-490.
39. Upadhyay, K.K., et al., *In vitro and In vivo Evaluation of Docetaxel Loaded Biodegradable Polymersomes.* Macromolecular Bioscience, 2010. **10**(5): p. 503-512.
40. Min, H.S., et al., *Liver-Specific and Echogenic Hyaluronic Acid Nanoparticles Facilitating Liver Cancer Discrimination.* Advanced Functional Materials, 2013: p. n/a-n/a.
41. Sugahara, K.N., et al., *Tissue-Penetrating Delivery of Compounds and Nanoparticles into Tumors.* Cancer Cell, 2009. **16**(6): p. 510-520.

42. Laakkonen, P., et al., *A tumor-homing peptide with a targeting specificity related to lymphatic vessels.* Nat Med, 2002. **8**(7): p. 751-5.
43. Herringson, T.P. and J.G. Altin, *Effective tumor targeting and enhanced anti-tumor effect of liposomes engrafted with peptides specific for tumor lymphatics and vasculature.* International Journal of Pharmaceutics, 2011. **411**(1–2): p. 206-214.
44. Wang, Z., et al., *LyP-1 Modification To Enhance Delivery of Artemisinin or Fluorescent Probe Loaded Polymeric Micelles to Highly Metastatic Tumor and Its Lymphatics.* Molecular Pharmaceutics, 2012. **9**(9): p. 2646-2657.
45. Karmali, P.P., et al., *Targeting of albumin-embedded paclitaxel nanoparticles to tumors.* Nanomedicine: Nanotechnology, Biology and Medicine. **5**(1): p. 73-82.
46. Roth, L., et al., *Transtumoral targeting enabled by a novel neuropilin-binding peptide.* Oncogene, 2012. **31**(33): p. 3754-3763.
47. Gonzalo, T., et al., *A new potential nano-oncological therapy based on polyamino acid nanocapsules.* Journal of Controlled Release. **169**(1–2): p. 10-16.
48. Lollo, G., et al., *Enhanced in vivo therapeutic efficacy of plitidepsin-loaded nanocapsules decorated with a new poly-aminoacid-PEG derivative.* International Journal of Pharmaceutics, 2015. **483**(1–2): p. 212-219.
49. Lozano, M.V., et al., *Intracellular delivery of docetaxel using freeze-dried polysaccharide nanocapsules.* Journal of Microencapsulation, 2012. **30**(2): p. 181-188.
50. Rivera-Rodríguez, G.R., M.J. Alonso, and D. Torres, *Poly-l-asparagine nanocapsules as anticancer drug delivery vehicles.* European Journal of Pharmaceutics and Biopharmaceutics, 2013. **85**(3, Part A): p. 481-487.
51. Moreira, J., et al., *Use of the Post-Insertion Technique to Insert Peptide Ligands into Pre-Formed Stealth Liposomes with Retention of Binding Activity and Cytotoxicity.* Pharmaceutical Research, 2002. **19**(3): p. 265-269.
52. Hoarau, D., et al., *Novel Long-Circulating Lipid Nanocapsules.* Pharmaceutical Research, 2004. **21**(10): p. 1783-1789.
53. Re, F., et al., *Functionalization of liposomes with ApoE-derived peptides at different density affects cellular uptake and drug transport across a blood-brain barrier model.* Nanomedicine: Nanotechnology, Biology and Medicine, 2011. **7**(5): p. 551-559.
54. Jin, R., P.J. Dijkstra, and J. Feijen, *Rapid gelation of injectable hydrogels based on hyaluronic acid and poly(ethylene glycol) via Michael-type addition.* Journal of Controlled Release, 2010. **148**(1): p. e41-e43.
55. Holzman, G., R.V. MacAllister, and C. Niemann, *THE COLORIMETRIC DETERMINATION OF HEXOSES WITH CARBAZOLE.* Journal of Biological Chemistry, 1947. **171**(1): p. 27-35.
56. Luo, Y., M.R. Ziebell, and G.D. Prestwich, *A Hyaluronic Acid−Taxol Antitumor Bioconjugate Targeted to Cancer Cells.* Biomacromolecules, 2000. **1**(2): p. 208-218.
57. Luo, Y. and G.D. Prestwich, *Synthesis and Selective Cytotoxicity of a Hyaluronic Acid−Antitumor Bioconjugate.* Bioconjugate Chemistry, 1999. **10**(5): p. 755-763.
58. Auzenne, E., et al., *Hyaluronic Acid-Paclitaxel: Antitumor Efficacy against CD44(+) Human Ovarian Carcinoma Xenografts.* Neoplasia (New York, N.Y.), 2007. **9**(6): p. 479-486.
59. Rosato, A., et al., *HYTAD1-p20: A new paclitaxel-hyaluronic acid hydrosoluble bioconjugate for treatment of superficial bladder cancer.* Urologic Oncology: Seminars and Original Investigations, 2006. **24**(3): p. 207-215.
60. Platt, V.M. and F.C. Szoka, *Anticancer Therapeutics: Targeting Macromolecules and Nanocarriers to Hyaluronan or CD44, a Hyaluronan Receptor.* Molecular Pharmaceutics, 2008. **5**(4): p. 474-486.
61. Jing, J., et al., *Type, Density, and Presentation of Grafted Adhesion Peptides on Polysaccharide-Based Hydrogels Control Preosteoblast Behavior and Differentiation.* Biomacromolecules, 2015. **16**(3): p. 715-722.

62. Palumbo, F.S., et al., *In situ forming hydrogels of hyaluronic acid and inulin derivatives for cartilage regeneration.* Carbohydrate Polymers, 2015. **122**: p. 408-416.
63. Novoa-Carballal, R., R. Riguera, and E. Fernandez-Megia, *Disclosing an NMR-Invisible Fraction in Chitosan and PEGylated Copolymers and Its Role on the Determination of Degrees of Substitution.* Molecular Pharmaceutics, 2013. **10**(8): p. 3225–3231.
64. Chen, Y.-H. and Q. Wang, *Establishment of CTAB Turbidimetric method to determine hyaluronic acid content in fermentation broth.* Carbohydrate Polymers, 2009. **78**(1): p. 178-181.
65. Oueslati, N., et al., *CTAB turbidimetric method for assaying hyaluronic acid in complex environments and under cross-linked form.* Carbohydrate Polymers, 2014. **112**(0): p. 102-108.
66. Song, J.-M., et al., *A simple method for hyaluronic acid quantification in culture broth.* Carbohydrate Polymers, 2009. **78**(3): p. 633-634.
67. Toti, U.S., et al., *Interfacial Activity Assisted Surface Functionalization: A Novel Approach to Incorporate Maleimide Functional Groups and cRGD Peptide on Polymeric Nanoparticles for Targeted Drug Delivery.* Molecular pharmaceutics, 2010. **7**(4): p. 1108-1117.
68. Elias, D.R., et al., *Effect of ligand density, receptor density, and nanoparticle size on cell targeting.* Nanomedicine: Nanotechnology, Biology and Medicine. **9**(2): p. 194-201.
69. Fakhari, A., et al., *Controlling ligand surface density optimizes nanoparticle binding to ICAM-1.* Journal of Pharmaceutical Sciences, 2011. **100**(3): p. 1045-1056.
70. Stefanick, J.F., et al., *A Systematic Analysis of Peptide Linker Length and Liposomal Polyethylene Glycol Coating on Cellular Uptake of Peptide-Targeted Liposomes.* ACS Nano, 2013. **7**(4): p. 2935-2947.
71. Fitch, R.M., *Principles of colloid and surface chemistry, by Paul C. Hiemenz, Marcel Dekker, New York, 1977, 516 pp. No Price given.* Journal of Polymer Science: Polymer Letters Edition, 1984. **22**(9): p. 508-509.
72. Walczyk, D., et al., *What the Cell "Sees" in Bionanoscience.* Journal of the American Chemical Society, 2010. **132**(16): p. 5761-5768.
73. Monopoli, M.P., et al., *Physical–Chemical Aspects of Protein Corona: Relevance to in Vitro and in Vivo Biological Impacts of Nanoparticles.* Journal of the American Chemical Society, 2011. **133**(8): p. 2525-2534.
74. Jiang, T., et al., *Dual-functional liposomes based on pH-responsive cell-penetrating peptide and hyaluronic acid for tumor-targeted anticancer drug delivery.* Biomaterials, 2012. **33**(36): p. 9246-9258.
75. Khalid, M., et al., *Long Circulating Poly(Ethylene Glycol)-Decorated Lipid Nanocapsules Deliver Docetaxel to Solid Tumors.* Pharmaceutical Research, 2006. **23**(4): p. 752-758.
76. Nassar, T., et al., *High Plasma Levels and Effective Lymphatic Uptake of Docetaxel in an Orally Available Nanotransporter Formulation.* Cancer Research, 2011. **71**(8): p. 3018-3028.
77. Hrkach, J., et al., *Preclinical Development and Clinical Translation of a PSMA-Targeted Docetaxel Nanoparticle with a Differentiated Pharmacological Profile.* Science Translational Medicine, 2012. **4**(128): p. 128ra39.
78. Choi, K.Y., et al., *Smart Nanocarrier Based on PEGylated Hyaluronic Acid for Cancer Therapy.* ACS Nano, 2011. **5**(11): p. 8591-8599.
79. Yoon, H.Y., et al., *Photo-crosslinked hyaluronic acid nanoparticles with improved stability for in vivo tumor-targeted drug delivery.* Biomaterials, 2013. **34**(21): p. 5273-5280.

Capítulo 3

Multifunctional hyaluronic acid and t-Lyp-1 nanocapsules: a strategy to simultaneously target and increase penetration into tumors

USC
UNIVERSIDADE
DE SANTIAGO
DE COMPOSTELA

Multifunctional hyaluronic acid and t-Lyp-1 nanocapsules: a strategy to simultaneously target and increase penetration into tumors

Este trabajo ha sido realizado en colaboración con Erea Borrajo y Anxo Vidal.

Cell Cycle and Oncology CiClOn Group, IDIS, CIMUS. (USC). Santiago de Compostela, Spain.

USC
UNIVERSIDADE
DE SANTIAGO
DE COMPOSTELA

Abstract

In general, passive targeting strategies using nanomedicines have failed to significantly concentrate the anticancer drugs in their ultimate targets (primary tumour and metastasis). As a consequence, these strategies have not led to a significant improvement in therapeutic effect of anticancer drugs. In addition to this limited targeting capacity, many of the drug nanocarriers reported so far had difficulties for getting across the tumour tissue. Here we report an advanced multifunctional technology, which exhibits a dual targeting behaviour (directed to CD44 and NRP1 cancer receptors) in addition to an improved penetration through the tumour stroma. The technology, which is based on hyaluronic acid (HA) nanocapsules, functionalized with the tumour homing peptide truncated Lyp-1 (t-Lyp-1), has been validated for the standard drug docetaxel. Hyaluronic acid (HA) is known to exhibit tumour targeting properties associated to its specific interaction with the CD44 receptor, present in cancer cells among others. On the other hand, t-Lyp-1 has been disclosed to promote tumour penetration in addition to its highly selective affinity to NRP1 receptor. The results of the pharmacokinetic and biodistribution study of docetaxel-loaded HA and HA-t-Lyp-1 nanocapsules evidenced the targeting capacity of both nanocarriers, however the drug accumulation in the tumour was dramatically higher for the t-Lyp-1 functionalized nanocapsules. The antitumour efficacy study revealed that HA-t-Lyp-1 nanocapsules decreased significantly the tumour growth and metastatic spreading through lymphatics. In conclusion, we report here for the first time the in vivo success of a multifunctional nanocarrier, which combines dual targeting with penetration enhancing properties. These; explain the extraordinary accumulation of the drug in the tumour (37 fold times higher than commercial treatment) and the capacity to, not only reduce tumour growth, but also hinder metastatic spreading.

1. Introduction

Nanomedicine science is contributing to the improvement of cancer therapies by helping anticancer drugs overcoming the biological barriers and reach their therapeutic targets. Chemotherapeutic drugs, such as paclitaxel and docetaxel, are known for their potent antitumoural effect; however, their indiscriminate biodistribution is responsible for serious side effects, which determines the balance efficacy/safety and the overall performance of these treatments [1, 2].

The most explored nanotechnology-based targeting strategy is the passive one. This relies on the use of drug nanocarriers that circulate in the blood stream for extended periods of time and take advantage of the high level of vascularization and permeability of many types of solid tumours, which enables the extravasation of nanocarriers from the blood vessels into the tumour tissue [3]. Nanoparticles with long circulating or "stealth" properties are characterized for having a hydrophilic coating, which provides them with a steric protection, thereby preventing their opsonization and subsequent clearance [4-10]. Such stealth properties have been mainly achieved by forming a hydrophilic polyethylene glycol (PEG) shell around the nanocarriers [6-8, 11-13]. However, some authors have brought up the so-called "PEG dilemma", which refers to the fact that PEG surface may have a negative effect in terms of the interaction with cancer cells [13-15].

The active targeting strategy refers to the use of stealth nanocarriers with an increased chemical affinity for receptors overexpressed in the membrane of cancer cells. This enhanced affinity is provided by the use of peptides, antibodies, nucleic acids among others, bound to the nanoparticles surface. The first targeting ligands proposed for the functionalization of micelles and liposomes were monoclonal antibodies [16-18]. Nevertheless, the immunogenicity, big size and instability of these molecules in organic solvents have hindered the translation of this technology to the clinic [19]. A more practical strategy relies on the use of Hyaluronic acid (HA), a hydrophilic and negatively charge biopolymer [20], with tumour targeting properties associated to its specific interaction with the CD44 receptor, which has widely reported to increase the capacity

for carrying drugs to tumour tissues [4, 21-25]. Nevertheless, the active targeting approach may be counter-balanced by the limited diffusion of nanocarriers across the tumour stroma [26-30]. In order to deal with this milestone, other authors have investigated the potential of a new class of tumour homing peptides, denominated CendR peptides [31-33]. These molecules have a multifunctional character, which, in addition to provide a selectivity towards specific tumour receptors [34-36], has showed the capacity to enhance the diffusion of the nanoparticles across the tumour [37]. Within this group of peptides, the truncated Lyp-1 (t-Lyp-1) with a high binding affinity for the neuropilin-1 (NRP1) receptor over-expressed in the majority of tumours, has shown a promising behavior [37].

In addition to the tumour tissue, a major target for most cancer treatments is lymphatic system [38-40], a natural niche for the spreading of metastatic cells. Nanotechnology can also help drugs reaching this specific compartment. In this regard, it is known that the physico-chemical properties of nanocarriers, such as hydrophilicity and particle size, can influence their access to the lymphatic circulation. More precisely, as in the case of passive tumour targeting, nanoparticles with a size close to 100 nm and a hydrophilic surface are those having greatest chances to diffuse passively from the blood circulation to the lymphatics [41-48].

Based on this previous knowledge, here we propose the use of Hyaluronic acid (HA) and HA-t-Lyp-1 nanocapsules loaded with the antitumoural drug Docetaxel (as described in Chapter 2). We have selected the HA-t-Lyp-1 conjugated with the highest modification level of t-Lyp-1 (substitution degree of 2.9%) based on its high cellular internalization, as observed in 2D and 3D *in vitro* studies (Annex 2 of this thesis). The presented nanocapsules fulfil a number of requisites such as small size, hydrophilic surface, adequate stability in plasma and good capacity for encapsulating and retaining the antitumoural drug. These properties may per se favour the drug accumulation in the tumour and the lymphatics mediated by a passive targeting [21, 41, 42, 49]. In addition, the polymer shell made of HA or HA-t-Lyp-1 may actively contribute to target the mentioned tissues through chemical interactions with CD44 [50-52] and NRP1 [37] cancer receptors, whereas, the presence of t-Lyp-1 may also facilitate the diffusion of the nanocapsules across the tumour tissue.

In this chapter we report the in vivo pharmacokinetics and biodistribution of docetaxel-loaded HA and HA-t-Lyp-1 nanocapsules in a metastatic lung cancer mouse model. In addition, the therapeutic effect of nanocapsules was studied in terms of reduction of tumour burden in lung and sentinel lymph node.

2. Materials and methods

2.1. Materials

Sodium hyaluronate (HA, Mw 57 KDa) was purchased from Lifecore Biomedical (USA). The truncated Lyp-1 peptide with the aminoacid sequence CGNKRTR was purchased from BCN peptides (Barcelona, Spain). Paclitaxel was purchased from Teva (Czech Republic). Taxotere was purchased from Actavis (EEUU). Hexadeciltrymethylammonium bromide (CTAB), phosphate buffered saline (PBS) and D-(+)-trehalose dehydrate, ethylenediaminetetraacetic acid (EDTA) ethylene glycol tetraacetic acid (EGTA), Tween-20, D-Luciferin for protein extracts, Sodium orthovanadate, β-Glycerophosphate and Protease inhibitor cocktail were purchased from Sigma-Aldrich (Spain). Sodium chloride (NaCl) and phenylmethylsulfonyl fluoride (PMSF) were purchased from Fisher-Scientific (Spain). Luciferin for in vivo imaging mice was purchased from Caliper (EEUU). Miglyol® 812, a neutral oil formed by esters of caprylic and capric fatty acids and glycerol, was donated by Cremer Oleo GmbH & Co (Germany). Docetaxel (DCX) was donated by Teva Pharmaceutical Industries (Israel). The surfactant Epikuron 145V, a phosphatidylcholine-enriched fraction of soybean lecithin, was donated by Cargill (Spain). Milli-Q water was used throughout the experiments and organic solvents were HPLC or MS grade.

2.2. Development of the orthotopic metastatic lung cancer model

Female athymic nude mice weighing about 20-25 g at the age of 8-12 weeks were used in the *in vivo* studies (Harlan Laboratories, Inc). The animals were acclimatized for at least 1 week before experimentation; they were housed in ventilated polypropylene cages at an average temperature of 22 ˚C, with exposure to 12 hours of light and 12 hours of darkness each day. All mice received a standard laboratory diet of food and water *ad libitum*. The experiments were carried out under Santiago de Compostela

University Bioethics Committee Rules and in compliance with the Principles of Laboratory Animal Care according to Spain national law.

The orthotopic lung cancer model that metastasizes to the mediastinal lymph nodes was adapted from *Cui et al* [53]. To generate this model, a suspension of $1x10^6$ non-small cell lung carcinoma luciferase expressing cells (A549Luc cell line) in PBS (50 µl) was injected through the intercostal space into the left lung of nude mice. During this procedure mice were anesthetized with 4% isoflurane inhalation. At different time points, luciferin was injected into the intraperitoneal cavity at a dose of 150 mg/kg body weight, approximately 5 minutes before imaging.

Luciferase bioluminescence was imaged under vaporized isofluorane anesthesia using an IVIS® Spectrum System that indicates both the presence of primary tumour growth and the cancer cell dissemination in a quantitative fashion 3 days after implantation. Dissemination of metastatic cancer cells through mediastinal lymph node could be detected ex vivo from day 13 after tumour implantation (as described in section "In vivo efficacy"). The presence of tumour cells in the lungs was moreover examined by histological analysis with a haematoxylin-eosin staining.

2.3. Pharmacokinetic and Biodistribution study

20 days after generating the orthotopic cancer model, mice were administered through tail vein by IV injection with Taxotere® (TXT, as Docetaxel commercial treatment), HA or HA-t-Lyp-1 nanocapsules in an aqueous solution of trehalose at 10% containing a total docetaxel dose of 10 mg/kg.

At selected time points blood samples were collected by jugular puncture in EDTA-containing tubes and centrifuged at 2000 g for 10 min at 4ºC for the collection of plasma samples. After blood extraction, the following tissues were harvested: heart, liver, spleen, kidney, tumour, brain and the main lymph nodes; mediastinal, cervical, axillar, inguinal and mesenteric. All these samples were rinsed with PBS and kept frozen at -80ºC until analysis.

Tissue samples were weighed and homogenized in 8mL of PBS 0.01M per g of tissue using a gentleMACS™ Dissociator (Miltenyi Biotec). Drug extraction was performed by protein precipitation methodology using acetonitrile. For this, 900 µL of acetonitrile containing 9ng of the internal standard (IS) were added to 100 µL of plasma or homogenized tissue sample. Then, this mixture was vortexed for 20 min, centrifuged at 20817 g for 5 min and 800 µL of the resulting supernatant were collected and evaporated to dryness (MiVac Duo Concentrator, Genevac) at 40ºC. Finally, the resulting dried samples were dissolved in 100 µL of mobile phase, filtered through 0.22 µm pore size (Millex-GV 4mm, Millipore) and transferred to a LC vial. Calibration standards were generated in the same way by spiking blank plasma or tissues with docetaxel standard solutions.

In order to quantify the docetaxel from tissue and plasma samples, we developed a liquid chromatography/tandem mass spectrometry method using paclitaxel as internal standard.

The UPLC system consisted of an Acquity UPLC® H-class system (Waters Corp) with thermostatized autosampler and a column compartment. Chromatography was performed on an Acquity UPLC® BEH C18 column (2.1 x 100mm, 1.7µm; Waters Corp). The following optimized parameters were employed: the mobile phase system consisted of 0.1% formic acid aqueous solution (A) and acetonitrile (B). A linear gradient program was used, with 80% to 20% of mobile phase A from 0 to 5 min, then from 5 to 5.5 min returns to 80% of A and it was kept up to 6 min for initial conditioning. The flow rate was 0.6 mL/min, the total run time was 6 min. Column temperature was maintained at 40 ºC and the autosampler was kept at 4 ºC. The volume injected was 10 µL. Under these conditions, DCX was eluted at 4.11 ± 0.02 min and IS at 4.17 ± 0.01 min.

The UPLC system was coupled to a Xevo® Triple Quadrupole Detector (TQD) (Waters Corp) with an electrospray ionization (ESI) interface. The following optimized mass parameters were employed: mass spectrometric detection was operated in positive mode and set up for multiple reaction monitoring (MRM) to monitor the transitions of m/z 830.4 → 304.1 and 830.4 → 549.2 for docetaxel and 854.6 → 286 and 854.6 → 569 for paclitaxel with auto dwell time conditions for both molecules. 525ºC was selected as source temperature and 150ºC as desolvation temperature, capillary voltage was 3.1 kV

and the cone voltage was 40 V and 20 V for docetaxel and paclitaxel respectively. Nitrogen was used for the desolvation and as cone gas at a flow rate of 600 L/h and 80 L/h repectively. Argon was used as the collision gas and the optimized collision energy was 30 eV for both DCX and IS.

Data acquisition and analysis were performed using TargetLynx v4.1 software (Waters Corp).

Docetaxel accumulation was expressed as % of the injected dose/g of tissue while drug concentration in plasma was expressed as µg of docetaxel/L of plasma. Pharmacokinetic parameters were analyzed using PKSolver [54] and data was fit to a non compartimental model.

2.4. In vivo efficacy

At day 20 and 27 after generating the orthotopic cancer model, mice were administered through tail vain by IV injection with Taxotere® (TXT, as docetaxel commercial treatment), HA or HA-t-Lyp-1 nanocapsules in an aqueous solution of trehalose at 10% containing a total docetaxel dose of 5 mg/kg. The animals were monitored daily for clinical signs of stress for the duration of the studies, and tumour evolution was followed by an IVIS® Spectrum System as described in section "Development of the orthotopic metastatic lung cancer model". Three different end time points were defined; 37 days or 19 days after tumour cell injection for non-treated mice and 47 days for treated mice. These end time points for non-treated mice will be used for comparative analysis with nanocapsules before start the treatment (day 19) and after treatment (day 37). It was not possible to kept non-treated mice until day 47 because of their accused tumoral growth. At these time points, animals were sacrificed for measuring luciferase activity in the protein extracts from lungs and mediastinal lymph nodes in order to quantify luciferase activity related with the tumour load. These tissues were homogenized in DIP buffer (50 mM pH 7.5, 150 mM NaCl, 1 mM EDTA, 2.5 mM EGTA, 0.1 % Tween-20,10 mM β-Glycerophosphate, 1 mM sodium orthovanadate, 0.1 M PMSF, 0.1 M NaF and protease inhibitors cocktail) using a tissue homogenizer (Polytron-Aggregate®, Kinematica). After centrifugation at 15000 g for 15 minutes the amount of protein in supernatants were quantified by a Bradford colorimetric method and the associated

luminescence was measured using a Lumat BL 9507 luminometer (Berthold Technologies). Results were expressed as relative luminescence units (RLU) per µg of extracted protein.

2.5. Statistical analysis

Statistical comparison was assessed using the Holm-Sidak method or t test (Graph Pad Prism software, version 6.0). Statistical significance was assigned for values of $p < 0.05$.

3. Results and discussion

A major challenge in the development of nano-oncologicals is the achievement of an adequate targeting of the cancer cells, not only at the tumour level but also at the level of the metastasis, which is often accumulated in the lymphatic compartment. In this work the *in vivo* fate of HA and HA-t-Lyp-1 nanocapsules was assessed in an orthotopic lung cancer model at an advanced metastatic state. This model consists of non-small cell lung carcinoma cells (A549), overexpressing both CD44 and NRP1 cellular receptors. Orthotopic tumour models are considered more clinically relevant and better predictive models of drug efficacy than standard subcutaneous models, owing to cancer cells are implanted directly into the organ of origin, reflecting the real situation much better than conventional subcutaneous xenograft models. In order to assess the capacity of the nanocapsule prototypes as anticancer drug carriers we evaluated their PK and biodistribution profile using a new LC-MS methodology. Then, the translation of the biodistribution profile into a therapeutic response has been assayed in terms of tumour load reduction in the primary tumour and in the sentinel lymph node.

3.1. Pharmacokinetic and biodistribution study

Figure 1 shows the plasma concentration-time curves of Docetaxel after IV administration in the form of the commercial formulation, Taxotere® (TXT) or associated to HA and HA-t-Lyp-1 nanocapsules. The overall appearance of these profiles is quite similar, however, the statistical analysis of the pharmacokinetic data (shown in Table 1) indicates that, although minor, there are significant differences in some pharmacokinetic parameters between nanocapsules and TXT. In particular, the longer MRT values for both nanocapsules compared with the commercial treatment could be related to the hydrophilic steric protection provided by the hyaluronic acid shell.

Besides, HA-t-Lyp-1 NCs present longer $t_{1/2}$, in contrast the clearance value is lower for HA NCs prototype. Globally, both prototypes appear to show similar blood permanence, as it can be figure out from Figure 1. Interestingly, the apparent distribution volume was the double for HA-t-Lyp-1 nanocapsules compared with HA nanocapsules and Taxotere®. This could be associated with the enhanced facility of HA-t-Lyp-1 to interact with tumour tissue thanks to its chemical affinity for NRP1 cellular receptor, but also thanks to its tissue penetrating ability upon binding this receptor.

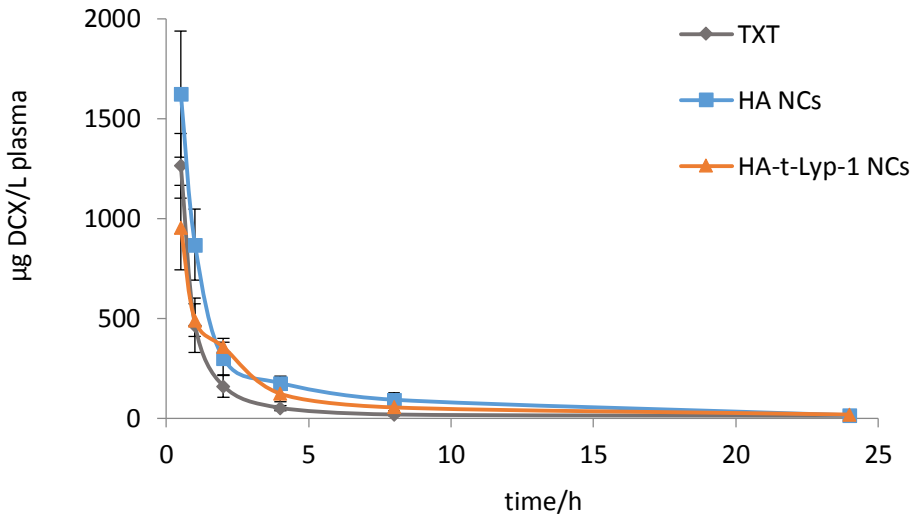

Figure 1. Docetaxel plasma concentration versus time for HA, HA-t-Lyp-1 NCs and Taxotere® after IV injection of equivalent docetaxel dose of 10 mg/kg. All the data are given as mean ± standard deviation (SD) of 5 replicates.

The capacity for prolonging the blood residence time was previously observed with other HA based nanocarriers [4, 23, 24, 55] and was attributed to the protection provided by the hydrophilic shell. In fact, different hydrophilic coated nanoparticles have shown a stealth effect [5-8]. Among them, polygutamic acid-polyethylene glycol and polyasparagine coated nanocapsules prepared in this group have exhibited increased half-life values [9, 10, 56]. This effect is expected to provide more opportunities for the nanocapsules to extravasate through the leaky tumour vessels into the tumour stroma and also into the lymphatics.

	$t_{1/2}$ (h)	$AUC_{0-\infty}$ ((mg/mL).h)	$MRT_{0-\infty}$ (h)	V (mL/kg)	Cl (mL/kg.h)
Taxotere®	5.40 ± 1.27	2.58 ± 0.35	2.89 ± 0.24	11.26± 0.60	3.93 ± 0.53
HA nanocapsules	5.75 ± 0.55	4.40 ± 1.11	4.25 ± 0.50*	9.89 ± 1.37	2.38 ± 0.62*
HA-t-Lyp-1 nanocapsules	8.43 ± 0.91*	3.16 ± 0.71	6.33 ± 0.42*	20.92 ± 6.19	3.27 ± 0.75

Table 1. Pharmacokinetic parameters for HA, HA-t-Lyp-1 NCs and Taxotere® after IV injection of equivalent docetaxel dose of 10 mg/kg, estimated with PKSolver program fitting the data to a non compartimental model. Significant differences between nanocapsules and Taxotere® (*) $p < 0.05$.

For biodistribution study, the concentration of docetaxel was determined in the lung, where the tumour was implanted and in the main lymph nodes (mediastinal, cervical, axillar, mesenteric and inguinal), where metastatic cells start to spread. In addition, the concentration of the drug was evaluated in major systemic organs, such as liver, spleen, kidney and heart. The percentage of the total injected dose of Docetaxel detected per gram of tissue was quantified using a newly developed LC-MS methodology.

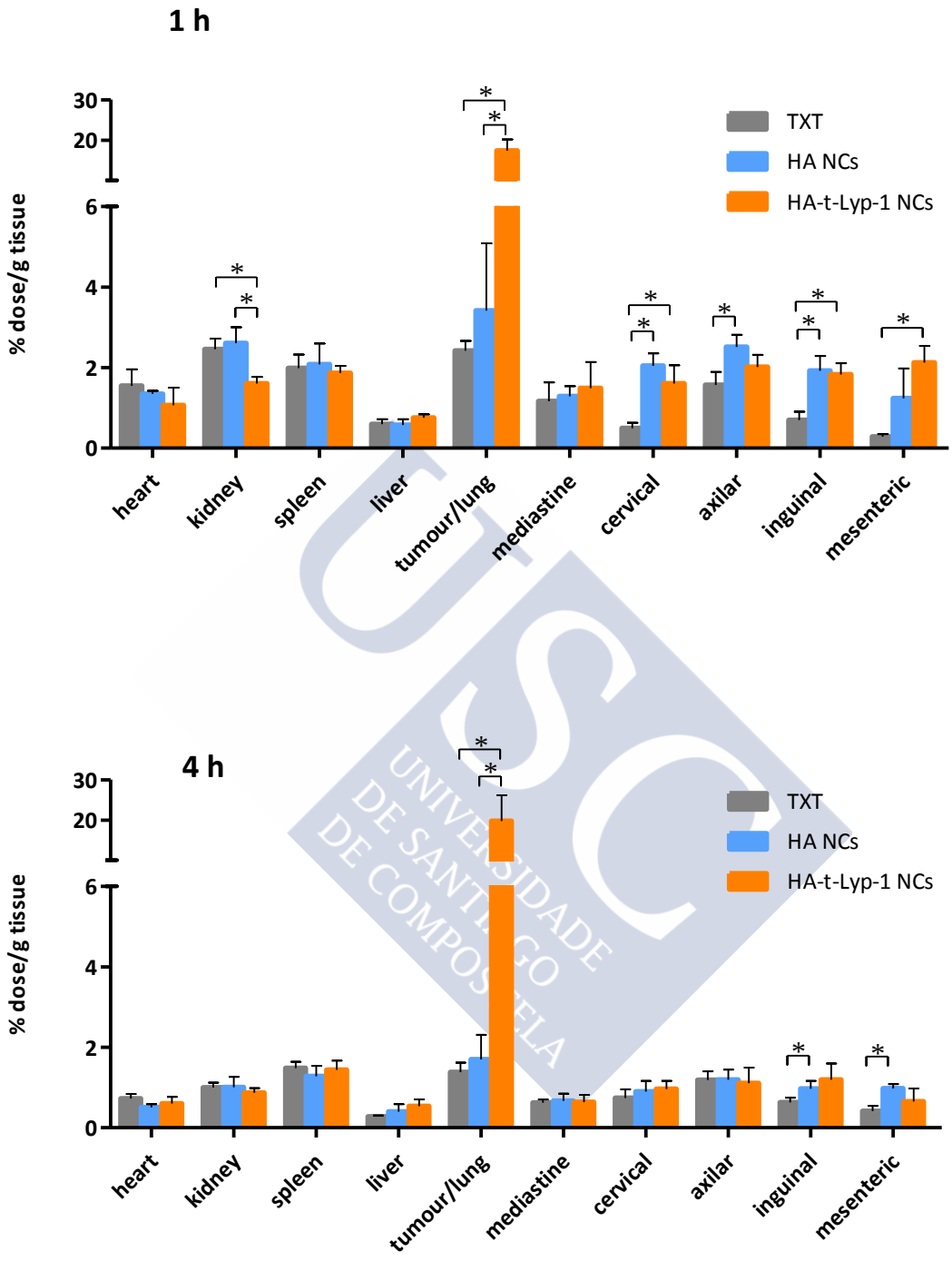

Figure 2. Docetaxel accumulation at 1 and 4 h in all tissues after IV administration of Taxotere®, HA and HA-t-Lyp-1 NCs at an equivalent docetaxel dose of 10 mg/kg. All data are given as mean ± standard deviation (SD) of 5 replicates. Significant differences between the treatments (*) $p < 0.05$.

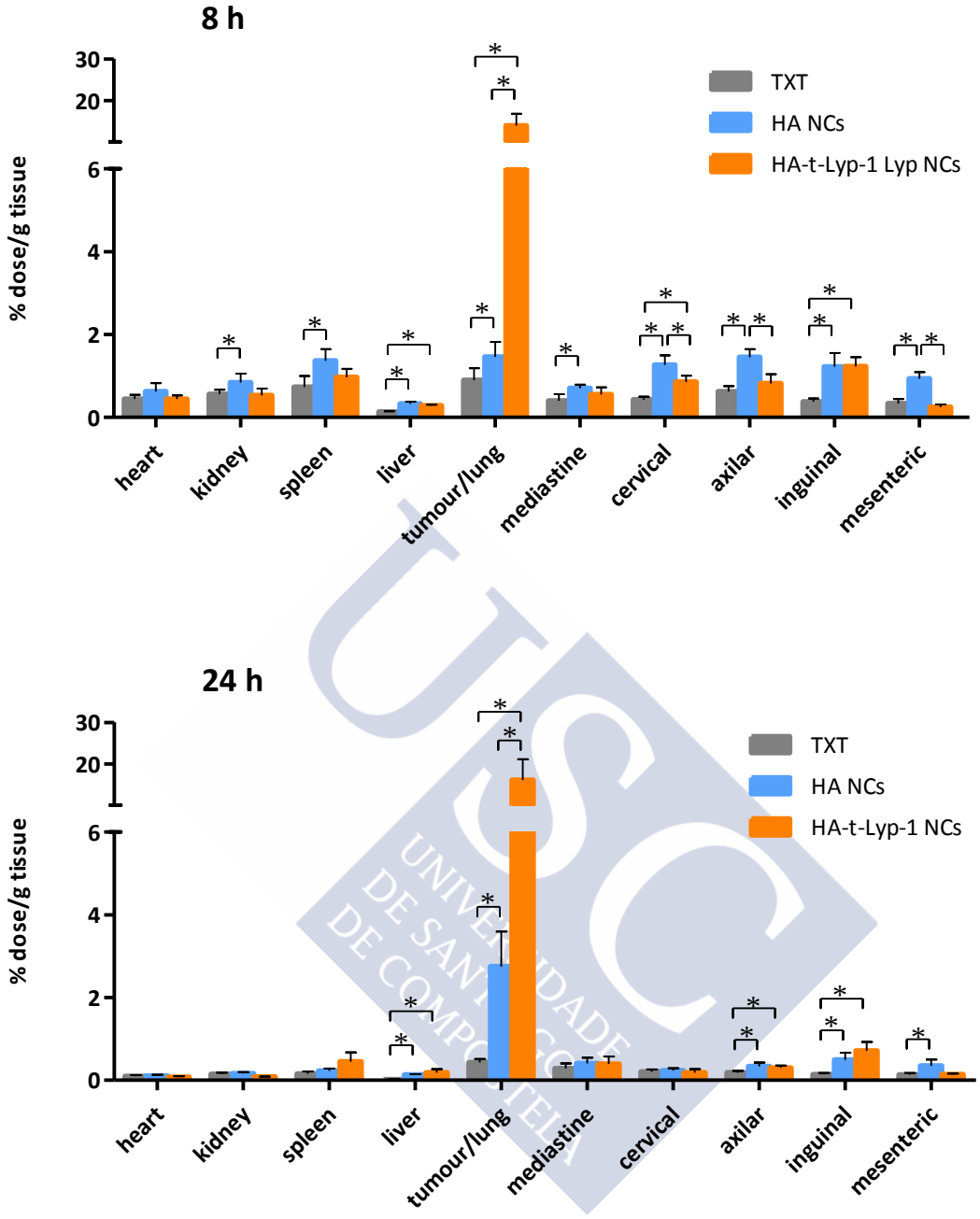

Figure 2. Docetaxel accumulation at 8 and 24h in all tissues after IV administration of Taxotere®, HA and HA-t-Lyp-1 NCs at an equivalent docetaxel dose of 10 mg/kg. All data are given as mean ± standard deviation (SD) of 5 replicates. Significant differences between the treatments (*) $p < 0.05$.

Overall, the analysis of the data indicates that the concentration of DCX in critical organs (hearth, kidney, spleen and liver) was similar for the different formulations. In contrast, the concentration of DCX in the tumour tissue was significantly higher for the nanoencapsulated docetaxel, as compared to Taxotere®. In the case of HA

nanocapsules, the differences were statistically significant at 8h and 24h, whereas in the case of HA-t-Lyp-1 nanocapsules the differences were statistically significant at all time points studied. On the other hand, the concentration of DCX in the lymph nodes was also significantly higher for the nanocapsules with respect to the commercial treatment, with statistically significant differences at almost all times.

Another particularly interesting observation is the low DCX accumulation in the liver and spleen achieved with both nanocapsule formulations. This is clearly in contrast with the data reported for many liposomes and functionalized nanocarriers, which have shown preferential clearance through these organs [4, 7, 8, 22, 24, 57-60]. It should be however noted that a slight but significant increase in DCX hepatic levels were observed for both nanocapsule prototypes (statistically significant differences at 8 and 24h), that could be attributed to the presence of a hyaluronic acid receptor for endocytosis (HARE) in the endothelium of liver [50, 61]. The detailed analysis of the tumour targeting capacity of the nanocapsules indicated that the drug concentration in the tumour increased over time reaching at 24 h up to a 6.3 and 36.6 times higher DCX concentration for HA and HA-t-Lyp-1 nanocapsules respectively, as compared with TXT. Consequently, these data underline the active targeting efficacy of both formulations, being this capacity particularly reinforced by the presence of t-Lyp-1 on the nanocapsules surface. The contribution of the “EPR effect” to this specific DCX accumulation in the tumour tissue cannot be discarded as described for other nanocarriers [8, 60]. However, the chemical affinity seems to be the major driving force for tumour accumulation. In fact, the similar PK profiles observed for both nanocapsules and the drastic difference in tumour accumulation underlines the tumour homing efficiency of t-Lyp-1. This difference is attributable to the high specificity of the main cellular receptor of t-Lyp-1 (NRP1) mostly located in tumour, in contrast with the wide distribution of CD44 over the body. On the other hand, the tissue specific penetration capacity of t-Lyp-1 is also expected to contribute to the DXC accumulation in the tumour tissue. This targeting effect has already been reported for HA-based nanocarriers [12, 13, 62-64] and also for t-Lyp-1 targeted nanocarriers [37]. However, to our knowledge, the high level of DCX accumulation in the tumour tissue, which reaches up to 20% of Docetaxel dose per gram

of tumour, associated with a minimal accumulation in the liver, has not been reported previously.

Finally, the results of the lymphatic accumulation of DCX underline the lymphatic targeting capacity of both types of nanocapsules. The increased level of DCX reached a maximum of 7.4 fold times accumulation (HA-t-Lyp-1 nanocapsules vs. TXT in the mesenteric lymph node at 1h). This increase of docetaxel levels does not present a clearly tendency in favour of one nanocapsule prototype, neither in favour of a specific type of lymph node. However, there is hardly difference between the three treatments in the case of sentinel lymph node (mediastine), probably due to a deficient lymphatic drainage at the proximity of the tumour [3]. Despite of this, the overall enhanced lymphatic accumulation may help preventing the metastatic spreading through the lymphatics whilst the high levels of DCX found in the tumour tissue may also reduce the arrival of new metastatic cells from primary tumour. Among the few references on the use of nanocarriers for enhancing the lymphatic accumulation of chemotherapeutic drugs after IV administration, there are pegylated liposomes and micelles [65-68]. These nanocarriers provided lymphatic accumulation levels ranging from 2 to 8 times, as compared to the corresponding commercial anticancer drug. These values are similar to those obtained with the nanocapsules prototypes proposed in this work and are expected to be related to the physico-chemical properties, notably, to the hydrophilic shell and to the small size [41, 42]. Besides, the presence of Lyve-1 HA receptors in lymphatic vessels [61, 69] could have also contributed to the enhanced lymphatic targeting capacity.

In conclusion, both nanocapsules presented increased capacity for the targeting of docetaxel to both the primary tumour and the lymphatics. In particular, those functionalized with t-Lyp-1 showed a noteworthy tumour accumulation. Therefore, it is expected that these nanocapsules can improve the efficacy of DCX inhibiting both metastatic cell spreading and primary tumour growth.

3.2. In vivo efficacy

Tumour inhibition was determined as luciferase activity in protein extracts associated with tumour cells from primary tumour (lungs) and sentinel lymph node (mediastinal nodes). Besides, luciferase activity was also monitored in vivo by IVIS in order to control tumour progression.

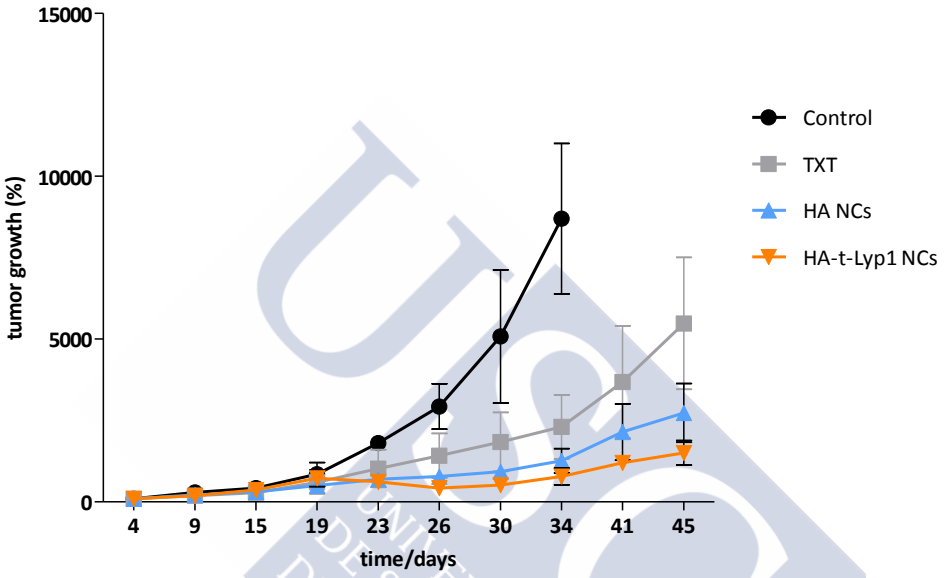

Figure 3. Tumour growth according raise of luciferase activity obtained by in vivo luminiscence after administration of a total dose of 10 mg/kg of Taxotere, HA and HA-t-Lyp-1 nanocapsules. All the data are given as mean ± standard deviation (SD) of 5 replicates.

Figure 3 shows the evolution of the tumour growth over the time based on the luminescence measured by IVIS. The results from this primary inspection indicate that DCX slows down tumour progression as compared with non-treated mice (control) and this effect is more pronounced for the nanocapsules than for the commercial formulation. Non-treated mice were sacrificed at day 37, because of their exponential tumour growth, weight loss and respiratory distress.

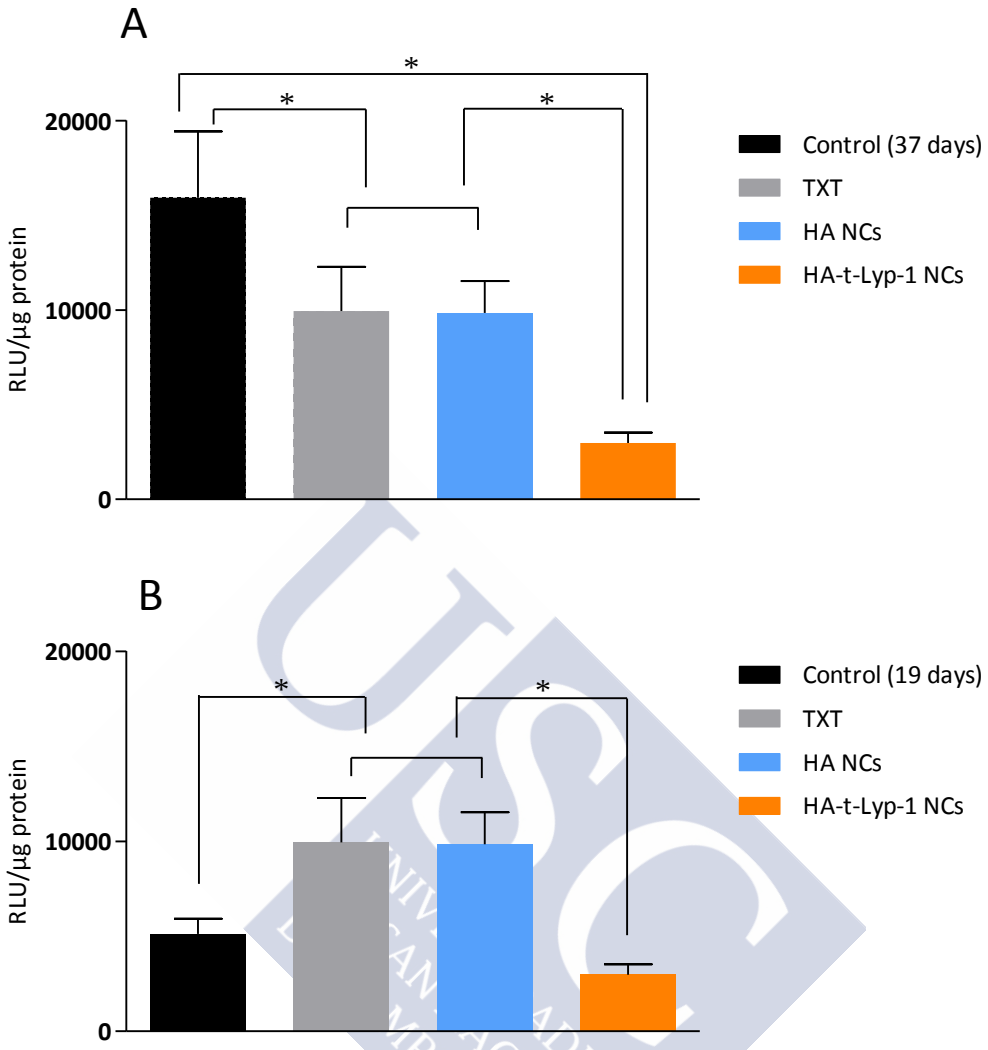

Figure 4. Quantification of luciferase activity in lungs ex vivo after IV administration of Taxotere®, HA and HA-t-Lyp-1 nanocapsules at an equivalent docetaxel dose of 10mg/kg versus control at 37 days (A) and control at 19 days (B). All the data are given as mean ± standard deviation (SD) of 5 replicates. Significant differences between the treatments (*) $p < 0.05$

The results of the quantitative analysis of luciferase activity after extracting the proteins from the tumour at the end of the experiment (day 47), are shown in Figure 4. According to these data, TXT and DCX-loaded HA nanocapsules show very similar tumour growth inhibition rate, whereas the t-Lyp-1 functionalized HA nanocapsules led to a significant reduction of the tumour burden. The limited effect of HA nanocapsules despite their 6.3 fold tumour accumulation as compared to Taxotere® could be related with the

potentially poor penetration of nanocarriers through the dense collagen extracellular matrix [26, 27] and the high interstitial fluid pressure [28, 29] of this advanced solid tumour mass, as previously reported for other nanocarriers [70, 71]. This hypothesis could also be supported by the differences between the results obtained with the luminescence IVIS monitoring and the quantitative analysis. Luciferase activity from IVIS shows a greater tumour reduction for DCX-loaded HA nanocapsules with respect to TXT, whilst this difference is not reflected by the quantitative ex vivo analysis. This might suggest that the IVIS signal proceeds from cells located in the tumour periphery rather than from the whole tumour tissue. The advanced mestastatic stage of this cancer model might aggravate the tumour physiology, hindering the penetration of HA nanocapsules within tumour tissue. On the other hand, the tissue specific penetration activity of t-Lyp-1 allows this prototype diffuse within tumour stroma, reaching a higher number of cancer cells. This would explain the translation of the 36.6 fold DCX accumulation in a markedly reduced tumour load compared with Taxotere®, in fact HA-t-Lyp-1 nanocapsules were able to revert tumour growth below tumour load before starting the treatment (control at day 19).

The therapeutic consequence of the enhanced tumour penetration capacity of CendR peptides has already been reported for other nanocarriers. For example albumin nanoparticles (Abraxane®) modified with cyclic Lyp-1 and iRGD allowed deeper diffusion in tumour stroma, followed by an enhanced antitumour effect as compared to non-modified albumin nanoparticles [31, 72].

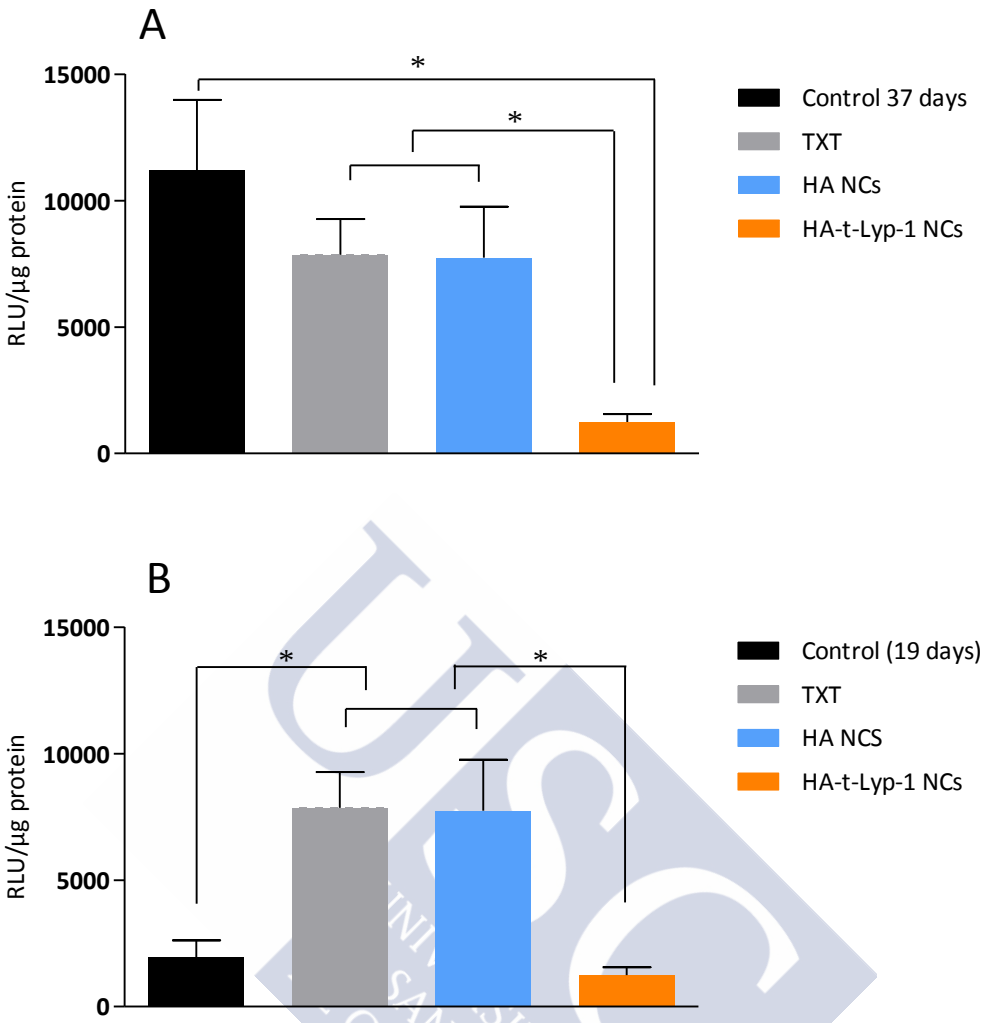

Figure 5. Quantification of luciferase activity in mediastinal lymph nodes ex vivo after IV administration of Taxotere®, HA and HA-t-Lyp-1 nanocapsules at an equivalent docetaxel dose of 10mg/kg versus control at 37 days (A) and control at 19 days (B). All the data are given as mean ± standard deviation (SD) of 5 replicates. Significant differences between the treatments (*) $p < 0.05$

The inhibition of the metastatic spreading through the sentinel lymph node is shown in Figure 5. As in the case of lung tumour load, HA nanocapsules and TXT exhibited a comparable anti-metastatic activity. In contrast, when comparing the metastatic load at day 19 and day 37, the conclusion is that HA-t-Lyp-1 nanocapsules are capable of inhibiting the metastatic spreading. Taking into account that the three treatments reached similar DCX levels in this affected lymph node in the biodistribution study, a possible explanation for the low metastatic load of animals treated with HA-t-Lyp-1 nanocapsules could be related to the prevention of the arrival of metastatic cells from

the primary tumour rather than a direct effect on the metastasis. Additionally, the increased DCX levels detected in the rest of lymphatics with both nanocapsules may also contribute to the anti-metastatic effect of these prototypes as compared with TXT, avoiding the spreading and colonization of other tissues through distant lymph nodes.

4. Conclusions

This chapter reports the *in vivo* fate of HA and HA-t-Lyp-1 nanocapsules as carriers for the active targeting of DCX. Mice bearing an orthotopic lung cancer in an advanced metastatic stage were intravenously administered with the commercial formulation TXT, and the docetaxel-loaded proposed nanocapsules. The biodistribution profile showed both prototypes, especially HA-t-Lyp-1 nanocapsules, present an active cancer cell targeting ability, associated to the specificity of its receptor and its tumour penetration properties. This targeting effect was eventually translated not only in the prevention of tumour growth but also on the inhibition of metastatic spreading. Overall, these results highlight the importance of enhancing drug tumour targeting and penetration, especially in the case of the worst prognostic situations where high interstitial fluidic pressure and dense collagen extracellular matrix are especially problematic [26-29].

References

1. de Weger, V.A., J.H. Beijnen, and J.H.M. Schellens, *Cellular and clinical pharmacology of the taxanes docetaxel and paclitaxel – a review.* Anti-Cancer Drugs, 2014. **25**(5): p. 488-494.
2. Chu, Q., et al., *Taxanes as first-line therapy for advanced non-small cell lung cancer: A systematic review and practice guideline.* Lung Cancer, 2005. **50**(3): p. 355-374.
3. Maeda, H., *Toward a full understanding of the EPR effect in primary and metastatic tumors as well as issues related to its heterogeneity.* Advanced Drug Delivery Reviews, (0).
4. Yang, X.-y., et al., *Hyaluronic acid-coated nanostructured lipid carriers for targeting paclitaxel to cancer.* Cancer Letters, 2013. **334**(2): p. 338-345.
5. Chen, D.-B., et al., *In Vitro and in Vivo Study of Two Types of Long-Circulating Solid Lipid Nanoparticles Containing Paclitaxel.* Chemical and Pharmaceutical Bulletin, 2001. **49**(11): p. 1444-1447.
6. Yang, T., et al., *Enhanced solubility and stability of PEGylated liposomal paclitaxel: In vitro and in vivo evaluation.* International Journal of Pharmaceutics, 2007. **338**(1–2): p. 317-326.
7. Ernsting, M.J., et al., *Preclinical pharmacokinetic, biodistribution, and anti-cancer efficacy studies of a docetaxel-carboxymethylcellulose nanoparticle in mouse models.* Biomaterials, 2012. **33**(5): p. 1445-1454.
8. Jiang, X., et al., *PEGylated poly(trimethylene carbonate) nanoparticles loaded with paclitaxel for the treatment of advanced glioma: In vitro and in vivo evaluation.* International Journal of Pharmaceutics, 2011. **420**(2): p. 385-394.
9. Lollo, G., et al., *Enhanced in vivo therapeutic efficacy of plitidepsin-loaded nanocapsules decorated with a new poly-aminoacid-PEG derivative.* International Journal of Pharmaceutics, 2015. **483**(1–2): p. 212-219.
10. Rivera-Rodriguez, G.R., et al., *In vivo evaluation of poly-l-asparagine nanocapsules as carriers for anti-cancer drug delivery.* International Journal of Pharmaceutics, 2013. **458**(1): p. 83-89.
11. Lollo, G., et al., *Polyglutamic acid–PEG nanocapsules as long circulating carriers for the delivery of docetaxel.* European Journal of Pharmaceutics and Biopharmaceutics, 2014. **87**(1): p. 47-54.
12. Choi, K.Y., et al., *Smart Nanocarrier Based on PEGylated Hyaluronic Acid for Cancer Therapy.* ACS Nano, 2011. **5**(11): p. 8591-8599.
13. Choi, K.Y., et al., *PEGylation of hyaluronic acid nanoparticles improves tumor targetability in vivo.* Biomaterials, 2011. **32**(7): p. 1880-1889.
14. Hatakeyama, H., H. Akita, and H. Harashima, *A multifunctional envelope type nano device (MEND) for gene delivery to tumours based on the EPR effect: A strategy for overcoming the PEG dilemma.* Advanced Drug Delivery Reviews, 2011. **63**(3): p. 152-160.
15. Wang, T., J.R. Upponi, and V.P. Torchilin, *Design of multifunctional non-viral gene vectors to overcome physiological barriers: Dilemmas and strategies.* International Journal of Pharmaceutics, 2012. **427**(1): p. 3-20.
16. Torchilin, V.P., *Immunoliposomes and PEGylated Immunoliposomes: Possible Use for Targeted Delivery of Imaging Agents.* ImmunoMethods, 1994. **4**(3): p. 244-258.
17. Warenius, H.M., et al., *Attempted targeting of a monoclonal antibody in a human tumour xenograft system.* European Journal of Cancer and Clinical Oncology, 1981. **17**(9): p. 1009-1015.

18. Leserman, L.D., et al., *Targeting to cells of fluorescent liposomes covalently coupled with monoclonal antibody or protein A.* Nature, 1980. **288**(5791): p. 602-604.
19. Kamaly, N., et al., *Targeted polymeric therapeutic nanoparticles: design, development and clinical translation.* Chemical Society reviews, 2012. **41**(7): p. 2971-3010.
20. Teijeiro, C., et al., *Polysaccharide-Based Nanocarriers for Drug Delivery*, in *Handbook of Nanobiomedical Research*. p. 235-277.
21. Choi, K.Y., et al., *Self-assembled hyaluronic acid nanoparticles for active tumor targeting.* Biomaterials, 2010. **31**(1): p. 106-114.
22. Choi, K.Y., et al., *Self-assembled hyaluronic acid nanoparticles as a potential drug carrier for cancer therapy: synthesis, characterization, and in vivo biodistribution.* Journal of Materials Chemistry, 2009. **19**(24): p. 4102-4107.
23. Peer, D. and R. Margalit, *Loading mitomycin C inside long circulating hyaluronan targeted nano-liposomes increases its antitumor activity in three mice tumor models.* International Journal of Cancer, 2004. **108**(5): p. 780-789.
24. Peer, D., Margalit, R., *Tumor-Targeted Hyaluronan Nanoliposomes Increase the Antitumor Activity of Liposomal Doxorubicin in Syngeneic and Human Xenograft Mouse Tumor Models.* Neoplasia, 2004. **6**(4): p. 343-353.
25. Oyarzun-Ampuero, F.A., et al., *Hyaluronan nanocapsules as a new vehicle for intracellular drug delivery.* European Journal of Pharmaceutical Sciences, 2013. **49**(4): p. 483-490.
26. Grantab, R., S. Sivananthan, and I.F. Tannock, *The Penetration of Anticancer Drugs through Tumor Tissue as a Function of Cellular Adhesion and Packing Density of Tumor Cells.* Cancer Research, 2006. **66**(2): p. 1033-1039.
27. Netti, P.A., et al., *Role of Extracellular Matrix Assembly in Interstitial Transport in Solid Tumors.* Cancer Research, 2000. **60**(9): p. 2497-2503.
28. Heldin, C.-H., et al., *High interstitial fluid pressure [mdash] an obstacle in cancer therapy.* Nat Rev Cancer, 2004. **4**(10): p. 806-813.
29. Jain, R.K., *Delivery of molecular and cellular medicine to solid tumors1.* Advanced Drug Delivery Reviews, 2001. **46**(1–3): p. 149-168.
30. RK, J., *Transport of molecules, particles, and cells in solid tumors.* Annual Review of Biomedical Engineering, 1999. **1**: p. 241-263.
31. Sugahara, K.N., et al., *Tissue-Penetrating Delivery of Compounds and Nanoparticles into Tumors.* Cancer Cell, 2009. **16**(6): p. 510-520.
32. Sugahara, K.N., et al., *Coadministration of a Tumor-Penetrating Peptide Enhances the Efficacy of Cancer Drugs.* Science, 2010. **328**(5981): p. 1031-1035.
33. Teesalu, T., et al., *C-end rule peptides mediate neuropilin-1-dependent cell, vascular, and tissue penetration.* Proceedings of the National Academy of Sciences, 2009. **106**(38): p. 16157-16162.
34. Ellis, L.M., *The role of neuropilins in cancer.* Molecular Cancer Therapeutics, 2006. **5**(5): p. 1099-1107.
35. Guttmann-Raviv, N., et al., *The neuropilins and their role in tumorigenesis and tumor progression.* Cancer Letters, 2006. **231**(1): p. 1-11.
36. Bagri, A., M. Tessier-Lavigne, and R.J. Watts, *Neuropilins in Tumor Biology.* Clinical Cancer Research, 2009. **15**(6): p. 1860-1864.
37. Roth, L., et al., *Transtumoral targeting enabled by a novel neuropilin-binding peptide.* Oncogene, 2012. **31**(33): p. 3754-3763.
38. Thiele, W. and J.P. Sleeman, *Tumor-induced lymphangiogenesis: A target for cancer therapy?* Journal of Biotechnology, 2006. **124**(1): p. 224-241.
39. Joyce, J.A. and J.W. Pollard, *Microenvironmental regulation of metastasis.* Nat Rev Cancer, 2009. **9**(4): p. 239-252.
40. Weaver, D.L., et al., *Pathologic analysis of sentinel and nonsentinel lymph nodes in breast carcinoma.* Cancer, 2000. **88**(5): p. 1099-1107.

41. Ryan, G.M., L.M. Kaminskas, and C.J.H. Porter, *Nano-chemotherapeutics: Maximising lymphatic drug exposure to improve the treatment of lymph-metastatic cancers.* Journal of Controlled Release, 2014. **193**(0): p. 241-256.
42. Svenson, S., *What nanomedicine in the clinic right now really forms nanoparticles?* Wiley Interdisciplinary Reviews: Nanomedicine and Nanobiotechnology, 2014. **6**(2): p. 125-135.
43. Vonarbourg, A., et al., *Parameters influencing the stealthiness of colloidal drug delivery systems.* Biomaterials, 2006. **27**(24): p. 4356-4373.
44. Dufort, S., L. Sancey, and J.-L. Coll, *Physico-chemical parameters that govern nanoparticles fate also dictate rules for their molecular evolution.* Advanced Drug Delivery Reviews, 2012. **64**(2): p. 179-189.
45. Lux, F., et al., *Ultrasmall Rigid Particles as Multimodal Probes for Medical Applications.* Angewandte Chemie International Edition, 2011. **50**(51): p. 12299-12303.
46. Park, J.-H., et al., *Magnetic Iron Oxide Nanoworms for Tumor Targeting and Imaging.* Advanced Materials, 2008. **20**(9): p. 1630-1635.
47. Faraji, A.H. and P. Wipf, *Nanoparticles in cellular drug delivery.* Bioorganic & Medicinal Chemistry, 2009. **17**(8): p. 2950-2962.
48. Abellan-Pose R, C.N., Alonso MJ, *Lymphatic Targeting of Nanosystems for Anticancer Drug Therapy.* Curr. Pharm. Des. In press.
49. Shen, Y., et al., *Synthesis and characterization of low molecular weight hyaluronic acid-based cationic micelles for efficient siRNA delivery.* Carbohydrate Polymers, 2009. **77**(1): p. 95-104.
50. Harada, H. and M. Takahashi, *CD44-dependent Intracellular and Extracellular Catabolism of Hyaluronic Acid by Hyaluronidase-1 and -2.* Journal of Biological Chemistry, 2007. **282**(8): p. 5597-5607.
51. Lesley, J., R. Hyman, and P.W. Kincade, *CD44 and Its Interaction with Extracellular Matrix*, in *Advances in Immunology*, J.D. Frank, Editor 1993, Academic Press. p. 271-335.
52. Knudson, C.B., *Hyaluronan and CD44: Strategic players for cell–matrix interactions during chondrogenesis and matrix assembly.* Birth Defects Research Part C: Embryo Today: Reviews, 2003. **69**(2): p. 174-196.
53. Cui, Z.Y., et al., *Mouse Orthotopic Lung Cancer Model Induced by PC14PE6.* Cancer Res Treat, 2006. **38**(4): p. 234-239.
54. Zhang, Y., et al., *PKSolver: An add-in program for pharmacokinetic and pharmacodynamic data analysis in Microsoft Excel.* Computer Methods and Programs in Biomedicine, 2010. **99**(3): p. 306-314.
55. Dan, P., et al., *Nanocarriers as an emerging platform for cancer therapy.* Nature Nanotechnology, 2007. **2**(12): p. 751-760.
56. Gonzalo, T., et al., *A new potential nano-oncological therapy based on polyamino acid nanocapsules.* Journal of Controlled Release. **169**(1–2): p. 10-16.
57. Rivkin, I., et al., *Paclitaxel-clusters coated with hyaluronan as selective tumor-targeted nanovectors.* Biomaterials, 2010. **31**(27): p. 7106-7114.
58. Ayen, W. and N. Kumar, *In Vivo Evaluation of Doxorubicin-Loaded (PEG)3-PLA Nanopolymersomes (PolyDoxSome) Using DMBA-Induced Mammary Carcinoma Rat Model and Comparison with Marketed LipoDox™.* Pharmaceutical Research, 2012. **29**(9): p. 2522-2533.
59. Karra, N., et al., *Antibody Conjugated PLGA Nanoparticles for Targeted Delivery of Paclitaxel Palmitate: Efficacy and Biofate in a Lung Cancer Mouse Model.* Small, 2013. **9**(24): p. 4221-4236.
60. Cheng, J., et al., *Formulation of functionalized PLGA–PEG nanoparticles for in vivo targeted drug delivery.* Biomaterials, 2007. **28**(5): p. 869-876.

61. Zhou, B., et al., *Identification of the Hyaluronan Receptor for Endocytosis (HARE).* Journal of Biological Chemistry, 2000. **275**(48): p. 37733-37741.
62. Yoon, H.Y., et al., *Photo-crosslinked hyaluronic acid nanoparticles with improved stability for in vivo tumor-targeted drug delivery.* Biomaterials, 2013. **34**(21): p. 5273-5280.
63. Lee, D.-E., et al., *Amphiphilic hyaluronic acid-based nanoparticles for tumor-specific optical/MR dual imaging.* Journal of Materials Chemistry, 2012. **22**(21): p. 10444-10447.
64. Yoon, H.Y., et al., *Tumor-targeting hyaluronic acid nanoparticles for photodynamic imaging and therapy.* Biomaterials, 2012. **33**(15): p. 3980-3989.
65. Ryan, G.M., et al., *PEGylated polylysine dendrimers increase lymphatic exposure to doxorubicin when compared to PEGylated liposomal and solution formulations of doxorubicin.* Journal of Controlled Release, 2013. **172**(1): p. 128-136.
66. Qin, L., et al., *Polymeric micelles for enhanced lymphatic drug delivery to treat metastatic tumors.* Journal of Controlled Release, 2013. **171**(2): p. 133-142.
67. Rafi, M., et al., *Polymeric micelles incorporating (1,2-diaminocyclohexane)platinum (II) suppress the growth of orthotopic scirrhous gastric tumors and their lymph node metastasis.* Journal of Controlled Release, 2012. **159**(2): p. 189-196.
68. Tan, R., et al., *Preparation of vincristine sulfate-loaded poly (butylcyanoacrylate) nanoparticles modified with pluronic F127 and evaluation of their lymphatic tissue targeting.* Journal of Drug Targeting, 2014. **22**(6): p. 509-517.
69. J R Fraser, W.G.K., T C Laurent, R N Cahill and N Vakakis, *Uptake and degradation of hyaluronan in lymphatic tissue.* Biochemical Journal, 1988. **256**: p. 153-158.
70. Wong, C., et al., *Multistage nanoparticle delivery system for deep penetration into tumor tissue.* Proceedings of the National Academy of Sciences, 2011. **108**(6): p. 2426-2431.
71. Yan, Z., et al., *Tumor-Penetrating Peptide Mediation: An Effective Strategy for Improving the Transport of Liposomes in Tumor Tissue.* Molecular Pharmaceutics, 2014. **11**(1): p. 218-225.
72. Karmali, P.P., et al., *Targeting of albumin-embedded paclitaxel nanoparticles to tumors.* Nanomedicine: Nanotechnology, Biology and Medicine. **5**(1): p. 73-82.

USC
UNIVERSIDADE
DE SANTIAGO
DE COMPOSTELA

Discusión general

USC
UNIVERSIDADE
DE SANTIAGO
DE COMPOSTELA

The design of actively targeted nanocarriers for the delivery of anticancer drugs is expected to contribute to a drastic improvement of oncological therapies. The combination of favorable physico-chemical properties, such as small size [1] and a hydrophilic surface [1], with the use of smart materials which endow nanocarriers with multifunctional capacity for specific interacting with tumour cells [2, 3] and promoting tumour penetration [4, 5], represents a promising strategy towards improving the therapeutic response of oncological drugs.

In this work, multifunctional hyaluronic acid (HA)-based nanocapsules were developed for the selective delivery of anticancer drugs. The natural polysaccharide, HA was expected to target the drug to the tumour tissue thanks to its specific interaction with the CD44 receptor, present in cancer cells. Additionally, the hydrophilic surface of the nanocapsules was supposed to provide the nanocapsules with stealth properties [6-11]. A subsequent multifunctional level was encompassed using the tumour homing peptide, truncated Lyp-1 (t-Lyp-1), conjugated to the hyaluronic acid backbone. This peptide has shown greatly selective affinity for cancer cells, mediated by NRP1 receptor, and an exceptional capacity to facilitate penetration across the tumour stroma [12]. The Figure 1 shows a schematic illustration of HA and HA-t-Lyp-1 nanocapsules.

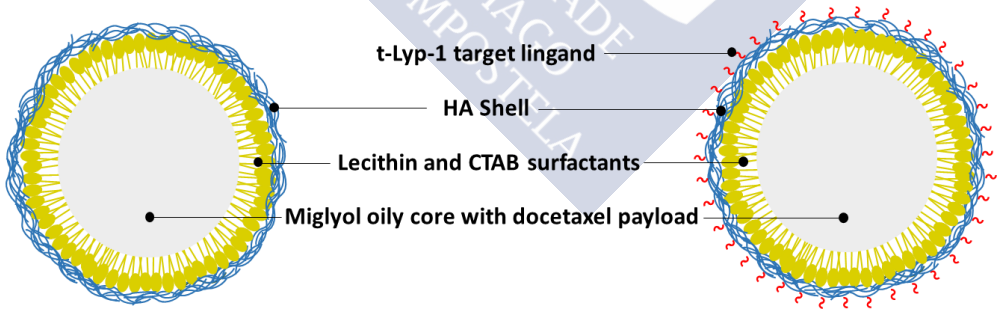

Figure 1. Illustration of HA nanocapsules (left) and HA-t-Lyp-1 nanocapsules (right)

For the development of the nanocapsules a new conjugate of hyaluronic acid with t-Lyp-1 was synthesized and characterized. This conjugate and plain hyaluronic acid were used for the formation of the nanocapsule's shell and the resulting prototypes were characterized in terms of physico-chemical properties, morphology, density of the HA and t-Lyp-1 shell, stability in plasma and docetaxel loading and release capacity. The in

vivo performance of these potential nanomedicines was assessed in a metastatic orthotopic lung cancer model. The pharmacokinetic and biodistribution profile were studied with special attention to the capacity of nanocapsules for carrying the drug to cancer cells in the primary tumour tissue and in the lymph nodes. Therefore, the translation of the biodistribution profile into a therapeutic response was also studied by determining the tumour load in both, primary tumour and sentinel lymph node.

Besides its attractive biological profile, the high number of carboxylic acid groups present in the hyaluronic acid backbone (1 carboxylic acid per disaccharide of HA) allows the conjugation of ligands via amide bond formation, using mild reaction conditions [13-17]. Despite this, the **conjugation of HA with the tumour homing peptide t-Lyp-1** has never been reported before. The functionalization of hyaluronic acid using different percentages of t-Lyp-1 was achieved according to a two-step synthetic approach (Figure 2). The peptide was linked through the thiol group of the cysteine residue located at terminal end of the peptide without compromising the distant epitopes responsible for the biological activity.

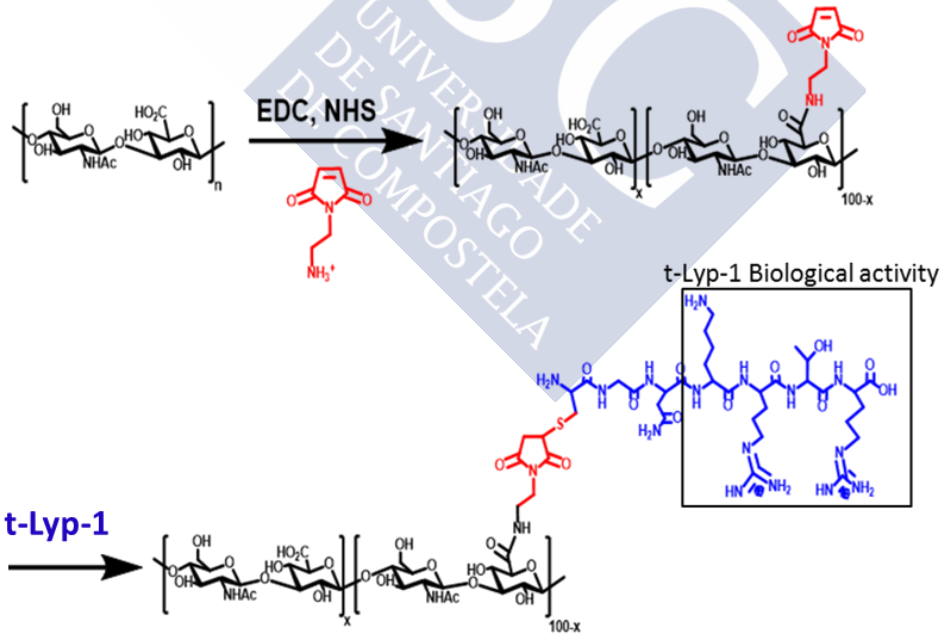

Figure 2. Two-step chemical reaction for obtaining HA-t-Lyp-1.

The resulting HA-t-Lyp-1 conjugates were characterized by ^{1}H-NMR. Among the different percentages of substitution obtained, those with the two lowest percentage of

peptide (substitution degree of 1.5 and 2.9% of t-Lyp-1 respect to carboxylic acid group of HA) were adequate for the formation of the nanocapsules, whereas higher percentages of the peptide led to the aggregation of the nanocapsules during the preparation process.

Nanocapsules using HA-t-Lyp-1 and plain HA were prepared using the solvent displacement technique, as previously disclosed by our group [18]. First, we conducted a study aimed to identify the critical formulation parameters that influenced on particle size in order to obtain small nanocapsules. These results are described in Annex 1 of this thesis. The nanocapsules developed consist on a Miglyol 812® oily core, used to dissolve docetaxel, lecithin Epikuron 145V and CTAB, as surfactants for the stabilization of the oily droplets and the mentioned polymer coating. Additionally, the cationic surfactant CTAB plays an important role, owing to its capactity to strongly interact with the polymer [19-21], thus, contributing to the stability of the systems. All of these materials, combined in the form of nanocapsules, have shown previously an acceptable toxicity profile [18, 22].

As shown in Table 1, the nanocapsules exhibited a size below 150 nm, which was considered to be adequate for and increased stability, reduced uptake by the mononuclear phagocytic system [1, 23, 24] and improved lymphatic drainage from blood vasculature to metastatic lymph nodes [25, 26]. The linking of the peptide to the HA shell led to a small increase in the particle size, an effect previously observed for other functionalized nanostructures [27, 28], and also to a reduction of the zeta potential. This could be logically explained by the substitution of the anionic carboxylate groups by the positive ammonium groups present in the peptide molecule. This result suggested that the t-Lyp-1 molecules are on the surface of the nanocapsules and, therefore, are available for active targeting.

	HA NCs	HA-t-Lyp-1 (DS 1.5%) NCs	HA-t-Lyp-1 (DS 2.9%) NCs
Size (nm)	112 ± 7	130 ± 12	149 ± 13
PI	0.1	0.1	0.1
Zeta potential (mV)	-49 ± 3	-31 ± 4	-27 ± 3
HA shell density (disaccharide	2.05 ± 0.19	2.33 ± 0.32	2.68 ± 0.15
t-Lyp-1 shell density (t-Lyp-1 molecules /nm2)	---	0.035 ± 0.005	0.079 ± 0.004
Docetaxel loading (w/w %)	1.54 ± 0.08	1.54 ± 0.11	1.53 ± 0.08

Table 1. Size, PI, Zeta potential, shell density and docetaxel loading capacity of HA and HA-t-Lyp-1 nanocapsules (t-Lyp-1 substitution degree, DS, of 1.5% and 2.9%). Results are presented as mean ± SD of 3 replicates.

On the other hand, the **HA and t-Lyp-1 shell density** analysis (Table 1), proved the presence of targeting molecules on the surface of the nanocapsules. This quantitative information about the density of targeting ligands is very interesting, as it is expected to have a strong influence on targeting ability of nanocarriers [29-31].

The confirmation of the **functionality of the hyaluronic shell and targeting ligand t-Lyp-1** with the CD44 and NRP1 receptors, respectively, was assessed using two and three dimensional cell culture models with A549 lung cancer cell line. The results of this study indicated that the internalization of the nanocapsules was dependent on the presence of t-Lyp-1 and, also, on the level of substitution degree (annex 2 of this thesis). Consequently with these results, we have selected HA-t-Lyp-1 nanocapsules with a DS 2.9% for the subsequent *in vivo* studies. These will be referred as HA-t-Lyp-1 nanocapsules henceforth in this document.

Once the functionality of the nanocapsules with respect to the cancer cells was verified, we found it critical to assess their **stability upon incubation in plasma**. The results reported in Chapter 2 of this thesis showed that the nanocapsules preserved their

nanometric size upon incubation in plasma for at least 24 hours. The interpretation of these results was that, according to previously reported information, the small size [1, 23], the high surface charge [32] and the steric protection provided by the HA shell [33, 34] could contribute to the stability of nanocapsules in plasma.

On the other hand, the **analysis of the drug loading and release capacity** showed that the oily core of these systems could efficiently load (above 1.5 %) and retain the hydrophobic antitumour drug docetaxel. The release kinetics profile for both formulations presented an initial burst as a consequence of the partition of the drug between the oily phase of nanocapsules and the external media, followed by a slow release phase. This release profile suggests that the core-shell structure of these nanocapsules, where the shell works as a barrier to the diffusion of DCX to the external media, is responsible for the bi-phasic profile. Similar results were observed for other HA-based nanocarriers, indicating the HA coating can help to control drug release [35-37].

The study of the pharmacokinetics and biodistribution profile of the DCX-loaded nanocapsules was performed in a metastatic orthotopic lung cancer model. Mice received by the tail vein the commercial treatment Taxotere®, HA and HA-t-Lyp-1 nanocapsules at an equivalent dose of 10 mg docetaxel/kg, at day 20 post implantation of the tumour cells.

	$t_{1/2}$ (h)	$AUC_{0-\infty}$ ((mg/mL).h)	$MRT_{0-\infty}$ (h)	V (mL/kg)	Cl (mL/kg.h)
Taxotere®	5.40 ± 1.27	2.58 ± 0.35	2.89 ± 0.24	11.26± 0.60	3.93 ± 0.53
HA NCs	5.75 ± 0.55	4.40 ± 1.11	4.25 ± 0.50*	9.89 ± 1.37	2.38 ± 0.62*
HA-t-Lyp-1 NCs	8.43 ± 0.91*	3.16 ± 0.71	6.33 ± 0.42*	20.92 ± 6.19	3.27 ± 0.75

Table 2. Pharmacokinetic parameters for HA, HA-t-Lyp-1 NCs and Taxotere® after IV injection of equivalent docetaxel dose of 10 mg/kg, estimated with PKSolver program fitting the data to a non-compartimental model. Significant differences between nanocapsules and Taxotere® (*) $p < 0.05$.

The results extracted from **pharmacokinetic analysis** (Table 2) show a minor contribution of both HA and HA-t-Lyp-1 nanocapsules in terms of prolonging the presence of DCX in the blood stream. The statistical analysis indicated that the MRT values were higher for both nanocapsules as compared to Taxotere®, and that the $t_{1/2,}$was only significantly extended for the t-Lyp-1-functionalized nanocapsules. Globally, both nanocapsules prototypes appear to show similar plasma concentration-time profiles, as it can be noted in Figure 1, Chapter 3. Although minor, the prolonged blood circulation of the nanocapsules could be attributed to the hydrophilic steric protection provided by the hyaluronic acid shell, (reported for other HA and hydrophilic polymer-coated nanocapsules [6-8, 38-41]), and also to their small size [1, 23, 42].

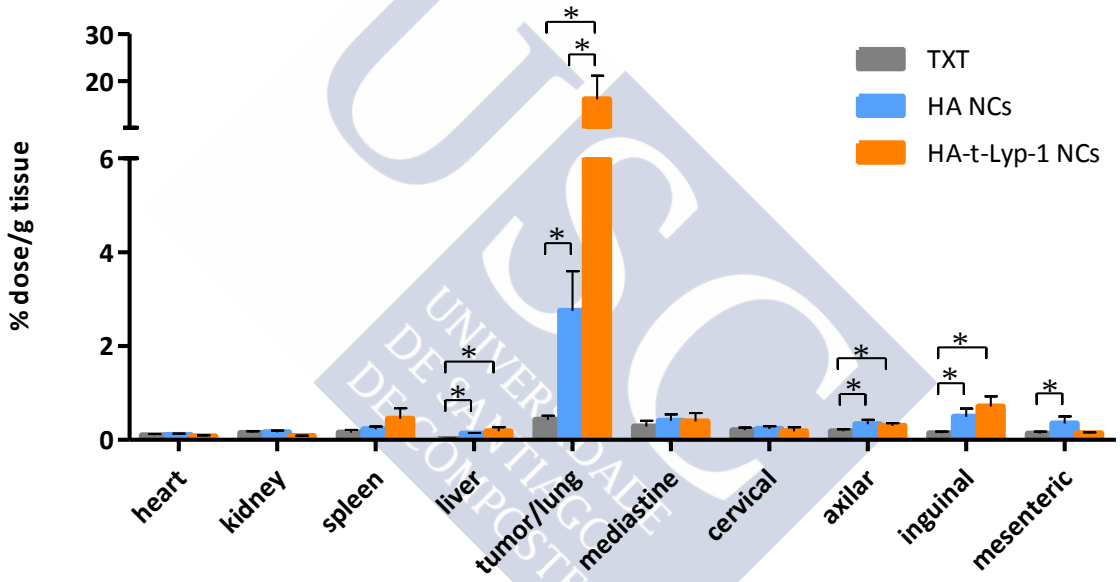

Figure 3. Docetaxel accumulation at 24h in all tissues after IV administration of Taxotere®, HA and HA-t-Lyp-1 NCs at an equivalent docetaxel dose of 10 mg/kg. All data are given as mean ± standard deviation (SD) of 5 replicates. Significant differences between three treatments (*) $p < 0.05$.

The results from the **biodistribution study** made clear the tumour homing efficiency of these prototypes. In fact, the DCX accumulation levels shown in Figure 3 indicate that the DCX tumour accumulation was much higher for the nanocapsules as compared to Taxotere®. Moreover, these differences were found to increase over time, reaching at the end of the study, values that were 6.3 and 36.6 times higher for the HA and t-Lyp-1-HA nanocapsules respectively. This extraordinary tumour uptake, observed especially to the actively targeted nanocapsules could also be complemented thanks to EPR effect,

similar to the one reported for other nanocarriers [43, 44]. On the other hand, the remarkable tumour homing efficiency achieved with HA-t-Lyp-1 points to the great contribution of the chemical affinity of this ligand towards the cellular receptor NRP1, mostly located in the tumour. Actually, the tumour targeting efficacy of both HA and t-Lyp-1 was assessed previously, nevertheless, t-Lyp-1 has disclosed excellent tumour selectivity, while the most reported limitation of HA is associated to the wide distribution of CD44 and to the presence of other HA receptors [6, 35, 38, 45, 46]. Another favourable point of the proposed nanocapsules is related to the limited docetaxel accumulation in non-targeted organs (most importantly, in the liver and spleen), in contrast with the results observed for other nanocarriers [7, 38, 43, 44, 47-54]. To our knowledge, the high level of tumour targeting efficiency (20% of injected dose per gram of tumour) associated to a low hepatic accumulation (maximum of 0.75% per gram of liver) presented in this work has not been reported previously. Furthermore, the results in Figure 3 and in Chapter 3 of this thesis, show a general enhanced lymphatic accumulation for both nanocapsule prototypes in relation with Taxotere®. This increase of docetaxel levels does not present a clearly tendency in favour of one nanocapsule prototype, neither in favour of a specific type of lymph node. However, there is hardly difference between the three treatments in the case of sentinel lymph node (mediastine), probably due to a deficient lymphatic drainage at the proximity of the tumour [55]. The lymphatic accumulation of the nanocapsules was considered to be a very positive outcome as it could help preventing the metastatic spreading through the lymphatics. Such lymphatic accumulation has also been reported for others hydrophilic small size nanocarriers ranging from 15 -115 nm [56-59], suggesting that the small size [25, 26] and the hydrophilic surface of the nanocapsules contributed to this enhanced lymphatic targeting capacity, besides, their affinity for the Lyve-1 HA receptor located in lymphatic vessels [60, 61] could also contribute to the capacity of these prototypes to reach the lymphatics.

For the analysis of the translation of the biodistribution profile into a potential **therapeutic response**, tumour bearing mice were IV injected with the three treatments at a dose of 5 mg docetaxel/kg at day 20 and 27 after the implantation of the tumour cells. Tumour inhibition was determined as luciferase activity in protein extracts

associated with tumour cells from primary tumour (lungs) and sentinel lymph node (mediastinal nodes). Besides, luciferase activity was also monitored in vivo by IVIS in order to control tumour progression.

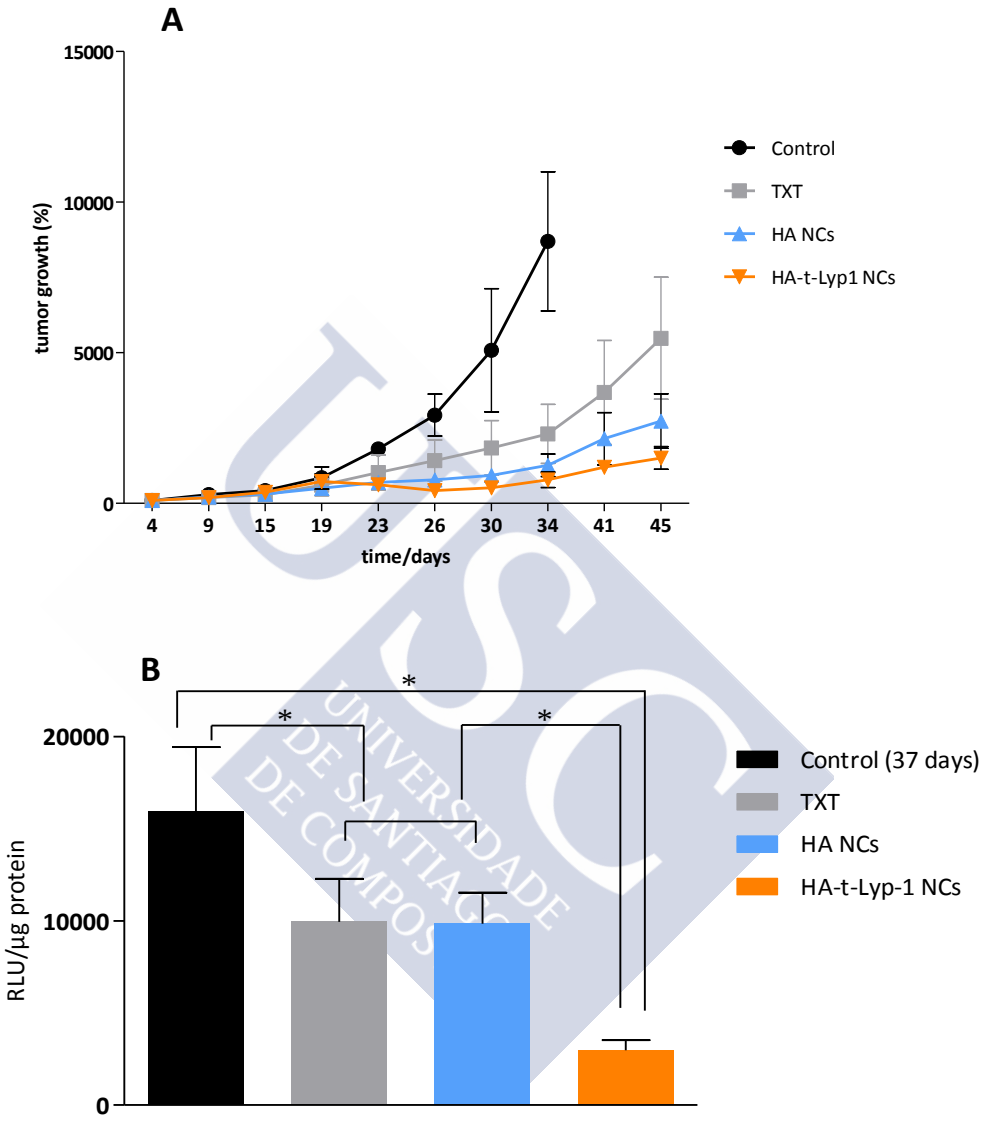

Figure 4. Quantification of luciferase activity in lungs in vivo (A) and ex vivo (B) after IV administration of Taxotere®, HA and HA-t-Lyp-1 nanocapsules at an equivalent docetaxel dose of 10 mg/kg versus control at 37 days. All the data are given as mean ± standard deviation (SD) of 5 replicates. Significant differences between three treatments (*) $p < 0.05$

As shown in Figure 4 B, the administration of HA-t-Lyp-1 nanocapsules led to an accentuated and significant tumour reduction as compared to Taxotere®, while the efficacy of HA nanocapsules in terms of tumour load resulted comparable to that

observed for the commercial treatment. We attribute these results to the problematic poor penetration of the nanocarriers through the tumour stroma [62-67]. The results of this quantitative analysis differs from those of the luciferase activity observed by IVIS shown in Figure 4 A, where the behaviour of HA and HA-t-Lyp-1 nanocapsules was similar. This discrepancy could be attributed to the different tissue distribution of both nanocarriers. Indeed, it could be hypothesized that the luciferase activity from IVIS mostly proceeds from tumour periphery rather than from the whole tumour tissue, suggesting that HA nanocapsules remained in this tumour periphery with restricted diffusion inside the tumour stroma, inhibiting more tumour cells in this area than Taxotere® as observed in IVIS. In other words, the transport of DCX in HA nanocapsules could have helped the tissue targeting, as noted by the biodistribution data, but not necessarily the access of the drug to the deeper tumour tissue. In contrast, the tumour penetration character of t-Lyp-1 allowed this prototype to diffuse across the tissue and reach globally a greater number of cancer cells, thus, resulting in a 36.6 fold DCX accumulation (vs free DCX) and in a markedly reduced tumour load. This enhanced tumour penetration technology of CendR peptides implicit in t-Lyp-1 [4, 5], has already been reported for other nanocarriers [12, 27, 68]. Nevertheless, this is the first data reported of the use of this sort of peptides for both the inhibition of tumoural growth and metastatic spreading.

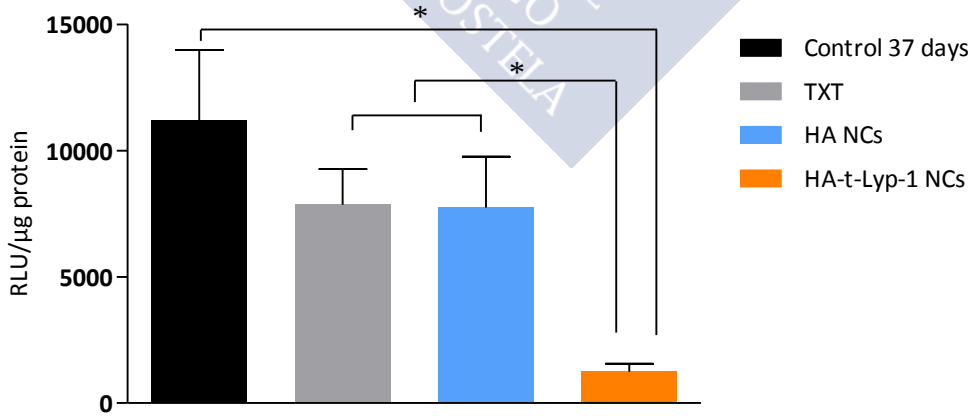

Figure 5. Quantification of luciferase activity in mediastinal lymph nodes ex vivo after IV administration of Taxotere®, HA and HA-t-Lyp-1 nanocapsules at an equivalent docetaxel dose of 10mg/kg versus control at 37 days. All the data are given as mean ± standard deviation (SD) of 5 replicates. Significant differences between three treatments (*) $p < 0.05$

With regard to the inhibition of the metastatic spreading through the sentinel lymph node (Figure 5), the results indicate that HA nanocapsules and Taxotere® present comparable metastatic load, whilst HA-t-Lyp-1 nanocapsules are capable of hindering the metastatic spreading. Given the fact that docetaxel levels in this lymph node were similar for the three treatments, this anti-metastatic effect could be a consequence of the reduction of cell migration from the primary tumour rather than from a direct effect on the metastatic cells. Although it was not possible to determine the metastatic spreading beyond the sentinel lymph node due to a minimum metastatic load required to detect luciferase acitivity, the increased docetaxel concentration found in the rest of lymph nodes for both types of nanocapsules might suggest their therapeutic advantage for avoiding the spreading and colonization of other tissues through distant lymph nodes.

Overall, this work presents the functionalization of the biopolymer HA with the tumour homing peptide t-Lyp-1. The subsequently developed nanocapsules with a polymer shell of HA and HA-t-Lyp-1 fulfil a number of important prerequisites for carrying antitumour drugs, such as favourable physico-chemical properties, optimal stability profile in plasma and an efficient capacity for associating antitumour drugs. The tumour homing efficiency of these prototypes through specific cellular receptors (CD44 and NRP1) was shown to have a dramatic impact on the biodistribution of the prototypes, this impact being especially relevant for HA-t-Lyp-1 nanocapsules. Besides, both nanocapsules formulations exhibited an augmented lymphatic accumulation. Finally, the antitumour activity study revealed HA-t-Lyp-1 nanocapsules are capable of markedly inhibiting the tumour growth and hinder metastatic spreading. In summary, these results highlight the synergistic role of the selective tumour targeting and the enhanced penetration in terms of achieving effective therapeutic response.

References

1. Vonarbourg, A., et al., *Parameters influencing the stealthiness of colloidal drug delivery systems.* Biomaterials, 2006. **27**(24): p. 4356-4373.
2. Brannon-Peppas, L. and J.O. Blanchette, *Nanoparticle and targeted systems for cancer therapy.* Advanced Drug Delivery Reviews, 2004. **56**(11): p. 1649-1659.
3. Jin, S.-E., H.-E. Jin, and S.-S. Hong, *Targeted Delivery System of Nanobiomaterials in Anticancer Therapy: From Cells to Clinics.* BioMed Research International, 2014. **2014**: p. 23.
4. Sugahara, K.N., et al., *Coadministration of a Tumour-Penetrating Peptide Enhances the Efficacy of Cancer Drugs.* Science, 2010. **328**(5981): p. 1031-1035.
5. Teesalu, T., et al., *C-end rule peptides mediate neuropilin-1-dependent cell, vascular, and tissue penetration.* Proceedings of the National Academy of Sciences, 2009. **106**(38): p. 16157-16162.
6. Peer, D. and R. Margalit, *Loading mitomycin C inside long circulating hyaluronan targeted nano-liposomes increases its antitumour activity in three mice tumour models.* International Journal of Cancer, 2004. **108**(5): p. 780-789.
7. Peer, D., Margalit, R., *Tumour-Targeted Hyaluronan Nanoliposomes Increase the Antitumour Activity of Liposomal Doxorubicin in Syngeneic and Human Xenograft Mouse Tumour Models.* Neoplasia, 2004. **6**(4): p. 343-353.
8. Dan, P., et al., *Nanocarriers as an emerging platform for cancer therapy.* Nature Nanotechnology, 2007. **2**(12): p. 751-760.
9. Harada, H. and M. Takahashi, *CD44-dependent Intracellular and Extracellular Catabolism of Hyaluronic Acid by Hyaluronidase-1 and -2.* Journal of Biological Chemistry, 2007. **282**(8): p. 5597-5607.
10. Lesley, J., R. Hyman, and P.W. Kincade, *CD44 and Its Interaction with Extracellular Matrix*, in *Advances in Immunology*, J.D. Frank, Editor 1993, Academic Press. p. 271-335.
11. Knudson, C.B., *Hyaluronan and CD44: Strategic players for cell–matrix interactions during chondrogenesis and matrix assembly.* Birth Defects Research Part C: Embryo Today: Reviews, 2003. **69**(2): p. 174-196.
12. Roth, L., et al., *Transtumoural targeting enabled by a novel neuropilin-binding peptide.* Oncogene, 2012. **31**(33): p. 3754-3763.
13. Luo, Y., M.R. Ziebell, and G.D. Prestwich, *A Hyaluronic Acid−Taxol Antitumour Bioconjugate Targeted to Cancer Cells.* Biomacromolecules, 2000. **1**(2): p. 208-218.
14. Luo, Y. and G.D. Prestwich, *Synthesis and Selective Cytotoxicity of a Hyaluronic Acid−Antitumour Bioconjugate.* Bioconjugate Chemistry, 1999. **10**(5): p. 755-763.
15. Auzenne, E., et al., *Hyaluronic Acid-Paclitaxel: Antitumour Efficacy against CD44(+) Human Ovarian Carcinoma Xenografts.* Neoplasia (New York, N.Y.), 2007. **9**(6): p. 479-486.
16. Rosato, A., et al., *HYTAD1-p20: A new paclitaxel-hyaluronic acid hydrosoluble bioconjugate for treatment of superficial bladder cancer.* Urologic Oncology: Seminars and Original Investigations, 2006. **24**(3): p. 207-215.
17. Platt, V.M. and F.C. Szoka, *Anticancer Therapeutics: Targeting Macromolecules and Nanocarriers to Hyaluronan or CD44, a Hyaluronan Receptor.* Molecular Pharmaceutics, 2008. **5**(4): p. 474-486.
18. Oyarzun-Ampuero, F.A., et al., *Hyaluronan nanocapsules as a new vehicle for intracellular drug delivery.* European Journal of Pharmaceutical Sciences, 2013. **49**(4): p. 483-490.

19. Chen, Y.-H. and Q. Wang, *Establishment of CTAB Turbidimetric method to determine hyaluronic acid content in fermentation broth.* Carbohydrate Polymers, 2009. **78**(1): p. 178-181.
20. Oueslati, N., et al., *CTAB turbidimetric method for assaying hyaluronic acid in complex environments and under cross-linked form.* Carbohydrate Polymers, 2014. **112**(0): p. 102-108.
21. Song, J.-M., et al., *A simple method for hyaluronic acid quantification in culture broth.* Carbohydrate Polymers, 2009. **78**(3): p. 633-634.
22. Rivera-Rodríguez, G.R., M.J. Alonso, and D. Torres, *Poly-l-asparagine nanocapsules as anticancer drug delivery vehicles.* European Journal of Pharmaceutics and Biopharmaceutics, 2013. **85**(3, Part A): p. 481-487.
23. Dufort, S., L. Sancey, and J.-L. Coll, *Physico-chemical parameters that govern nanoparticles fate also dictate rules for their molecular evolution.* Advanced Drug Delivery Reviews, 2012. **64**(2): p. 179-189.
24. Lux, F., et al., *Ultrasmall Rigid Particles as Multimodal Probes for Medical Applications.* Angewandte Chemie International Edition, 2011. **50**(51): p. 12299-12303.
25. Ryan, G.M., L.M. Kaminskas, and C.J.H. Porter, *Nano-chemotherapeutics: Maximising lymphatic drug exposure to improve the treatment of lymph-metastatic cancers.* Journal of Controlled Release, 2014. **193**(0): p. 241-256.
26. Svenson, S., *What nanomedicine in the clinic right now really forms nanoparticles?* Wiley Interdisciplinary Reviews: Nanomedicine and Nanobiotechnology, 2014. **6**(2): p. 125-135.
27. Sugahara, K.N., et al., *Tissue-Penetrating Delivery of Compounds and Nanoparticles into Tumours.* Cancer Cell, 2009. **16**(6): p. 510-520.
28. Toti, U.S., et al., *Interfacial Activity Assisted Surface Functionalization: A Novel Approach to Incorporate Maleimide Functional Groups and cRGD Peptide on Polymeric Nanoparticles for Targeted Drug Delivery.* Molecular pharmaceutics, 2010. **7**(4): p. 1108-1117.
29. Elias, D.R., et al., *Effect of ligand density, receptor density, and nanoparticle size on cell targeting.* Nanomedicine: Nanotechnology, Biology and Medicine. **9**(2): p. 194-201.
30. Fakhari, A., et al., *Controlling ligand surface density optimizes nanoparticle binding to ICAM-1.* Journal of Pharmaceutical Sciences, 2011. **100**(3): p. 1045-1056.
31. Stefanick, J.F., et al., *A Systematic Analysis of Peptide Linker Length and Liposomal Polyethylene Glycol Coating on Cellular Uptake of Peptide-Targeted Liposomes.* ACS Nano, 2013. **7**(4): p. 2935-2947.
32. Heurtault, B., et al., *Physico-chemical stability of colloidal lipid particles.* Biomaterials, 2003. **24**(23): p. 4283-4300.
33. Jiang, T., et al., *Dual-functional liposomes based on pH-responsive cell-penetrating peptide and hyaluronic acid for tumour-targeted anticancer drug delivery.* Biomaterials, 2012. **33**(36): p. 9246-9258.
34. Santander-Ortega, M.J., et al., *Hydration forces as a tool for the optimization of core-shell nanoparticle vectors for cancer gene therapy.* Soft Matter, 2012. **8**(48): p. 12080-12092.
35. Upadhyay, K.K., et al., *In vitro and In vivo Evaluation of Docetaxel Loaded Biodegradable Polymersomes.* Macromolecular Bioscience, 2010. **10**(5): p. 503-512.
36. Choi, K.Y., et al., *Smart Nanocarrier Based on PEGylated Hyaluronic Acid for Cancer Therapy.* ACS Nano, 2011. **5**(11): p. 8591-8599.
37. Yoon, H.Y., et al., *Photo-crosslinked hyaluronic acid nanoparticles with improved stability for in vivo tumour-targeted drug delivery.* Biomaterials, 2013. **34**(21): p. 5273-5280.
38. Yang, X.-y., et al., *Hyaluronic acid-coated nanostructured lipid carriers for targeting paclitaxel to cancer.* Cancer Letters, 2013. **334**(2): p. 338-345.

39. Gonzalo, T., et al., *A new potential nano-oncological therapy based on polyamino acid nanocapsules.* Journal of Controlled Release. **169**(1–2): p. 10-16.
40. Lollo, G., et al., *Enhanced in vivo therapeutic efficacy of plitidepsin-loaded nanocapsules decorated with a new poly-aminoacid-PEG derivative.* International Journal of Pharmaceutics, 2015. **483**(1–2): p. 212-219.
41. Rivera-Rodriguez, G.R., et al., *In vivo evaluation of poly-l-asparagine nanocapsules as carriers for anti-cancer drug delivery.* International Journal of Pharmaceutics, 2013. **458**(1): p. 83-89.
42. Faraji, A.H. and P. Wipf, *Nanoparticles in cellular drug delivery.* Bioorganic & Medicinal Chemistry, 2009. **17**(8): p. 2950-2962.
43. Jiang, X., et al., *PEGylated poly(trimethylene carbonate) nanoparticles loaded with paclitaxel for the treatment of advanced glioma: In vitro and in vivo evaluation.* International Journal of Pharmaceutics, 2011. **420**(2): p. 385-394.
44. Cheng, J., et al., *Formulation of functionalized PLGA–PEG nanoparticles for in vivo targeted drug delivery.* Biomaterials, 2007. **28**(5): p. 869-876.
45. Lee, D.-E., et al., *Amphiphilic hyaluronic acid-based nanoparticles for tumour-specific optical/MR dual imaging.* Journal of Materials Chemistry, 2012. **22**(21): p. 10444-10447.
46. Choi, K.Y., et al., *Self-assembled hyaluronic acid nanoparticles for active tumour targeting.* Biomaterials, 2010. **31**(1): p. 106-114.
47. Rivkin, I., et al., *Paclitaxel-clusters coated with hyaluronan as selective tumour-targeted nanovectors.* Biomaterials, 2010. **31**(27): p. 7106-7114.
48. Choi, K.Y., et al., *Self-assembled hyaluronic acid nanoparticles as a potential drug carrier for cancer therapy: synthesis, characterization, and in vivo biodistribution.* Journal of Materials Chemistry, 2009. **19**(24): p. 4102-4107.
49. Ayen, W. and N. Kumar, *In Vivo Evaluation of Doxorubicin-Loaded (PEG)3-PLA Nanopolymersomes (PolyDoxSome) Using DMBA-Induced Mammary Carcinoma Rat Model and Comparison with Marketed LipoDox™.* Pharmaceutical Research, 2012. **29**(9): p. 2522-2533.
50. Karra, N., et al., *Antibody Conjugated PLGA Nanoparticles for Targeted Delivery of Paclitaxel Palmitate: Efficacy and Biofate in a Lung Cancer Mouse Model.* Small, 2013. **9**(24): p. 4221-4236.
51. Ernsting, M.J., et al., *Preclinical pharmacokinetic, biodistribution, and anti-cancer efficacy studies of a docetaxel-carboxymethylcellulose nanoparticle in mouse models.* Biomaterials, 2012. **33**(5): p. 1445-1454.
52. Park, J.-H., et al., *Systematic Surface Engineering of Magnetic Nanoworms for In vivo Tumour Targeting.* Small, 2009. **5**(6): p. 694-700.
53. Herringson, T.P. and J.G. Altin, *Effective tumour targeting and enhanced anti-tumour effect of liposomes engrafted with peptides specific for tumour lymphatics and vasculature.* International Journal of Pharmaceutics, 2011. **411**(1–2): p. 206-214.
54. Ishida, T., et al., *Spleen plays an important role in the induction of accelerated blood clearance of PEGylated liposomes.* Journal of Controlled Release, 2006. **115**(3): p. 243-250.
55. Maeda, H., *Toward a full understanding of the EPR effect in primary and metastatic tumours as well as issues related to its heterogeneity.* Advanced Drug Delivery Reviews, (0).
56. Ryan, G.M., et al., *PEGylated polylysine dendrimers increase lymphatic exposure to doxorubicin when compared to PEGylated liposomal and solution formulations of doxorubicin.* Journal of Controlled Release, 2013. **172**(1): p. 128-136.
57. Qin, L., et al., *Polymeric micelles for enhanced lymphatic drug delivery to treat metastatic tumours.* Journal of Controlled Release, 2013. **171**(2): p. 133-142.

58. Rafi, M., et al., *Polymeric micelles incorporating (1,2-diaminocyclohexane)platinum (II) suppress the growth of orthotopic scirrhous gastric tumours and their lymph node metastasis.* Journal of Controlled Release, 2012. **159**(2): p. 189-196.
59. Tan, R., et al., *Preparation of vincristine sulfate-loaded poly (butylcyanoacrylate) nanoparticles modified with pluronic F127 and evaluation of their lymphatic tissue targeting.* Journal of Drug Targeting, 2014. **22**(6): p. 509-517.
60. J R Fraser, W.G.K., T C Laurent, R N Cahill and N Vakakis, *Uptake and degradation of hyaluronan in lymphatic tissue.* Biochemical Journal, 1988. **256**: p. 153-158.
61. Zhou, B., et al., *Identification of the Hyaluronan Receptor for Endocytosis (HARE).* Journal of Biological Chemistry, 2000. **275**(48): p. 37733-37741.
62. Grantab, R., S. Sivananthan, and I.F. Tannock, *The Penetration of Anticancer Drugs through Tumour Tissue as a Function of Cellular Adhesion and Packing Density of Tumour Cells.* Cancer Research, 2006. **66**(2): p. 1033-1039.
63. Netti, P.A., et al., *Role of Extracellular Matrix Assembly in Interstitial Transport in Solid Tumours.* Cancer Research, 2000. **60**(9): p. 2497-2503.
64. Heldin, C.-H., et al., *High interstitial fluid pressure [mdash] an obstacle in cancer therapy.* Nat Rev Cancer, 2004. **4**(10): p. 806-813.
65. Jain, R.K., *Delivery of molecular and cellular medicine to solid tumours1.* Advanced Drug Delivery Reviews, 2001. **46**(1–3): p. 149-168.
66. Wong, C., et al., *Multistage nanoparticle delivery system for deep penetration into tumour tissue.* Proceedings of the National Academy of Sciences, 2011. **108**(6): p. 2426-2431.
67. Yan, Z., et al., *Tumour-Penetrating Peptide Mediation: An Effective Strategy for Improving the Transport of Liposomes in Tumour Tissue.* Molecular Pharmaceutics, 2014. **11**(1): p. 218-225.
68. Karmali, P.P., et al., *Targeting of albumin-embedded paclitaxel nanoparticles to tumours.* Nanomedicine: Nanotechnology, Biology and Medicine. **5**(1): p. 73-82.

Conclusiones / Conclusions

USC
UNIVERSIDADE
DE SANTIAGO
DE COMPOSTELA

El trabajo experimental descrito en la presente tesis, se ha enfocado al diseño de plataformas nanométricas denominadas nanocápsulas, con propiedades multifuncionales que les permitan dirigir selectivamente fármacos citostáticos a las células tumorales. De los resultados obtenidos se han extraído las siguientes conclusiones:

1. Se ha sintetizado un nuevo conjugado químico consistente en ácido hialurónico modificado con el péptido t-Lyp-1, con distintos grados de sustitución (1.5 y 2.9 %). Dicho conjugado fue utilizado para la obtención de nanocápsulas funcionalizadas en su superficie.

2. Se han obtenido por primera vez nanocápsulas constituidas por un núcleo oleoso con una cubierta de ácido hialurónico o de ácido hialurónico conjugado con t-Lyp-1 con un tamaño comprendido entre 112 – 149 nm y una carga superficial negativa (-49 y -25mV). Estas nanocápsulas presentaron una adecuada estabilidad en medios biológicos y una eficiente capacidad para asociar y retener el fármaco.

3. Los resultados obtenidos en los estudios llevados a cabo en cultivos celulares en 2 y 3 dimensiones permitieron demostrar la existencia de una interacción específica de las nanocápsulas a través de sus receptores CD44 y NRP1 en la línea celular de cáncer de pulmón A549, siendo las nanocápsulas con mayor grado de modificación de t-Lyp-1 (grado de sustitución 2.9 %) las que muestran una mayor internalización celular. Por consiguiente las nanocápsulas de HA y las modificadas con un grado de sustitución del 2.9 % fueron seleccionadas para los posteriores estudios *in vivo*.

4. Los resultados obtenidos en los estudios *in vivo* llevados a cabo en un modelo tumoral de cáncer de pulmón metastático, pusieron de manifiesto la extraordinaria acumulación del fármaco en el tejido tumoral (pulmón), tras la

administración de ambos prototipos de nanocápsulas, especialmente las funcionalizadas con t-Lyp-1 que logran un aumento de 37 veces en la concentración obtenida comparado con el tratamiento comercial Taxotere®. Además, ambos prototipos de nanocápsulas permitieron incrementar los niveles de fármaco en los nodos linfáticos, en comparación con el Taxotere®.

5. El estudio de la respuesta terapéutica en el citado modelo tumoral, permitió demostrar la capacidad de las nanocápsulas modificadas con t-Lyp-1 para inhibir notablemente el crecimiento tumoral en el tumor primario, además de frenar drásticamente la diseminación metastática.

The experimental work reported in this thesis, has been oriented to the design and development of multifunctional nanocapsules, with the capacity to target anti-tumoral drugs to cancer cells. Overall, the results have led to the following conclusions:

1. A novel chemical conjugate consisting in hyaluronic acid modified with the peptide t-Lyp-1, with different substitution degrees (1.5 y 2.9%) was synthesized. This biomaterial was used for the production of t-Lyp-1 surface modified hyaluronic acid nanocapsules.

2. Nanocapsules made of hyaluronic acid modified or not with t-Lyp-1 with a size between 112 – 149 nm and a negative surface charge (-49 y -25mV) were originally produced and characterized. Furthermore, these nanocapsules were shown to be stable in plasma and presented an adequate capacity for loading and retaining the anticancer drug docetaxel.

3. The *in vitro* cell cultures performed in 2 and 3 dimensions models showed that the nanocapsules have a specific interaction with A549 lung tumour cell line through their CD44 and NRP1 receptors, being nanocapsules with a higher substitution degree of t-Lyp-1 (substitution degree 2.9 %) those with a higher internalization rate. Therefore, HA and modified nanocapsules with a substitution degree of 2.9 % were selected for *in vivo* studies.

4. The *in vivo* studies carried out in a metastatic lung cancer model evidenced the extraordinary capacity of tumour accumulation after administration of both nanocapsules prototypes, especially for t-Lyp-1-functionalized nanocapsules that achieved a concentration increment of 37 times respect to the commercial treatment Taxotere®. Additionally, both prototypes of nanocapsules, led to a significant increase in the drug levels in the lymphatic nodes compared with Taxotere® treatment.

5. The study of the therapeutic response in this above mentioned tumour model, indicated that the t-Lyp-1-modified nanocapsules were able to inhibit tumour load in primary tumour and, more importantly, to reduce drastically the metastatic spreading.

Anexos

USC
UNIVERSIDADE
DE SANTIAGO
DE COMPOSTELA

Anexo 1

Polimeric nanocapsules for drug delivery to the lymphatic system: effect of the particle size

Este trabajo ha sido realizado en colaboración con Raquel Abellán.

Nanobiofar Group, IDIS, CIMUS. Universidad de Santiago de Compostela, Spain.

USC
UNIVERSIDADE
DE SANTIAGO
DE COMPOSTELA

Abstract

Previous work by our group has shown that polimeric nanocapsules larger than 200 nm have potential as vehicles for the intravenous administration of the anticancer drug docetaxel. The objective of this study was to elucidate whether a reduction in the nanocapsules size might facilitate their access to the lymphatic system. To do so, we developed polimeric nanocapsules with a particle size close to 100 nm, using the solvent displacement technique. During the preparation process, we analyzed the effect that several formulation parameters have on the characteristics of polymeric nanocapsules. From the data obtained during these experiments, we identified the best conditions to create nanocapsules in the 80–120 nm size range.

1. Introduction

There is significant evidence suggesting that polymeric nanocarriers have the potential for the targeted delivery of anticancer drugs to the tumor tissue. Indeed, some of them, *i.e*. docetaxel-loaded poly(lactic acid-glycolic acid)-polyethylene glycol (PLGA-PEG) nanoparticles [1], polyglutamic acid (PGA)-paclitaxel and PGA-camptothecin conjugates [2] are currently being used in Phase II and Phase III clinical trials. Several polymeric micelles based on PGA-PEG (NK012, NC-6004, NC-4016), are also under clinical evaluation for the delivery of SN38, cisplatin and oxaliplatin [3,4]. Our group has contributed to this field of research by designing polymeric nanocapsules, consisting of a lipid core surrounded by a polymer shell [5–7]. This nanocarrier exhibits competitive advantages over other delivery nanovehicles. Namely, its oily core, which enables the encapsulation of high loads of hydrophobic drugs and their polymer shell, helps to preserve its stability and control the release of the encapsulated drugs.

Despite the advances achieved on the use of nanocarriers for the delivery of drugs to the tumor tissue, researchers in the field are becoming to realize the advantages that targeting the drug to the lymphatic system would give them. Nowadays it is accepted that an important limitation of the conventional intravenous chemotherapy lies on the inability of cytotoxic drugs to reach metastatic cells, which frequently accumulate in the

lymphatic system [14]. The goal of our study is to bypass this limitation by designing polymer nanocapsules specifically tailored for the delivery of drugs to the lymphatic system. Previous studies have shown that nanosystems up to 100 nm in size, and a hydrophilic and negatively charged surface administered subcutaneously may be easily drained by the lymphatic system [15–17]. Similarly, these small nanocarriers administered by the intravenous route may have the capacity to extravasate from the tumor-associated blood vessels and cross the tumor interstice before entering the functional peritumoral lymphatic vessels [18,19]. The information reported so far in this regard indicates that nanocarriers with a size close to 100 nanometers are the most appropriate based on their ability to reach the lymphatic capillaries from the interstice and remain entrapped in the lymphatic system [15,20].

The production of nanocapsules with a size close to 100 nm presents a technological challenge since conventional preparation techniques usually yield nanocapsules larger than 200 nm [21]. Smaller nanocapsules have been produced by phase inversion-based methods using high surfactant concentrations and high temperatures [22]. As an alternative, in the present work, we have adapted a mild and easily scalable solvent diffusion method through systematic screening of the formulation parameters, in order to identify the optimal conditions for the preparation of nanocapsules with simple and flexible composition and a reduced particle size suitable for the lymphatic targeting of drugs.

2. Materials and methods

2.1. Materials

Miglyol®812, a neutral oil composed by esters of caprylic and capric fatty acids and glycerol, was donated by Sasol Germany GmbH (Germany). The surfactant Epikuron® 145V, a deoiled phosphatidylcholine enriched fraction of soybean lecithin, was donated by Cargill (Spain). Hexadecyltrimethylammonium bromide (CTAB), poly-L-glutamic acid (PGA; Mw 15-50 kDa), poly-L-asparagine (PASN; Mw 5-15 kDa), benzalkonium chloride and poloxamer 188 (Pluronic® F68) were purchased from Sigma-Aldrich (Spain). Methoxy-poly(ethylene glycol)-block-poly(L-glutamic acid sodium salt) (PGA-PEG; Mw

35 kDa), a diblock copolymer composed by poly-L-glutamic acid (chains length 15 kDa) and 57% of PEG (w/w, chains length 20 kDa) was supplied by Alamanda Polymers (USA).

2.2. Preparation of nanoemulsions and polimeric nanocapsules

Anionic nanoemulsions were prepared by the solvent displacement method, following the procedure previously described by our group [9]. Briefly, 30 mg of Epikuron® 145V were dissolved in 0.25 ml of ethanol. After mixing, 125 µl of Miglyol®812 and 9.5 ml of acetone were also incorporated. This organic phase was immediately added to 20 ml of ultrapure water, at room temperature and under magnetic stirring, which led to the instantaneous formation of the nanoemulsion. Solvents were evaporated under vacuum at 37 ºC (Buchi Labortechnik AG, Flawil, Switzerland) up to a final volume of 10 ml.

The influence of the parameters indicated in the **Table 1** on the particle size was investigated. In each set of experiments one single parameter was changed at a time while the other formulation variables were kept at the values described for the nanoemulsion used as reference.

Temperature of AP	4, 25, 40°C
AP:OP Volume Ratio	2:1, 3:1, 4.5:1
Oil Concentration in the OP *	11.8, 5.9, 2.9, 1.5, 0.7 mg/ml
Addition Rate of the OP	Direct addition of the whole volume (10 ml) *vs.* aliquots of 250 µl/15 seconds

AP: aqueous phase. OP: organic phase. *: constant oil:lecithin mass ratio of 4:1.

Table 1. Formulation parameters studied in order to assess their influence on the particle size distribution of the nanoemulsion.

After selecting the optimal formulation conditions to obtain nanoemulsions of suitable droplet size (AP at 4 ºC, AP:OP 2:1, C=3.7 mg/ml, OP addition in aliquots), the cationic surfactant hexadecyltrimethylammonium bromide (CTAB) was incorporated to the organic phase as an ethanolic solution. To determine the minimum amount required, different concentrations of CTAB (1 to 5.7% w/w) were tested.

Nanocapsules were prepared according to the optimized procedure (3.9% w/w of CTAB), by replacing the aqueous phase by the polimeric aqueous solution of hayaluronic acid, polyglutamic acid, polyglutamic acid-polyethilenglycol or polyasparagine.

2.3. Physicochemical characterization

The size and the polydispersity index of the nanosystems were analyzed by photon correlation spectroscopy (PCS) after appropriate dilution with ultrapure water. Each analysis was performed at 25 °C with an angle detection of 90°. The zeta potential (ζ) was determined by laser Doppler anemometry (LDA) after dilution with KCl 1mM. The PCS and LDA analysis were performed in triplicate using a Zetasizer Nano ZS® (Malvern Instruments, Malvern, UK).

3. Results and discussion

Previous studies from our group have shown the potential of 200 nm polymeric nanocapsules to be used as vehicles for the delivery of anticancer drugs. Given the importance the size of the particles has in the nanocarriers access to the lymphatic system, herein we report experimental conditions designed to obtain 100 nm nanocapsules with different polymer shells; Hyaluronic acid, polyglutamic acid, polyglutamic acid-polyethilenglycol and polyasparagine, as well as their characterization. Prior to the formation and characterization of the said nanocapsules, we performed a thoughtful analysis of the oil-in water emulsification process, as described below.

3.1. Preparation of nanoemulsions and polimeric nanocapsules

It is well known that the physicochemical properties of drug carriers play a critical role in their ability to reach the tumor and the lymphatics following either intravenous or subcutaneous administration [20]. Among these properties, size is particularly important since it determines both access to and retention into the lymphatic system. Some authors have reported that small lipid nanosystems with particle sizes from tens of nanometers up to 100 nm [25], an anionic charge [26], and a hydrophilic surface [27] are suitable for passive targeting to the lymphatic system, following subcutaneous administration.

Polimeric nanocapsules previously reported by our group were produced by the solvent displacement technique with a particle size in the 200 nm-500 nm range [28]. As indicated before, the main aim of this work has been to identify the experimental factors that are crucial in the particle size distribution during the preparation of polimeric nanocapsules. In order to identify these parameters, we selected an anionic nanoemulsion constituted solely by oil and lecithin as our starting point. We evaluated how temperature, oil concentration, aqueous phase:organic phase volume ratio, and mixing rate of these two phases affected the particle size distribution of the resulting polimeric nanocapsules. The results showed that the temperature has no effect on the size of the resulting nanoemulsions (Table 1 Supporting information) whereas an increase in the AP:OP volume ratio produces slightly smaller nanoemulsions (**Table 2A**). The greatest effect on the size was achieved by reducing the oil and surfactant concentration as reflected in **Table 2B** [29]. The reduction of the lipidic components leads to a homogeneous and monodisperse population of nanoemulsions with smaller droplet size (under 100 nm). This result is in line with previous studies reporting the preparation of polyester nanocapsules, although the size of these nanocapsules was above 200 nm [29,30]. On the other hand, a slow addition of the organic phase over the aqueous one (10 ml in 40 fractions, rate 250 µl/15 seconds), instead of direct addition, also led to a considerable reduction of droplet size. The supersaturation phenomenon that occurs when the total volume of both phases are mixed together could explain this effect. This process, which constitutes the driving force of the particle formation, determines the nucleation rate and thus influences the resulting particle size [31,32]. The slow mixing of both phases (*i.e.* by the addition in aliquots), could increase the nucleation rate and led to an increase in the number of smaller particles. These results concur with those obtained by other groups when studying the influence of the mixing rate in the preparation of nanoemulsions [32] and nanoparticles [31]. Therefore, we simultaneously applied both strategies, the reduction of the lipid components and the slow mixing of aqueous and oily phases, in order to obtain small droplet sizes without a drastic reduction of the lipidic components that could compromise production yield and/or drug loading.

Table 2A. Effect of the aqueous phase:organic phase (AP:OP) volume ratio on the mean size and polydispersity index of the nanoemulsion (mean ± SD, n=3).

AP:OP Volume Ratio	2:1	3:1	4.5:1
Size (nm)	178 ± 1	159 ± 7	155 ± 0
P.I.	0.1	0.1	0.1

Table 2B. Effect of the oil concentration and addition method of the organic phase on the mean droplet size and polydispersity index of the nanoemulsion (mean ± SD, n=3).

Addition Method	Direct addition of the whole volume (10 ml)					40 fractions of 250 µl/15 seconds	
Oil Concentration (mg/ml)	11.8	5.9	2.9	1.5	0.7	11.8	2.9
Size (nm)	178 ± 1	163 ± 6	134 ± 9	109 ± 5	87 ± 14	149 ± 11	99 ± 4
P.I.	0.1	0.1	0.1	0.1	0.1	0.2	0.2

In order to facilitate the deposition of the anionic polymers, such as HA, onto the oily cores, we introduced the cationic surfactant CTAB at concentrations between 1 and 5.7% (w/w). **Figure 1** shows how the addition of CTAB reversed the zeta potential from -60 mV to positive values. For the 1% CTAB concentration, a great enlargement of the droplet size was observed together with high polydispersity, a result that was attributed to the aggregation produced by charge neutralization. The 3.9% CTAB concentration led to the formation of positively charged oily droplets with the smallest particle size. Therefore, this concentration was selected for the preparation of nanocapsules.

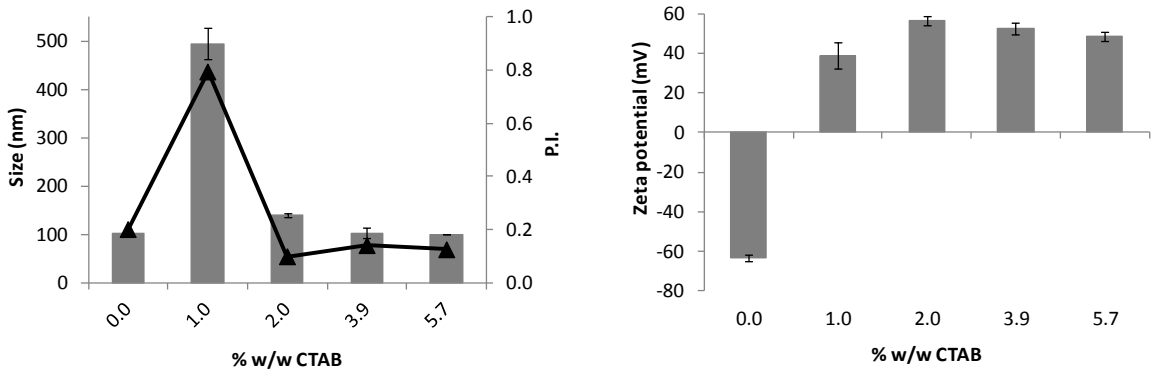

Figure 1. Physicochemical characterization of cationic nanoemulsions prepared with hexadecyltrimethylammonium bromide (CTAB). Size (represented by columns) and polydispersity index (P.I., shown as lines) and zeta potential.

For the preparation of polymeric based nanocapsules, the corresponding polymer was added to the aqueous phase during the preparation. **Table 3** shows the physicochemical characteristics of these nanocarriers. As expected, the addition of anionic polymers reversed the positive zeta potential to negative values, indicating the polymer deposition over the cationic oily droplets.

Formulation	Size (nm)	P.I.	ζ Potential (mV)
Cationic NE	103 ± 10	0.1	+52 ± 3
HA NCs	112 ± 7	0.1	-49 ± 3
PGA NCs	99 ± 3	0.1	-51 ± 6
PGA-PEG NCs	116 ± 5	0.1	-29 ± 5
PASN NCs	111 ± 2	0.1	-25 ± 9

Table 3. Physicochemical characteristics of the cationic nanoemulsion (NE) and the HA, PGA, PGA-PEG and PASN nanocapsules (NCs). (mean ± SD; n=3).

4. Conclusions

Herein we report, for the first time, the synthesis and characterization of a variety of 100 nm polimeric nanocapsules (HA, PGA, PGA-PEG and PASN) using the solvent displacement technique.

References

[1] Hrkach J, Von Hoff D, Mukkaram Ali M, Andrianova E, Auer J, Campbell T, et al. Preclinical development and clinical translation of a PSMA-targeted docetaxel nanoparticle with a differentiated pharmacological profile. Sci. Transl. Med. 2012;4:128ra39.

[2] González-Aramundiz JV, Lozano MV, Sousa-Herves A, Fernandez-Megia E, Csaba N. Polypeptides and polyaminoacids in drug delivery. Expert Opin. Drug Deliv. 2012;9:183–201.

[3] Duro-Castano A, Conejos-Sánchez I, Vicent M. Peptide-Based Polymer Therapeutics. Polymers (Basel). 2014;6:515–51.

[4] Matsumura Y, Kataoka K. Preclinical and clinical studies of anticancer agent-incorporating polymer micelles. Cancer Sci. 2009;100:572–9.

[5] Lozano M V, Torrecilla D, Torres D, Vidal A, Domínguez F, Alonso MJ. Highly efficient system to deliver taxanes into tumor cells: docetaxel-loaded chitosan oligomer colloidal carriers. Biomacromolecules 2008;9:2186–93.

[6] Oyarzun-Ampuero FA, Rivera-Rodríguez GR, Alonso MJ, Torres D. Hyaluronan nanocapsules as a new vehicle for intracellular drug delivery. Eur. J. Pharm. Sci. 2013;49:483–90.

[7] Hervella P, Alonso-Sande M, Ledo F, Lucero ML, Alonso MJ, Garcia-Fuentes M. PEGylated Lipid Nanocapsules with Improved Drug Encapsulation and Controlled Release Properties. Curr. Top. Med. Chem. 2014;14:1115–23.

[8] Verma N, Kumar K, Kaur G, Anand S. L-asparaginase: a promising chemotherapeutic agent. Crit. Rev. Biotechnol. 2007;27:45–62.

[9] Gonzalo T, Lollo G, Garcia-Fuentes M, Torres D, Correa J, Riguera R, et al. A new potential nano-oncological therapy based on polyamino acid nanocapsules. J. Control. Release 2013;169:10–6.

[10] Lollo G, Rivera-Rodriguez GR, Bejaud J, Passirani C, Benoit JP, García-Fuentes M, et al. Polyglutamic acid-PEG nanocapsules as long circulated carriers for the delivery of docetaxel. Eur. J. Pharm. Biopharm. 2014;87:47–54.

[11] Lollo G, Hervella P, Calvo P, Avilés P, Guillén MJ, Garcia-Fuentes M, et al. Enhanced in vivo therapeutic efficacy of plitidepsin-loaded nanocapsules decorated with a new poly-aminoacid-PEG derivative. Int. J. Pharm. 2015;483:212–9.

[12] Rivera-Rodríguez GR, Alonso MJ, Torres D. Poly-L-asparagine nanocapsules as anticancer drug delivery vehicles. Eur. J. Pharm. Biopharm. 2013;85:481–7.

[13] Rivera-Rodriguez GR, Lollo G, Montier T, Benoit JP, Passirani C, Alonso MJ, et al. In vivo evaluation of poly-l-asparagine nanocapsules as carriers for anti-cancer drug delivery. Int. J. Pharm. 2013;458:83–9.

[14] Xie Y, Bagby TR, Cohen M, Forrest ML. Drug delivery to the lymphatic system: importance in future cancer diagnosis and therapies. Expert Opin. Drug Deliv. 2009;6:785–92.

[15] Oussoren C, Zuidema J, Crommelin DJA, Storm G. Lymphatic uptake and biodistribution of liposomes after subcutaneous injection. II. Influence of liposomal size, lipid composition and lipid dose. Biochim. Biophys. Acta 1997;261–72.

[16] Oussoren C, Storm G. Lymphatic uptake and biodistribution of liposomes after subcutaneous injection: III. Influence of surface modification with poly(ethyleneglycol). Pharm. Res. 1997;14:1479–84.

[17] Rao DA, Forrest ML, Alani AWG, Kwon GS, Robinson JR. Biodegradable PLGA Based Nanoparticles for Sustained Regional Lymphatic Drug Delivery. J. Pharm. Sci. 2010;99:2018–31.

[18] Proulx ST, Luciani P, Dieterich LC, Karaman S, Leroux J-C, Detmar M. Expansion of the lymphatic vasculature in cancer and inflammation: New opportunities for in vivo imaging and drug delivery. J. Control. Release 2013;172:550–7.

[19] Qin L, Zhang F, Lu X, Wei X, Wang J, Fang X, et al. Polymeric micelles for enhanced lymphatic drug delivery to treat metastatic tumors. J. Control. Release 2013;171:133–42.

[20] Abellan-Pose R, Csaba N, Alonso MJ. Lymphatic Targeting of Nanosystems for Anticancer Drug Therapy. Curr. Pharm. Des. Accepted.

[21] Mora-Huertas CE, Fessi H, Elaissari A. Polymer-based nanocapsules for drug delivery. Int. J. Pharm. 2010;385:113–42.

[22] Heurtault B, Saulnier P, Pech B, Venier-Julienne M-C, Proust J-E, Phan-Tan-Luu R, et al. The influence of lipid nanocapsule composition on their size distribution. Eur. J. Pharm. Sci. 2003;18:55–61.

[23] Lee SH, Yoo SD, Lee KH. Rapid and sensitive determination of paclitaxel in mouse plasma by high-performance liquid chromatography. J. Chromatogr. Biomed. Sci. Appl. 1999;724:357–63.

[24] Santander-Ortega MJ, Lozano-López M V, Bastos-González D, Peula-García JM, Ortega-Vinuesa JL. Novel core-shell lipid-chitosan and lipid-poloxamer nanocapsules: stability by hydration forces. Colloid Polym. Sci. 2009;288:159–72.

[25] Oussoren C, Storm G. Liposomes to target the lymphatics by subcutaneous administration. Adv. Drug Deliv. Rev. 2001;50:143–56.

[26] Kaur CD, Nahar M, Jain NK. Lymphatic targeting of zidovudine using surface-engineered liposomes. J. Drug Target. 2008;16:798–805.

[27] Moghimi SM. The effect of methoxy-PEG chain length and molecular architecture on lymph node targeting of immuno-PEG liposomes. Biomaterials 2006;27:136–44.

[28] Hervella P, Lollo G, Oyarzún-Ampuero F, Rivera G, Torres D, Alonso M. Nanocapsules as carriers for the transport and targeted delivery of bioactive molecules. In: Da Silva AL, Trindade T, editors. Nanocomposite Particles for Bio-Applications - Materials and Bio-Interfaces. Pan Stanford Publishing Pte Ltd; 2011. page 45–68.

[29] Calvo P, Sanchez A, Martinez J, Lopez M, Calonge M, JC P, et al. Polyester Nanocapsules as New Topical Ocular Delivery Systems for Cyclosporin A. Pharm. Res. 1996;13:311–5.

[30] Calvo P, Remunan-Lopez C, Vila-Jato J, Alonso M. Development of positively charged colloidal drug carriers:chitosan-coated polyester nanocapsules and submicron-emulsions. Colloid Polym. Sci. 1997;275:46-53.

[31] Lince F, Marchisio DL, Barresi AA. Strategies to control the particle size distribution of poly-epsilon-caprolactone nanoparticles for pharmaceutical applications. J. Colloid Interface Sci. 2008;322:505–15.

[32] Mitri K, Vauthier C, Huang N, Menas A, Ringard-Lefebvre C, Anselmi C, et al. Scale-up of Nanoemulsion Produced by Emulsification and Solvent Diffusion. J. Pharm. Sci. 2012;101:4240–7.

Anexo 2

Internalization of HA and HA-t-Lyp-1 nanocapsules in 2 and 3 dimensional cell co-cultures

Este trabajo ha sido realizado en colaboración con M. Alonso-Nocelo[1], A. Vidal[2], Rafael López[1] y M. de la Fuente[1]

[1]Translational Medical Oncology Group, Health Research Institute of Santiago de Compostela (IDIS) Clinical University Hospital/SERGAS, Santiago de Compostela, Spain.

[2]Cell Cycle and Oncology Group CiClOn, IDIS, CIMUS. (USC). Santiago de Compostela, Spain.

USC
UNIVERSIDADE
DE SANTIAGO
DE COMPOSTELA

1. Objectives of this work:

- To evaluate the ability of HA and HA-t-Lyp-1 nanocapsules to be internalized by receptor-mediated endocytosis (CD44 for HA and NRP1 for t-Lyp-1)
- To evaluate the ability of HA and HA-t-Lyp-1 nanocapsules to interact with cancer cells in a 3D tumour model under dynamic conditions.
- To evaluate their specific interaction with tumour cells in a 3D co-culture tumor model (tumour cells and lymphocytes).

2. Materials and methods

2.1. Expression of CD44 and NRP1 receptors in A549 lung cancer cell line.

NRP1 (t-Lyp-1 peptide receptor) and CD44 (hyaluronan receptor) expression was validated in the lung adenocarcinoma cell line A549 (ATCC® CCL-185™). Cells were grown as 2D conventional monolayers and also 3D mono-cultures. Then, they were then fixed in 4% paraformaldehyde, washed with PBS and incubated with rabbit anti-human NRP1 (Abcam) and mouse anti-human CD44 (Dako M7082) primary antibodies. Texas Red conjugated goat anti-rabbit and Alexa-Fluor 488 conjugated goat anti-mouse secondary antibodies (Jackson Immunoresearch Laboratories, Inc.) were incubated for 1h at room temperature in the dark. Samples were mounted with Mowiol™ mounting medium (Calbiochem, UK).

2.2. 2D cell culture studies in FACS Analysis

Lung adenocarcinoma cell line A549 (ATCC® CCL-185™) was grown in DMEM Dulbecco's modified Eagle's Medium) supplemented with 10% fetalbovine serum and 5% Penicillin streptomycin (GIBCO®). For FACS analysis, cells were seeded in 24 well plates at $7.5x10^4$ cells/well in supplemented medium for 24 hours. Afterwards, the medium was removed and dilutions of DiD loaded Hyaluronan nanocapsules (HA NCs), and t-LyP-1 decorated hyaluronan nanocapsules (with substitution degrees of t-Lyp-1 of 1.5 and 2.9 %) were added to the wells at a fluorescent probe concentration of 0.5 µg/ml. Experiments were performed at 37ºC and 4ºC. Control isotype antibodies (i.e. non-specific antibodies to

assess blocking specificity) and anti-CD44 and anti-NRP1 antibodies were used at 4ºC to block the receptors. After 1h of incubation, cells were washed and recovered by trypsinization. Cells were rinsed with PBS and resuspended in 500µL of PBS-FBS 2% for the analysis using a FACScan (BS Biosciences)

2.3. Preparation of the 3D tumour model and nanocapsules perfusion

For 3D mono-cultures, Alvetex scaffolds (Reinnervate) were placed on a 6 well plate. Cells were seeded into the scaffolds following the manufacturer´s protocol. Briefly, a cell suspension at a concentration of $7.5x10^5$ cells was prepared and pipetted on the surface of the scaffold dropwise. 3D co-cultures were seeded as previously described, but from a cell suspension containing $5x10^5$ cells of each cell type. Carefully, scaffolds were placed in the incubator for 4 hours. Then, 10mL of fresh culture medium were added along each well´s edge. Cells were allowed to grown in the scaffold for 48 hours.Scaffolds were placed inside a bioreactor coupled to an automatic syringe pump for nanocapsules perfusion. DiD loaded HA NCs and HA-t-Lyp-1 NCs (with substitution degrees of t-Lyp-1 of 1.5 and 2.9 %) were diuted in cell culture medium at a fluorescent probe concentration of 0.5 µg/mL. Then, they were pumped through the co-cultures at a flow rate of 250 µL/h for 2 hours, followed by a washing cycle of cold PBS at a flow rate of 600 µL/h.

2.4. 3D confocal studies

3D cultures were removed using a scalpel, rinsed gently with PBS and fixed with in 4% paraformaldehyde. 3D mono-cultures were stained using rabbit anti-human NRP1 (Abcam) and mouse anti-human CD44 (Dako M7082) primary antibodies. 3D co-cultures were stained using Actin-Phalloidin FITC conjugated (Sigma-Aldrich) and rabbit anti-human CD3 (Dako IR553) primary antibodies. Texas Red conjugated goat anti-rabbit and Alexa-Fluor 488 conjugated goat anti-mouse secondary antibodies (Jackson Immunoresearch Laboratories, Inc) were incubated for 1h at room temperature in the dark. Samples were mounted with MowiolTM mounting medium (Calbiochem). Cell-population specific uptake of the NCs was analysed by LCSM at 63x magnification. Images were captures with a scanning speed of 400 Hz and image resolution of 1024 x 1024 pixels.

3. Results

3.1. NRP1 and CD44 receptors expression

Immunofluorescence of NRP1 and CD44 receptors revealed their expression in both 2D (Figure 1 A-B) and 3D cultures (Figure 1 C-D) of A549 cells. As it can be observed, and in agreement with previous studies (1-4), NRP1 expression was observed not only in the tumour cell line, but importantly, its expression was confirmed in our 3D model. Therefore, A549 cells and 3D models based on this cell line are a good model to test HA and HA-t-Lyp-1 nanocapsules.

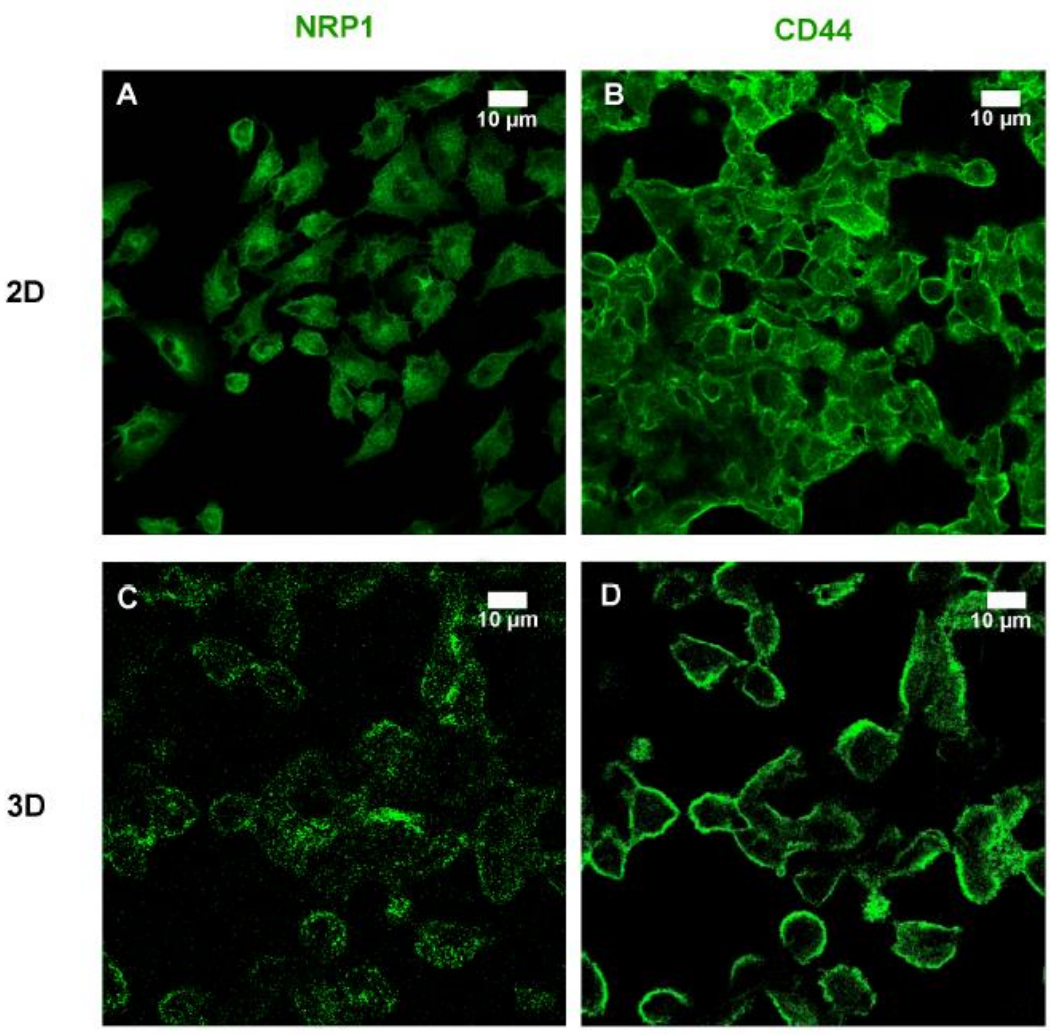

Figure 1: NRP1 and CD44 receptors expression in 2D (A-B green) and 3D cultures (C-D green) of tumour cells by confocal microscopy.

3.2. Mechanistic studies in 2D cultures

As obserbed in Figure 2, the 3 formulations (HA, HA-t-Lyp-1 DS 1,6% and HA-t-Lyp-1 DS 3% NCs) were successfully uptake by cancer cells at 37ºC. At this temperature, both adsorptive and receptor-mediated endocytosis tipically account for the internalization of NCs. Thus, to explore if HA NCs and HA-t-Lyp-1 NCs could enter the cells after their specific interaction with the targeted receptors, mechanistic studies were subsequently performed at 4ºC (at this temperature adsoptive-mediated endocytosis and vesicle formation are blocked) (Figure 2B). The 3 formulations showed a reduction of the mean intensity DiD fluorescence when blocking CD44 receptor. NRP1 receptor blocking showed a smaller reduction on NCs uptake compared to CD44, a fact that could somehow be expected. Even if the inhibition of the internalization of HA-t-Lyp-1 NCs could have been effective, these formulations could still entry cells through CD44-hyaluronan interactions, as CD44 is widely and ubiquitously expressed in this cell line. However, blocking both receptors exhibited a higher reduction on DiD fluorescence for the modified t-Lyp-1 NCs, even if significant differences among the 3 formulations are not reported. For visualization, cells blocked with both CD44 and NRP1 were also observed under the confocal microscope upon incubation of t-Lyp-1 decorated and HA NCs and HA-t-Lyp-1 NCs (Figure 2C). Results revealed that the internalization of t-Lyp-1 modified NCs is less efficient than plain HA NCs after the simultaneous blocking of CD44 and NRP1, in agreement with the FACS analysis data.

Altogether, results indicate a CD44 specific interaction mediating in part the internalization of the NCs in tumour cells, and suggest that the modification with t-Lyp-1 could favour their selectivity towards tumour cells.

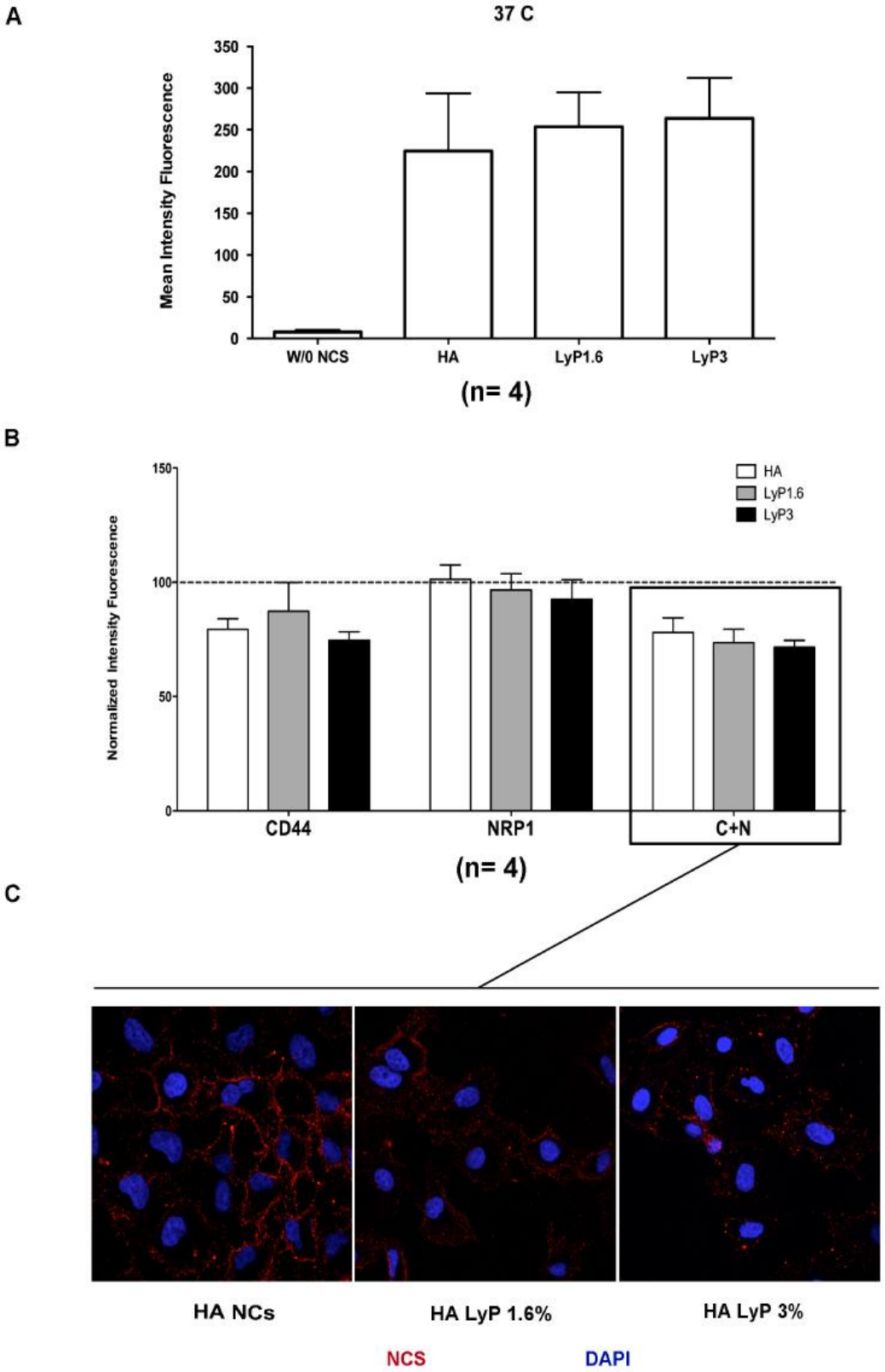

Figure 2: Flow cytometry analysis of NCs uptake at 37ºC (A) and 4ºC (B). Graph bars represent % of normalized mean DiD intensity fluorescence when blocking receptor mediated endocytosis. (C) 2D cell uptake studies at 4ºC, blocking CD44 and NRP1 receptors. NCs (red) and nuclei (blue).

3.3. Cellular upake studies in 3D Mono-Cultures of tumour cells.

Immunofluorescence of CD44 (Figure 3A) and NRP1 (Figure 3B) receptors confirmed a higher expression of CD44 compared to NRP1. Internalization studies under dynamic conditions at 37ºC showed as t-Lyp-1 modified NCs are apparently more efficiently internalized than plain HA NCs (Figure 3C). Results suggest as the interaction of t-Lyp-1 with NRP1 could improve the retention of the NCs in the 3D network.

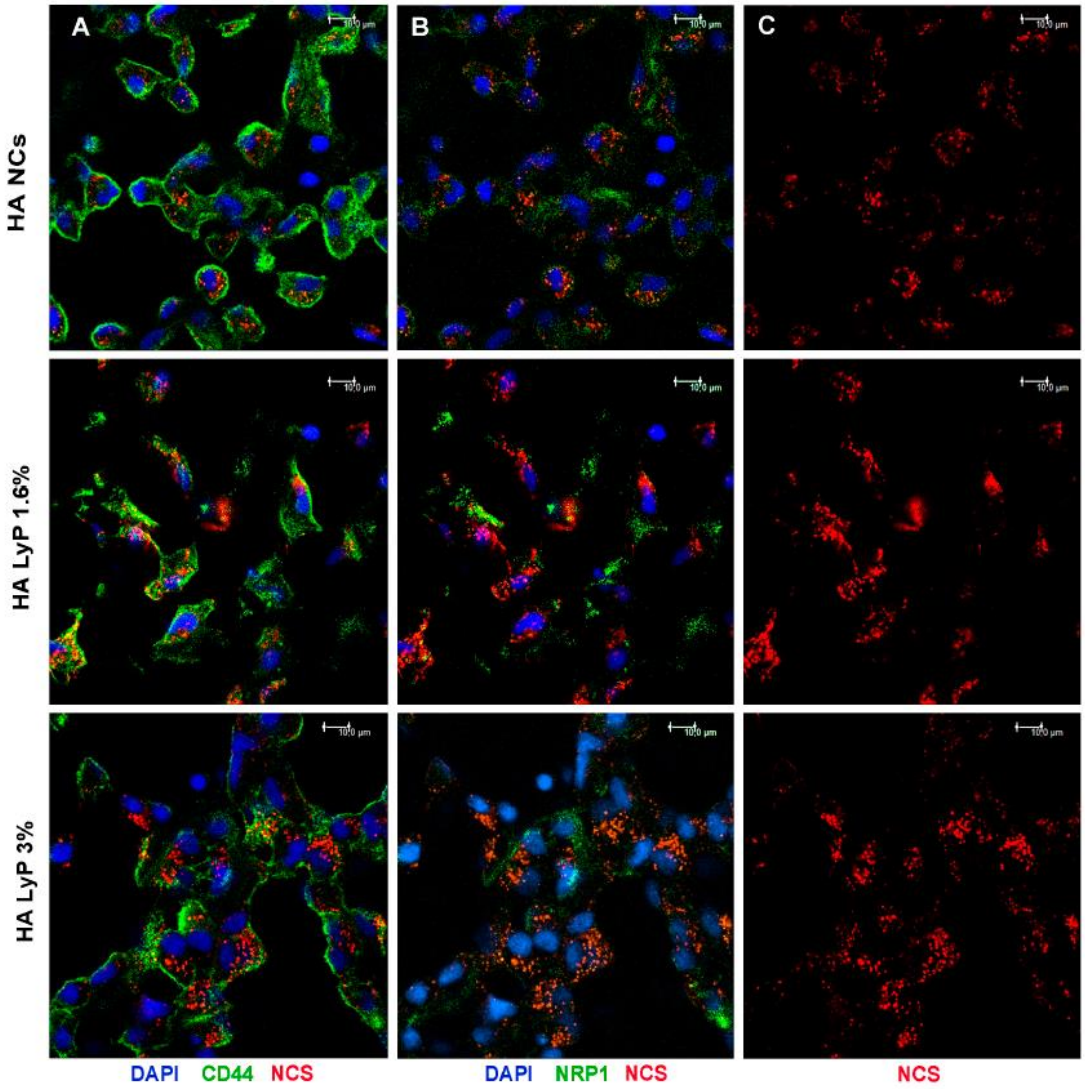

Figure 3: immunofluorescence of 3D mono-culture after NCs perfusion at 37ºC. Green channel, CD44 (A) and NRP1 (B). Blue channel corresponds to cell nuclei counterstained with DAPI (A, B). Red channel correspond to DiD loaded into the NCs (A, B, C). Red channel is depicted without staining the cells for a better appreciation (C).

3.4. Cellular uptake studies in 3D co-cultures of tumour cells and lymphocytes

Immunofluorescence of actin (cytoskeleton marker) and CD3 (lymphocytes specific marker) was done after perfusion with the purpose of differentiating both cell populations, i.e. tumour cells and lymphocytes (Figure 4A). Results revealed that the 3 formulations were preferentially internalized in the tumour cells rateher than in the lymphocytes (Figure 4B). In agreement to the results reported in 3D mono-cultures of A549 cells (Figure 3C). HA-t-Lyp-1 NCs seemed to interact more efficiently with the tumour cells with respect to the unmodified HA NCs.

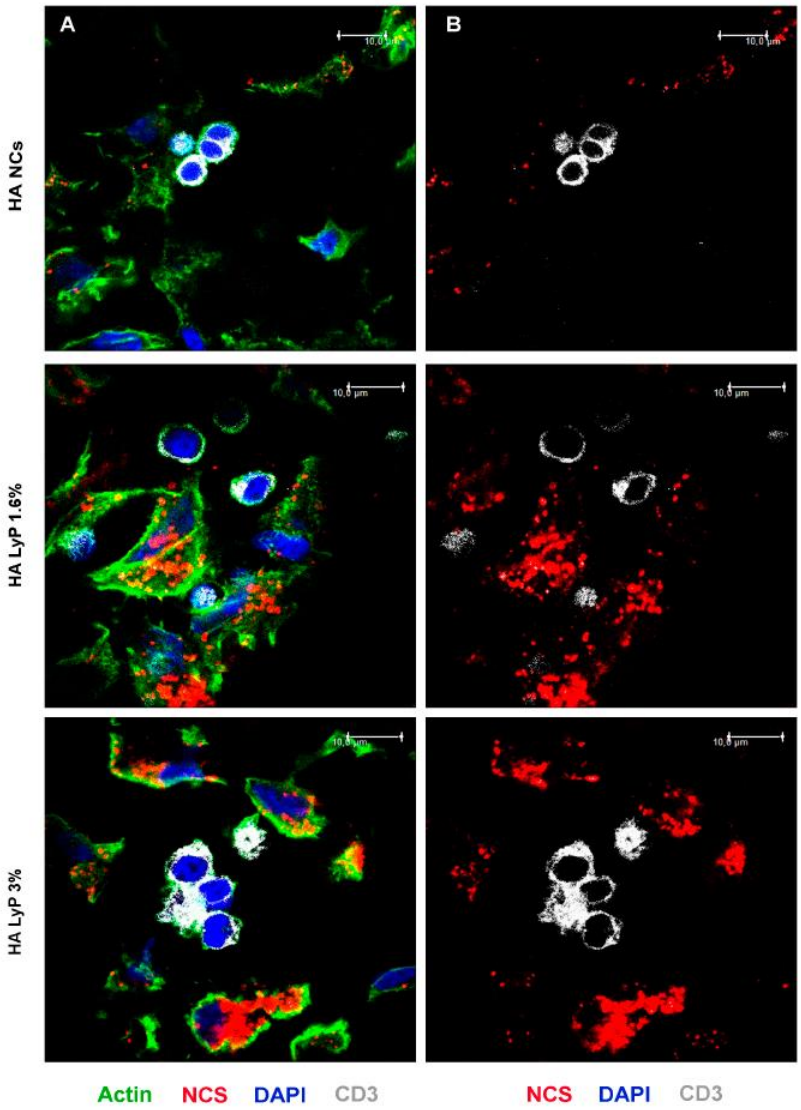

Figure 4: immunofluorescence of 3D co-culture after NCs perfusion at 37ºC. (A) green channel: acti, white channel: CD3 receptor. Blue channel: cell nuclei counterstained with DAPI. Red channel: DiD loaded NCs. (A, B) Red channel is depicted with CD3 staining for a better visualization of NCs that were not internalized by the lymphocytes (B).

4. Conclusion

We have probed the ability of HA and HA-t-Lyp-1 nanocapsules to interact and accumulate in A549 lung cancer cells in a selective fashion. Mechanistic studies indicate that the internalization is at least partially mediated by interaction with the CD44 receptor. Additionally, we have observed as the modification with t-Lyp-1 improve their accumulation in a 3D tumour model. This fact could be attributed to the dynamic flow favouring t-Lyp-1 penetrating properties, improving NCs targeted interaction and distribution along the 3D model, in agreement with previous nanoparticle perfusion-driven studies (5-7).

References

1. Ding M, Liu L, Hu C, Liu Y, Qiao Y, Jiang X. Expression of VEG Expression of VEGFR2 and NRP-1 in non-small cell lung cancer and their clinical significance Chin J Cancer Res. 2014 Dec; 26(6): 669–677.
2. Imoh S. Okon, Kathleen A. Coughlan, Cheng Zhang, Cate Moriasi, Ye Ding, Ping Song, Wencheng Zhang, Guangpu Li, and Ming-Hui Zou. Protein kinase LKB1 promotes RAB7-mediated neuropilin-1 degradation to inhibit angiogenesis J Clin Invest. 2014 Oct;124(10):4590-602
3. Jia H, Cheng L, Tickner M, Bagherzadeh A, Selwood D, Zachary I. Neuropilin-1 antagonism in human carcinoma cells inhibits migration and enhances chemosensitivity. Br J Cancer. 2010 Feb 2;102(3):541-52.
4. Chaudhary B, Khaled YS, Ammori BJ, Elkord E. Neuropilin 1: function and therapeutic potential in cancer. Cancer Immunol Immunother. 2014 Feb;63(2):81-99.
5. Ng CP, Pun SH. A perfusable 3D cell-matrix tissue culture chamber for in situ evaluation of nanoparticle vehicle penetration and transport. Biotechnol Bioeng. 2008 Apr 15;99(6):1490-501.
6. Goodman TT, Ng CP, Pun SH. 3-D tissue culture systems for the evaluation and optimization of nanoparticle-based drug carriers. Bioconjug Chem. 2008 Oct;19(10):1951-9.
7. Alonso-Nocelo M, Abellán-Pose R, Vidal A, Csaba N, Abal M, Alonso MJ, et al. A 3-D tumor-infiltrated lymph node model for the evaluation of targeted therapies. Unpublished

Anexo 3

Toxicity and mechanistic behavior of hyaluronan-based drug nanocarriers on zebrafish embryos

Este trabajo ha sido elaborado en colaboración con Elena S. Yebra-Pimentel, Jorge Guerra-Varela y Laura Sánchez. Genetic Department, Veterinary Faculty, University of Santiago de Compostela, Lugo, 27002, Spain.

USC
UNIVERSIDADE
DE SANTIAGO
DE COMPOSTELA

Abstract

Nanoparticles have several applications in biopharmaceutics, as they can improve the biological effect of the drugs they carry. However, an assessment of their potential hazard to human beings must be performed. Within biomaterials used in this field, hyaluronic acid (HA) is one of the most functional materials explored due to its biocompatibility and viscoelasticity together with its selectivity to different cell types. In this work, fish embryo toxicity (FET) test of two prototypes of HA-coated nanocapsules (the first one, HA-NC, comprises a cationic surfactant, and the second, PrHA-NC, avoids this surfactant by using the positive polymer coating protamine, Pr) and the analog non-HA coated nanocarrier (nanoemulsion, NE) was conducted on zebrafish embryos. Results indicate that NE is the most toxic nanocarrier as it causes 100% of mortality, and HA-NC and Pr-HA-NC cause mortalities of 17.71 ± 5.14% and 13.04 ± 3.01% respectively at the highest concentration tested. Uptake studies indicate that HA-NC is not internalized by the embryo, even in early-dechorionated ones, whereas PrHA-NC is able to cross the chorion and reach embryo cells. This effect has been attributed to the cell penetrating peptide ability of Pr, which highlights its potential use for high patient compliance administration route where crossing a biological barrier is a critical step.

1. Introduction

Zebrafish (*Danio rerio*) has emerged as a useful model organism in biomedicine and focused increasing attention for drug discovery (MacRae and Peterson, 2015). This species exhibits biological similarity when compared with more complex organisms like rodents and humans, and its genome has been completely sequenced showing more than 70% of its genes in common with humans (Zon & Peterson, 2005). Zebrafish has high fecundity so it is possible to perform experiments with a high number of individuals with statistically robust results and it is ideal for toxicological analysis due to embryos can be exposed to different products via aqueous solutions (McGrath & Qi Li, 2008).

Nanotechnology is a new science, born at the beginning of the century, which involves the use of structures that have at least one dimension in the nanoscale (Lin *et al*., 2012).

A wide range of applications of these nanocarriers include therapeutic purposes like transporting vaccines, genes, and drugs. However, nanocarriers may pose a risk to human health and the environment, which should be evaluated. In recent years it has exponentially increased the literature documenting the toxicity of a wide range of nanomaterials (Duan *et al.,* 2013; Kovriznych *et al.,* 2013). Toxicology models used in published studies comprise cell cultures and more complex analysis performed *in vivo* with biological models such as mouse or zebrafish.

Moreover, molecular analyses of embryo zebrafish indicate that these embryos can be a good model for testing new particles under the European REACH initiative (Yang *et al*. 2009). The existing literature on nanomaterials toxicity studies in zebrafish embryos is very recent and is mainly based on analysis of toxicity of metal nanoparticles, mainly gold and silver (Asharani *et al*., 2008; Cunningham *et al*., 2013)

In aquatic organisms, substances can pass through the skin and biological barriers when dissolved in the aquatic medium or by direct introduction (e.g. oral administration, injection) (Braunbeck *et al*., 2004; Asharani *et al*., 2008; Schubert *et al*., 2014). At an embryonic stage, the chorion permeability is an important assessment for the uptake of nanomaterials being necessary to test its influence in embryo toxicity test (Kim & Tanguay, 2014). The chorion can be removed manually or with an enzymatic treatment with pronase (Westerfield 2007). Previous studies show that enzymatic dechorionation with proteases as pronase does not offer a reproducible survival rate and might undetectably damage the embryos (Henn & Braunbeck, 2010). In addition, 24 hours post-fertilization (hpf) is the earliest stage at which rate survival average is appropriated to the acceptance criteria related to negative control mortality (≤ 10%).

The aim of the present study is to evaluate the toxicity in zebrafish embryos of a nanoemulsion (NE) HA free and two prototypes of nanocapsules (NC) with HA: first, HA-NC (hyaluronan nanocapsules) has a cationic surfactant, and the second PrHA -NC (protamine hyaluronan nanocapsules), avoids the use of the surfactant by introducing a second polymer coat of protamine (Pr). Thus, we will analyze whether the presence of HA in the polymeric shell is beneficial to reduce the toxicity of these type of nanosystem.

2. Materials and methods

2.1. Breeding stock maintenance

A breeding stock of wild-type adult zebrafish was kept on a recirculating water system at 26 ± 1 ºC, and has been fed three times a day with dry commercial flakes (Tetramin®) and brine shrimp (*Artemia spp*.). Females and males are constantly held together at a 14h/10h light: dark photoperiod. Tap water has been purified and dechlorinated by reverse osmosis and adjusted to optimal parameters (Westerfield, 2007). Fish are macroscopically free of apparent symptoms of disease and have not been subjected to any pharmaceutical treatment for the previous two months to the spawning. All the experiments have been performed in compliance with the relevant laws of animal experimentation and were approved by the Bioethical Committee for animal experimentation CEEA-LU (University of Santiago of Compostela).

2.2 Nanosystem preparation

Sodium hyaluronate (HA, MW 57 KDa) was purchased from Lifecore Biomedical (Chaska, MN, USA). Miglyol® 812, neutral oil formed by esters of caprylic and capric fatty acids and glycerol, was donated by Cremer Oleo GmbH & Co (Germany). The surfactant Epikuron® 145V, a phosphatidylcholine-enriched fraction of soybean lecithin, was donated by Cargill (Spain). Protamine sulphate purchased from Yuki Gosei, Japan. PEG-Stearate (Simulsol® M52) was obtained from Seppic (France). α-tocopherol (Vitamin E) was supplied by Merck (Germany). 1,1´-Dioctadecyl-3,3,3´,3´-tetramethylindodicarbocyanineperchlorate (DiD) was obtained from Molecular Probes-Invitrogen (USA). Hexadeciltrymethylammonium bromide (CTAB), Rhodamine 6G and sodium phosphate monobasic were purchased from Sigma-Aldrich (Spain). Milli-Q water was used throughout the experiments and organic solvents were HPLC degree.

Both prototypes were prepared by solvent displacement technique with slight modifications to the procedure described previously (Oyarzun-Ampuero *et al*., 2013). This method consists on adding by dropwise the organic phase containing oil and surfactants into an aqueous phase containing the coating polymer under magnetic stirring. After nanocapsules formation organic solvents were removed by rotaevaporation.

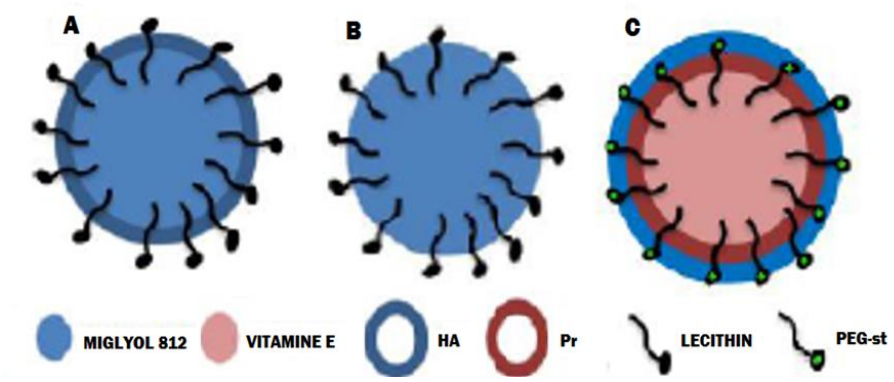

Figure 1. Nanosystem structure. A: HA-NC; B: NE; C: PrHA-NC

In the case of HA-NC (Figure 1), the organic phase was composed by 4.75 mL of acetone and 0.2t5 mL of ethanol containing 0.75 mg/mL of Epikuron® 145v, 0.15MG/ML of CTAB and 2.96 mg/mL of Miglyol® 812. The aqueous phase consists of 10 mL of hyaluronic acid solution (0.25 mg/mL). The nanoemulsion (NE, Figure 1 B) was obtained with the same procedure replacing the hyaluronic acid solution for 10 mL of water.

PrHA-NC (Figure 1.C) were prepared in two steps. First, protamine nanocapsules were prepared adding an organic phase composed by 4.75 mL of acetone and 0.25 mL of ethanol with 1.2 mg/mL of PEG-stearate and 3 mg/mL of Vitamin E into 10 mL of water phase with 0.125 mg/mL of protamine. After solvent evaporation, 4 mL of nanocapsule suspension were incubated with 1 mL of an aqueous solution of hyaluronic acid (8 mg/mL) in order to get an electrostatic interaction between protamine and hyaluronic acid.

Fluorescent labeled nanocapsules were prepared adding an ethanolic aliquot of 50 and 100 µg/mL of DiD (in the case of HA-NC and NE) or Rho6G (in PrHA-NC) into the organic phase for hyaluronic acid or protamine-hyaluronic acid NCs respectively, according to the capacity of each nanocarrier for retain the fluorescent probe.

The nanostructures obtained were isolated by ultracentrifugation (Optima™ L-90K Ultracentrifuge, Beckman Coulter; Fullerton, CA) at 84035g for 1 h at 15 °C. Then infranatant was removed from the media and nanocarriers were diluted to a known concentration.

2.2.1. Physicochemical characterization

Particle size and polydispersion index (PDI) were determined by photon correlation spectroscopy (PCS). Samples were diluted in Milli-Q Water and the analysis was carried out at 25 ºC with an angle detection of 173º. Zeta potential measurements were performed by laser Doppler anemometry (LDA) and the samples were diluted in 1mM KCl aqueous solution. PCS and LDA analyses were performed in triplicate using a NanoZS® (Malvern Instruments, Malvern, UK).

2.2.2. Quantification of nanosystem formation yield

Yield in the process of nanosystems preparation was performed with a gravimetric assay. Three batches of isolated nanosystems were placed in a vial, freeze-dried and accurately weighted with an analytical balance (A & D instruments, GR 200, UK). The percent yield was estimated by difference between the total weight of all components used in the preparation and the weight of isolated nanosystems after lyophilization. For Pr-HA NCs this percentage was calculated without taking into account the HA amount due to this polymer is added in a greater excess compared with protamine polymer.

2.2.3. Release of fluorescence

The release of DiD and Rhodamine 6G from the nanosystems was also studied simulating the zebrafish assay conditions, in order to/This will guarantee that signals observed could be associated exclusively, to them and not to free fluorophores. For these studies three batches of isolated nanosystems were diluted up to 1:10 dilution in a phosphate buffer (pH 7, sink conditions), and maintained under horizontal shaking. At 0, 4 and 24 h, 1 mL of each batch was isolated by ultracentrifugation and the infranatant containing the released fluorescent was collected for its quantification.

The estimation of the release (%) was calculated by difference between the free fluorescence obtained dissolving an aliquot of infranatant after nanosystem isolation, and the initial fluorescence attached to nanosystems. The initial fluorescence attached to nanosystems was determined by diluting an aliquot of isolated nanosystems before diluting with phosphate buffer.

Fluorescence quantification was performed by UV spectrophotometry at 646 nm for DiD *(*DU® 730, Beckman Coulter*)* in acetonitrile, and at 530/590 525 nm for Rho 6G (Mithras LB 940, Berthold Technologies) in ethanol.

2.2.4. Stability studies in zebrafish media

The physical integrity of nanosystems in the zebrafish conventional embryo media, called E3 (OECD 203 annex 2, 1992: 294mg/L $CaCl_2 \cdot 2H_20$, 123.25 mg/L Mg $SO_4 \cdot 7H_20$, 64.75Mg/L $NaHCO_3$, 5.75 mg/L KCl), and in sterile dechlorinated tap water (SDTW) was assessed. Three different batches of each nanosystem were diluted in this medium and were maintained under horizontal shaking at room temperature to simulate zebrafish living conditions. At 0, 2, 24 y 48 h particle size, PDI and zeta potential were controlled as described in section 2.2.1. Physicochemical characterization.

2.3. Nanosystem toxicity assays in zebrafish embryos

Embryos aged 4-5 hours post-fertilization (hpf) were exposed for 96 hours to different nanosystem suspensions at 26 ± 1 ºC, following the OECD fish embryo toxicity (FET) test (OECD Test No. 236, 2013). In brief, 24 eggs were transferred into 24-well plates with one embryo per well. Twenty wells were filled with 2 mL of increasingly concentrations of nanosystem suspensions and the remaining four wells acted as internal-plate negative control. Based on preexistent publications related to toxicity assays of similar polymeric nanosystems on zebrafish embryos (Duan et al., 2013; Hu *et al*., 2011), theoretical concentrations performed were 30, 60, 90 and 120 µg/mL. Negative control consisted on SDTW, as the instability of these nanosystems in conventional embryo medium (OECD Test No. 203 Annex 2, 1992) has been demonstrated by changes on size and Z potential (data not shown). ZnO nanoparticles 10 µg/mL (CAS 1314-13-2, Sigma Aldrich) were used as positive control, as its toxicity has been well studied and demonstrated (Zhu *et al.,* 2009). Lethal endpoints (embryo coagulation, lack of somite formation, non-detachment of the tail and lack of heartbeat) were observed every 24 hours under inverse microscope (Nikon TMS Nº3) until the end of the test (96hpf). All experiments have been performed in triplicate.

2.3.1. Data analysis

Data analysis was performed by probit analysis (Finney, 1952) using ToxRat Professional 2.10.2.1 (ToxRat Solutions, Alsddorf, Germany) and Microsoft Excel (v 2013, Microsoft, Inc, Reddemond, WA). Data are shown in terms of mean ± standard deviation, considering $\alpha = 0.05$.

It has been demonstrated that ignoring mortality in the negative control can result in underestimated LC_{50} (Hoekstra, 1987) even at such low percentages as 10% accepted by FET OECD Protocol. Therefore, data were corrected for control mortality with Abbott´s formula, where X is the % mortality of treated embryos and Y is the % mortality in the control embryos (Abbott, 1925).

$$Corrected\ \% = \frac{X - Y}{100 - Y}\ x\ 100$$

In order to determinate the NOEC (*no observed effect concentration*) and LOEC (*lowest observed effect concentration*) pair-wise comparisons between treatment and control have been performed by Fisher's exact binomial test with Bonferroni Correction. Pair-wise comparisons are performed sequentially using the adjusted $\alpha^* = \alpha/(k-1)$, were k is the number of comparisons (Holm, 1979). No effect (H_0) is accepted if the probability (p) is > than α^*.

2.4. Nanocapsules uptake and biodistribution scanning

In order to get a better understanding of nanocapsules activity, their distribution was followed by confocal microscopy, due to the fluorophores included into the core. HA-NC and NE, labeled with DiD, were excited at 646 nm, and PrHA-NC, labeled with RhO6G were excited at 525 nm. Signal was acquired at 655 and 565 nm respectively.

Resulted images slides can be sum, enhanced or analyzed using ImageJ® software.

2.4.1. Uptake of nanocapsules suspensions

Some of the 0 hpf embryos exposed to 120 µg/mL fluorescent nanosystem suspension (from FET analysis) were randomly selected at different and observed under confocal

microscopy (Leica TC5 SPSX) to analyze their substance uptake both in chorioned phase (48hpf) and non-chorioned phase (96hpf). Not exposed embryos were also observed as negative control in order to discriminate nanosystem fluorescence from the typical zebrafish autofluorescence, peaked in 570 and 630 nm (Billinton & Knight, 2001; Shi *et al.,* 2009).

As both NCs were dyed with different fluorophores, NCs were also mixed together at a concentration of 60 mg/mL each, to compare different uptake capacity and biodistribution.

In case of finding no NC uptake, experiments were repeated with early- dechorionated embryos in order to facilitate the uptake by increasing the contact time between the nanocapsules and naked embryo. 24 hpf embryos were manually dechorionated with sharply pointed forceps (Dumont No 5). This could help to unveil some of the chorion properties, limiting diffusion until the developing embryo. To avoid injury of naked embryos, which otherwise might occur through direct contact with plastic materials, the bottom of the wells have been covered with 2% agarose (Henn & Braunbeck, 2010). Control experiments with SDTW were conducted to ensure that mechanical dechorionation does not effect on embryonic development. If the NC does not enter even so, NCs microinjections took place.

2.4.2 Biodistribution of injected nanocapsules

In case that nanocapsules does not enter the body by diffusion, forced uptake was carried out by microinjecting the nanoparticles inside the embryo yolk. Here, the aim is checking the presence of the nanocapsules inside the yolk and its biodistribution and mobility inside the embryo.

Embryos aged 4-5, 24 and 48 hpf were microinjected (Narishige IM-31) with s HA-NC and PrHA-NC at doses 0.15 and 0.3 µg/mL following the next conditions: Pressure = 12 kPa; Pore diameter = 25 µm; Time = 10 ms; Volume = 10 nL. Microneedles (Harvard apparatus) were made with a puller (Narishige PC-10). Embryos aged 24 and 48 hpf were anesthetized with 75 µM MS-222 (CAS 212-956-8) before the injection (Westerfield, 2007). Negative control embryos were microinjected with SDTW.

Microinjected embryos were randomly selected and observed under confocal microscopy 24 and 48 and 96 hours post-injection (hpi) to confirm the suitability of this

uptaking method and to analyze nanocapsules dynamics inside the embryo's body.

3. Results

3.1. Nanosystem characterization

Nanostructures formation was easily observed for the opalescent appearance of the organic and aqueous phase mixture. These nanosystems have a size below 200 nm, with a unimodal distribution. Nanocapsules have negative surface charge, which was attributed to anionic nature of HA, while non-polymer coated nanoemulsion has a strong positive charge due to the positive ammonium groups of CTAB (Table 1).

Nanosystems	Size (nm)	P.I.	Z potential (mV)
HA-NC	112 ± 7	0.1	-49 ± 3
PrHA-NC	157 ± 3	0.1	-30 ± 4
NE	104 ± 8	0.1	+52 ± 2
ZnO-NP	< 100	0.8	+ 26.5

Table 1. Physico-chemical characteristics of nanocapsules

The encapsulation of fluorescent probes into the oily core of NCs did not produce any effect on their physicochemical properties.

3.1.1. Quantification of nanosystems formation yield

Yield experiments allowed to determinate the real dose administrated to zebrafish embryos instead of reporting a theoretical value that underestimates the toxicity values.

Yield studies on NCs formation showed that both NCs prototypes presented similar production efficiency (above 50%). For Pr-HA NCs this percentage was calculated without taking into account the HA amount due to this polymer is added in a greater excess compared with protamine polymer (Table 2).

	HA-NCs	PrHA-NC	NE
Yield formation (%)	58.1 ± 0.7	53.6 ± 1.8	78.6 ± 8.8

Table 2. Yield percentage of nanosystem formation

In the case of nanoemulsion this production rate increased to 78%. A possible explanation of this higher yield may be due to the polymers facilitate the solubility of the oil into the aqueous phase reducing the nanoprecipitation process that is the driving force of NCs formation.

3.1.2. Control release of fluorescent probe

Encapsulation efficiency and control release studies with different fluorescent probes served to select de most appropriate option for each nanocarrier according to its capacity for encapsulating and retaining it efficiently.

HA-NCs and NE with the same core and surfactants could encapsulate approximately 77% of DiD and, moreover, hold it encapsulated up to 24h (Table 3).

	Encapsulation efficiency (%)	Release at 0h	Release at 2h	Release at 24h
HA-NC	70 ± 9	28 ± 5	30 ± 17	23 ± 1
PrHA-NC	39 ± 11	24 ± 3	20 ± 3	18 ± 5
NE	67 ± 20	30 ± 7	29 ± 2	

Table 3. Encapsulation efficiency and release rate of fluorescent probes at zebrafish assay conditions.

PrHA-NCs encapsulated around 40% of Rho 6G added in the preparation; therefore a loading increase to 100 g/mL was necessary to get a similar fluorescent concentration in both NCs. The release study showed that PrHA-NCs retained approximately 80% of the encapsulated fluorescent up to 24h (Table 3).

The use of these fluorophores allowed to perform zebrafish studies ensuring that the fluorescent signals observed could be associated to the nanocapsules.

3.1.3. Stability studies in ZF media

Toxicity test must be performed under conditions that do not compromise the nanostructure nature of the prototypes and therefore maintain the same structure than for a biomedical application.

Nanocarriers suffered from aggregation in a medium frequently used for zebrafish embryos (E3 medium). This medium is composed of different salts ($NaHCO_3$, KCl, $Mg\ SO_4$ and $CaCl_2$), with high ionic strength causing the fast aggregation of nanocarriers (data not shown).

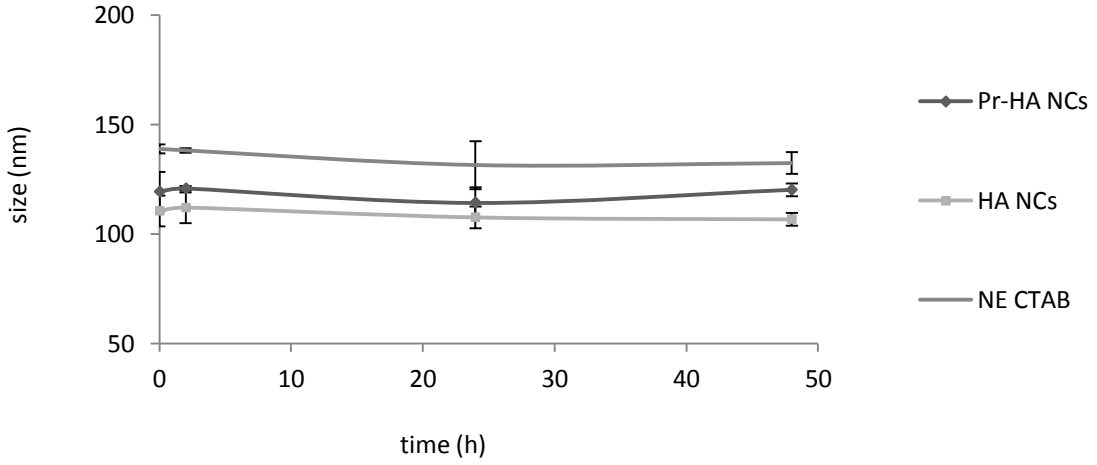

Figure 3. Size evolution of nanocarriers in SDTW

SDTW is another alternative used as zebrafish breeding media. All prototypes resulted to be completely stable in this media without any change in size, IP or Z potential (Figure 3). Accordingly, zebrafish studies were performed diluting nanocarriers in SDTW ensuring the validity of these studies.

3.2. Nanosystem effects on embryo's mortality

Taking into account the yield formation percentage of nanosystems, theoretical concentrations were corrected resulting in the real concentrations represented in table 4.

	Theoretical concentration (µg/mL)	Yield formation (%)	Real concentration (µg/mL)
HA-NC	30	58.1 ± 0.7	17.43 ± 0.12
	60		34.86 ±0.24
	90		52.29 ± 0.37
	120		69.72 ± 0.49
PrHA-NC	30	53.6 ± 1.8	16.08 ± 0.29
	60		32.16 ± 0.58
	90		48. 24 ± 0.87
	120		64.32 ± 1.16
NE	30	78.6 ± 8.8	23.58 ±2.64
	60		47.16 ±5.28
	90		70.74 ± 7.92
	120		94.32 ± 10.56

Table 4. Theoretical and real concentrations used.

Results indicate that exposition to NE produces mortality rates significantly greater than prototypes with HA coating. While NE exposition produces 100% of mortality at the end of the test even at lowest concentration tested (Figure 4), the percentage of mortality achieved at the highest concentration at the end of the test for HA-coated nanosystems is 17.71 ± 5.14 % and 13.04 ± 3.01 % for prototypes HA-NC and PrHA-NC respectively (Figure 4). Thus, LC_{50} for both prototypes with HA is much greater than 69.72 µg/mL, the highest concentration tested, while LC_{50}, NOEC or LOEC for the NE could not be determined because of inappropriate data.

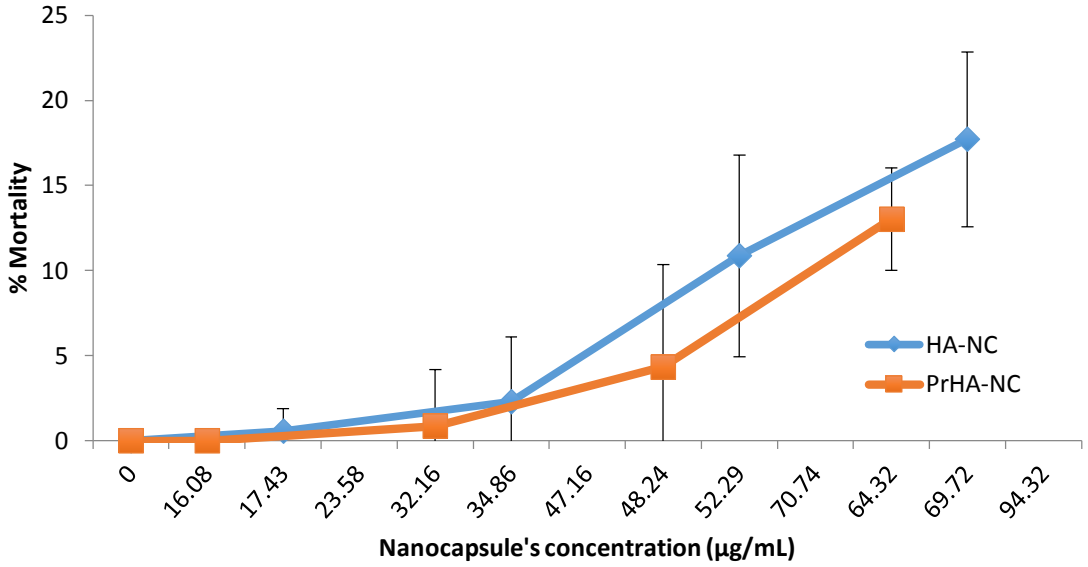

Figure 4. Mortality caused by suspended nanocapsules

Pair-wise comparisons following Fisher's exact binomial test show no significant differences between the control and any of PrHA-NC nanocapsules solutions (α<p; α=0.013; p=0.017), while there are statistically significant differences between the highest concentration of HA-NC and the control (α>p; α =0.013; p=0.001). For prototype HA-NC, NOEC and LOEC are 52.29 and 69.72 µg/mL, while for prototype PrHA-NC are >64.32 and ≥64.32 µg/mL.

All the data are corrected for the mortality in the negative control and all the requirements of the FET (OECD Test No. 236, 2013) were accomplished, as in negative control mortality was ≤ 10% and hatching rate ≥ 80%, and mortality in positive control was ≥ 80% even in the first observation (24 hpf).

3.3. Nanocapsules embryo uptake and biodistribution scanning

Taking advantage of the NCs possibility of internalizing fluorophores and transparency of zebrafish embryos, an uptake and biodistribution assay was carried out checking the results with a confocal microscope. Using embryos from FET analysis, NCs uptake from a suspension and NCs biodistribution from a yolk microinjection were evaluated.

3.3.1. Uptake of suspended nanocapsules

Confocal image analyses suggest a different behavior between both nanocapsule prototypes. NE uptake and biodistribution was not possible to assess because the used

concentrations caused embryo mortality and consequent increase of autofluorescence due necrotic cells, impossible to differentiate from fluorophore (Edwin & Jackman 1981) (Salinas-Madrigal & Sotelo-Avila, 1986) (Tamosiunas *et al*., 2004).

The chorion protects the embryo until dechorionation, at 48-52 hpf, and may be a barrier to the uptake of this nanoparticles. In order to clear up if the chorion prevents the nanoparticles to reach the target, embryos just before hatching (48hpf) were analyzed under confocal microscopy. In the case of prototype HA-NC, aggregates were observed on the external surface of the chorion, but images from the central slides discard their presence inside the embryo or perivitelline space (Figure 5).

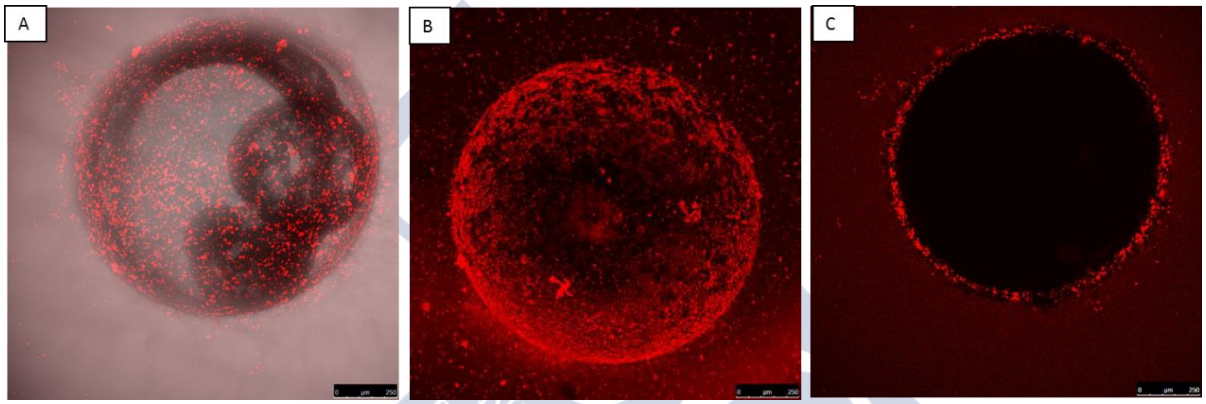

Figure 5. Embryo aged 48hpf exposed to 120µg/mL HA-NC. A: Maximum projection in black and white and fluorescence, z0-z49. B: Maximum projection in fluorescence, z0-z49 C: Slides z23-z26. Scale bar: 250µm.

In the case of prototype PrHA-NC some nanocapsules were observed attached to the chorion as well. However, most of them had passed through the chorion and were in the perivitelline space and in the surface of embryo's skin, as is deducible from the central slides images (Figure 6).

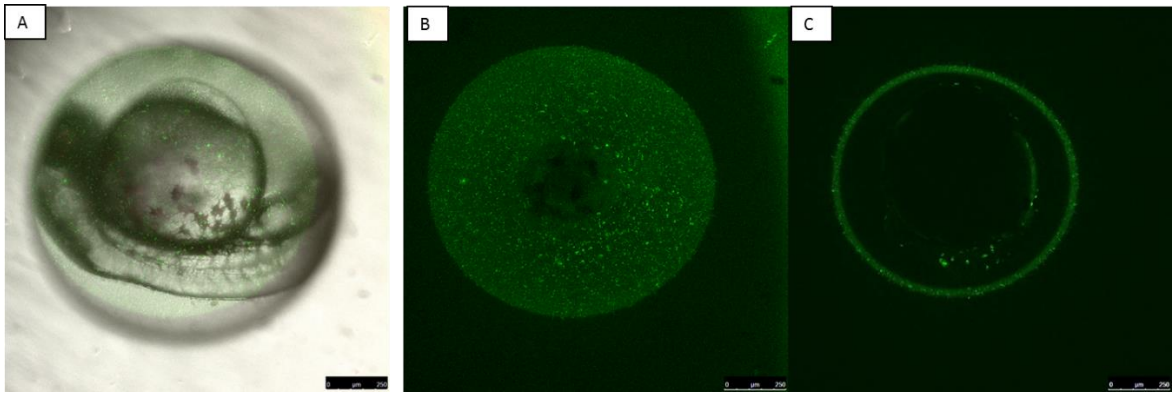

Figure 6. Embryo aged 48hpf exposed to 120µg/mL PrHA-NC. A: Maximum projection in black and white and fluorescence, z0-z41. B: Maximum projection in fluorescence, z0-z41 C: Slides z22-z25. Scale bar: 250 µm.

Embryos exposed to SDTW with a mixture of both prototypes during 48 hours show the same results, observing PrHA-NC in the inner area of the chorion, perivitelline space and embryo's skin, while HA-NC are in the outer surface of the chorion and stuck to it (Figure 7).

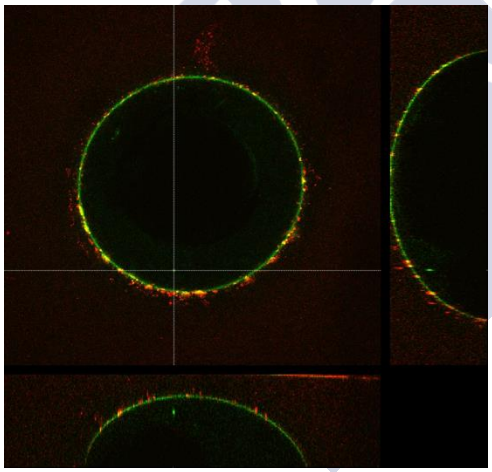

Figure 7. Embryo aged 48hpf exposed to 60 µg/mL of each HA-NC and PrHA-NC, z46. 10x.

Increasing exposure time until 96 hpf (hatched embryos), again HA-NC lack of uptake was again observed (Figure 8), comparing with the uptake of prototype PrHA-NC (Figure 9).

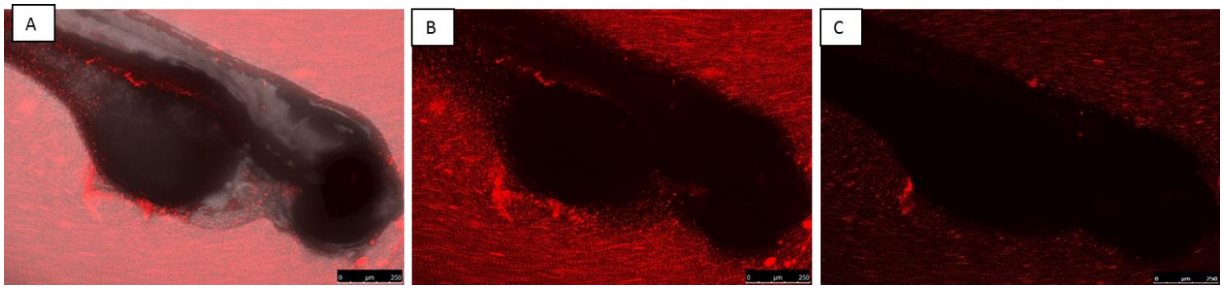

Figure 8. Embryo aged 96 hpf exposed to 120µg/mL HA-NC. A: Maximum projection in black and white and fluorescence, z0-z91. B: Maximum projection in fluorescence, z0-z91. C: Slides z41-z44. Scale bar: 250 µm.

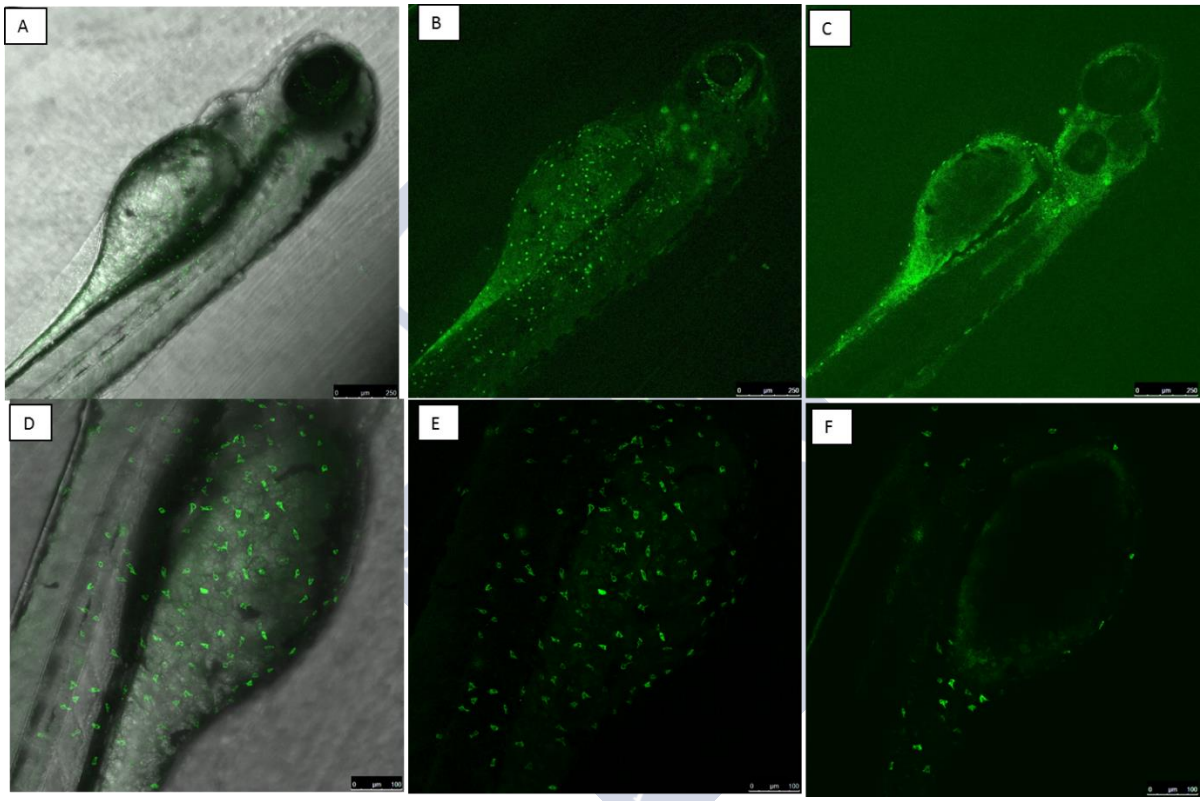

Figure 9. Embryo aged 96 hpf exposed to 120µg/mL PrHA-NC. A: Maximum projection in black and white and fluorescence, z0-z28. B: Maximum projection in fluorescence, z0-z28. C: Slides z12-z15. D: Maximum projection in black and white and fluorescence, z0-z58; E: Maximum projection in fluorescence, z0-z58; F: Slids z32-z35. Scale bars: (A-C) 250 µm, (D-F) 100 µm.

PrHA-NC are present inside the embryos body, specially concentrated in the skin and yolk but avoiding structures like the eye, othic vesicle, heart and dorsal yolk musculature (Figure 9 C).

Analyzing yolk area at 20x (Figure 9, D-F) it is observable the presence of multiple particles of dispersed sizes (87.18 ± 51.57 μm^2) and similar shape. These structures are

present in the surface of the yolk and skin and are very similar in terms of morphology and size to macrophages (Mathias *et al*.,2009; Singer *et al*., 2010; Colucci-Guycon *et al*., 2011; Fenaroli *et al.,* 2014).

Despite early artificial dechorionation is not the routine procedure for toxicity assays, taking into account the presence of canals in the chorion surface that can inhibit the uptake of some substances depending on its size and molecular weight (Creton, 2004), chorion was mechanically removed in embryos aged 24 hpf and the embryos were exposed to a suspension of HA-NC 120 µg/mL. After 48 hours post exposition, again, results indicate the lack of uptake by the embryo (Data not shown).

3.3.2. Biodistribution of injected nanocapsules

HA-NC did not move from the injection point. When observing 0 hpf injected embryos at 24 hpi (Figure 10), vast majority of red signal is forming aggregates inside the yolk, and small proportion migrated through the injection hole in the yolk to the perivitelline space. Embryos 48 and 96 hpi confirm the same pattern (Figure 11).

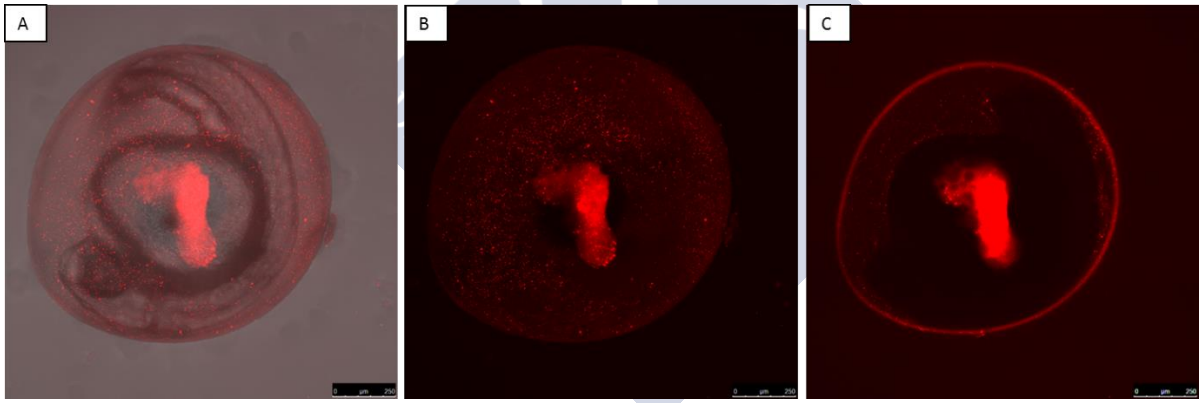

Figure 10. Embryo injected with HA-NC at 0hpf, after 24hpi. A: Maximum projection in black and white and fluorescence, z0-z80; B: Maximum projection in fluorescence, z0-z80; C: Slides z38-z41. Scale bar: 250µm

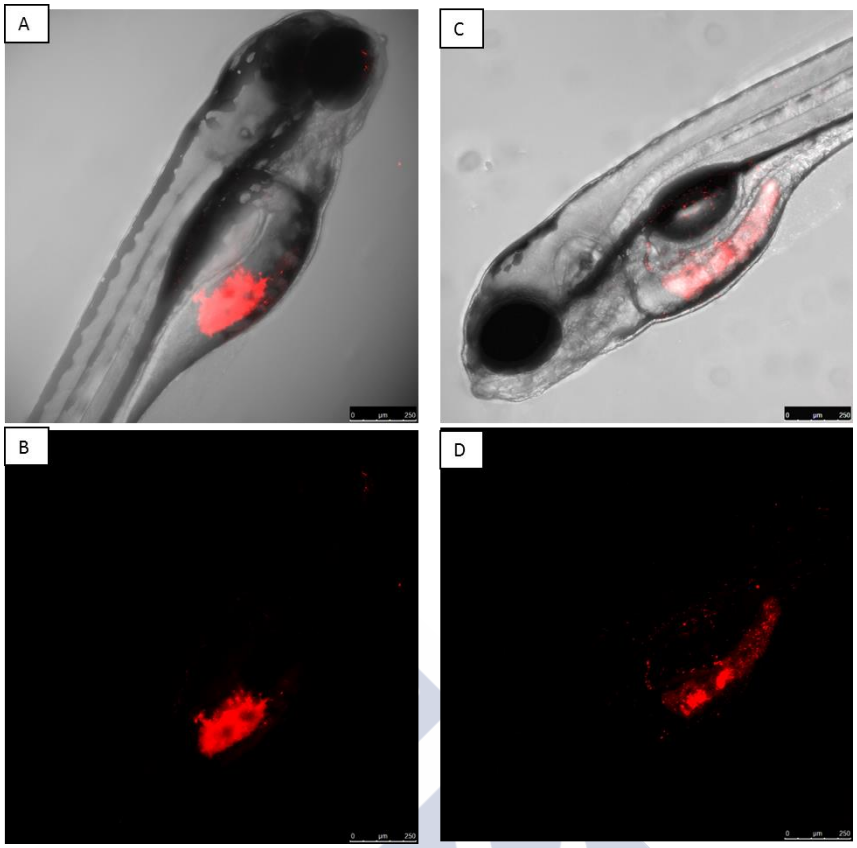

Figure 11. Embryo injected with HA-NC. A-B: at 24 hpf, after 48 hpi. Maximum projection in black and white and fluorescence, z0-z41 (A), Maximum projection in fluorescence, z0-z41 (B). C-D:at 48 hpf, after 96 hpi. Maximum projection in black and white and fluorescence, z0-z27 (C) Maximum projection in fluorescence, z0-z27 (D). Scale bar: 250µm

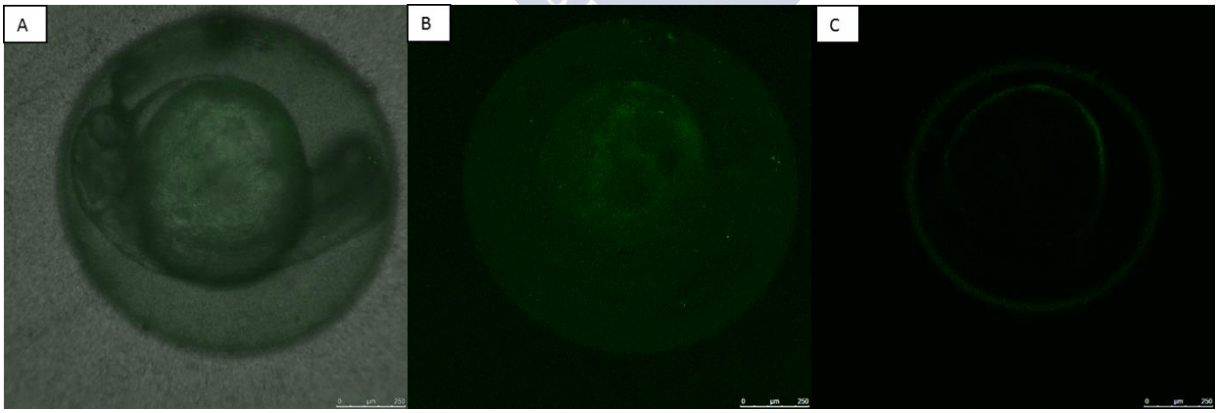

Figure 12. Embryo injected with PrHA-NC at 0hpf, after 24hpi. A: Maximum projection in black and white and fluorescence, z0-z62; B: Maximum projection in fluorescence, z0-z62; C: Slides z21-z24. Scale bar: 250µm

In case of PrHA-NC, both 24hpi (Figure 12) and 48-96hpi (Figure 13) the signal is distributed in the whole volume of the yolk sac instead of forming aggregates, but again

any migration can be observed to neighbor organs.

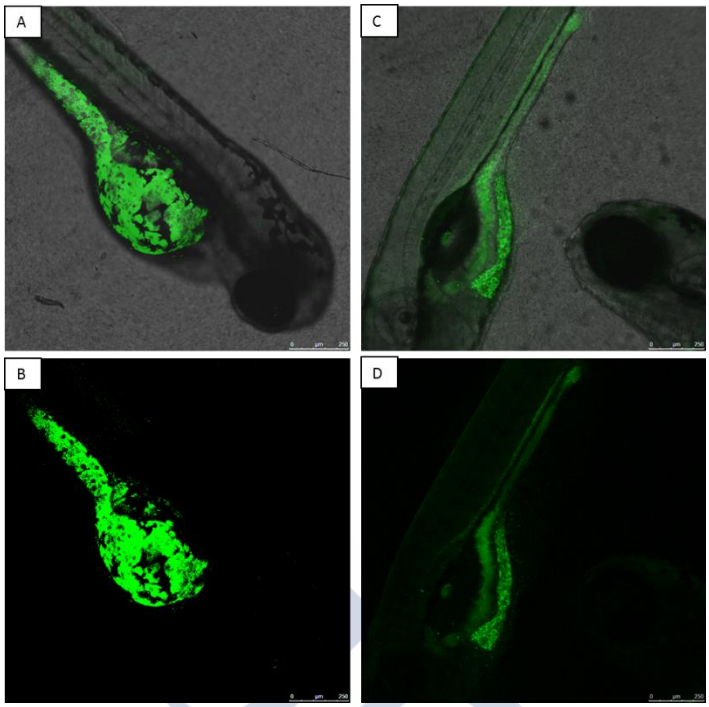

Figure 13. Embryo injected with PrHA-NC A-B: At 24 hpf, after 48 hpi. Maximum projection in black and white and fluorescence, z0-z26 (A).Maximum projection in fluorescence,. z0-z26 (B); C-D: At 48 hpf, after 96 hpi. Maximum projection in black and white and fluorescence, z0-z21 (C) Maximum projection in fluorescence, z0-z21 (D). Scale bar: 250 µm.

4. Discussion

Zebrafish embryos represent the model species for toxicology analysis (OECD test No. 236, 2013). In addition, they are frequently used as vertebrate model, complementary to murine models, for human biomedical applications (e.g. drug delivery systems).

In the last decade, many different types of nanosystems (NS) are being put into practice in numerous fields, providing possible exposures as much to humans as to environmental life.

In this work, 3 related nanosystems (HA-NC, PrHA-NC and NE) were analyzed for toxicology and embryo uptake to evaluate its application as drug nanocarriers.

As a first step, main physicochemical properties (size, morphology, PDI and Z potential) were described because their relevance in toxicology analyses (Bai *et al.*, 2010).

Moreover, it has been already described that variations in size and shape (Ispas *et al*., 2009) or Z potential (Cunningham *et al*., 2013; Lee *et al*., 2013) can play important roles on toxicity over zebrafish embryos. NS size ranged from 157 ± 3 (PrHA-NC) to 104 ± 8 nm (NE), which is slightly smaller than 200-400 nm, normally used as drug delivery systems (Hu *et al*., 2011). Regarding Z potential, this can be positive or negative, influenced by surface properties, as polymer and/or surfactant. This will partly establish nanoparticle aggregations, cell interactions… In our cases, HA provides to HA-NC and PrHA-NC of negative Z potential – (49±3) and – (30±4) mV respectively because of its high anionic charge. Moreover, PrHA-NC exhibits an increase in the charge explained by a second polymeric coating of protamine, arginine rich cationic peptide. On the other hand, NE shows positive charge (52±2) mV due to lack of polymeric coatings.

Related to NS structure, media where NS are resuspended represents a crucial issue for a proper application outcome. E3 appears, likely, as the most common media where zebrafish embryos are raised during early development, and a widespread media for NS toxicity evaluation using zebrafish embryos along the bibliography. Surprisingly, nanocarriers here analyzed suffered from aggregation in E3, causing variations in size, PI and Z potential. It could be provoked because E3 is composed by a multivalent inorganic salt solution, which can interact with the surfactant or the polymeric coating, responsible of NS stability (Bai *et al*., 2010)

Afterwards, NS were tested in SDTW for 96 h, and results demonstrated no changes in size, PI and Z potential parameters. From these results, we strongly recommend to analyze the exact media to use.

Concerning the toxicological assays on NS suspensions, NE turn out to be the most hazardous composition, much more than HA-NC or PrHA-NC. Paying attention to their structures and physicochemical characterization, the increased mortality caused by the exposition to NE is due to both, the presence of CTAB and the high positive surface charge. CTAB has been already demonstrated toxic from cell culture and algae to rat (Ray *et al*., 2009; Liang *et al.,* 2013), and appears easily accessible in the NE structure. However, HA-NC although also possess CTAB in its composition, its toxicity is much lower because of the presence of a HA polymeric coating. Similar results to HA-NC in the

FET test were the results for PrHA-NC, which also presents the external HA polymer coating. NE was not injected due to the high toxicity obtained in the FET test.

Focusing on possible differences to explain such results, attention should not be paid in the oily compounds of the internal cavity (Myglyol and Vitamine E), since they are neutral and present low density, but the key is the surfactant and Z potential. PrHA-NC uses as stabilizing agent, PEG-st, non-toxic biodegradable compound that hydrates the polymeric coating improving its biodistribution (Mosqueira *et al*., 2001; Prego *et al*., 2006), whereas HA-NC carries CTAB, highly toxic as previously explained.

In order to evaluate the possible applications of the NC tested, a series of nanoparticles uptake analyses were carried out. For this purpose, advantage was taken of embryo transparency and fluorescent nanocapsule labeling. Zebrafish offers a unique system to easily visualize *in vivo* phenomena, as uptake or biodistribution (Fenaroli *et al*., 2014). NE uptake was not evaluated because high levels of mortality in the FET test. As a result with nanocapsule solutions, embryos always internalized PrHA-NC, as much as in embryos with chorion (crossing the chorion and periviteline space, reaching the embryo cells), as in early dechorionated embryos (to overtake chorion limitations); but never HA-NC. Protamine can facilitate internalization of the PrHA-NC into the embryo. Administration way is expected to be transdermal or through the gills, but not oral. Mouth opening will not take place until 72 hpf (Kimmel *et al*., 1995).

In the case of prototype PrHA-NC suspended in the media, after 96 hpf multiple spots containing Rho6G can be observed on the zebrafish skin, reminding macrophages. Immunolabeling of L-plastin or Sudan black labeling should be done to distinguish them from neutrophils (Mathias *et al.,* 2009). Macrophages have been observed to be involved in inflammatory responses during cancer and metastasis (Benito-Martin *et al*., 2015). This tumor associated macrophages (TAM) have controversial functions, as they are shown to express growth factors and promote angiogenesis of tumor tissues as well as anti-tumor processes (Bingle *et al.,* 2002; Shih *el al*., 2006). More work should be done to demonstrate if PrHA-NC are phagocyted by macrophages. If that was the case this prototype would be a promising nanocarrier for antitumor drugs in tumors in where TAM are an important component of tumor tissue stroma.

When the uptake was forced by microinjection, both NC were visualized inside the yolk. Nevertheless, they did not diffuse to nearby tissues, perhaps, again, due to the yolk nature, affecting nanocapsule stability. Those cases where small amount of NC can be found out of the yolk could be explained because of very limited biodistribution, or releases of nanocapsules during the microinjection procedures, as much in the perivitelline space as in the developing cells of the embryo.

5. Conclusions

We can conclude that prototypes PrHA-NC and HA-NC designed by the group Nanobiofar cause a reduced mortality on zebrafish embryos comparing with the mortality of NE; being PrHA-NC a promising nanocarrier, especially with those drugs must cross biological barriers.

References

Abbott WS. A method of computing the effectiveness of an insecticide. *J Econ Entomol 1925; 18: 265-267.*

Al-Qadi S, Grenha A & Remuñán-López C. Microspheres loaded with polysaccharide nanoparticles for pulmonary delivery: Preparation, structure and surface analysis. *Carboydrate Polymers* 2011; 86:25-34.

Asharani PV, Wu YL, Gong Z & Valiyaveettil S. Toxicity of silver nanoparticles in zebrafish models. *Nanotechnology* 2008; 19(25): 255102.

Bai W, Zhang Z, Tian W, He X, Ma Y, Zhao Y, Chai Z. Toxicity of zinc oxide nanoparticles to zebrafish embryo: a physicochemical study of toxicity mechanism. *J Nanopart Res* 2010; 12:1645-1654.

Benito-Martin A, Giannatale AD, Ceder S & Peinado H. The new deal: a potential role for secreted vesicles in innate immunity and tumor progression. *Front Immunol* 2015. 6(66):doi:10.3389/fimmu.2015.00066.eCollection 2015.

Billinton N, Knight AW. Seeing the Wood through the trees: A review of techniques for distinguishing green fluorescent protein from endogenous autofluorescence. *Anal Biochem* 2001; 291: 175-197.

Bingle L, Brown NJ & ewis CE. The role of tumour-associated macrophages in tumour progression: implications for new anticancer therapies. *J Pathol* 2002; 196(3):254-65.

Colucci-Guyon E, Tinevez JY, Renshaw SA & Herbomel P. Strategies of professional phagocytes in vivo: unlike macrophages, neutrophils engulf only surface-associated microbes. *J Cell Sci* 2011; 124:3053-3059

Creton R. The calcium pump of the endoplasmic reticulum plays a role in midline signaling during early zebrafish development. *Developmental Brain Research* 2004; 151: 33-41.

Cunninghtam S, Brennan-Fournet ME, Ledwith D, Byrnes L & Joshi L. Effect of Nanoparticle Stabilization and Physicochemical Properties on Exposure Outcome: Acute Toxicity of Silver Nanoparticle Preparations in Zebrafish (Danio rerio). *Environ. Sci Technol* 2013; 47: 3883-3892.

Duan J, Yu Y, Shi H, Tian L, Guo C, Huang P, Zhou X, Peng S, Su Z. Plos One 2013; 8(9):e74606. Doi:10.1371/journal.pone.0074606.

Edwin EE & Jackman R. Nature of the autofluorescent material in cerebrocortical necrosis. *J Neurochem* 1981; 37(4):1054-6

Fako VE & Furgeson DY. Zebrafish as a correlative and predictive model for assessing biomaterial nanotoxicity. *Adv Drug Deliver Rev* 2009; 61(6): 478-486.

Fenaroli F, Westmoreland D, Benjaminsen J, Kolstad T, Skjeldal FM, Meijer AH, van der Vaart M, Ulanova L, Roos N, Nyström B, Hildahl J & Griffiths G. Nanoparticles as drug delivery system against Tuberculosis in Zebrafish Embryos: Direct Visualization and Treatment. *ACS Nano* 2014; 8:7014-7026.

Finney, DJ. Probit Analysis. Cambridge, Cambridge University Press. 1952.

Fraser JRE, Laurent TC & Laurent UBG. Hyaluronan: its nature, distribution, function and turnover. *Journal of Internal Medicine* 1997; 2242:27-33

Gou ML, Shi HS, Guo G, Men K, Zhang J, Zheng L, Li ZY, Luo F, Quian ZY, Zhao X & Wei YQ. Improving anticancer activity and reducing systemic toxicity of doxorubicin by self-assembled polymeric micelles. *Nanotechnology* 2011; 22: 095102-095113.

Henn K, Braunbeck T. Dechorionation as a tool to improve the fish embryo toxicity test (FET) with the zebrafish (*Danio rerio*). *Comp Biochem Phys C* 2010; 153: 91-98.

Hoekstra JA. Acute bioassays with control mortality. *Water Air Soil Poll* 1987; 35: 311-317.

Hu YL, Qi W, Han F, Shao JZ & Gao JG. Toxicity evaluation of biodegradable chitosan nanoparticles using zebrafish embryo model. *Inte J Nanomedicine* 2011; 6: 3351-3359.

Ispas C, Andreescu D, Patel A, Goia D, Andreescu S & Wallace KN. Toxicity and developmental defects of different sizes and shape nickel nanoparticles in zebrafish. *Environ Sci Technol* 2009; 43:6349-6356.

Kim KT & Tanguay RL. The role of chorion on toxicity of silver nanoparticles in the embryonic zebrafish assay. *Environ Helath Toxicol* 2014. 29:e2014021

Kimmel CB, Ballard WW, Kimmel SR, Ullmann B & Schiling TF. Stages of embryonic development of the zebrafish. *Developmental dynamics* 1995; 203:253-310.

Kogan G, Soltés L, Stern R & Gemeiner P. Hyaluronan acid: a natural biopolymer with a broad range of biomedical and industrial applications. *Biotechnol Lett* 2007; 29:17-25.

Kovriznych JA, Sotnikova R, Zeljenkova D, Rollerova E, Szabova E & Wimmerova S. Acute toxicity of 31 different nanoparticles to zebrafish (Danio rerio tested in adulthood and in early life stages-comparative study. *Interdisip Toxicol* 2013; 6(2):67-73

Lee KJ, Browning LM, Nallathamby PD & Xu XHN. Study of charge-dependent transport and toxicity of peptide-functionalized silver nanoparticles using zebrafish embryos and single nanoparticle plasmonic spectroscopy. *Chem Res Toxicol.* 2013; 26(6): 904-917.

Liang Z, Ge F, Zeng H, Xu Y, Peng F& Wong M. Influence of cetyltrimethyl ammonium bromide on nutrient uptake and cell responses of *Chlorella vulgaris. Aquatic Toxicology* 2013; 138:81-87.

Lin S, Zhao Y, Nel AE & Lin S. Zebrafish: An In Vivo Model for Nano EHS Studies. Small 2012

Mathias JR, Dodd ME, Walters KB, Yoo SK, Ranheim EA & Huttenlocher A. Characterization of zebrafish larval inflammatory macrophages. *Dev Comp Immunol* 2009; 33(11):1212-1217.

Maeda H, Bharate GY & Daruwalla J. Polymeric drugs for efficient tumor-targeted drug delivery based on EPR-effect. *Eur J Pharm Biopharm* 2009; 71(13):409-19.

McGrath P & Li CQ. Zebrafish: a predictive model for assessing drug-induced toxicity. *Drug Discov Today* 2008; 13(9-10): 394-401.

Mizrahy S, Raz SR, Hasgaard M, Liu H, Soffer-Tsur N, Cohen K, Dvash R, Landdsman-Milo D, Bremer MGEG, Moghimi SM & Peer D. Hyaluronan-coated nanoparticles: The influence of the molecular weight on CD44-hyaluronan interaction and on the immune response. *J Control Release* 2011; 156(2):231-238.

Mosqueira VCF, Legrand P, Morgat JL, Vert M, Mysiakine E, Gref R, Devissaguet JP & Barratt G. Biodistribution of long-circulating PEG-Grafted Nanocapsules in mice: Effects of PEG chain Length and density. *Pharmaceutical Research* 2001; 18_ 1411-1419.

Organization for Economic Co-operation and Development (OECD). Guidelines for the testing of chemicals. Section 2. Test No. 203. Fish, acute toxicity test. 1992

Organization for Economic Co-operation and Development (OECD). Test No 236. Fish embryo acute toxicity (FET) test. 2013

Oyarzun-Ampuero FA, Rivera-Rodriguez GR, Alonso MJ, Torres D. Hyaluronan nanocapsules as a new vehicle for intracellular drug delivery, *Eur. J. Pharm. Sci.,* 2013; 49, 483-490.

Prego C, Torres D, Fernandez-Megia E, Novoa-Carballal R, Quiñoá E & Alonso MJ. Chitosan-PEG nanocapsules as new carriers for oral peptide delivery. Effect of chitosan pegylation degree. *J Control Release* 2006; 111(3):299-308.

Ray PC, Yu H & Fu PP. Toxicity and Environmental Risks of Nanomaterials: Challenges and Future Needs. *J Environ Schi Health C Environ Carcinog Ecotoxicol Rev* 2009; 27:1-35.

Salinas-Madrigal L & Soelo-Avila C. Morphologic diagnosis of acute tubular necrosis (ATN) by autofluorescence. *Am J Kidney Dis* 1986; 7(1):84-7

Schubert S, Keddig N, Hanel R & Kammann U. Microinjection into zebrafish embryos (*Danio rerio*)- a useful tool in aquatic toxicity testing?.*Environ Sci Eur* 2014. 26-32.

Shi X, Teo LS, Pan X, Chong SW, Kraut R, Korzh V, Wohland T. Probing events with single molecule sensitivity in zebrafish and Drosophila embryos by fluorescence correlation spectroscopy. *Dev Dynam* 2009; 238:3156-3167.

Shih JY, Yuan A, Chen JJW & Yang PC. Tumor-associated macrophage: Its role in cancer invasion and metastasis. *Journal of Cancer Molecules* 2006; 2(3):1101-106.

Singer JT, Phennicie RT, Sullivan MJ, Porter LA, Shaffer VJ, Kim CH. Broad-host-range plasmids for red fluorescent protein labeling of gram-negative bacteria for use in the zebrafish model system. *Appl Environ Microbiol* 2010. 76 (11):3467-74

Tamosiunas M, Makaryceva J, Labanauskiene J, Bagdonas S, Aleksandraviciene C, Didziapetriene J, Griciute L& Rotomskis R. Autofluorescence of transplantable hepatoma A22 (MH-A22): prospects of tumor tissue optical biopsy. *Exp Oncol* 2004; 26(2).118-24

Westerfield M. The zebrafish book: A guide for the laboratory use of zebrafish (Danio rerio). 5th ed. Eugene: University of Oregon Press, 2007

Yang XY, Li YX, Li M, Zhang L, Feng LX & Zhang N. Hyaluronic acid-coated nanostructured lipid carriers for targeting paclitaxel to cancer. *Cancer Letters* 2013; 334: 338-345.

Zhu X, Wang J, Zhang X, Chang Y, Chen Y. The impact of ZnO nanoparticle aggregates on the embryonic development of zebrafish. *Nanotechnology* 2009; 20 (19):195103.

Zon LI & Peterson RT. In vivo drug discovery in the zebrafish. Nat Rev Drug Discov 2005;4:35-44.

USC
UNIVERSIDADE
DE SANTIAGO
DE COMPOSTELA